

School of Civil and Mechanical Engineering

**Physical Parameter Identification of Time-Varying Structure Using
Partial Measurements**

Ning Yang

This thesis is presented to the Degree of

Doctor of Philosophy

of

Curtin University

August 2021

DECLARATION

To the best of my knowledge and belief this thesis contains no material previously published by any other person except where due acknowledgement has been made.

Signature:

02/08/2021

Date:

CHAPTER 1 ABSTRACT

Direct identification of physical parameters, such as, physical stiffness and damping parameters of linear structures, plays a significant role in structural health assessment. Vibration-based techniques have been developed to identify the physical parameters of time-invariant structures in the field of structural health monitoring (SHM) [1]. However, structural physical parameters may vary under severe loading conditions, such as strong seismic and wind loads, as well as other environmental effects, e.g., temperature and/or corrosion effect. Effective methods are therefore also needed to identify the dynamic characteristics of time-varying structures, adaptively assess and evaluate the performance of time-varying structural systems [2, 3].

Relevant studies have been conducted in the time-domain and time-frequency domain. The state space model based methods have shown a high efficiency in the time-domain to track the change of physical parameters [4-12]. Among these methods, the Kalman filter (KF) series methods have been commonly used with an outstanding feature that only incomplete measurements are required in the identification process [6-12]. Based on KF series methods, the time-varying physical parameters can be identified by introducing the fading-factor to adjust the state prediction covariance matrix in real time. However, it is difficult to determine the optimal fading-factor. As a result, some of these methods were proposed based on an empirical factor [6] or the empirical formula [7, 8]. Furthermore, the adaptive factor matrix at each time instant is developed, but it is computational expensive [9, 10]. In addition, the time-varying physical parameters can be identified by updating the process noise covariance in KF series methods [11, 12], which also depends on the selection of empirical factors.

The time-frequency domain methods that are developed to identify the structural time-varying physical parameters mainly refer to the wavelet multiresolution (WM) based methods [13-20]. Most of these methods expand the time-varying structural physical parameters into scale coefficients, and then identify these coefficients by the linear least-squares estimation [13-19]. However, complete measurements of structural responses at all degrees of freedom (DOFs) are required in these methods, which is impractical for real applications. To overcome the limitation on full observations, a novel method has been proposed recently to identify the time-varying physical parameters of linear structures under known excitations using partial measurements [20]. Nevertheless, such method is only applicable for linear time-varying structures with known excitations, and it is required to expand all physical parameters (including time-varying parameters and time-invariant parameters) into scale coefficients based on WM.

Overall, there are still some difficulties and limitations in the identification of time-varying physical parameters, including: (1) the number of sensors is large, because the full observations of all the displacement, velocity, and acceleration responses are needed. Furthermore, the known external excitation is required; (2) There is a lack of effective identification methods for the large-scale time-varying structures. Although the substructure technique provides a feasible manner for the identification of large-scale structures, determining the interaction forces between adjacent substructures is still a great challenge in the case of unavailable observations at the interface of substructures; (3) The identification of nonlinear time-varying physical parameters is more difficult than that of linear time-varying structures; (4) The identification of gradually varying physical parameters is more challenging than that of abruptly changing physical parameters, for example, the identification of the gradually-varying cable force is worth of further studies; (5) The diagnosis of structural damage is an important purpose of identifying the physical

parameters of time-varying structures. Nevertheless, detecting structural damage by using partial measurements still needs investigations, etc.

It is noted that measuring the displacement, velocity and acceleration responses of all DOFs is unrealistic and uneconomic in practical engineering, and the external load information is often difficult to obtain directly. Therefore, it is suggested to investigate the identification methods for time-varying physical parameters by using only partially measured responses under unknown excitations, and explore suitable identification methods for large-scale structures, nonlinear systems, and gradually varying systems. Moreover, a novel method is desired to diagnosis the structural damage using only partial structural measurements. It is more in line with the requirements of engineering practices, which has more theoretical research value and engineering significance.

Thus, in this thesis, the followings are investigated step by step, including: “Chapter 2: Simultaneous identification of structural time-varying physical parameters and unknown excitations using partial measurements”, “Chapter 3: Identification of time-varying large-scale structures by integrated sub-structural and wavelet multiresolution approach with partial measurements”, “Chapter 4: Identification of time-varying nonlinear structural physical parameters by integrated WMA and UKF/UKF-UI”, “Chapter 5: Identification of gradually varying physical parameters based on discrete cosine transform using partial measurements” and “Chapter 6: Structural damage diagnosis based on the temporal moment of partially measured structural responses”. The methods in Chapters 2 – 5 are proposed based on the KF series methods and the Kalman filter under unknown input series methods. These proposed methods improve the traditional methods based on the WM analysis, and overcome the shortcomings of full observations of all displacement, velocity and acceleration responses. Additionally, the identification of time-varying physical parameters under unknown loads is discussed. In

Chapter 6, a structural damage detection algorithm based on temporal moments by using only incomplete measured structural response is proposed, which shows a good accuracy in structural damage diagnosis with noise resistance. The contents of each chapter are introduced as follows.

Chapter 2: Simultaneous identification of structural time-varying physical parameters and unknown excitations using partial measurements.

Current structural time-varying physical parameters identification methods based on WM analysis need full measurements of structural acceleration, velocity and displacement responses together with the external excitation information, which greatly restricts their applications in practice [14-19]. Inspired by the merits of both the recently developed data fusing based Kalman filter under unknown input (KF-UI) [21] and the WM analysis, this chapter aims to overcome the limitations of previous WM-based methods for the identification of time-varying physical parameters. An algorithm is proposed by integrating the WM analysis and the data fusion based KF-UI to identify structural time-varying systems and the unknown excitations using only partially measured structural responses. In the proposed algorithm, structural mass is assumed time-invariant and known while structural stiffness and damping parameters are time-varying and unknown, the structure is subjected to unknown excitation, and only partial measurements of structure responses are observed. The WM analysis is utilized to expand the structural time-varying physical parameters at a multi-scale profile, which transforms the time-varying physical parameter identification into equivalent estimation of time-invariant scale coefficients. To overcome the previously mentioned limitation on requiring full measurements of structural responses and external excitations, the advantage of the data fusion based KF-UI is adopted to identify structural state using only partial measurements of structural responses. Finally, the scale coefficients of WM

analysis are estimated by the nonlinear least-squares optimization, and structural time-varying physical parameters and the unknown external loads are also identified accordingly. The effect of noise can be minimized based on the noise immunity of the KF-UI. Three numerical examples including various scenarios (e.g. suddenly or gradually varying of structural physical parameters) simulated on the shear-type frame, beam and plane frames under unknown excitations have validated the proposed algorithm. Furthermore, experimental data of a three-story time-varying frame from the Research Center of Earthquake Engineering in Taipei [22] are utilized to validate the proposed algorithm.

The proposed identification approach in Chapter 2 contains the following main procedures:

(1) Based on the WM expansion, the time-varying structural physical parameters are approximately expressed by a truncated WM analysis in the discrete form with the resolution level J and unknown wavelet scale coefficients. Then, the identification task is transformed into estimating the time-invariant coefficients in WM analysis.

(2) With given wavelet scale coefficients, structural full responses at all DOFs together with the unknown excitation can be estimated by the data fusion based KF-UI using partially measured structural responses. The identified structural responses and unknown external excitations are implicit functions of the wavelet scale coefficients.

(3) The unknown wavelet scale coefficients are estimated by solving a nonlinear optimization problem with the objective function using the nonlinear least-squares estimation.

(4) With the estimated wavelet scale coefficients, structural time-varying physical parameters can be reconstructed by WM, and structural external excitations can also be identified simultaneously.

The main contributions of this chapter are listed as follows. (i) A novel algorithm is proposed for simultaneously identifying structural time-varying parameters and unknown external excitations using only partial measurements instead of full measurements of structural responses at all DOFs; (ii) The unknown excitations to the time-varying structures are considered and identified; (iii) The effect of measurements noise is minimized due to the fact that KF-UI approach itself can include the influences of modelling error and measurements noise. Such an identification algorithm is not available in the literature.

Similar as other previous WM-based methods for time-varying parameter identification, the proposed algorithm in Chapter 2 may not be effective for large size structures considering the difficulty in the multiple-parameter optimization problem. This is the drawback of the proposed method. This difficulty can be solved by the sub-structural identification approach. Such relevant research is conducted in Chapter 3 and is briefly summarized as follows.

Chapter 3: Identification of time-varying large-scale structures by integrated sub-structural and wavelet multiresolution approach with partial measurements.

Method developed in Chapter 2 requires to expand all physical parameters (including time-varying parameters and time-invariant parameters) into scale coefficients based on WM. The number of expanded coefficients increases greatly as the structural size increases, making it difficult to obtain a global optimal solution especially when the quality of the collected data is poor. Therefore, the proposed method is still applicable to small-scale structures with a small number of DOFs.

For the parametric identification of large-scale structures, sub-structural identification technique is more efficient [23-29]. However, these methods are mostly used to identify the parameters of time-invariant systems. For time-varying systems, Shi and Chang [15, 16] used the sub-structural identification technique to identify the time-varying physical parameters of a numerical 10-story shear frame and a 3-story experimental shear building model. Each structure was divided into several small size substructures, and WM was adopted to identify the time-varying physical parameters of each substructure. Recently, Wang et al. [19] presented a wavelet transform and sub-structural algorithm to track the abrupt stiffness degradation of a numerical 7-story shear frame and a laboratory 3-storey shear-type structure. However, measurements of complete structural responses of acceleration, velocity and displacement responses at every DOF including those at sub-structural interfaces, were needed for each substructure in the above studies. With the full measurements of structural responses and known excitations, the identification can be accomplished by the simple linear least-squares estimation. Although sub-structural technique provides a very useful tool for parametric identification of large-scale structures, it is still a challenging task to properly model the interaction forces between adjacent substructures without the fully measured responses at the sub-structural interfaces.

Based on the above literature review of current existing methods, it is obvious that there are still some limitations in identifying the time-varying physical parameters of large-scale structures. This chapter aims to circumvent these limitations and propose a novel approach for the identification of time-varying physical parameters of large-scale

structures by integrating sub-structural and WM methods using only partially measured structural responses. Two main technical innovation aspects are summarized as follows:

1. Substructure identification is conducted based on the partial observations of sub-structural responses.

Usually, dynamic responses at the sub-structural interfaces are required in the previous sub-structural identification techniques, which limits the practical applications [24, 26]. Interaction forces between adjacent substructures can be considered as ‘unknown inputs’ to the substructure of interest. The generalized Kalman filter under unknown input (GKF-UI), which was recently proposed for the identification of time-invariant systems by the authors [30], is used to identify each substructure with only partial measurements of sub-structural responses without measurements at the interface DOFs. Then, the identification of a large-scale structure is transformed to the identification of each substructure independently, which greatly simplifies the identification of the time-varying structural parameters of the large-scale structure in the optimization problem.

2. Localization of time-varying physical parameters is conducted to reduce the number of expanded scale coefficients and ensure a global optimal solution.

In this chapter, a fading-factor generalized extended Kalman filter under unknown input (FGEKF-UI) is proposed to firstly locate the time-varying physical parameters in each substructure, in which the unknown sub-structural interaction forces are regarded as “additional unknown inputs” imposed to the target substructure. Then only the time-varying parameters are expanded by WM, greatly reducing the number of expanded scale

coefficients compared with the current WM based methods for the identification of time-varying structures, since all physical parameters including time-varying and time-invariant parameters are expanded into scale coefficients in the latter.

Inspired by the merits of sub-structural identification technique and WM analysis for time-varying parameters, a novel two-step approach is proposed in this chapter for the identification of time-varying physical parameters of large-scale structures using only partially measured structural responses. In this study, structural mass is assumed time-invariant and known, while structural stiffness and damping are time varying parameters to be identified. A large-scale structure is divided into several substructures, and the sub-structural interaction forces are treated as ‘additional unknown inputs’ to the target substructure. Each substructure is identified in a parallel manner with a two-step procedure. In the first step, the time-varying sub-structural physical parameters are located by the FGEKF-UI algorithm. In the second step, these parameters are expanded into fewer scale coefficients by the WM analysis, therefore the identification of time-varying systems is transformed into the identification of time-invariant scale coefficients together with the time-invariant physical parameters. Then, the GKF-UI algorithm is used for the identification of sub-structural state under unknown inputs using data fusion of partial measurements. Finally, the scale coefficients and time-invariant physical parameters are estimated by solving a nonlinear optimization problem, and the original unknown time-varying structural physical parameters are reconstructed by the estimated scale coefficients. Numerical results of identifying time-varying physical parameters of a 30-story shear frame and a three-span truss bridge model demonstrate that the proposed

approach can effectively identify the abruptly changing, gradually varying and time-invariant stiffness and damping parameters. The structures investigated in this chapter are of relatively larger-scale compared with the numerical structures in the previous WM-based studies. Moreover, the external excitations can be unknown in both cases and can also be identified.

The main contributions of this chapter are listed as follows:

(1) A new two-step approach is proposed for the identification of large-scale linear structures with time-varying physical parameters using only partially measured structural responses;

(2) FGEKF-UI is firstly proposed to locate the time-varying parameters and enable dimensionality reduction of scale coefficients to the greatest extent, resulting in only a few variables involved in the optimization process;

(3) GKF-UI is used to estimate the sub-structural state, where the known interaction forces and full observations are not required, and observations at the interface are not required either. The effect of measurement noise is minimized, owing to that GKF-UI algorithm itself can include the influence of modelling error and measurement noise;

(4) The proposed approach can be applied to each substructure independently by parallel computing, which greatly simplifies the difficulties in identifying large-scale time-varying structural parameters.

Chapter 4 Identification of time-varying nonlinear structural physical parameters by integrated WMA and UKF/UKF-UI

Methods proposed in Chapters 2 and 3 are based on the assumption of the linear structural model. However, under strong external loads such as earthquake, strong wind, impact and explosion, engineering structural components may respond nonlinearly [31-33]. In recent years, many researchers have carried out in-depth researches on the identification of nonlinear structural characteristics and presented a variety of identification methods, including time-domain [34-37], frequency-domain [39] or time-frequency analysis methods [39-43]. However, the parameters of nonlinear models are assumed to be steady in most of these methods, only a few efforts have been attempted on the identification of time-varying nonlinear systems. Adaptive identification techniques based on the Kalman Filter (KF) have the potential to track time-varying parameters of hysterically degrading structures [10, 44, 45], which exploited the track factor, adaptive correction factor, or adaptive factor matrix to deal with the evolution of system variation. The challenging issue is that either these adaptive algorithms have strong subjectivity on empirical factors [45], or it is time-consuming in calculating the optimal matrix at each time-step [44]. The WMA based method mentioned above can also be used to identify the time-varying nonlinear systems. For instance, Chang and Shi [14] proposed a method to identify the time-varying physical parameters and model parameters in the Bouc-Wen hysteresis model based on WMA. However, this method needs full information on the structural displacement, velocity, acceleration responses, and excitation. Furthermore, in addition to the stiffness and damping parameters, the parameters in the nonlinear model are also needed to be expanded by WMA, which increases the complexity than the identification of linear systems.

With partial measurements, the extended Kalman filter (EKF) and unscented Kalman filter (UKF) [46] have been commonly used in the identification of nonlinear time-invariant systems. Compared with EKF, UKF is more superior as it does not need the calculation of the Jacobian matrix and a linearization-based approximation of the nonlinear system, realizing an on-line identification with a better recognition accuracy [47]. Furthermore, UKF method for the case of unknown excitations has been derived and successfully applied to the physical parameter identification of nonlinear systems under unknown loads [48]. However, these methods are only suitable for the time-invariant systems. Adaptive UKF methods have been proposed for the identification of time-varying structures, combining with the adjustment of error covariance [49, 50] or the adjustment of noise covariance matrix [51, 52]. This may depend on the fading factors in most of the developed methods. However, if the fading factors are not selected properly, one may only roughly determine which parameter has the most possibility of varying property, but the change degree is difficult to be accurately determined. Moreover, all these adaptive methods are derived on the premise of known excitation. To the best knowledge of the authors, there is a lack in the identification of time-varying nonlinear systems under unknown excitations.

In addition, it should be pointed out that the existing WMA based methods are only applicable to structures with a small number of elements [14-20]. The reason is that the number of scale coefficients in the least-squares optimization process will increase with the number of elements, which makes it difficult to obtain the global optimal solution especially when the quality of observation data is poor. The “divide and conquer” idea of

the sub-structural based methods provides a feasible strategy for the identification of structures with more elements [23-29]. Many scholars have also introduced the concept of substructure analysis into the identification of nonlinear structures [53-56]. However, these methods are mostly used to identify the parameters of time-invariant systems, and they still have some shortcomings such as the difficulties in determining the interface forces, the incapability of parallel identification, and the existence of propagation errors [57]. Shi and Chang [15, 16] presented an offline sub-structural method to identify the time-varying nonlinear shear-type buildings based on WMA. Nevertheless, the method requires all the displacement, velocity and acceleration responses inside and at the interfaces of the substructure. Further development and studies on identification techniques for time-varying nonlinear structures with more elements are still needed.

Based on the above-mentioned detailed literature, most WMA based methods are used to identify the physical parameters of time-varying linear systems, while only a few studies are conducted for the time-varying nonlinear systems. In addition, these methods require full measurements of displacement, velocity, acceleration and external loads. Furthermore, all physical parameters including time-varying and time-invariant parameters are expanded by WMA, which leads to a significant increase in the number of scale coefficients. Therefore, two-step identification processes are proposed in this chapter to identify the physical parameters of time-varying nonlinear systems by using partial measurements. Three cases are discussed respectively.

The first case is the identification of time-varying nonlinear structures with a small number of elements under known excitations. The time-varying physical parameters are

located by the fading-factor unscented Kalman filter (FUKF) in the first step, and the method integrating WMA with UKF is proposed to identify the time-varying physical parameters in the second step, which uses partially measured acceleration responses. A numerical example of a 6-story time-varying nonlinear shear frame under known seismic acceleration is provided, with abruptly changing or gradually varying parameters, to verify the effectiveness of the first proposed identification process. The proposed identification process contributes to reducing the number of scale coefficients, since not all physical parameters are required to be expanded after the locations of time-varying physical parameters are detected. Most importantly, only partial response measurements are needed in the identification process, with a clear improvement compared with the previous WMA based methods which require response measurements at all DOFs.

Considering that the external loads are always hard to measure in practical situations, the study is extended to the second case, that is, the identification of time-varying nonlinear structures with a small number of elements but under unknown excitations. Herein, the improved unscented Kalman filter under unknown input (UKF-UI) method proposed by the authors [48] is adopted. The time-varying physical parameters are located by the proposed fading-factor UKF-UI (FUKF-UI) in the first step, and the method integrating WMA with UKF-UI is proposed to identify the physical parameters using partially measured acceleration and displacement responses in the second step. Numerical study on a truss structure is conducted to identify the time-varying parameters and unknown excitations simultaneously. The proposed identification process meets the needs of practical engineering applications, since the physical parameters of time-varying

nonlinear system can be identified by using partial response measurements under unknown excitations.

The last case is the identification of time-varying nonlinear structures with more number of elements under unknown excitations, which is investigated based on the sub-structural method. The time-varying physical parameters of the whole structure are located by the proposed FUKF-UI method in the first step. In the second step, the whole structure is divided into several substructures and the unknown interaction force is considered as the fictitious “unknown input”. Therefore, each substructure can be identified in parallel using the proposed WMA integrated with UKF-UI method. Numerical study on a 10-story shear frame demonstrates that the proposed identification process is effective for the identification of structures with more number of elements under unknown excitations. With partial response measurements, each substructure can be identified in parallel without measuring the interaction forces.

Chapter 5 Identification of time-varying nonlinear structural physical parameters by integrated WMA and UKF/UKF-UI

Change in physical parameters of civil engineering structures is a gradual process in most circumstances. For instance, the cumulative structural damage evolves from minor to severe, leading to gradually changing vibration characteristics [58]. For the vehicle-bridge coupling system, the mass distribution of the system varies with time due to the moving of vehicles, which also results in the gradually varying features of the system [59-61]. Tracking the gradual evolution process and identifying the gradually changing physical parameters accurately is still a challenging issue that is worth of investigation.

The core of the WM-based method is to reparametrize the time-varying model by wavelet basis for the purpose of reducing the dimensionality of the inverse problem and computational complexity. Then, the unknown physical parameters are equal to the product of the scale coefficients and the base functions. However, the wavelet basis function is not particularly suitable for the decomposition of gradually changing parameters. The reason is that relatively more scale coefficients should be retained to guarantee the accuracy of reconstructed gradually changing parameters, while a large number of scale coefficients may result in the convergence to local optimization results, especially when the measured structural responses are contaminated by a high-level noise. Furthermore, the determination of appropriate mother function and decomposition level in WM is a pending issue that is not yet well resolved [62]. Besides, the boundary effect of WM is also inevitable. Therefore, other decomposition basis which is more suitable for gradually changing parameters should be investigated to reduce the number of coefficients as much as possible. Discrete cosine transform (DCT) is a kind of transformation defined for analysing real signals [63]. A series of DCT coefficients are obtained in frequency domain after transformation. Most importantly, energy concentration is a very valuable property of DCT, that is, a majority of energy in natural signals (e.g., sound and image) is concentrated in the low frequency range, promoting the wide application of DCT in data compression [64, 65]. In addition, some researchers have adopted DCT for the identification of unknown parameters benefitting from the dimensional reduction of DCT [66, 67]. Zhang [68] used the DCT basis and wavelet basis to expand the same gradually changing signal, and then compared the sparsity of DCT

coefficients and scale coefficients, respectively. Results showed that DCT coefficients contained more coefficients close to zero, demonstrating a better sparsity. It means that DCT instead of WM can use less number of coefficients to express the original gradually changing signal. Considering that the energy of vibration of civil engineering structures is mainly distributed in the low-frequency component [18], therefore, it is worth decomposing the gradually varying physical parameters into low-order DCT coefficients, especially when the measured responses are polluted by a high-level noise.

Cable is a common time-varying system. With the advantages of low cost, high bearing capacity and wind stability, cables have been widely used as the main components in long-span bridges [69-71]. Under complex load conditions and harsh environmental effects, the structural cable condition inevitably deteriorates by a number of issues, such as fatigue, corrosion and prestress loss, which can introduce negative effects on the cable, such as weakening the stiffness and reducing the bearing capacity, and eventually leading to cable fracture, which endangers the safety of the cable-supported bridges [72]. Therefore, the identification of cable force plays an indispensable role in the SHM of cable-supported bridges. Specifically, the existing cable force identification methods can be roughly divided into five categories: lift-off method, load cell method, magnetic flux leakage method, fiber Bragg grating method and vibration-based method [72]. As an indirect measurement method, the vibration-based methods have the advantages of simple installation, convenient operation, reusability, high precision and low price [73, 74]. Although many in-depth studies have been carried out, most of the proposed methods can only be used to estimate the average value of cable forces in a specific duration. However,

the cable force is time-varying subjected to the live load in the long-span cable-supported bridge. The average cable force value may not be used to evaluate the fatigue damage of the cable accurately. Therefore, it is of great theoretical significance and engineering application importance to develop the identification method of time-varying cable force for the safety assessment of bridges. Some attempts have been conducted to obtain the time-varying cable tension from the dynamic responses of cables [72, 75-80]. It shall be noted that the varying cable force is in the form of gradual change in the abovementioned studies.

Inspired by the merits of DCT and KF series methods, this chapter proposes novel two-step approaches for the identification of gradually varying physical parameters of structural cables under known and unknown excitations, respectively. In this study, the structural mass is a known and time-invariant parameter, and only partially measured structural responses are used for the identification of gradually varying physical parameters. Approach I is proposed for the case of time-varying system identification under known excitations. The gradually varying physical parameters are localized by the fading-factor extended Kalman filter (FEKF) algorithm in the first step, and then identified by the proposed DCT integrated with KF method. Approach II is proposed to conduct the time varying system identification under unknown excitations. In this approach, the gradually varying physical parameters are localized by the proposed fading-factor extended Kalman filter under unknown input (FEKF-UI) algorithm, and identified by the proposed DCT integrated with Kalman filter under unknown input (KF-UI) method. Moreover, considering that the stay cable is a common time-varying system as its cable

force changes with time under the combined action of vehicle load and wind load, it is investigated as a case study in this paper. The discrete equation of motion of stay cables in modal domain is given and the steps of identifying the time-varying cable force by the proposed approach I are presented. Results obtained from numerical studies on Nanjing Yangtze River No. 3 Bridge and experimental tests on the scaled cable demonstrate that the change of cable force can be identified by using only one acceleration response on the cable, with or without the anemometer installed on the bridge.

The main contributions of this paper are listed as follows.

(1) Novel two-step approaches are proposed for the identification of gradually varying physical parameters of linear structures using only partially measured structural responses;

(2) FEKF-UI is firstly proposed to locate the time-varying parameters under unknown input. Locating the time-varying parameters aids to reduce the number of coefficients involved in the optimization process;

(3) DCT is used to expand the gradually varying physical parameters instead of previous WM analysis. It is more suitable for the decomposition of gradually changing parameters, which can retain less coefficients to reconstruct the original physical parameters. Thus, the proposed approaches are robust even when the measurements are polluted by high-level noises. In addition, the boundary effect of WM is avoided;

(4) It is further extended to the identification of gradually changing physical parameters under unknown excitations. Both the time-varying parameters and the unknown excitations are identified simultaneously.

Chapter 6 Structural damage diagnosis based on the temporal moment of partially measured structural responses

Damage detection of civil structures is still a challenging task, since current damage detection methods are either insensitive to local structural damage or sensitive to measurement noise. It is noted that methods based on statistical moment of structural responses are proposed and shown to be an efficient tool because of its good noise immunity [81-95]. Generally speaking, a significant advantage of the method based on statistical moment of structural responses is that it is not only sensitive to local structural damage but also insensitive to measurement noise. However, the limitation is that it can only be applied when the number of measured responses is less than that of the structural stiffness, greatly restricting the application in engineering practice. Given the above, an improved temporal moment-based damage detection (TMBDD) method is proposed in this chapter. Firstly, structural incomplete acceleration responses are measured and divided into a series of time segments. Then, the temporal moments of the measured accelerations and those of the calculated accelerations are obtained respectively, and the objective error function between them is constructed. Finally, the structural stiffness can be estimated by minimizing the objective error function. The validity of the method is verified by numerical examples and experimental model respectively.

Compared with the previous work, the proposed algorithm has the following innovations: 1) The proposed algorithm only needs partial observed structural acceleration responses. Moreover, the number of measured acceleration responses is less than that of the structural stiffness. 2) This method shows a good accuracy in structural

damage diagnosis with noise resistance.

Keywords: Time-varying physical parameter identification; Partial observation; Unknown input; Wavelet transform; Kalman filter; Discrete cosine transform; Temporal moment

References

1. Amezquita-Sanchez JP, Adeli H. Signal processing techniques for vibration-based health monitoring of smart structures. *Archives of Computational Methods in Engineering*. 2016; 23(1): 1-15.
2. Wang ZC, Ren WX, Chen GD. Time-frequency analysis and applications in time-varying/nonlinear structural systems: A state-of-the-art review. *Advances in Structural Engineering*. 2018; 21: 1562-1584.
3. Ni PH, Li J, Hao H, Xia Y, Wang X, Lee JM, Jung KH. Time-varying system identification using variational mode decomposition. *Structural Control & Health Monitoring*. 2018; 25(6): e2175.
4. Lin JW, Betti R, Smyth AW, Longman RW. On-line identification of nonlinear hysteretic structural systems using a variable trace approach. *Earthquake Engineering and Structural Dynamics*. 2001; 30(9):1279-1303.
5. Askari M, Yu Y, Zhang CW, Samali B, Gu XY. Real-time tracking of structural stiffness reduction with unknown inputs, using self-adaptive recursive least-square and curvature-change techniques. *International Journal of Structural Stability and Dynamics*. 2019; 19(10):1950123.
6. Bisht SS, Singh MP. An adaptive unscented Kalman filter for tracking sudden stiffness changes. *Mechanical Systems and Signal Processing*. 2014; 49(1-2):181-195.
7. Yuen KV, Kuok SC. Online updating and uncertainty quantification using nonstationary output-only measurement. *Mechanical Systems and Signal Processing*. 2016; 66-67:62–77.

8. Yuen KV, Kuok SC, Dong L. Self-calibrating Bayesian real-time system identification. *Computer-Aided Civil and Infrastructure Engineering*. 2019; 34: 806–821.
9. Yang JN, Lin SL, Huang HW, Zhou L. An adaptive extended Kalman filter for structural damage identification. *Structural Control & Health Monitoring*. 2006; 13: 849–867.
10. Huang Q, Xu YL, Liu HJ. An efficient algorithm for simultaneous identification of time-varying structural parameters and unknown excitations of a building structure. *Engineering Structures*. 2015; 98:29–37.
11. Yang YH, Nagayama T, Xue K. Structure system estimation under seismic excitation with an adaptive extended Kalman filter. *Journal of Sound and Vibration*. 2020; 489:115690.
12. Wang N, Li L, Wang Q. Adaptive UKF-based parameter estimation for Bouc-Wen model of magnetorheological elastomer materials. *Journal of Aerospace Engineering*. 2019; 32(1): 04018130.
13. Ghanem R, Romeo F. A wavelet-based approach for the identification of linear time-varying dynamical systems. *Journal of Sound and Vibration*. 2000; 234(4):555-576.
14. Chang CC, Shi YF. Identification of time-varying hysteretic structures using wavelet multiresolution analysis. *International Journal of Non-Linear Mechanics*. 2010; 45(1): 21-34.
15. Shi YF, Chang CC. Substructural time-varying parameter identification using wavelet multiresolution approximation. *Journal of Engineering Mechanics*. 2012; 138(1):50-59.
16. Shi YF, Chang CC. Wavelet-based identification of time-varying shear-beam buildings using incomplete and noisy measurement data. *Nonlinear Engineering*. 2013; 2(1-2): 29-37.
17. Xiang M, Xiong F, Shi YF, Dai KS, Ding ZB. Wavelet multi-resolution approximation of time-varying frame structure. *Advances in Mechanical Engineering*. 2018; 10(8):1-19.
18. Wang C, Ren WX, Wang ZC, Zhu HP. Time-varying physical parameter identification of shear type structures based on discrete wavelet transform. *Smart Structures and Systems*. 2014; 14(5): 831-845.
19. Wang C, Ai DM, Ren WX. A wavelet transform and substructure algorithm for tracking the abrupt stiffness degradation of shear structure. *Advances in Structural Engineering*. 2019; 22(5): 1136-1148.

20. Chen SY, Lu JB, Lei Y, Identification of time-varying systems with partial acceleration measurements by synthesis of wavelet decomposition and Kalman filter. *Advances in Mechanical Engineering*. 2020; 12(6):168781402093046.
21. Liu LJ, Zhu JJ, Su Y, Lei Y. Improved Kalman filter with unknown inputs based on data fusion of partial acceleration and displacement measurements. *Smart Structures and Systems*. 2016; 17(6): 903-915.
22. Weng JH, Loh CH. Recursive subspace identification for on-line tracking of structural modal parameter. *Mechanical Systems and Signal Processing*. 2011; 25(8):2923-2937.
23. Yuen KV, Huang K. Identifiability-enhanced Bayesian frequency-domain substructure identification. *Computer-Aided Civil and Infrastructure Engineering*. 2018; 21(4):280-291.
24. Lei Y, Liu C, Jiang YQ, Mao YK. Substructure based structural damage detection with limited input and output measurements. *Smart Structures and Systems*. 2013; 12(6): 619-640.
25. Lei Y, Wu DT, Lin Y. A decentralized control algorithm for large-scale building structures. *Computer-Aided Civil and Infrastructure Engineering*. 2012; 27(1): 2-13.
26. Li J, Hao H. Substructure damage identification based on wavelet-domain response reconstruction. *Structural Health Monitoring*. 2014; 13(4): 389-405.
27. Li J, Law SS. Damage identification of a target substructure with moving load excitation. *Mechanical Systems and Signal Processing*. 2012; 30: 78-90.
28. Weng S, Zhu HP, Li PH, Xia Y, Ye L. Construction of orthogonal projector for the damage identification by measured substructural flexibility. *Measurement*. 2016; 88: 441-455.
29. Weng S, Zhu HP, Xia Y, Li JJ, Tian W. A review on dynamic substructuring methods for model updating and damage detection of large-scale structures. *Advances in Structural Engineering*. 2020; 23(3): 584-600.
30. Huang JS, Rao YP, Qiu H, Lei Y. Generalized algorithms for the identification of seismic ground excitations to building structures based on generalized Kalman filtering under unknown input. *Advances in Structural Engineering*. 2020; 23(5):136943322090622.
31. Quaranta G, Lacarbonara W, Masri SF. A review on computational intelligence for identification of nonlinear dynamical systems. *Nonlinear Dynamics*. 2020; 99:1709-1761.

32. Xu Y, Wei SY, Bao YQ, Li H. Automatic seismic damage identification of reinforced concrete columns from images by a region-based deep convolutional neural network. *Structural Control and Health Monitoring*. 2019; 26(3): e2313.
33. Xu B, He J, Dyke SJ. Model-free nonlinear restoring force identification for SMA dampers with double Chebyshev polynomials: approach and validation. *Nonlinear Dynamics*. 2015; 82(3):1-16.
34. Wei S, Peng ZK, Dong XJ, Zhang WM. A nonlinear subspace-prediction error method for identification of nonlinear vibrating structures. *Nonlinear Dynamics*. 2018; 91:1605-1617.
35. He J, Xu B, Masri SF. Restoring force and dynamic loadings identification for a nonlinear chain-like structure with partially unknown excitations. *Nonlinear Dynamics*. 2012; 69(1-2): 231-245.
36. Lei Y, Luo SJ, He MY. Identification of model-free structural nonlinear restoring forces using partial measurements of structural responses. *Advances in Structural Engineering*. 2016; 20(1): 69-80.
37. Xu B, Li J, Dyke SJ, Deng BC, He J. Nonparametric identification for hysteretic behavior modelled with a power series polynomial using EKF-WGI approach under limited acceleration and unknown mass. *International Journal of Non-linear Mechanics*. 2019: 103324
38. Cheng CM, Peng ZK, Zhang WM, Meng G. Volterra-series-based nonlinear system modeling and its engineering applications: a state-of-the-art review. *Mechanical Systems and Signal Processing*. 2017; 87: 340-364.
39. Qu HY, Li TT, Chen GD. Multiple analytical mode decompositions for nonlinear system identification from forced vibration. *Engineering Structures*. 2018; 173: 979-986.
40. Li H, Mao CX, Ou JP. Identification of hysteretic dynamic systems by using hybrid extended Kalman filter and wavelet multiresolution analysis with limited observation. *Journal of Engineering Mechanics*. 2013; 139(5): 547-558.
41. Ghanem R, Romeo F. A wavelet-based approach for model and parameter identification of non-linear systems. *International Journal of Non-Linear Mechanics*. 2001; 36(5): 835-859.
42. Kougioumtzoglou IA, Spanos PD. An identification approach for linear and nonlinear time-

- variant structural systems via harmonic wavelets. *Mechanical Systems & Signal Processing*. 2013; 37(1-2): 338-352.
43. Yang Y, Peng ZK, Dong XJ, Zhang WM, Meng G. Nonlinear time-varying vibration system identification using parametric time–frequency transform with spline kernel. *Nonlinear Dynamics*. 2016; 85(3): 1679-1694.
 44. Yang JN, Lin SL. On-line identification of non-linear hysteretic structures using an adaptive tracking technique. *International Journal of Non-Linear Mechanics*. 2004; 39(9): 1481–1491.
 45. Mu HQ, Kuok SC, Yuen KV. Stable robust extended Kalman filter. *Journal of Aerospace Engineering*. 2016; B4016010.
 46. Julier SJ, Uhlmann JK, Durrant-Whyte HF. A new approach for filtering nonlinear systems. *Proc. Am. Control Conf.* 1995; 3: 1628–1632.
 47. Astroza R, Alessandri A, Conte JP. Finite element model updating accounting for modeling uncertainty. *Mechanical Systems & Signal Processing*. 2019; 115(15): 782-800.
 48. Lei Y, Xia DD, Erazo K, Nagarajaiah S. A novel unscented Kalman filter for recursive state-input-system identification of nonlinear systems. *Mechanical Systems and Signal Processing*. 2019; 127(15):120-135.
 49. Jwo DJ, Yang CF, Chuang CH, Lee TY. Performance enhancement for ultra-tight GPS/INS integration using a fuzzy adaptive strong tracking unscented Kalman filter. *Nonlinear Dynamics*. 2013; 73(1-2): 377-395.
 50. Hu GG, Wang W, Zhong YM, Gao BB, Gu CF. A new direct filtering approach to INS/GNSS integration. *Aerospace Science and Technology*. 2018; 77: 755-764.
 51. Wang N, Li L, Wang Q. Adaptive UKF-based parameter estimation for Bouc-Wen model of magnetorheological elastomer materials. *Journal of Aerospace Engineering*. 2019; 32(1): 04018130.
 52. Gaviria CA, Montejo LA. Monitoring physical and dynamic properties of reinforced concrete structures during seismic excitations. *Construction and Building Materials*. 2019; 196: 43-53.
 53. Ni PH, Xia Y, Li J, Hao H. Improved decentralized structural identification with output only measurements. *Measurement*. 2018; 122: 597–610.

54. Su TL, Tang ZY, Peng LY, Bai YT, Kong JL. Model updating for real time dynamic substructures based on UKF algorithm. *Earthquake Engineering and Engineering Vibration*. 2020; 19(2): 413-421.
55. Kumar RK, Shankar K. Parametric identification of structures with nonlinearities using global and substructure approaches in the time domain. *Advances in Structural Engineering*. 2009;12(2):195-210.
56. Tao DW, Zhang DY, Li H. Structural seismic damage detection using fractal dimension of time-frequency feature. *Key Engineering Materials*. 2013; 558:554-560.
57. Lei Y, He MY, Liu C, Lin SZ. Identification of tall shear buildings under unknown seismic excitation with limited output measurements. *Advances in Structural Engineering*. 2013; 16(11):1839-1850.
58. Xin Y, Li J, Hao H. Enhanced vibration decomposition method based on multisynchrosqueezing transform and analytical mode decomposition. *Structural Control & Health Monitoring*. 2021; 28: e2730.
59. Li JT, Zhu XQ, Law SS, Samali B. Time-varying characteristics of bridges under the passage of vehicles using synchroextracting transform. *Mechanical Systems and Signal Processing*. 2020; 140:106727.1-106727.19.
60. Zhu XQ, Law SS. Recent developments in inverse problems of vehicle-bridge interaction dynamics. *Journal of Civil Structural Health Monitoring*. 2016; 6(1): 107-128.
61. Tian YD, Wang L, Zhang J. Time-varying frequency-based scaled flexibility identification of a posttensioned concrete bridge through vehicle-bridge interaction analysis. *Structural Control & Health Monitoring*. 2021; 28: e2631.
62. Silik A, Noori M, Altabey WA, Ghiasi R. Selecting optimum levels of wavelet multi-resolution analysis for time-varying signals in structural health monitoring. *Structural Control & Health Monitoring*. 2021; e2762.
63. Ahmed N, Natarajan T, Rao KR. Discrete cosine transform. *IEEE Transactions on Computers*. 1974; C-23:90-93.
64. Garcia-Hernandez JJ, Gomez-Flores W. Detection of AAC compression using MDCT-based features and supervised learning. *Journal of Experimental & Theoretical Artificial*

- Intelligence. 2021; 10:1-18.
65. Holub V, Fridrich J. Low-complexity features for JPEG steganalysis using undecimated DCT. *IEEE Transactions on Information Forensics & Security*. 2015; 10(2):219-228.
 66. Eom KB. Analysis of acoustic signatures from moving vehicles using time-varying autoregressive models. *Multidimensional Systems and Signal Processing*. 1999; 10(4):357-378.
 67. Aleardi M. Discrete cosine transform for parameter space reduction in linear and non-linear AVA inversions. *Journal of Applied Geophysics*. 2020; 179:104106.
 68. Zhang S. Study the method of under sampling flight data reconstruction based on compressive sensing. Master Thesis, Civil Aviation University of China, China, May 2015. (In Chinese)
 69. Alamdari MM, Khoa NLD, Wang Y, Samali B, Zhu XQ. A multi-way data analysis approach for structural health monitoring of a cable-stayed bridge. *Structural Health Monitoring*. 2019; 18(1):35-48.
 70. Li SL, Wei SY, Bao YQ, Li H. Condition assessment of cables by pattern recognition of vehicle-induced cable tension ratio. *Engineering Structures*. 2018; 155(15): 1-15.
 71. Kim SW, Jeon BG, Kim NS, Park JC. Vision-based monitoring system for evaluating cable tensile forces on a cable-stayed bridge. *Structural Health Monitoring*. 2013; 12(5-6): 440-456.
 72. Zhang X, Peng JY, Cao MS, Damjanovic D, Ostachowicz W. Identification of instantaneous tension of bridge cables from dynamic responses: STRICT algorithm and applications. *Mechanical Systems and Signal Processing*. 2020; 142: 106729.
 73. Li H, Ou JP. The state of the art in structural health monitoring of cable-stayed bridges. *Journal of Civil Structural Health Monitoring*. 2016; 6:43-67.
 74. Zhang LX, Qiu GY, Chen ZS. Structural health monitoring methods of cables in cable-stayed bridge: a review. *Measurement*. 2020; 168:108343.
 75. Li H, Zhang FJ, Jin YZ. Real-time identification of time-varying tension in stay cables by monitoring cable transversal acceleration. *Structural Control & Health Monitoring*. 2014; 21:1100–1117.

76. Bao YQ, Shi ZQ, Beck JL, Li H, Hou TY. Identification of time-varying cable tension forces based on adaptive sparse time-frequency analysis of cable vibrations. *Structural Control & Health Monitoring*. 2016; 24(3).
77. Bao YQ, Guo YB, Li H. A machine learning-based approach for adaptive sparse time-frequency analysis used in structural health monitoring. *Structural Health Monitoring*. 2020; 19(6): 1963–1975
78. Yang YC, Li SL, Nagarajaiah S, Li H, Zhou P. Real-time output-only identification of time-varying cable tension from accelerations via complexity pursuit. *Journal of Structural Engineering*. 2016; 142(1):1-10.
79. Xue SL, Shen RL. Real time cable force identification by short time sparse time domain algorithm with half wave. *Measurement*. 2020; 152:107355.
80. Wang C, Zhang J, Zhu HP. A combined method for time-varying parameter identification based on variational mode decomposition and generalized Morse wavelet. *International Journal of Structural Stability and Dynamics*. 2020; 10:2050077.
81. Farrar CR, Duffey TA, Doebling SW, Nix DA. A statistical pattern recognition paradigm for vibration-based structural health monitoring. *Structural & Multidisciplinary Optimization*. 2000; 41 (1):57-64.
82. Impollonia N, Failla I, Ricciardi G. Parametric statistical moment method for damage detection and health monitoring. *ASCE-ASME Journal of Risk and Uncertainty in Engineering Systems, Part A: Civil Engineering*. 2016.
83. Lei Y, Yang N, Xia DD. Probabilistic structural damage detection approaches based on structural dynamic response moments. *Smart Structures and Systems*. 2017; 20(2):207-217.
84. Sohn H, Farrar CR, Hunter NF, Worden K. Structural health monitoring using statistical pattern recognition techniques. *Journal of Dynamic Systems Measurement and Control*. 2003; 123(4):706-711.
85. Wang DS, Chen Z, Wei X, Zhu HP. Experimental investigation of damage identification in beam structures based on the strain statistical moment. *Advances in Structural Engineering*. 2016; 20(5):747-758.
86. Wang DS, Xiang W, Zhu HP. Damage identification in beam type structures based on

- statistical moment using a two-step method. *Journal of Sound and Vibration*. 2014; 333(3):745-760.
87. Wang DS, Xiang W, Zhu HP. Damage identification in a plate structure based on strain statistical moment. *Advances in Structural Engineering*. 2014; 17(11):1639-1655.
 88. Xia Y, Hao H. Statistical damage identification of structures with frequency changes. *Journal of Sound and Vibration*. 2003; 263(4):853-870.
 89. Yang Y, Li JL, Zhou CH, Law SS, Lv L. Damage detection of structures with parametric uncertainties based on fusion of statistical moments. *Journal of Sound and Vibration*. 2018; 442:200-219.
 90. Yu L, Zhu JH. Nonlinear damage detection using higher statistical moments of structural responses. *Structural Engineering and Mechanics*. 2015; 54(2):221-237.
 91. Zhang J, Xu YL, Li J. Integrated system identification and reliability evaluation of stochastic building structures. *Probabilistic Engineering Mechanics*. 2011; 26(4):528-538.
 92. Zhang J, Xu YL, Li J, Xia Y, Li JC. A new statistical moment-based structural damage detection method. *Earthquake Engineering & Engineering Vibration*. 2008; 12(1).
 93. Zhang J, Xu YL, Li J, Xia Y, Li JC. Statistical moment-based structural damage detection method in time domain. *Earthquake Engineering and Engineering Vibration*. 2013; 1291(1):1671-3664.
 94. Zhang J, Xu YL, Xia Y, Li J. Generalization of the statistical moment-based damage detection method. *Structural Engineering and Mechanics*. 2011; 38(6):715-732.
 95. Zhou P, Wang DS, Zhu HP. A novel damage indicator based on the electromechanical impedance principle for structural damage identification. *Sensors*. 2018; 18(7):2199.

ACKNOWLEDGEMENTS

I am so lucky to be the first student enrolled in the joint PhD program of Curtin University and Xiamen University. I would like to take this opportunity to express my sincere gratitude and respect to my supervisors Prof. Hong Hao and Associate Prof. Jun Li at Curtin University, and Prof. Ying Lei at Xiamen University, for their expert guidance and consistent patience. They have offered me valuable suggestions throughout my PhD study and raised me to a higher stage of research.

Secondly, I would like to thank the staff in the School of Civil and Mechanical Engineering for their friendly and kind help. I would also like to thank all members of my research centre, Centre for Infrastructure Monitoring and Protection (CIMP) for helping me from my research to personal life.

Thirdly, I would like to thank China Scholarship Council for the scholarship, and Curtin University for the CIPRS and Research Stipend Scholarship for sponsoring me for my research.

Lastly, I would like to thank my parents and husband who have shared the happiness in my golden time and unconditionally supported me when I face difficulties.

LIST OF PUBLICATIONS

Chapter 2

Lei Y, Yang N. Simultaneous identification of structural time-varying physical parameters and unknown excitations using partial measurements. *Engineering Structures*, 2020, 214:110672.

Chapter 3

Lei Y, Yang N, Li J, Hao H, Huang JS. Identification of time-varying large-scale structures by integrated sub-structural and wavelet multiresolution approach with partial measurements. *Engineering Structures*, 2021. (Under review).

Chapter 4

Yang N, Li J, Lei Y, Hao H. Identification of time-varying nonlinear structural physical parameters by integrated WMA and UKF/UKF-UI. *Nonlinear Dynamics*, 2021. DOI: 10.1007/s11071-021-06682-y. (In Press)

Chapter 5

Yang N, Lei Y, Li J, Hao H. Identification of gradually varying physical parameters based on discrete cosine transform using partial measurements. *Structural Control and Health Monitoring*, 2021. (Under review).

Chapter 6

Yang N, Luo SJ, Lei Y. Structural damage diagnosis based on the temporal moment of partially measured structural responses. *Journal of Aerospace Engineering*, 2021, 34(1): 04020106.

STATEMENT OF CONTRIBUTION OF OTHERS

The work presented in this thesis was primarily designed, numerically and experimentally conducted, and the manuscripts and thesis are written by Ning Yang. Contributions by supervisors and others are described as follows. The signed contribution forms are attached in the appendix.

Chapter 2

Prof. Ying Lei at Xiamen University helped to define the research scope and objective of this study. Prof. Ying Lei also revised and edited the manuscript, provided professional input toward data analysis and results discussion.

Chapter 3

Prof. Hong Hao, Associate Prof. Jun Li and Prof. Ying Lei revised and edited the manuscript, provided professional input toward data analysis and results discussion. Dr. Jinshan Huang helped to conduct the numerical examples.

Chapter 4

Prof. Hong Hao, Associate Prof. Jun Li and Prof. Ying Lei revised and edited the manuscript, provided intellectual ideas for data analysis and results discussion.

Chapter 5

Associate Prof. Jun Li considered the real application of the proposed methods for civil engineering, offered valuable suggestions for improving the reliability and applicability of these methods. Associate Prof. Jun Li also helped to provide test data of the cable force experiment. Prof. Hong Hao, Associate Prof. Jun Li and Prof. Ying Lei all revised and edited the manuscript.

Chapter 6

Prof. Ying Lei revised and edited the manuscript, provided intellectual ideas for data analysis and results discussion. Mrs. Sujuan Luo helped to conduct the numerical simulations and experimental test.

LIST OF RELEVANT ADDITIONAL PUBLICATIONS

- Lei Y, Yang N, Xia DD. Probabilistic structural damage detection approaches based on structural dynamic response moments. *Smart Structures and Systems*, 2017, 20(2):207-217.
- Yang N, Wang JX, Rao YP, Lei Y. Identification of unknown inputs considering structural parametric uncertainties. *International Journal of Lifecycle Performance Engineering*, 2019, 3(2):187-209.
- Lei Y, Zhang FB, Zhang YL, Yang N. Identification of distributed dynamic loading in one-spatial dimension based on combing wavelet decomposition and KF-UI. *Journal of Aerospace Engineering*, 2021, 34(4): 04021025.
- Lei Y, Qi CK, Wu JM, Huang JS, Yang N. Identification of parameters of high-rise shear-type buildings and unknown seismic excitations using sparse measurements. *Engineering Mechanics*. DOI: 10.6052/j.issn.1000-4750.2020.10.0716.

TABLE OF CONTENTS

CHAPTER 1 ABSTRACT	1
ACKNOWLEDGEMENTS	30
LIST OF PUBLICATIONS	31
STATEMENT OF CONTRIBUTION OF OTHERS	32
LIST OF RELEVANT ADDITIONAL PUBLICATIONS.....	33
TABLE OF CONTENTS	34
CHAPTER 2 Simultaneous identification of structural time-varying physical parameters and unknown excitations using partial measurements	35
CHAPTER 3 Identification of time-varying large-scale structures by integrated sub-structural and wavelet multiresolution approach with partial measurements	68
CHAPTER 4 Identification of time-varying nonlinear structural physical parameters by integrated WMA and UKF/UKF-UI	109
CHAPTER 5 Identification of gradually varying physical parameters based on discrete cosine transform using partial measurements.....	153
CHAPTER 6 Structural damage diagnosis based on the temporal moment of partially measured structural responses	197
APPENDIX I.....	217
APPENDIX II	222
BIBLIOGRAPHY DISCLAIMER.....	227

CHAPTER 2 Simultaneous identification of structural time-varying physical parameters and unknown excitations using partial measurements

ABSTRACT

Structural systems often exhibit time-varying dynamic characteristics during their service life due to serve hazards and/or environmental erosion. Therefore, the identification of time-varying structural systems is important. So far, methods based on wavelet multiresolution (WM) analysis have been proposed for the identification of structural time-varying physical parameters. However, full information on both complete structural responses and external excitations were requested in previous approaches, which greatly restricts their applications in practice. To overcome this severe limitation, an algorithm is proposed in this paper for simultaneous identification of structural time-varying physical parameters and unknown external excitations using only partially measured structural responses. The proposed algorithm is based on the integration of WM analysis and the Kalman filter with unknown input (KF-UI) algorithm recently developed by the authors. Firstly, structural time-varying physical parameters are decomposed by WM expansion, transforming the identification task into time-invariant scale coefficients estimation. Then, the KF-UI algorithm is used for simultaneous identification of structural state and unknown excitations using partially measured structural responses. Finally, the scale coefficients are estimated by nonlinear least-squares optimization and the original time-varying physical parameters are re-constructed. Numerical simulations and an experimental test are conducted to validate the proposed algorithm.

This chapter was published in *Engineering Structures* with the full bibliographic citation as follows: Lei Y, Yang N. Simultaneous identification of structural time-varying physical parameters and unknown excitations using partial measurements. *Engineering Structures*, 2020, 214:110672.

1. Introduction

Structural system identification is an important issue and has received great attention [1]. So far, the identification of time-invariant structural systems has been widely investigated and various vibration-based techniques have been developed [2-3]. However, structures usually exhibit time-varying behavior in their service process due to severe hazards (e.g. strong seismic and wind loads) and complex internal degradation. It is more suitable to adopt time-varying models for dynamic behavior description and life-cycle management than the time-invariant models. Therefore, it is essential to investigate the identification of structural time-varying physical parameters.

Generally, the currently existing identification methods for time-varying structural systems can be categorized into time-domain and time-frequency-domain classifications. Time-domain identification methods mainly include the time series-based methods [4-5] and the state-space model-based methods [6-10]. For example, the time-varying autoregressive moving average model (TV-ARMA) has been proposed as a time series-based method to recognize the time-varying modal parameters such as frequency and damping ratio [5]. Simultaneously, many identification methods have been presented based on state-space models. For example, empirical approaches based on the track factor [6] or adaptive correction factor [7] have been developed, and the adaptive factor matrix has been proposed to track arbitrary changes in structural parameters [8]. However, updating the adaptive factor matrix by optimization at each time instant is computational inefficiency. Moreover, the Bayesian-based method by online updating noise covariance matrix has been presented to treat time-varying systems [9-10]. Time-frequency domain methods mainly focus on the Hilbert transform (HT) and the wavelet-based methods [11], e.g., the empirical mode decomposition (EMD) based HT [12-14], the variational mode decomposition (VMD) based HT [15], and the analytical mode decompositions (AMD) based HT [16-19] have been developed for estimating time-varying parameters of linear and nonlinear structural systems.

Wavelet transform (WT) is another widely used time-frequency analysis tool for time-varying signal processing and structural damage detection [20-23] as it reveals the detail and approximation information by multiresolution analysis. In particular, some methodologies based on wavelet multiresolution (WM) analysis have been proposed to identify structural time-varying physical parameters [24-30]. These methods can be mainly divided into two categories: one is expanding the response signals by WM and capturing the time-varying characteristics by least-squares with a sliding window [25] or the state-space method [26], and the other one is transforming the time-varying stiffness and damping parameters into wavelet coefficients, then identify them by the least-squares estimation [27-30]. Although satisfactory identification results for structural time-varying physical parameters have been obtained by these methods, full measurements of structural responses (including acceleration, velocity, and displacement) and external excitations are requested in these methodologies, which greatly restricts their applications in practice.

On the other hand, the Kalman filter (KF) [31] has been widely utilized for structural state estimation using only partially observed structural responses. However, in the classical KF approach, external excitation information is needed [31-32]. Although some KF based methods have been developed to identify the unknown input before, improvements are still needed as their derivation processes were relatively complicated, and most importantly, severe ‘drift’ phenomenon existed in the identification results by these previous methods [33-34]. Recently, a data fusion based Kalman filter with unknown inputs (KF-UI) algorithm has been proposed by the authors to identify structural state and unknown excitations simultaneously [35], which is directly derived according to the KF framework to make the derivation process much clearer and simpler, and the ‘drift’ phenomenon is avoided by the data fusion of accelerations and displacements. However, this KF-UI cannot be directly adopted to identify structural time-varying physical parameters.

In view of the above-mentioned literature, current structural time-varying physical parameters identification methods based on WM analysis need full measurements of structural

acceleration, velocity and displacement responses together with the external excitation information, which greatly restricts their applications in practice. Inspired by the merits of both the recently proposed data fusing based KF-UI and the WM analysis, this paper aims to overcome the limitations of previous WM-based methods for the identification of time-varying physical parameters. An algorithm is proposed by integrating the WM analysis and the data fusion based KF-UI to identify structural time-varying systems and the unknown excitations using only partially measured structural responses. In the proposed algorithm, structural mass is assumed time-invariant and known while structural stiffness and damping parameters are time-varying and unknown, the structure is subjected to unknown excitation, and only partial measurements of structure responses are observed. The WM analysis is utilized to expand the structural time-varying physical parameters at a multi-scale profile, which transforms the time-varying physical parameter identification into equivalent time-invariant scale coefficient estimation. To overcome the previously mentioned limitation on requiring full measurements of structural responses and external excitations, the advantage of the data fusion based KF-UI is adopted to identify structural state using only partial measurements of structural responses. Finally, the scale coefficients of WM analysis are estimated by the nonlinear least-squares optimization, and structural time-varying physical parameters and the unknown external loads are also identified accordingly. The effect of noise can be minimized based on the noise immunity of the KF-UI. Three numerical examples including the various scenarios of time-varying structural physical parameters in a 3-story shear frame, a simply supported beam, and a plane frame, respectively are used to test the efficiency of the proposed algorithm. Furthermore, experimental data of a three-story time-varying frame from the Research Center of Earthquake Engineering in Taipei [36] are utilized to validate the proposed algorithm.

The main contributions of this paper list as follows. (i) Propose a simultaneous identification algorithm for structural time-varying parameters and unknown external excitations using only partial measurements instead of full measurements of structural responses at all DOFs; (ii) Consider the unknown excitations to the time-varying structures and identify the unknown

excitations simultaneously; (iii) Minimize the effect of measurements noise due to the fact that KF-UI approach itself can include the influences of modeling error and measurements noise.

The remaining part of the paper is organized as: In section 2, the details of the proposed algorithm are presented. In section 3, three numerical examples including various scenarios of structural time-varying physical parameters in different types of models are utilized to test the performance of the proposed algorithm. In section 4, an experimental test of a three-story time-varying frame is utilized to further validate the proposed algorithm. Finally, some conclusions with further research issues are presented in the conclusion part.

2. The proposed identification algorithm

The wavelet multiresolution (WM) analysis is used to expand structural time-varying physical parameters in the process of the proposed method for system identification.

2.1. Wavelet multiresolution expansion

The WM analysis can expand a signal into approximate and detailed parts at multi-scale levels. For any continuous signal $f(t)$ with finite energy, it can be orthogonally expanded as [27-30]:

$$f(t) = \sum_{l=-\infty}^{\infty} c_{J,l} \phi_{J,l}(t) + \sum_{j=J}^{\infty} \sum_{l=-\infty}^{\infty} d_{j,l} \varphi_{j,l}(t) \quad (1)$$

where $\phi_{J,l}(t) = 2^{J/2} \phi(2^J t - l)$ and $\varphi_{j,l}(t) = 2^{j/2} \varphi(2^j t - l)$ are the scale function and the mother wavelet function, respectively, $c_{J,l}$ is the scale coefficient at the level J , and $d_{j,l}$ is the detail or wavelet coefficient at the level j . For a discrete signal $f(t_n)$ sampled with N_t number of points, the discrete form of Eq. (1) can be written as:

$$f(t_n) = \sum_l c_{J,l} \phi_{J,l}(2^J n - l) + \sum_{j=1}^J \sum_l d_{j,l} \varphi_{j,l}(2^j n - l), \quad n = 1, 2, 3, \dots, Nt \quad (2)$$

Usually, the energy of the signal mainly concentrates on the low-frequency components. The discrete signal $f(t_n)$ can be represented by a cut-down WM expansion up to the scale level J , i.e., $f(t_n)$ is approximated as [27]:

$$f(t_n) \approx \sum_l c_{J,l} \phi_{J,l}(2^J n - l), \quad n = 1, 2, 3, \dots, Nt \quad (3)$$

In this paper, structural stiffness and damping are time-varying and unknown. By expanding the stiffness and viscous damping coefficients according to Eq. (3), Eq. (4) can be derived as [27-30]:

$$k_i(t_n) \approx \sum_{l_i^k} k_{J_i^k, l_i^k} \phi_{J_i^k, l_i^k}^k(2^{J_i^k} n - l_i^k); c_i(t_n) \approx \sum_{l_i^c} c_{J_i^c, l_i^c} \phi_{J_i^c, l_i^c}^c(2^{J_i^c} n - l_i^c), \quad n = 1, 2, 3, \dots, Nt \quad (4)$$

in which, $k_i(t_n)$ and $c_i(t_n)$ represent the i -th stiffness and damping parameter at time t_n , respectively, $k_{J_i^k, l_i^k}$ is the corresponding decomposed scale coefficient for stiffness k_i at the J_i^k resolution scale, and $c_{J_i^c, l_i^c}$ is the damping scale coefficient at the J_i^c resolution scale, l_i^k and l_i^c are the numbers of scale coefficients for the parameters k_i and c_i , respectively. If the scale coefficient $k_{J_i^k, l_i^k}$ and $c_{J_i^c, l_i^c}$ are estimated, the time-varying physical parameter $k_i(t_n)$ and $c_i(t_n)$ can be reconstructed through Eq. (4). Therefore, the task of identifying time-varying structural physical parameters is converted to the identification of time-invariant scale coefficients based on the WM expansion.

2.2 Previous identification based on wavelet multiresolution expansion

The governing equation of a multi degrees-of-freedom (MDOFs) linear time-varying structural system is described by:

$$\mathbf{M}\ddot{\mathbf{x}}(t) + \mathbf{C}(t)\dot{\mathbf{x}}(t) + \mathbf{K}(t)\mathbf{x}(t) = \boldsymbol{\eta}f(t) \quad (5)$$

where $\mathbf{x}(t)$, $\dot{\mathbf{x}}(t)$ and $\ddot{\mathbf{x}}(t)$ are the vector of structural displacement, velocity, and acceleration response time history, respectively. \mathbf{M} represents the structural mass matrix which is assumed to be time-invariant with a known value. $\mathbf{K}(t)$ and $\mathbf{C}(t)$ denote the stiffness and damping matrix with time-varying parameters, respectively. $\mathbf{f}(t)$ is an external excitation vector with the influence matrix $\boldsymbol{\eta}$. When the sampling time is $n=1, 2, \dots, Nt$, the corresponding discrete format for Eq.(5) is:

$$\mathbf{M}\ddot{\mathbf{x}}(t_n) + \mathbf{C}(t_n)\dot{\mathbf{x}}(t_n) + \mathbf{K}(t_n)\mathbf{x}(t_n) = \boldsymbol{\eta}\mathbf{f}(t_n) \quad (6)$$

In previous approaches based on WM analysis for the identification of time-varying physical parameters, the preconditions are that the full responses of structural displacement, velocity, and acceleration are observed, and the external excitation $\mathbf{f}(t)$ is assumed known. Under these prerequisites, by substituting the expansion of stiffness and damping parameters in Eq. (4) into Eq. (6), Eq. (6) can be re-written as:

$$\boldsymbol{\Theta}\boldsymbol{\theta} = \mathbf{Y} \quad (7)$$

in which

$$\boldsymbol{\Theta} = \mathbf{Q}\mathbf{W}$$

$$\boldsymbol{\theta} = [c_{J_1^s, J_1^s}, \dots, c_{J_1^s, J_1^s}, k_{J_1^k, J_1^k}, \dots, k_{J_1^k, J_1^k}]^T; \mathbf{Y} = [\boldsymbol{\eta}\mathbf{f}(t_1) - \mathbf{M}\ddot{\mathbf{x}}(t_1), \boldsymbol{\eta}\mathbf{f}(t_2) - \mathbf{M}\ddot{\mathbf{x}}(t_2), \dots, \boldsymbol{\eta}\mathbf{f}(t_{N_t}) - \mathbf{M}\ddot{\mathbf{x}}(t_{N_t})]^T \quad (8)$$

in which \mathbf{W} is the corresponding WM matrix contains the wavelet scale functions in Eq.(4), and the matrix \mathbf{Q} is related to the measured structural displacement, velocity responses at all DOFs, which is specified as shown in Eq. (9).

$$\mathbf{Q} = \begin{bmatrix} \boldsymbol{\psi}[t_1] & 0 & \dots & 0 \\ 0 & \boldsymbol{\psi}[t_2] & \dots & 0 \\ \vdots & \vdots & \ddots & \vdots \\ 0 & 0 & \dots & \boldsymbol{\psi}[t_{N_t}] \end{bmatrix}, \boldsymbol{\psi}[t_{N_t}] = [\dot{\mathbf{x}}(t_{N_t}) \quad \mathbf{x}(t_{N_t})] \quad (9)$$

If all structural responses are measured, it's obvious that the matrix Θ is known because it's constituted by the measured structural displacement, velocity, and the wavelet scale functions. The output matrix Y is also known because the mass matrix, acceleration, and the external excitation are all preset information. The vector θ is unknown as it contains the unknown wavelet scale coefficients from the expansion of stiffness and damping parameters in Eq. (4). Then, the unknown stiffness and damping scale coefficients can be obtained from Eq. (7) by the linear least-squares estimation. More detailed derivation of the previous identification method based on WM expansion refers to [27-30].

However, requiring full measurements of all structural responses is impractical. Also, it is often difficult to obtain accurate excitation information. Herein, an improved identification algorithm to overcome these limitations is studied. It is based on the integration of WM expansion of time-varying stiffness and damping parameters and the data fusing based KF-UI recently developed by the authors [35] with limited measurements of structural responses.

2.3 Identify structural state and excitation by KF-UI with given scale coefficients

When the above linear time-varying structural system is subjected to unknown external excitations, its governing equation can be re-written as:

$$M\ddot{x}(t) + C(t)\dot{x}(t) + K(t)x(t) = \eta^u f^u(t) \quad (10)$$

where $f^u(t)$ is the unknown input vector with the influence matrix η^u . With the given wavelet scale coefficients for the time-varying stiffness and damping parameters, structural physical parameters can be reconstructed through Eq. (4). The data fusing based KF-UI proposed by the authors is utilized herein for the identification of structural system under unknown inputs.

Eq. (8) can be transformed into the system state equation. Describe the state equation in the discrete form based on the zero-order holder (ZOH) discretization:

$$X_{k+1} = A_k X_k + B_k f_k^u + w_k \quad (11)$$

where \mathbf{x}_k is the system state vector at time $t = k\Delta t$, \mathbf{A}_k is the state transfer matrix, \mathbf{B}_k is the influence matrix of the unknown input vector \mathbf{f}_k^u , and \mathbf{w}_k is the modeling error assumed as a Gaussian white noise vector with zero mean and a covariance matrix \mathbf{Q}_k .

Given partial structural responses, the discrete observation equations can be expressed as:

$$\mathbf{y}_{k+1} = \mathbf{H}_{k+1} \mathbf{x}_{k+1} + \mathbf{D}_{k+1} \mathbf{f}_{k+1}^u + \mathbf{v}_{k+1} \quad (12)$$

where \mathbf{y}_{k+1} is the measured response vector at time $t = (k+1)\Delta t$, \mathbf{H}_{k+1} and \mathbf{D}_{k+1} are measurement matrices associated with structural state and external force vectors, respectively, and \mathbf{v}_{k+1} is the measurement noise vector, which is also assumed as a Gaussian white noise vector with zero mean and a covariance matrix \mathbf{R}_{k+1} .

The proposed KF-UI contains two procedures [35]. First, $\tilde{\mathbf{x}}_{k+1|k}$ is predicted as:

$$\tilde{\mathbf{x}}_{k+1|k} = \mathbf{A}_k \hat{\mathbf{x}}_{k|k} + \mathbf{B}_k \hat{\mathbf{f}}_{k|k}^u \quad (13)$$

where $\tilde{\mathbf{x}}_{k+1|k}$, $\hat{\mathbf{x}}_{k|k}$, and $\hat{\mathbf{f}}_{k|k}^u$ denote the predicted \mathbf{x}_{k+1} , estimated \mathbf{x}_k , and \mathbf{f}^u at time $t = k\Delta t$, respectively.

Then, the estimated $\hat{\mathbf{x}}_{k+1}$ in the measurement update procedure is derived as: [35]

$$\hat{\mathbf{x}}_{k+1|k+1} = \tilde{\mathbf{x}}_{k+1|k} + \mathbf{K}_{k+1} (\mathbf{y}_{k+1} - \mathbf{H}_{k+1} \tilde{\mathbf{x}}_{k+1|k} - \mathbf{D}_{k+1} \hat{\mathbf{f}}_{k+1|k+1}^u) \quad (14)$$

where $\hat{\mathbf{x}}_{k+1|k+1}$ and $\hat{\mathbf{f}}_{k+1|k+1}^u$ denote the estimated \mathbf{x}_{k+1} and \mathbf{f}_{k+1}^u given the observations $\mathbf{y}_1, \mathbf{y}_2, \dots, \mathbf{y}_{k+1}$, respectively, \mathbf{K}_{k+1} is the Kalman gain matrix which can be derived as: [35]

$$\mathbf{K}_{k+1} = \tilde{\mathbf{P}}_{k+1|k} \mathbf{H}_{k+1}^T (\mathbf{H}_{k+1} \tilde{\mathbf{P}}_{k+1|k} \mathbf{H}_{k+1}^T + \mathbf{R}_{k+1})^{-1} \quad (15)$$

in which $\tilde{\mathbf{P}}_{k+1|k}$ is the error covariance of the predicted $\tilde{\mathbf{x}}_{k+1|k}$.

If the number of measured responses is no less than that of the unknown inputs, $\hat{\mathbf{f}}_{k+1|k+1}^u$ can be obtained by the least-squares estimation as: [35]

$$\hat{\mathbf{f}}_{k+1|k+1}^u = \mathbf{S}_{k+1} \mathbf{D}_{k+1}^T \mathbf{R}_{k+1}^{-1} (\mathbf{I} - \mathbf{H}_{k+1} \mathbf{K}_{k+1}) (\mathbf{y}_{k+1} - \mathbf{H}_{k+1} \hat{\mathbf{x}}_{k+1|k+1}) \quad (16)$$

where \mathbf{I} denotes a unit matrix, and $\mathbf{S}_{k+1} = [\mathbf{D}_{k+1}^T \mathbf{R}_{k+1}^{-1} (\mathbf{I} - \mathbf{H}_{k+1} \mathbf{K}_{k+1}) \mathbf{D}_{k+1}]^{-1}$.

Also, the error covariance matrices are expressed as: [35]

$$\hat{\mathbf{P}}_{k+1|k+1}^X = (\mathbf{I} + \mathbf{K}_{k+1} \mathbf{D}_{k+1} \mathbf{S}_{k+1} \mathbf{D}_{k+1}^T \mathbf{R}_{k+1}^{-1} \mathbf{H}_{k+1}^T) (\mathbf{I} - \mathbf{K}_{k+1} \mathbf{H}_{k+1}) \tilde{\mathbf{P}}_{k+1|k}^X \quad (17)$$

$$\hat{\mathbf{P}}_{k+1|k+1}^f = \mathbf{S}_{k+1} \quad (18)$$

$$\hat{\mathbf{P}}_{k+1|k+1}^{Xf} = (\hat{\mathbf{P}}_{k+1|k+1}^{fX})^T = -\mathbf{K}_{k+1} \mathbf{D}_{k+1} \mathbf{S}_{k+1} \quad (19)$$

Moreover, the drift problem in the identification results by previous identification approaches can be effectively overcome by the data fusion of acceleration and displacement measurements in the proposed KF-UI [35]. Thus, the observation equation in Eq. (12) can be expressed as:

$$\mathbf{Y}_{k+1} = \begin{Bmatrix} \mathbf{Y}_{k+1}^a \\ \mathbf{Y}_{k+1}^d \end{Bmatrix} = \begin{bmatrix} \mathbf{E}_{k+1}^a & \mathbf{F}_{k+1}^a \\ \mathbf{L}_s & \mathbf{0} \end{bmatrix} \begin{Bmatrix} \mathbf{x}_{k+1} \\ \dot{\mathbf{x}}_{k+1} \end{Bmatrix} + \begin{Bmatrix} \mathbf{G}_{k+1} \\ \mathbf{0} \end{Bmatrix} \mathbf{f}_{k+1}^u + \mathbf{v}_{k+1} = \mathbf{H}_{k+1} \mathbf{X}_{k+1} + \mathbf{D}_{k+1} \mathbf{f}_{k+1}^u + \mathbf{v}_{k+1} \quad (20)$$

where \mathbf{E}_{k+1}^a and \mathbf{F}_{k+1}^a are matrices related to observed accelerations, \mathbf{L}_s represents the location of displacement sensors, and \mathbf{G}_{k+1} denotes the influence matrix of unknown inputs on the acceleration responses [35].

2.4 Scale coefficient estimation by nonlinear optimization

In the above identification procedures, the identified structural state vector and the unknown excitation depend on the values of wavelet scale coefficients $k_{J_i^k, l_i^k}$ and $c_{J_i^c, l_i^c}$ in the WM expansion of structural stiffness and damping parameters by Eq.(4). Then, structural acceleration responses can be estimated by the following formula as:

$$\hat{\mathbf{x}} = \mathbf{M}^{-1} (\boldsymbol{\eta}^u \hat{\mathbf{f}}^u - \mathbf{K} \hat{\mathbf{x}} - \mathbf{C} \dot{\hat{\mathbf{x}}}) \quad (21)$$

Therefore, the estimated acceleration vector $\hat{\mathbf{x}}$ is also an implicit function of the scale coefficients which can be expressed as $\hat{\mathbf{x}} = \hat{\mathbf{x}}(\mathbf{k}_{J_i^k, l_i^k}, \mathbf{c}_{J_i^c, l_i^c})$, in which $\mathbf{k}_{J_i^k, l_i^k}$ and $\mathbf{c}_{J_i^c, l_i^c}$ denote the scale coefficient vector of $k_{J_i^k, l_i^k}$ and $c_{J_i^c, l_i^c}$, respectively.

Finally, the scale coefficient vector \mathbf{k}_{J^k, I^k} and \mathbf{c}_{J^c, I^c} can be estimated through a nonlinear optimization problem by minimizing the following objective function as:

$$\Delta(\mathbf{k}_{J^k, I^k}, \mathbf{c}_{J^c, I^c}) = \left\| \left(\ddot{\mathbf{x}}_m - \mathbf{H}_a \hat{\mathbf{x}}(\mathbf{k}_{J^k, I^k}, \mathbf{c}_{J^c, I^c}) \right) \right\|_2^2 \quad (22)$$

where \mathbf{H}_a denotes the located matrix of partial acceleration measurement $\ddot{\mathbf{x}}_m$. By solving the above optimization problem, the optimal \mathbf{k}_{J^k, I^k} and \mathbf{c}_{J^c, I^c} could be obtained. Afterward, structural time-varying stiffness and damping parameters can be reconstructed through Eq. (4).

Herein, the command ‘lsqnonlin’ with Levenberg-Marquardt (LM) algorithm in MATLAB is applied to solve the nonlinear least-squares problem. The default stopping criterion of the LM algorithm in MATLAB is used. The initial values of scale coefficients play a critical role in the nonlinear least-squares estimation. Considering that the change of structural parameters is caused by an external load, it is less possible for the structural parameters to have a sudden change or gradual change in the initial stage of vibration in practice. Therefore, in the initial stage, that is, when the physical parameters are time-invariant, the EKF-UI method can be used to estimate the unknown physical parameters and set them as the initial values of time-varying structural parameters. The EKF-UI method can identify the unknown time-invariant physical parameters by limited measurements when the excitation is unknown. Such a method is also proposed by the authors and has been published before [37]. Then the initial values of scale coefficients can be calculated by the estimated initial physical parameters based on the WM transformation.

Besides, particular attention should be paid to the selection of wavelet scale function and resolution scale. On one hand, the number of coefficients that need to be optimized is greatly increased with a small resolution scale. It is more likely that the optimization problem in Eq. (22) cannot get the global optimal solution, and over-fine fitting of time-varying physical parameters will also amplify the influence of high-frequency noise, so the decomposition level is not recommended to be too small. On the other hand, too many high-order energies and details in signals will be lost when the resolution level is too high, which will lead to lower accuracy of physical parameter identification. Therefore, the choice of wavelet scale function and resolution

scale is an important issue. Usually, the DbN wavelet has been widely used in time-varying physical parameter identification because of its superior orthogonal properties and compact support characteristics. Chang and Shi [29] suggested that the Db1 wavelet is appropriate for abrupt change. Herein, the Db1 wavelet is chosen as the scale function for the abrupt change of structural physical parameters while Db3 is adopted for the gradual change of physical parameters. Concerning the selection of the resolution scale, the orthogonal forward regression (OFR) algorithm [29-30] is used to determine a suitable resolution scale and reduce the number of the estimated wavelet coefficients. It is well known that selecting the most appropriate scale function and resolution scale is still a challenging problem in the wavelet analysis and further investigations are needed in the follow-up research.

2.5 Summary of the proposed identification procedures

Fig.1 shows the flowchart of the proposed identification procedure.

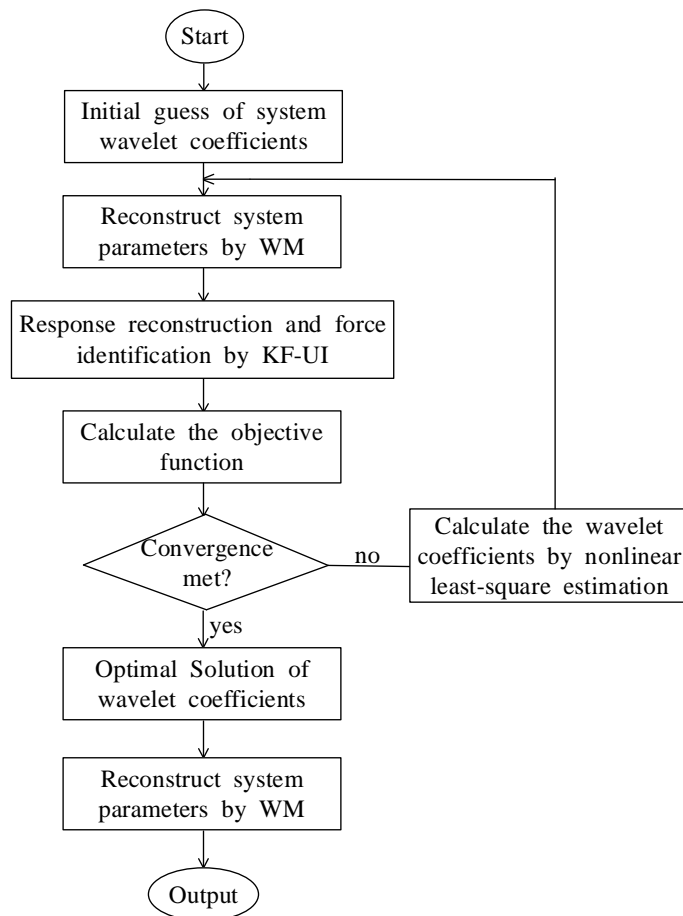


Fig. 1. Procedure of the simultaneous identification algorithm

In summary, the proposed identification algorithm contains the following main procedures:

(1) Based on the WM expansion, the time-varying structural physical parameters are approximately expressed by a truncated WM analysis in the discrete form with the resolution level J and unknown wavelet scale coefficients as shown in Eq. (4). Then, the identification task is transformed into estimating time-invariant coefficients in WM analysis.

(2) With given wavelet scale coefficients, structural full responses at all DOFs together with the unknown excitation can be estimated by the data fusion based KF-UI using partially measured structural responses through Eqs.(10)-(20). The identified structural responses and unknown external excitations are implicit functions of the wavelet scale coefficients.

(3) The unknown wavelet scale coefficients are estimated by solving a nonlinear optimization problem with the objective function shown in Eq. (22) using the nonlinear least-squares estimation.

(4) With the estimated wavelet scale coefficients, structural time-varying physical parameters can be reconstructed by Eq. (4), and structural external excitations can also be identified simultaneously.

3. Numerical example validations

In this paper, three numerical examples for the identification of various time-varying structural physical parameters in different types of structural models are used to validate the proposed algorithm.

3.1 Example 1: A 3-story time-varying shear frame under unknown seismic excitation

A numerical example is given to recognize the time-varying stiffness and damping coefficient of a three-story shear frame under unknown seismic excitation. The mass of the frame is assumed to be known with $m_1 = m_2 = m_3 = 2500\text{kg}$. The sampling frequency is 50Hz and the sampling time is 10s, thus there are 1503 stiffness parameters and 1503 damping parameters to be identified in total. Only two accelerometers are deployed on the 1st and 3rd floors, respectively. To avoid the drifts in the identification results, the displacement response at the 1st floor is also

measured. To consider the influence of measurement noise, all the measured structural responses are polluted by white noise with 1% in root mean square (RMS). The frame is stimulated by the EL-Centro earthquake excitation. The three-story time-varying shear frame model is shown in Fig.2.

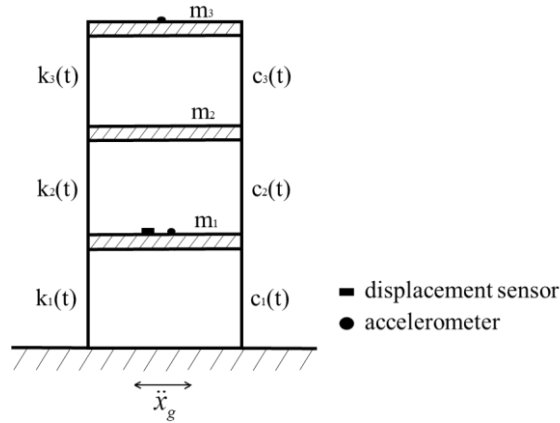


Fig. 2. Three-story time-varying shear frame model

Three different scenarios of time-varying structural physical parameters are simulated in this example. Case I: multi abruptly varying stiffness and time-invariant damping parameters; Case II: both time-varying stiffness and damping parameters; Case III: gradually varying and abruptly varying stiffness parameters with time-invariant damping parameters.

3.1.1 Case I: multi abruptly varying stiffness and time-invariant damping parameters

In this case, it is assumed that sudden reduction occurs on the structural stiffness parameters k_1 and k_3 respectively, while parameters k_2 and c_i ($i=1,2,3$) remain constant. The changes in the physical parameters are specified as shown in Eq. (23). Herein, Db1 is adopted as the scale function for abruptly varying case [29] and scale level $J=7$ is used to expand the abruptly varying stiffness and invariant damping parameters. Thus, there are totally 24 unknown scale coefficients to be optimized in the nonlinear least-squares estimation.

$$\begin{aligned}
k_1 &= \begin{cases} 250 \text{ kN/m}, & 0 \leq t < 5.2 \text{ s} \\ 200 \text{ kN/m}, & 5.2 \leq t \leq 10 \text{ s} \end{cases} \\
k_2 &= 200 \text{ kN/m}, \quad 0 \leq t \leq 10 \text{ s} \\
k_3 &= \begin{cases} 180 \text{ kN/m}, & 0 \leq t < 7.6 \text{ s} \\ 140 \text{ kN/m}, & 7.6 \leq t \leq 10 \text{ s} \end{cases} \\
c_1 = c_2 = c_3 &= 2.5 \text{ kN} \cdot \text{s/m}, \quad 0 \leq t \leq 10 \text{ s}
\end{aligned} \tag{23}$$

Figs.3-4 show the identified time-varying or time-invariant structural stiffness and damping parameters with comparison to their exact values, respectively. It is illustrated that the proposed algorithm can accurately track the abrupt change of structural stiffness parameters.

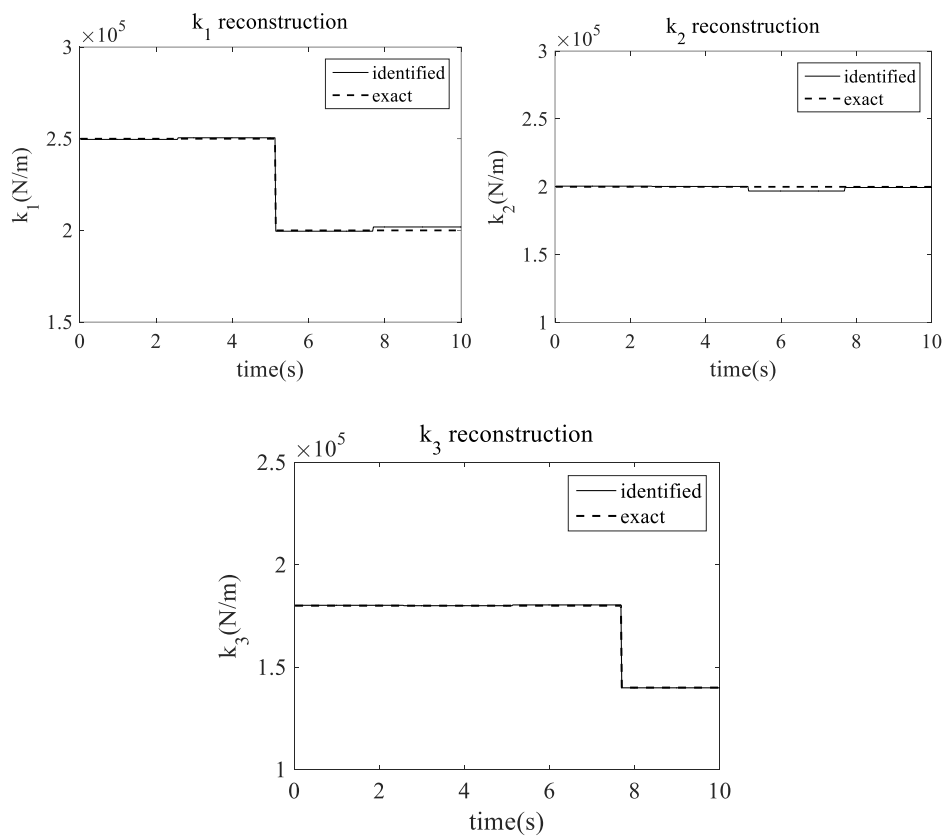


Fig. 3. Identified time-varying stiffness of the 3-story shear frame in case I

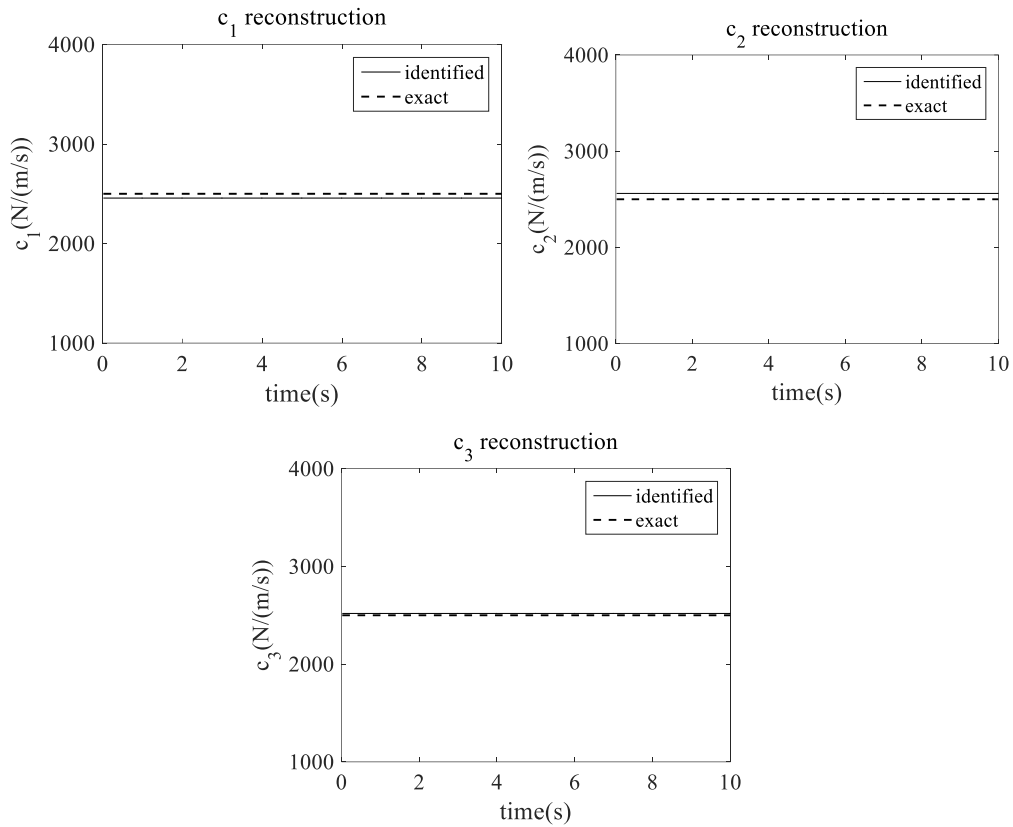


Fig. 4. Identified damping of the 3-story shear frame in case I

Based on the proposed algorithm, all unmeasured structural responses can be identified. Some identified structural displacement and velocity responses are compared with their exact values in Fig.5. It is noted that the identified structural responses are in agreement with their exact values.

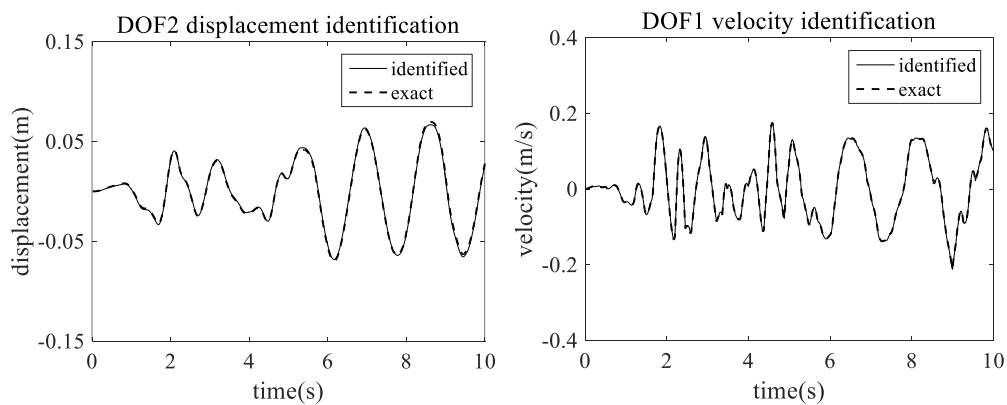


Fig. 5. Identified displacement and velocity of the 3-story shear frame in case I

Moreover, the identified earthquake acceleration agrees with the exact one, as shown in Fig.

6.

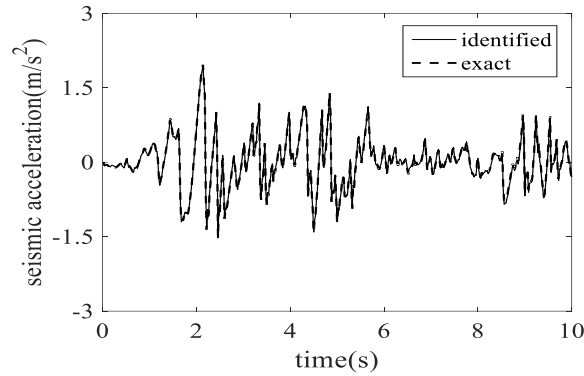


Fig.6. Identified seismic acceleration to the 3-story shear frame in case I

3.1.2. Case II: both time-varying stiffness and damping parameters

Different from the case I, the damping parameters are also time-varying in case II. It is assumed c_1 and c_3 suddenly increase according to Eq. (24), while other stiffness and damping parameters are consistent with those in case I. The number of the unknown scale coefficients is the same with that in case I.

$$\begin{aligned}
 k_1 &= \begin{cases} 250 \text{ kN/m}, & 0 \leq t < 5.2 \text{ s} \\ 200 \text{ kN/m}, & 5.2 \text{ s} \leq t \leq 10 \text{ s} \end{cases} & c_1 &= \begin{cases} 2.5 \text{ kN}\cdot\text{s/m}, & 0 \leq t < 5.2 \text{ s} \\ 3.0 \text{ kN}\cdot\text{s/m}, & 5.2 \text{ s} \leq t \leq 10 \text{ s} \end{cases} \\
 k_2 &= 200 \text{ kN/m}, & 0 \leq t \leq 10 \text{ s} & c_2 &= 2.5 \text{ kN}\cdot\text{s/m}, & 0 \leq t \leq 10 \text{ s} \\
 k_3 &= \begin{cases} 180 \text{ kN/m}, & 0 \leq t < 7.6 \text{ s} \\ 140 \text{ kN/m}, & 7.6 \text{ s} \leq t \leq 10 \text{ s} \end{cases} & c_3 &= \begin{cases} 2.5 \text{ kN}\cdot\text{s/m}, & 0 \leq t < 7.6 \text{ s} \\ 2.8 \text{ kN}\cdot\text{s/m}, & 7.6 \text{ s} \leq t \leq 10 \text{ s} \end{cases}
 \end{aligned} \quad (24)$$

From Fig.7, it is noted that the identified time-varying stiffness parameters are in good agreement with the exact values. The identified time-varying damping parameters are not so accurate as shown in Fig. 8, but it is well known that it is hard to accurately identify damping parameters. Although the changing time can be tracked, the recognition errors are larger than those of stiffness parameters because the damping coefficients orders are much smaller than those of stiffness parameters. The identification of damping coefficients is more sensitive to noise [27].

As indicated in Fig.9, the identified earthquake ground acceleration is entirely precise in this case.

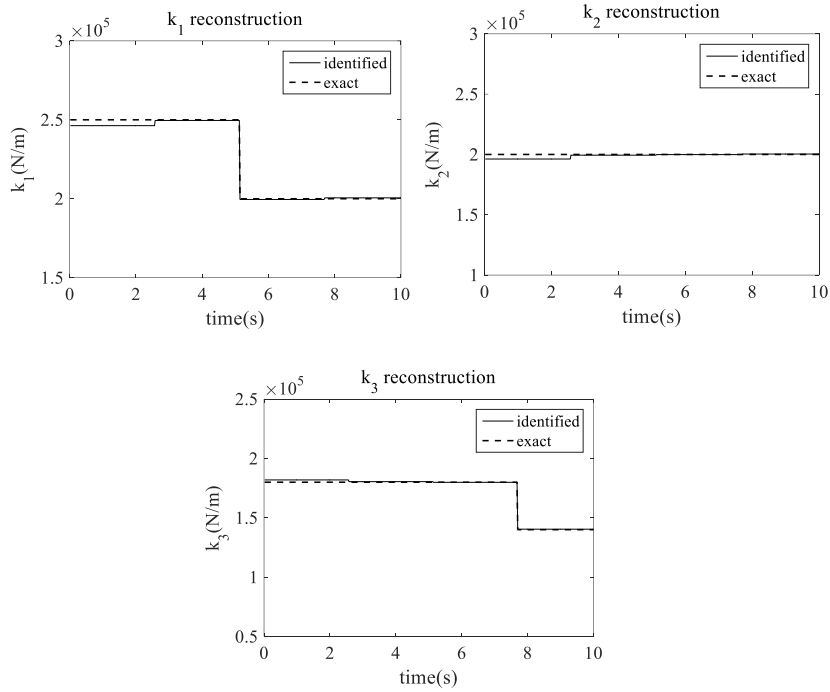


Fig. 7. Identified time-varying stiffness of the 3-story shear frame in case II

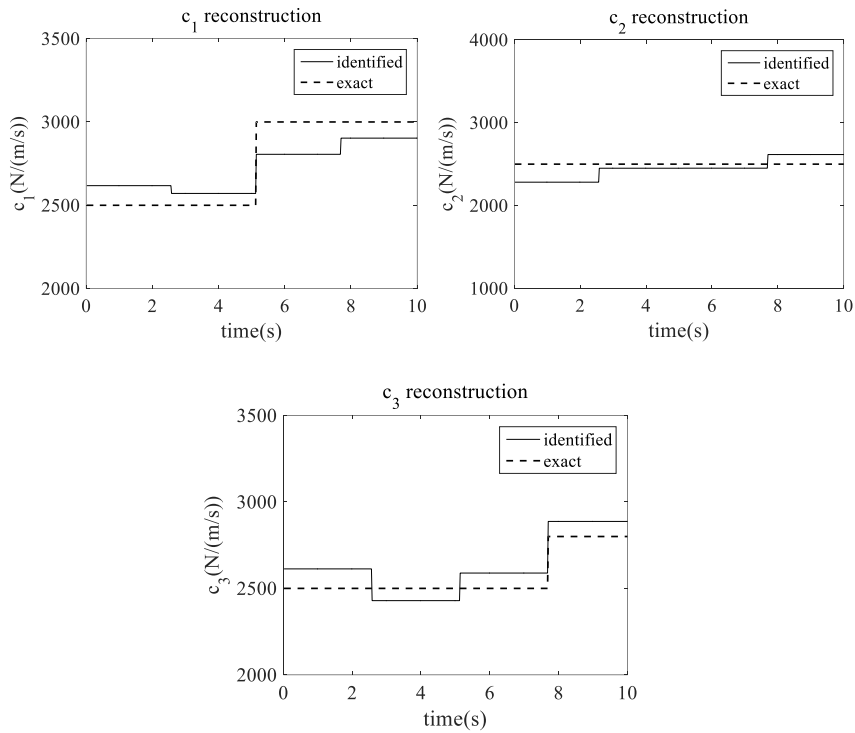


Fig. 8. Identified time-varying damping of the 3-story shear frame in case II

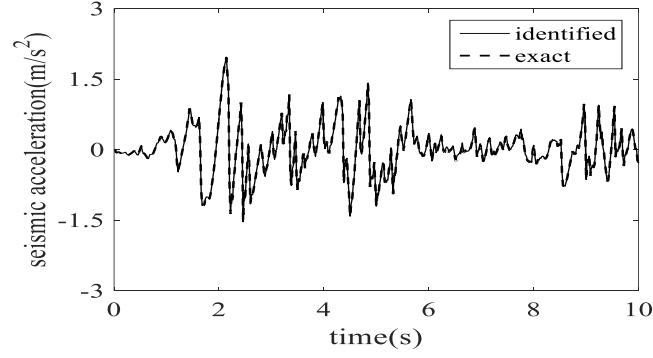


Fig.9. Identified seismic acceleration to the 3-story shear frame in case II

3.1.3. Case III: Gradually varying and abruptly varying stiffness with time-invariant damping

To further verify the proposed algorithm for the identification of gradually time-varying type, it is assumed that the time-varying k_1 is set to be in a linear form. The changes in the physical parameters are specified as shown in Eq. (25).

$$\begin{aligned}
 k_1 &= \begin{cases} 250 \text{ kN/m}, & 0 \text{ s} \leq t < 4 \text{ s} \\ -12.5t + 300 (\text{kN/m}), & 4 \text{ s} \leq t \leq 8 \text{ s} \\ 200 \text{ kN/m}, & 8 \text{ s} < t \leq 10 \text{ s} \end{cases} \\
 k_2 &= 200 \text{ kN/m}, \quad 0 \text{ s} \leq t \leq 10 \text{ s} \\
 k_3 &= \begin{cases} 180 \text{ kN/m}, & 0 \text{ s} \leq t < 5.2 \text{ s} \\ 140 \text{ kN/m}, & 5.2 \text{ s} \leq t \leq 10 \text{ s} \end{cases} \\
 c_1 = c_2 = c_3 &= 2.5 \text{ kN}\cdot\text{s/m}, \quad 0 \text{ s} \leq t \leq 10 \text{ s}
 \end{aligned} \tag{25}$$

For the decomposition of gradually varying stiffness parameter k_1 , Db3 is selected as the wavelet function with the scale level $J=5$. The number of unknown stiffness scale coefficients is 24.

Fig.10 illustrates that both the gradually and abruptly time-varying stiffness parameters in this example can be well-identified. The identification results of damping parameters are also acceptable, but these results are not shown herein due to page limitations.

Again, the identified ground acceleration is quite accurate in this case, as shown in Fig. 11.

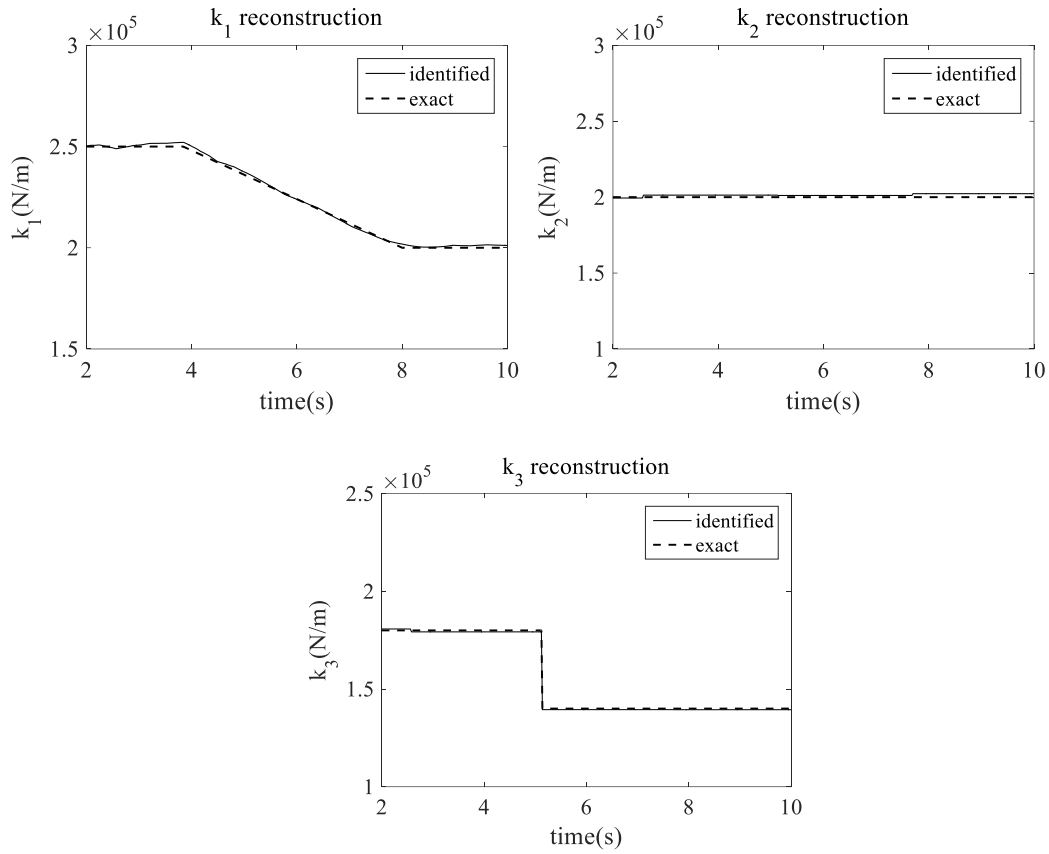


Fig.10. Identified time-varying stiffness of the 3-story shear frame in case III

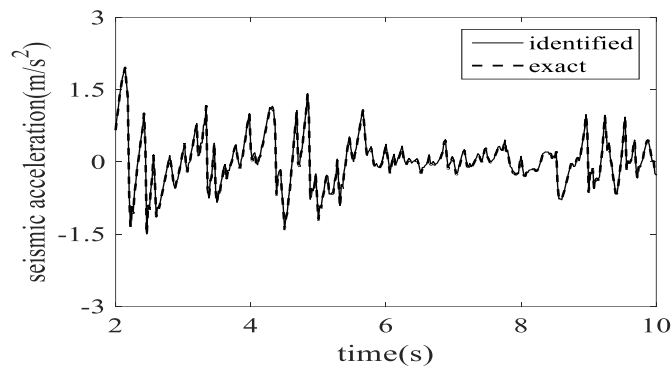


Fig.11. Identified seismic acceleration to the 3-story shear frame in case III

3.2 Example 2: A simply supported beam under unknown external excitation

Considering only shear-type frames were studied in most previous literature, a time-varying beam-type structure is investigated as another numerical example. As shown in Fig.12, a simply supported beam is divided into four finite elements. The model is built based on the Euler-Bernoulli theory. There are 8 DOFs in total, including 3 vertical displacement DOFs and 5 rotation

DOFs. The length of each element is $l=1.5\text{m}$ with uniformly distributed mass 7850kg/m , and the Rayleigh damping is adopted with the first two damping ratios being 0.03. A white noise excitation is acted on the 2nd DOF of the beam. The sampling frequency is 50Hz and the sampling time is 10s , thus 2004 stiffness parameters need to be identified in total. Only three accelerometers are deployed at the 2nd, 4th, and 6th DOFs, respectively. For data fusion, two displacement sensors fixed on the 2nd and 4th DOF are used. In this example, responses of the rotation DOFs are non-essential. The measured structural responses are polluted by white noise with 1% in RMS. Two cases of time-varying stiffness parameters are investigated as follows.

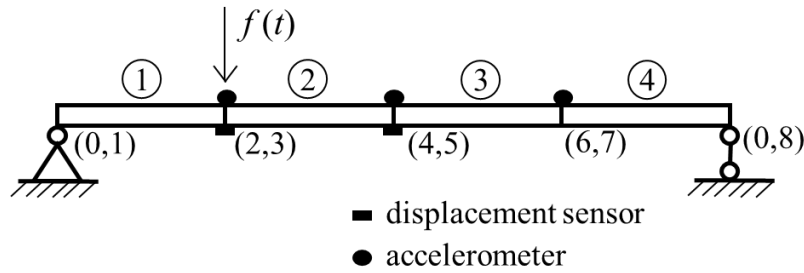


Fig.12. A simply supported beam with time-varying stiffness parameters

3.2.1. Case I: multi abruptly varying stiffness

In case I, it is assumed that the changes of stiffness parameter k_2 and k_3 are linear while the physical parameters k_1 and k_4 are time-invariant. The values of stiffness parameters are specified in Eq. (26). Also, Db1 is utilized as the wavelet function with the resolution scale $J=7$. Thus, there are totally 16 unknown stiffness scale coefficients to be optimized in the nonlinear least-squares estimation.

$$\begin{aligned}
 k_1 &= 20\text{ kN/ m, } 0\text{ s} \leq t \leq 10\text{ s} \\
 k_2 &= \begin{cases} 20\text{ kN/ m, } 0\text{ s} \leq t < 5.2\text{ s} \\ 17\text{ kN/ m, } 5.2\text{ s} \leq t \leq 10\text{ s} \end{cases} \\
 k_3 &= \begin{cases} 20\text{ kN/ m, } 0\text{ s} \leq t < 7.6\text{ s} \\ 18\text{ kN/ m, } 7.6\text{ s} \leq t \leq 10\text{ s} \end{cases} \\
 k_4 &= 20\text{ kN/ m, } 0\text{ s} \leq t \leq 10\text{ s}
 \end{aligned} \tag{26}$$

Fig.13 shows the identified time-varying stiffness parameters of this simply supported beam model, which are in favorable agreement with the exact time-varying curves. Furthermore, all

responses and external excitations can be estimated accurately. For saving space, only the identified external excitation is shown and compared with its exact time history in Fig.14.

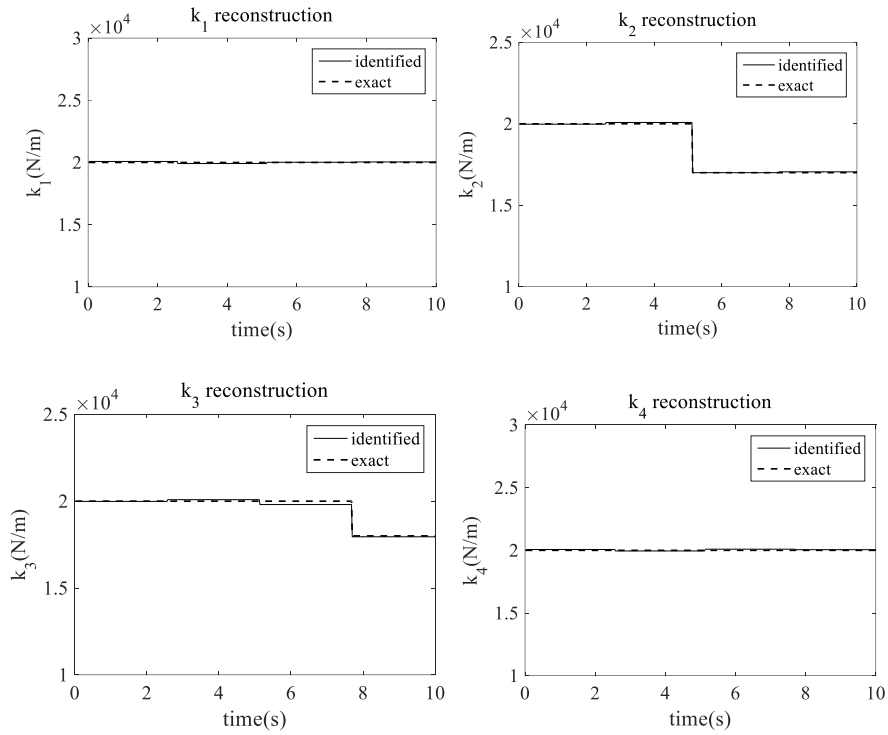


Fig.13. Identified time-varying stiffness of the beam in case I

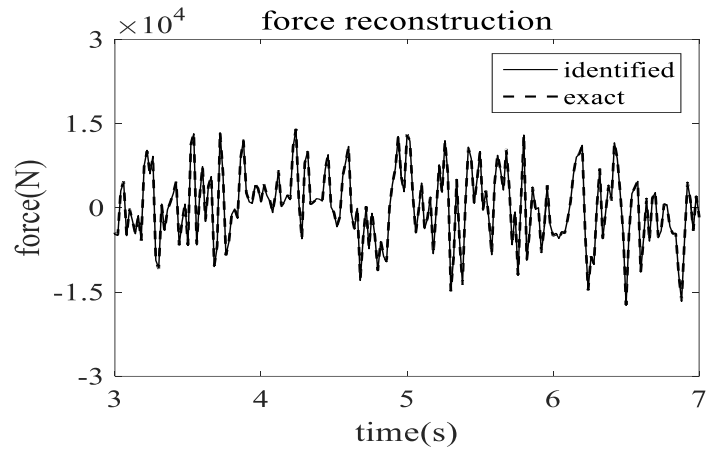


Fig.14. Identified external excitation to the beam in case I

3.2.2. Case II: gradually varying and abruptly varying stiffness

In this case, structural physical parameters are consistent with those in case I, except that k_3 is in a gradually varying trend as:

$$k_3 = \begin{cases} 20 \text{ kN/m}, & 0 \leq t < 2.5 \text{ s} \\ -1.8t + 24.6 (\text{kN/m}), & 2.5 \text{ s} \leq t \leq 4.8 \text{ s} \\ 16 \text{ kN/m}, & 4.8 \text{ s} < t \leq 10 \text{ s} \end{cases} \quad (27)$$

Analogously, Db3 is selected as the wavelet scale function for the expansion of gradually varying parameter k_3 and the scale level is $J=4$. The number of unknown stiffness scale coefficients is 44 in total.

Fig.15 shows the identified time-varying stiffness parameters. Although the recognition error is greater when the stiffness changes gradually, it is still within an acceptable range. Furthermore, all responses and external excitations can be identified and the identified external excitation is shown and compared with its exact time history in Fig.16.

Summarizing the two identification cases, it is shown that the proposed algorithm is also effective in identifying the time-varying structural physical parameters of beam-type structures subjected to unknown external excitations.

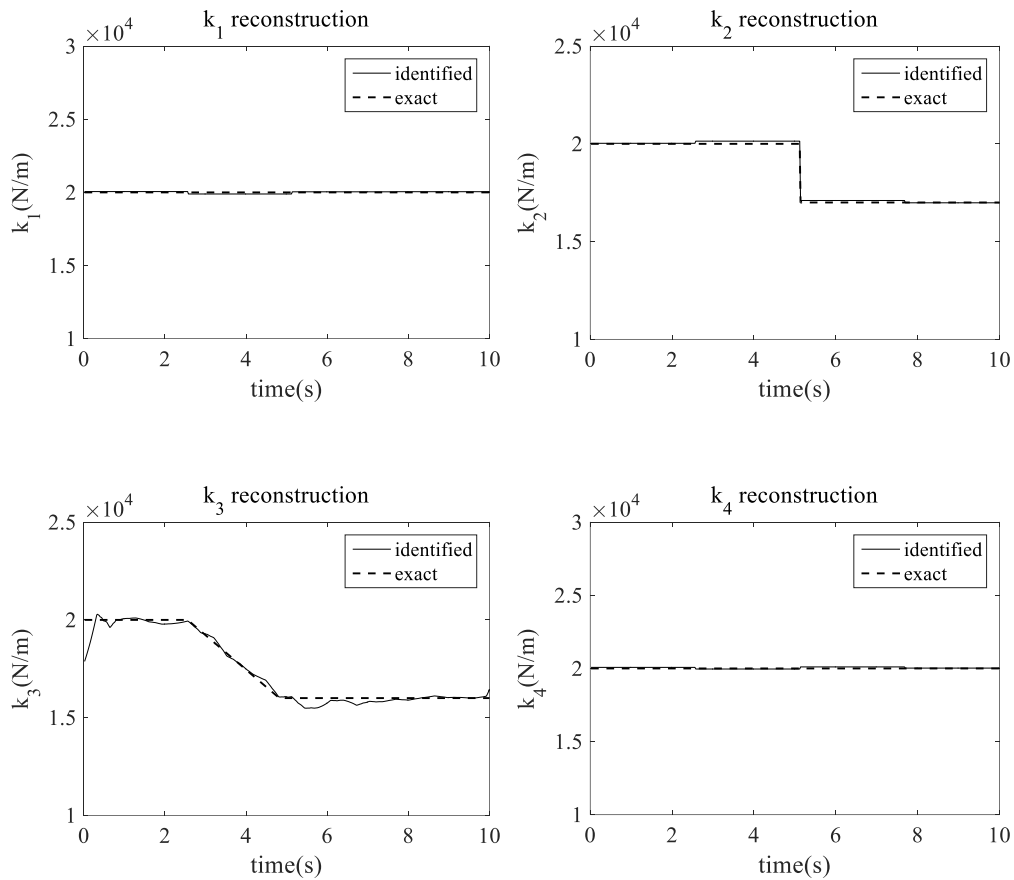


Fig.15. Identified time-varying stiffness of the beam in case II

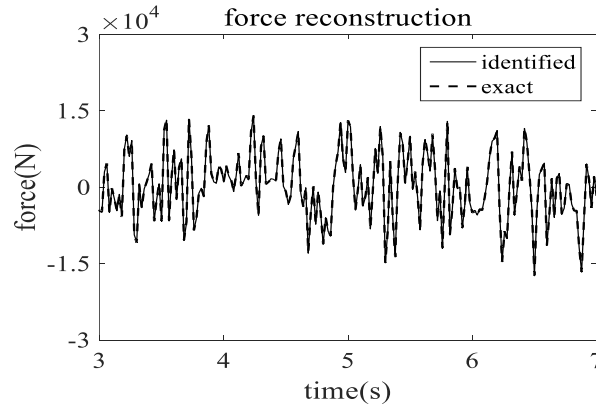


Fig.16. Identified external excitation to the beam in case II

3.3 Example 3: A plane frame under unknown seismic excitation

To further validate the proposed algorithm for the identification of time-varying physical parameters in complex structures, the time-varying physical parameters identification of a two-dimensional (2D) plane frame shown in Fig. 17 is investigated.

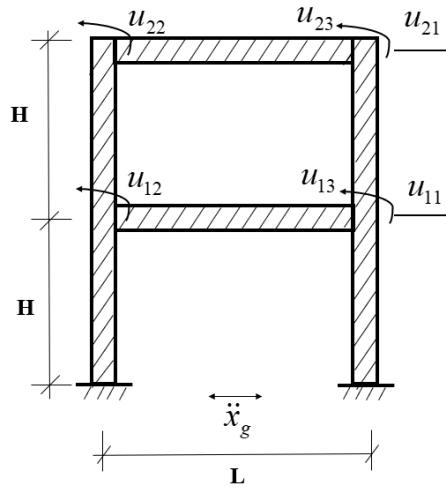


Fig.17. A time-varying one-bay two-story plane frame model

This frame studied herein is one bay and two-story with linear elements of four columns and two beams [30]. Neglecting axis deformation of the rigid frame, only six DOFs including two horizontal DOFs and four rotational ones are considered. The same uniform mass density with $m=240\text{kg/m}$ is used for all columns and beams. The height of the column is $H=5\text{m}$ and the length of the beam is $L=6\text{m}$. The frame is excited by the El-Centro earthquake ground motion. The

sampling frequency is 50Hz and the sampling time is 10s. Acceleration responses of u_{11} , u_{12} , u_{21} , and u_{22} DOFs in Fig.17 are used as measurements for identification. Since rotational accelerations are hard to be measured, it is usually a good approximation to assume that rotational motion at a joint is related to the horizontal motion through the static deflection relation [38-39]. Herein, the rotational accelerations are estimated from the measured horizontal acceleration. Also, two horizontal displacements of the u_{11} and u_{21} DOF are used for data fusing. All the measured structural responses are contaminated by white noise with 1% RMS on account of noise influence.

In this numerical illustration, the linear stiffness $i(t) = EI(t)/L$ is considered as a time-varying parameter to reflect the time-varying property of the member, that is the six linear stiffness parameters i_{1l} , i_{1r} , i_{2l} , i_{2r} , i_{1b} , i_{2b} are time-varying, in which the first subscript denotes the story number while the second index indicates the left column (l), right column (r), and the beam (b), respectively. It is assumed the stiffness parameters vary abruptly as: i_{1l} is reduced from 4000kN·m to 3400kN·m at 5.12 second, i_{1b} is changed from 3500kN·m to 2800kN·m at 7.68 second, $i_{1r}=i_{2l}=i_{2r}=4000\text{kN}\cdot\text{m}$ and $i_{2b}=3500\text{kN}\cdot\text{m}$. Db1 is used as the mother function in this case and the resolution scale is chosen as $J=7$ to expand the stiffness parameters. The number of unknown stiffness scale coefficients is 24 in total. Viscous damping coefficient is assumed for each DOF in the plane frame, respectively [30]. Herein, damping coefficients are assumed constant as: $c_{1l}=50\text{kN}\cdot\text{s/m}$, $c_{1r}=c_{1r}=10\text{kN}\cdot\text{s/m}$, $c_{2l}=20\text{kN}\cdot\text{s/m}$, and $c_{2r}=c_{2r}=70\text{kN}\cdot\text{s/m}$.

According to the identified results shown in Fig.18, it is validated that the proposed algorithm is capable of identifying time-varying stiffness parameters in the plane frame model. Furthermore, the identified earthquake ground acceleration to the plane frame by the proposed algorithm is satisfactory, as shown in Fig. 19.

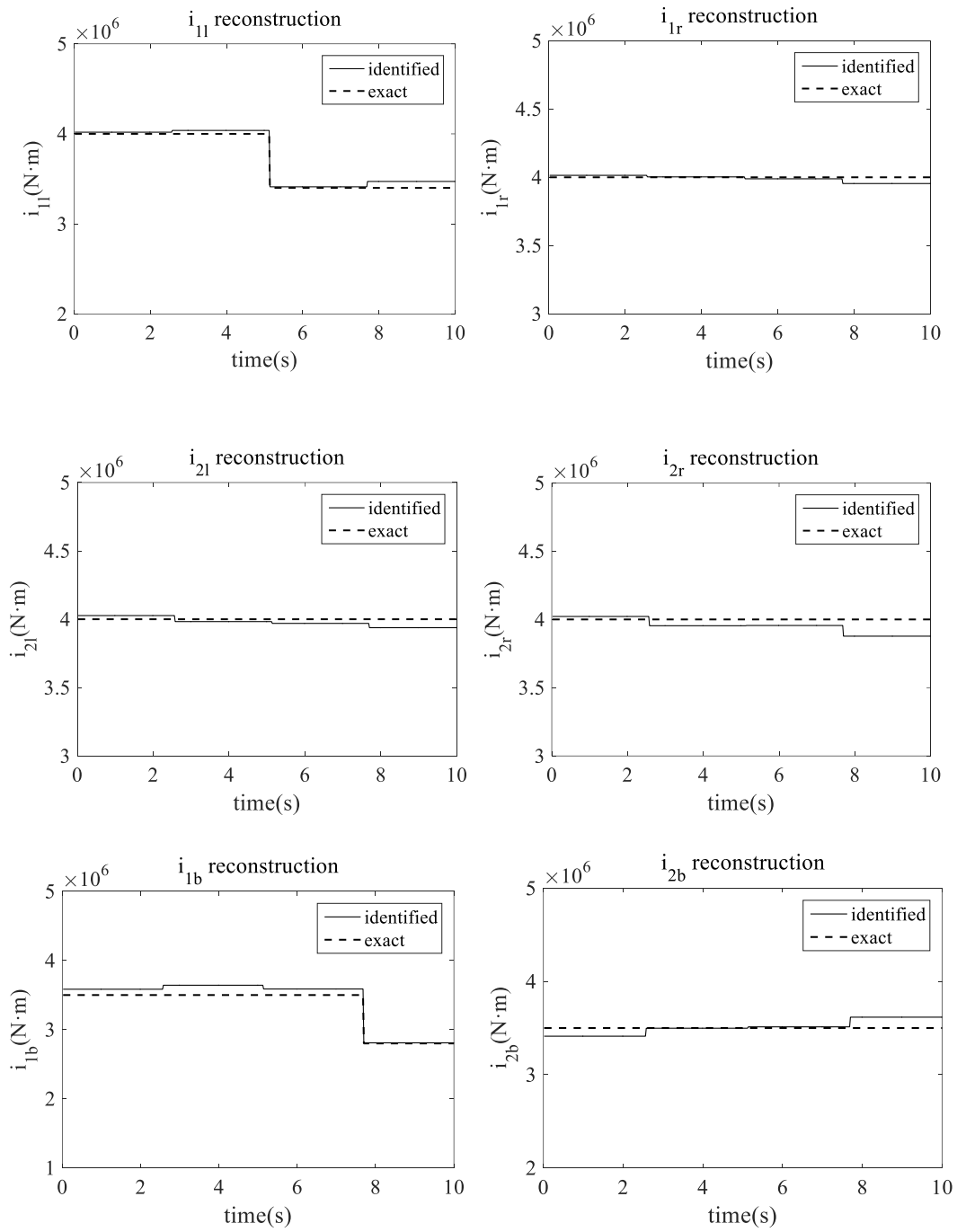


Fig. 18. Identified time-varying stiffness of the plane frame

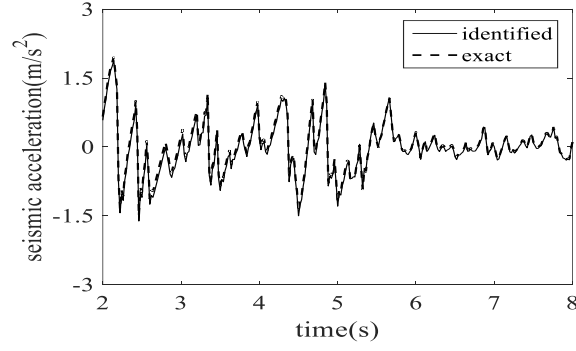


Fig.19. Identified external excitation to the plane frame

4. Experimental verification

To further verify the effectiveness of the proposed algorithm, an experiment test with a three-story steel frame is used to identify the sudden change of stiffness parameter. The experiment was completed in the Research Centre of Earthquake Engineering in Taiwan [36]. As shown in Fig.20, the structure was placed on the seismic shaking table and the ground acceleration was measured by the accelerometer fixed on the table. To simulate the suddenly changing stiffness of the 1st floor, a locking system supported by a V-shaped bracing was assembled on the first floor and the locking system could be released at any time during the process of earthquake excitation, so the frame can display abruptly time-varying characteristics [36].

The structural system is a lumped mass reduced-order structural model with three DOFs and the lumped mass of each floor is known as 6000kg. The damping parameters are selected according to [36]. The structural stiffness matrix \mathbf{K} is unknown. Different from the stiffness matrix of traditional shear frames, the stiffness matrix \mathbf{K} herein contains all elements naming k_{ij} ($i = 1, 2, 3, j = 1, 2, 3$) in the i -th row and the j -th column. Inter-story stiffness k_m ($m = 1, 2, 3$) can be obtained as shown in Eq.(28) [36]:

$$k_m = \sum_{i=m}^3 \sum_{j=m}^3 k_{ij} \quad (m = 1, 2, 3) \quad (28)$$

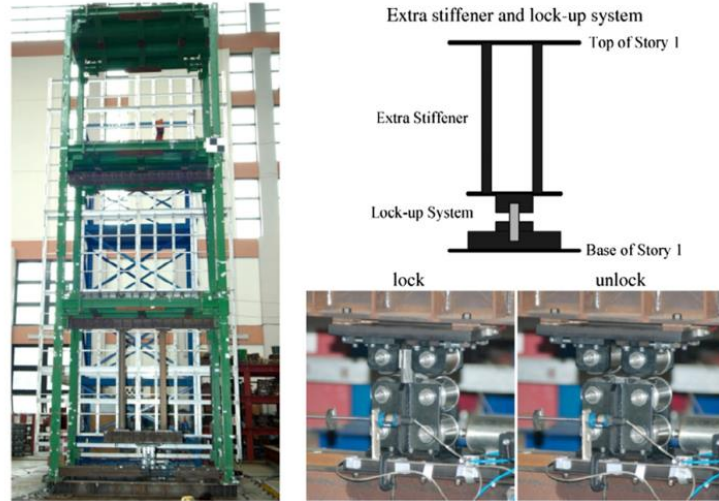


Fig.20. A 3-story steel frame with a lock-up system on the 1st floor (referred to [36])

In the experiment, sensors for measuring acceleration, velocity, and displacement were installed on each floor, but only the collected acceleration data of the 1st and 3rd floor and displacement data of the 1st floor are used in the proposed algorithm. The sampling time interval is 0.02s and the whole sampling time is 30s. Thus, take k_1 as an example, the stiffness parameters of the first floor are 1500 in total. Adopt the mother function Db1 and the scale level $J=6$ to expand the abruptly varying stiffness k_1 , thus 24 unknown stiffness scale coefficients of the first floor participate in the nonlinear optimization. The 6th-order Butterworth band-pass filter is adopted pre-processing the collected data to remove the high-frequency noise influence. The stiffness parameters before and after the sudden change together with the unknown ground acceleration of the shaking table are identified by the proposed algorithm in this paper.

From the comparison for the time-varying inter-story stiffness parameters shown in Fig.21, it is demonstrated that not only the abrupt change of k_1 can be tracked but also the time-invariant inter-story stiffness k_2 and k_3 can be identified. Moreover, the unknown acceleration of the shaking table can also be identified as shown in Fig. 22. The experimental testing case is more complex compared with those numerical simulation studies, so the identified seismic acceleration deviates from the measured value, but the error is still within the acceptable range in the experimental test.

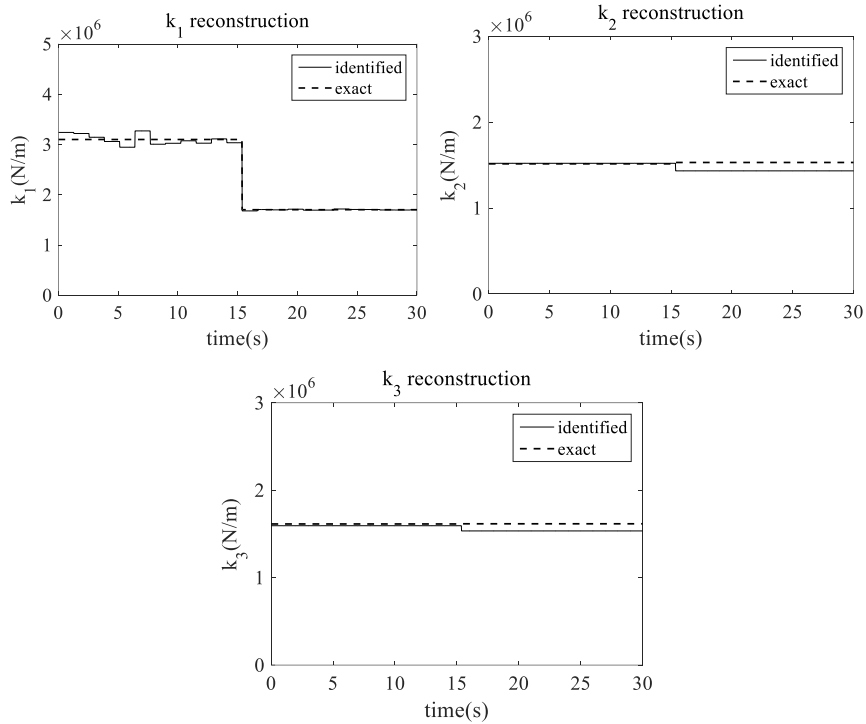


Fig. 21. Identified time-varying inter-story stiffness of the experimental steel frame

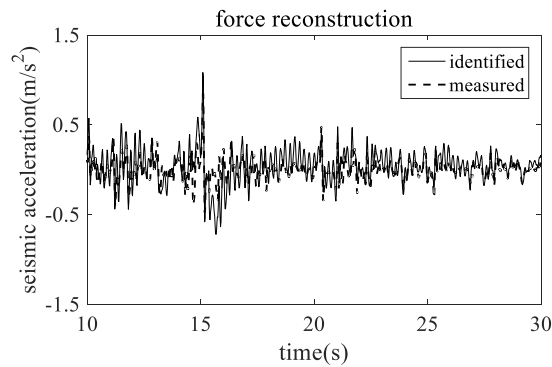


Fig. 22. Identified acceleration of the shaking table in the experimental test

5. Conclusions

It is necessary to investigate an effective algorithm for the identification of time-varying structural systems. Current identification approaches based on the WM analysis request the full structural response measurements. Moreover, external excitations to the structures are also needed to be known or assumed. To overcome these limitations, an algorithm is proposed for simultaneous identification of structural time-varying physical parameters and unknown external

excitation only using limited observed responses. Structural time-varying physical parameters are expanded using a discrete wavelet basis and resolution scale. Structural responses and unknown excitations are estimated by the data fusion based KF-UI approach developed by the authors with partially measured responses and pre-assumed scale coefficients. The KF-UI approach can include the influence of measurement noise as a measurement noise vector is considered in the observation equation. The expanded scale coefficients are estimated by solving a nonlinear optimization problem. Afterward, structural time-varying parameters are reconstructed accordingly, and the unknown external excitations can be identified simultaneously.

Three numerical examples including various sceneries (e.g. suddenly or gradually varying of structural physical parameters) in the shear-type frame, beam and plane frame under unknown excitations have validated the proposed algorithm. Moreover, an experimental shaking table test for a time-varying frame further validates the effectiveness of the proposed algorithm. The proposed novel algorithm is effective for simultaneous identification of structural time-varying physical parameters and unknown excitations only using partially measured responses of structures, which is suitable for practical application. Such an identification algorithm is not available in the literature.

In this paper, the selection of appropriate resolution scale in the wavelet analysis is an important but a challenging task. Further related investigations are needed in the follow-up research. Similar to other previous WM-based approaches for time-varying parameter identification, the proposed algorithm is not applicable for large size structures due to the difficulty in the multiple-parameter optimization problem. This is the drawback of the proposed method. This difficulty can be solved by the sub-structural identification approach. Such relevant research is being conducted and identification results will be published subsequently.

Acknowledgments

This work is supported by the National Natural Science Foundation of China via Grant No.51678509. The authors appreciate the support from Professor Loh at National Taiwan University for providing experimental data on a three-story steel frame with stiffness changes.

References

- [1] Ou JP, Li H. Structural health monitoring in mainland China: review and future trends. *Structural Health Monitoring* 2010; 9(3):219–231.
- [2] Doebling SW, Farrar CR, Prime MB. A summary review of vibration-based damage identification methods. *Shock and Vibration* 1998; 30(2): 91-105.
- [3] Doebling SW, Farrar CR, Prime MB, Shevitz DW. Damage identification and health monitoring of structural and mechanical systems from changes in their vibration characteristics: a literature review. No. LA-13070-MS. Los Alamos National Laboratory Report 1996; LA-13070-MS.
- [4] Grenier Y. Time-dependent ARMA modeling of nonstationary signals. *IEEE Transactions on Acoustics, Speech, and Signal Processing* 1983; 31(4): 899-911.
- [5] Poulimenos AG, Fassois SD. Parametric time-domain methods for non-stationary random vibration modelling and analysis- A critical survey and comparison. *Mechanical Systems and Signal Processing* 2006; 20(4): 763-816.
- [6] Lin JW, Betti R, Smyth AW, Longman RW. On-line identification of nonlinear hysteretic structural systems using a variable trace approach. *Earthquake Engineering and Structural Dynamics* 2010; 30(9): 1279-1303.
- [7] Huang, Q, Xu YL, Liu HJ. An efficient algorithm for simultaneous identification of time-varying structural parameters and unknown excitations of a building structure. *Engineering structures* 2015; 98: 29-37.
- [8] Yang JN, Lin SL. On-line identification of non-linear hysteretic structures using an adaptive tracking technique. *International Journal of Non-Linear Mechanics* 2004; 39(9):1481-1491.
- [9] Mu HQ, Kuok SC, Yuen KV. Stable robust extended Kalman filter. *Journal of Aerospace Engineering* 2016; B4016010.
- [10] Yuen KV, Huang K. Real-time substructural identification by boundary force modeling. *Structural Control and Health Monitoring* 2018; 25: e2151.
- [11] Wang ZC, Ren WX, Chen GD. Time-frequency analysis and applications in time-varying/nonlinear structural systems: A state-of-the-art review. *Advances in Structural Engineering* 2018; 21: 1562-1584.
- [12] Chen J, Zhao G. Numerical and experimental investigation on parameter identification of time-varying dynamical system using Hilbert Transform and Empirical Mode Decomposition. *Mathematical Problems in Engineering* 2014; 2: 1-15.
- [13] Yang JN, Lei Y, Pan SW, Huang N. System identification of linear structures based on Hilbert-Huang spectral analysis. Part 1: normal modes. *Earthquake Engineering and Structural Dynamics* 2003; 32: 1443–1467.

- [14] Yang JN, Lei Y, Pan SW, Huang N. System identification of linear structures based on Hilbert-Huang spectral analysis. Part 2: complex modes. *Earthquake Engineering and Structural Dynamics* 2003; 32:1533–1554.
- [15] Ni PH, Li J, Hao H, Xia Y, Wang XY, Lee JM, Jung KH. Time-varying system identification using variational mode decomposition. *Structural Control and Health Monitoring* 2018; 25: e2175.
- [16] Chen GD, Wang ZC. A signal decomposition theorem with Hilbert transform and its application to narrowband time series with closely spaced frequency components. *Mechanical Systems and Signal Processing* 2012; 28: 258-279.
- [17] Wang ZC, Chen GD. Analytical mode decomposition with Hilbert transform for modal parameter identification of buildings under ambient vibration. *Engineering Structures* 2014; 59:173-184.
- [18] Liu JL, Zheng JY, Wei XJ, Ren WX, Laory I. A combined method for instantaneous frequency identification in low frequency structures. *Engineering Structures* 2019; 194: 370-383.
- [19] Qu HY, Li TT, Chen GD. Multiple analytical mode decompositions for nonlinear system identification from forced vibration. *Engineering Structures* 2018; 173: 979-986.
- [20] Huang CS, Liu CY, Su WC. Application of Cauchy wavelet transformation to identify time-variant modal parameters of structures. *Mechanical Systems and Signal Processing* 2016; 80: 302–323.
- [21] Xin Y, Hao H, Li J. Time-varying system identification by enhanced Empirical Wavelet Transform based on Synchroextracting Transform. *Engineering Structures* 2019; 196: 109313.
- [22] Yang YC, Nagarajaiah S. Blind identification of damage in time-varying systems using independent component analysis with wavelet transform. *Mechanical Systems and Signal Processing* 2014; 47(1-2): 3-20.
- [23] Li H, Mao CX, Ou JP. Identification of hysteretic dynamic systems by using hybrid extended Kalman Filter and Wavelet Multiresolution analysis with limited observation. *Journal of Engineering Mechanics* 2013; 139(5):547-558.
- [24] Ghanem R, Romeo F. A wavelet-based approach for the identification of linear time-varying dynamical systems. *Journal of Sound and Vibration* 2000; 234(4): 555-576.
- [25] You Q, Shi ZY, Shen L. Damage detection in time-varying beam structures based on wavelet analysis. *Journal of Vibroengineering* 2012; 14:291-304.
- [26] Xu X, Shi ZY, You Q. Identification of linear time-varying systems using a wavelet-based state-space method. *Mechanical Systems and Signal Processing* 2012; 26: 91-103.

- [27] Wang C, Ren WX, Wang ZC, Zhu HP. Time-varying physical parameter identification of shear type structures based on discrete wavelet transform. *Smart Structures and Systems* 2014; 14(5):831-845.
- [28] Wang C, AiDM, Ren WX. A wavelet transform and substructure algorithm for tracking the abrupt stiffness degradation of shear structure. *Advances in Structural Engineering* 2019; 22(5): 1136-1148.
- [29] Chang CC, Shi YF. Identification of time-varying hysteretic structures using wavelet multiresolution analysis. *International Journal of Non-Linear Mechanics* 2010; 45(1): 21-34.
- [30] Xiang M, Xiong F, Shi YF, Dai KS, Ding ZB. Wavelet multi-resolution approximation of time-varying frame structure. *Advances in Mechanical Engineering* 2018;10(8):1–19.
- [31] Kalman RE. A new approach to linear filtering and prediction problems. *Journal of Basic Engineering* 1960; 82(1): 35–45.
- [32] Lei Y, Jiang YQ, Xu ZQ. Structural damage detection with limited input and output measurement signals. *Mechanical Systems and Signal Processing* 2012; 28:229-243.
- [33] Azam S, Chatzi E, Papadimitriou C. A dual Kalman filter approach for state estimation via output-only acceleration measurements. *Mechanical System and Signal Process* 2015; 60:866–886.
- [34] Naets F, Cuadrado J, Desmet W. Stable force identification in structural dynamics using Kalman filtering and dummy-measurements. *Mechanical Systems and Signal Processing* 2015; 50-51: 235-248.
- [35] Liu LJ, Zhu JJ, Su Y, Lei Y. Improved Kalman filter with unknown inputs based on data fusion of partial acceleration and displacement measurement. *Smart Structures and Systems* 2016; 17(6): 903-915.
- [36] Weng JH, Loh CH. Recursive subspace identification for on-line tracking of structural modal parameter. *Mechanical Systems and Signal Processing* 2011; 25(8):2923-2937.
- [37] Liu LJ, Su Y, Zhu JJ, Lei Y. Data fusion based EKF-UI for real-time simultaneous identification of structural systems and unknown external inputs. *Measurement* 2016; 88: 456-467.
- [38] Ling XL, Haldar A. Element level system identification with unknown input with Rayleigh damping. *Journal of Engineering Mechanics* 2004;130(8):877-885.
- [39] Yang JN, Huang HW, Pan SW. Adaptive quadratic sum-squares error for structural damage identification. *ASCE Journal of Engineering Mechanics* 2009; 135(2): 67-77.

CHAPTER 3 Identification of time-varying large-scale structures by integrated sub-structural and wavelet multiresolution approach with partial measurements

ABSTRACT

Currently, most wavelet multiresolution (WM) based methods for the identification of time-varying structural physical parameters request the full measurements of all structural responses. All physical parameters including time-varying and time-invariant parameters are expanded by WM, so it is only applicable to small-scale structures with a few degree-of-freedom (DOFs). In this paper, based on the sub-structural identification technique, a novel two-step approach is proposed to identify the time-varying physical parameters of large-scale structures under unknown external excitations using only partially measured responses. A large-scale structure is divided into several substructures. For a substructure concerned, the unknown interaction forces from neighboring structures are treated as ‘additional unknown inputs’ imposed to the substructure, so the identification of large-scale structure can be transformed to the identification of each substructure with parallel computing in two steps. In the first step, the fading-factor generalized extended Kalman filter under unknown input (FGGEKF-UI) algorithm is proposed to locate the time-varying physical parameters in each substructure. In the second step, a synthesized method is developed for the quantitative identification of time-varying physical parameters based on the integration of WM analysis and the generalized Kalman filter under unknown input (GKF-UI) proposed by the authors. The time-varying structural physical parameters distinguished in the first step are expanded into scale coefficients by WM analysis. Then, the time-invariant physical parameters and the scale coefficients of time-varying physical parameters are identified by performing the nonlinear optimization with an objective function established by the proposed GKF-UI algorithm. Finally, the estimated scale coefficients are used to reconstruct the original time-varying structural physical parameters. Several numerical examples are used to demonstrate the effectiveness of the proposed approach.

Lei Y, Yang N, Li J, Hao H, Huang JS. Identification of time-varying large-scale structures by integrated sub-structural and wavelet multiresolution approach with partial measurements. *Engineering Structures*, 2021. (Under review)

1. Introduction

Many vibration-based techniques have been developed to identify the physical parameters of time-invariant structures in the field of structural health monitoring (SHM) [1, 2]. However, structural dynamic parameters often change owing to severe hazards, e.g. strong seismic and wind loads, as well as other environmental effects, e.g., temperature or corrosion effect. Effective methods need to be investigated to identify the dynamic characteristics of time-varying structures, assess and adaptively evaluate the performance of time-varying structural systems [3].

Therefore, particular attentions have been concentrated on the modal parameters identification of time-varying structures [4]. Some methods in the time-domain, e.g., the time-varying autoregressive moving average model (TV-ARMA) [5,6], have been proposed to identify the time-varying modal parameters. Many time-frequency domain methods have also been developed to successfully estimate the time-varying modal parameters and detect the structural damage [7, 8]. For example, the HT based methods, such as Empirical Mode Decomposition (EMD)[9], Variational Mode Decomposition (VMD)[10] and Analytical Mode Decomposition (AMD) [11, 12], and methods based on the wavelet decomposition, such as Empirical Wavelet Transform (EWT) [13], wavelet transform with independent component analysis (ICA) [14] and the synchrosqueezed wavelet transform [15, 16], etc.

On the other hand, direct identification of physical parameters, such as physical stiffness and damping parameters of time-varying linear structures, is more intuitive to assess the time-varying systems [1]. Relevant studies have been conducted in the time-domain and time-frequency domain. The state space model-based methods [17-21], have shown a high efficiency in the time-domain to track the change of physical parameters by introducing the fading-factor related to the

time-varying parameters. However, it is difficult to select the most optimal fading-factor. Therefore, some of these methods were proposed based on an empirical fading-factor [17-20]. In addition, researches to find the most optimal fading-factor were attempted by updating the adaptive factor matrix at each time instant [21], but it is computational expensive for large-scale structures. The time-frequency domain methods based on the wavelet multiresolution (WM) have been developed to identify the structural time-varying physical parameters [22-26]. These methods expand the physical parameters of time-varying structures into scale coefficients, which are identified by the linear least-squares estimation. However, these methods are not suitable for large-scale structures due to the reason that complete measurements of all structural responses are required, which is impractical for real applications. To overcome this limitation on full observations, some novel methods have been proposed [27,28] recently by the authors to identify the time-varying physical parameters of linear structures under known or unknown excitations using only partial measurements of structural responses. However, it is required to expand all physical parameters (including time-varying parameters and time-invariant parameters) into scale coefficients based on WM. The number of expanded coefficients increases greatly as the structural size increases, making it difficult to obtain a global optimal solution especially when the quality of the collected data is poor. Therefore, the proposed methods are still applicable to small-scale structures with a small number of degree-of-freedom (DOFs).

For the parametric identification of large-scale structures, sub-structural identification technique is more efficient [29-35]. However, these methods are mostly used to identify the parameters of time-invariant systems. For time-varying systems, Shi and Chang [22,23] used the sub-structural identification technique to identify the time-varying physical parameters of a

numerical 10-story shear frame and a 3-story experimental shear building model. Each structure was divided into several small size substructures, and WM was adopted to identify the time-varying physical parameters of each substructure. Recently, Wang et al. [24] presented a wavelet transform and sub-structural algorithm to track the abrupt stiffness degradation of a numerical 7-story shear frame and a lab experimental 3-story shear-type structure. However, measurements of complete structural responses of acceleration, velocity and displacement responses at every DOF including the one at sub-structural interfaces, were needed for each substructure in the above studies. With the full measurements of structural responses and known excitations, the identification can be accomplished by the simple linear least-squares estimation. Although sub-structural technique provides a very useful tool for parametric identification of large-scale structures, it is still a challenging task to properly consider the interaction forces between adjacent substructures without the fully measured responses at the sub-structural interfaces.

Based on the above literature review of current existing methods, it is noted that there are still some limitations in identifying the time-varying physical parameters of large-scale structures. This paper aims to circumvent these limitations and propose a novel approach for the identification of time-varying physical parameters of large-scale structures by integrating sub-structural and WM methods using only partially measured structural responses. Two main technical innovation aspects are summarized as follows:

1. Substructure identification based on the partial observations of sub-structural responses.

Usually, dynamic responses at the sub-structural interfaces are required in the previous sub-structural identification techniques, which limits the practical applications [30,32]. Interaction forces between adjacent substructures can be considered as ‘unknown inputs’ to the substructure

of interest. The generalized Kalman filter under unknown input (GKF-UI), which was recently proposed for the identification of time-invariant systems by the authors [36], is used to identify each substructure with only partial measurements of sub-structural responses without measurements at the interface DOFs. Then, the identification of a large-scale structure is transformed to the identification of each substructure independently, which greatly simplifies the identification of the time-varying structural parameters of the large-scale structure in the optimization problem.

2. Localization of time-varying physical parameters to reduce the number of expanded scale coefficients and ensure a global optimal solution.

In this paper, a fading-factor generalized extended Kalman filter under unknown input (FGEKF-UI) is proposed to firstly locate the time-varying physical parameters in each substructure, in which the unknown sub-structural interaction forces are regarded as “additional unknown inputs” imposed to the target substructure. Then only the time-varying parameters are expanded by WM, greatly reducing the number of expanded scale coefficients compared with the current WM based methods for the identification of time-varying structures, as all physical parameters including time-varying and time-invariant parameters are expanded into scale coefficients in the latter.

Inspired by the merits of sub-structural identification technique and WM analysis for time-varying parameters, a novel two-step approach is proposed in this paper for the identification of time-varying physical parameters of large-scale structures using only partially measured structural responses. In this study, structural mass is assumed time-invariant and known, while structural stiffness and damping are time varying parameters to be identified. A large-scale

structure is divided into several substructures, and the sub-structural interaction forces are treated as ‘additional unknown inputs’ to the target substructure. Each substructure is identified in a parallel manner with two-step. In the first step, the time-varying sub-structural physical parameters are located by the FGEKF-UI algorithm. In the second step, these parameters are expanded into fewer scale coefficients by the WM analysis, so the identification of time-varying systems is transformed into the identification of time-invariant scale coefficients together with the time-invariant physical parameters. Then, the GKF-UI algorithm is used for the identification of sub-structural state under unknown inputs using data fusion of partial measurements. Finally, the scale coefficients and time-invariant physical parameters are estimated by solving a nonlinear optimization problem, and the original unknown time-varying structural physical parameters are reconstructed by the estimated scale coefficients. Numerical studies of identifying the abruptly and/or gradually time-varying parameters of a 30-story shear frame and a three-span truss bridge with 55 members are conducted to demonstrate the effectiveness of the proposed two-step approach.

The remaining parts of the paper are organized as follows. In Section 2, previous identification of sub-structural time-varying parameters based on WM expansion is briefly introduced for the completeness of this manuscript. In Section 3, the details of the proposed two-step approach are presented, in which Section 3.1 investigates the localization of time-varying physical parameters in each substructure using FGEKF-UI algorithm; Section 3.2 introduces the integrated WM and GKF-UI algorithm; and Section 3.3 summaries the procedures of the proposed approach. In Section 4, two numerical identification examples including a 30-story shear frame and a three-span truss bridge are presented to validate the performance of the proposed approach

in identifying various scenarios of time-varying physical parameters of large-scale structures.

Finally, some conclusions with further research issues are presented in the conclusions.

2. Previous identification of sub-structural time-varying parameters based on WM analysis

Shi and Chang [22, 23] and Wang et al. [24] presented novel methods to identify the time-varying parameters based on the combination of sub-structural technique and WM analysis. For brevity but without losing generality, the main idea and formulas are briefly introduced as follows.

After dividing a large-scale structure into several substructures, the equation of motion of the target sub-structural system can be written as [30,31]

$$\mathbf{M}_s \ddot{\mathbf{x}}_s(t) + \mathbf{C}_s(t) \dot{\mathbf{x}}_s(t) + \mathbf{K}_s(t) \mathbf{x}_s(t) = \boldsymbol{\eta}_s \mathbf{f}_s(t) + \boldsymbol{\eta}_s^u \mathbf{f}_s^u(t) \quad (1)$$

in which $\boldsymbol{\eta}_s^u = [\boldsymbol{\eta}_{se}^u \quad \boldsymbol{\eta}_{sb}^u]$, $\mathbf{f}_s^u = [\mathbf{f}_{se}^u \quad \mathbf{f}_{sb}^u]^T$. In Eq.(1), the subscript s represents ‘substructure’; $\mathbf{x}_s(t)$, $\dot{\mathbf{x}}_s(t)$, and $\ddot{\mathbf{x}}_s(t)$ are the sub-structural displacement, velocity, and acceleration vector, respectively; \mathbf{M}_s means the underlying sub-structural mass matrix which is time-invariant and known; $\mathbf{K}_s(t)$ and $\mathbf{C}_s(t)$ denote the sub-structural stiffness and damping matrix respectively, which are assembled by the time-varying parameters to be estimated; $\mathbf{f}_s(t)$ is the known external excitation vector applied on the substructure with the influence matrix $\boldsymbol{\eta}_s$, and $\mathbf{f}_s^u(t)$ is the unknown input vector of the substructure with the influence matrix $\boldsymbol{\eta}_s^u$, $\mathbf{f}_s^u(t)$ is composed of the actual unknown external excitation vector $\mathbf{f}_{se}^u(t)$ and the unknown sub-structural interaction force vector $\mathbf{f}_{sb}^u(t)$, $\boldsymbol{\eta}_{se}^u$ and $\boldsymbol{\eta}_{sb}^u$ are their influence matrices, respectively. Rewrite Eq. (1) into the corresponding discrete format, one can have

$$\mathbf{M}_s \ddot{\mathbf{x}}_s(n) + \mathbf{C}_s(n) \dot{\mathbf{x}}_s(n) + \mathbf{K}_s(n) \mathbf{x}_s(n) = \boldsymbol{\eta} \mathbf{F}(n) \quad (2)$$

where $n=1, 2, \dots, Nt$, $\boldsymbol{\eta} = [\boldsymbol{\eta}_s \quad \boldsymbol{\eta}_s^u]^T$, $\mathbf{F}(n) = [\mathbf{f}_s(n) \quad \mathbf{f}_s^u(n)]^T$, and Nt is the number of sampled points.

WM analysis can decompose an arbitrary signal into approximate and detailed portions in different scale levels, expressed as the summation of the high-frequency and low-frequency components, respectively [24, 25]. When the signal energies mainly centralize on the low-frequency components, physical parameters including stiffness and damping coefficients throughout the whole time-domain can be expanded in the wavelet domain as

$$k_{s,i}(n) \approx \sum_{l_i^k} k_{J_i^k, l_i^k} \phi_{J_i^k, l_i^k}(2^{J_i^k} n - l_i^k), \quad c_{s,i}(n) \approx \sum_{l_i^c} c_{J_i^c, l_i^c} \phi_{J_i^c, l_i^c}(2^{J_i^c} n - l_i^c) \quad (3)$$

where $k_{s,i}(n)$ and $c_{s,i}(n)$ denote the i -th stiffness and damping parameter in the target substructure, respectively. $k_{J_i^k, l_i^k}$ is the scale coefficient for stiffness $k_{s,i}$ at the resolution scale J_i^k , and $c_{J_i^c, l_i^c}$ is the corresponding damping scale coefficient at the resolution scale J_i^c . l_i^k and l_i^c are the numbers of stiffness and damping scale coefficients, respectively. $\phi_{J_i^k, l_i^k}$ and $\phi_{J_i^c, l_i^c}$ are the scale functions in the WM analysis. From Eq. (3), the time-varying physical parameters can also be reconstructed based on the estimated scale coefficient vectors $\mathbf{k}_{J_i^k, l_i^k}$ and $\mathbf{c}_{J_i^c, l_i^c}$ accordingly.

Under the condition that: (a) sub-structural displacement, velocity and acceleration responses of the target substructure, including the ones at the sub-structural interface, are fully observed inside the target substructure; and (b) external excitation and interaction force (that is, $\mathbf{F}(n)$) are assumed to be known, Eq. (2) can be expressed by substituting the scale coefficients of stiffness and damping parameters by WM analysis in Eq. (3) as

$$\boldsymbol{\varepsilon}_s \boldsymbol{\zeta}_s = \mathbf{Y}_s \quad (4)$$

in which

$$\boldsymbol{\zeta}_s = \left[c_{J_1^c, J_1^c}, \dots, c_{J_m^c, J_m^c}, k_{J_1^k, J_1^k}, \dots, k_{J_m^k, J_m^k} \right]^T, \quad \mathbf{Y}_s = \begin{Bmatrix} \boldsymbol{\eta}\mathbf{F}(1) - \mathbf{M}_s \ddot{\mathbf{x}}_s(1) \\ \vdots \\ \boldsymbol{\eta}\mathbf{F}(Nt) - \mathbf{M}_s \ddot{\mathbf{x}}_s(Nt) \end{Bmatrix} \quad (5)$$

where m is the number of the elements, and $\boldsymbol{\varepsilon}_s$ is constituted by the measured sub-structural displacement and velocity responses at all DOFs, and the wavelet scale functions in Eq. (3). Thus, with known interaction forces, known external excitations and full responses in the substructure, the expanded unknown scale coefficients vector $\boldsymbol{\zeta}_s$ can be easily obtained from Eq. (4) by the linear least-squares estimation [22-26]. However, the assumption that the external and interface forces and responses at all DOFs are known is impractical. In addition, such method needs to expand all physical parameters into scale coefficients. It is more feasible and effective to distinguish the time-varying parameters qualitatively and then concentrate on identifying the scale coefficients of those time-varying parameters. Therefore, a novel two-step approach is proposed for the identification of time-varying parameter of large-scale structures based on the sub-structural technique using only partially measured structural responses.

3. The proposed two-step identification approach

In the proposed two-step identification approach, a large-scale structure is divided into several substructures. The sub-structural interaction forces are considered as ‘additional unknown inputs’ to the target substructure. Each substructure is identified using partial measurements in parallel following the two steps. The first step is to locate the time-varying physical parameters in the substructure using the proposed FGEKF-UI. The second step performs the WM analysis of time-varying structural physical parameters and establishes objective function based on GKF-UI. The scale coefficients are estimated by performing nonlinear optimization. It should be noted that “generalized” means that FGEKF-UI and GKF-UI are efficient even when structural measurement/observation equations do not contain the unknown excitations. That is, when the sub-structural interaction forces are treated as ‘additional unknown inputs’ to the target

substructure, it is unnecessary to measure the responses at the substructure interfaces. This is crucial for large-scale structures as it may be impractical to place sensors at all DOFs of interfaces. Each of the integrated techniques is presented in the following subsections.

3.1 Step 1: Locate the time-varying physical parameters in the substructure using FGEKF-UI algorithm.

FGEKF-UI is firstly proposed to locate the time-varying physical parameters in the substructure based on the GEKF-UI algorithm proposed by the authors [37-39]. GEKF-UI can be used to simultaneously identify the structural parameters and unknown excitations, even when structural measurement/observation equations do not contain the unknown excitations. However, GEKF-UI can only be adopted in the identification of time-invariant systems. Herein, a fading-factor is adopted to extend its application to the identification of time-varying systems.

By defining a $2n+l$ dimensional augmented state vector $\mathbf{Z}_s = \{\mathbf{x}_s^T, \dot{\mathbf{x}}_s^T, \boldsymbol{\theta}_s^T\}^T$, in which $\boldsymbol{\theta}_s$ is the vector of unknown sub-structural parameters including stiffness and damping parameters,

Eq. (1) can be rewritten into the following state space equation as

$$\begin{aligned} \dot{\mathbf{Z}}_s = \begin{Bmatrix} \dot{\mathbf{x}}_s \\ \ddot{\mathbf{x}}_s \\ \dot{\boldsymbol{\theta}}_s \end{Bmatrix} &= \begin{Bmatrix} \dot{\mathbf{x}}_s \\ -\mathbf{M}_s^{-1}[\mathbf{C}_s(t)\dot{\mathbf{x}}_s(t) + \mathbf{K}_s(t)\mathbf{x}_s(t)] \\ \mathbf{0} \end{Bmatrix} + \begin{Bmatrix} \mathbf{0} \\ \mathbf{M}_s^{-1}\boldsymbol{\eta}_s^u \\ \mathbf{0} \end{Bmatrix} \mathbf{f}_s^u + \begin{Bmatrix} \mathbf{0} \\ \mathbf{M}_s^{-1}\boldsymbol{\eta}_s \\ \mathbf{0} \end{Bmatrix} \mathbf{f}_s + \mathbf{w}_s \\ &= g(\mathbf{Z}_s) + \mathbf{B}_s^u \mathbf{f}_s^u + \mathbf{B}_s^c \mathbf{f}_s + \mathbf{w}_s \end{aligned} \quad (6)$$

in which $g(\cdot)$ is a nonlinear function, \mathbf{w}_s is the process noise (or model noise) with zero mean and a covariance matrix $E[\mathbf{w}_s \mathbf{w}_s^T] = \mathbf{Q}_s$.

Data fusion of partially measured displacement and acceleration responses is utilized to prevent the drifts in the identified displacement and unknown excitations based on previous algorithms [37]. Therefore, the measurement equation is written as

$$\begin{aligned} \mathbf{y}_{s,k+1} &= \begin{bmatrix} \ddot{\mathbf{x}}_{s,k+1}^m \\ \mathbf{x}_{s,k+1}^m \end{bmatrix} = \begin{bmatrix} -\mathbf{L}_s^a \mathbf{M}_s^{-1} [\mathbf{C}_{s,k+1} \dot{\mathbf{x}}_{s,k+1} + \mathbf{K}_{s,k+1} \mathbf{x}_{s,k+1}] \\ \mathbf{L}_s^d \mathbf{x}_{s,k+1} \end{bmatrix} + \begin{bmatrix} \mathbf{L}_s^a \mathbf{M}_s^{-1} \boldsymbol{\eta}_s^u \\ \mathbf{0} \end{bmatrix} \mathbf{f}_{s,k+1}^u + \begin{bmatrix} \mathbf{L}_s^a \mathbf{M}_s^{-1} \boldsymbol{\eta}_s \\ \mathbf{0} \end{bmatrix} \mathbf{f}_{s,k+1} + \mathbf{v}_{s,k+1} \quad (7) \\ &= h(\mathbf{Z}_{s,k+1}) + \mathbf{D}_s^u \mathbf{f}_{s,k+1}^u + \mathbf{D}_s^c \mathbf{f}_{s,k+1} + \mathbf{v}_{s,k+1} \end{aligned}$$

in which $\mathbf{y}_{s,k+1}$, $\ddot{\mathbf{x}}_{s,k+1}^m$, and $\mathbf{x}_{s,k+1}^m$ represent the observation, the measured acceleration, and the measured displacement at the time instant $t = (k+1)\Delta t$ inside the substructures, respectively. Δt is the sampling interval. \mathbf{L}_s^a and \mathbf{L}_s^d are sensor location matrices associated with the acceleration and displacement measurements, respectively. $h(\cdot)$ is a nonlinear function. $\mathbf{v}_{s,k+1}$ is the measurement noise assumed as a Gaussian white noise process, with mean value of zero and covariance matrix of $E[\mathbf{v}_{s,k+1} \mathbf{v}_{s,k+1}^T] = \mathbf{R}_{s,k+1}$.

It can be seen from Eq. (7) that $\mathbf{D}_s^u = \mathbf{0}$ if no accelerometers are installed at the locations of unknown forces, i.e. at the sub-structural interfaces or the locations of actual unknown forces, resulting in that $\mathbf{f}_{s,k+1}^u$ will not appear in the measurement equation. GEKF-UI algorithm was proposed to process the identification of time-invariant systems when $\mathbf{D}_s^u = \mathbf{0}$ [37]. According to this, the FGEKF-UI is developed by extending the GEKF-UI for the identification of time-varying substructures under the condition that interface measurements are not available.

Let $\hat{\mathbf{Z}}_{s,k|k}$ be the estimated augmented state vector at the time instant $t = k\Delta t$, the state equation is linearized at $\hat{\mathbf{Z}}_{s,k|k}$ by using the first order Taylor series expansion

$$\dot{\mathbf{Z}}_s = \mathbf{G}_{s,k|k} \mathbf{Z}_s + \mathbf{B}_s^u \mathbf{f}_s^u + \mathbf{B}_s^c \mathbf{f}_s + \left[g(\hat{\mathbf{Z}}_{s,k|k}) - \mathbf{G}_{s,k|k} \hat{\mathbf{Z}}_{s,k|k} \right] + \mathbf{w}_s \quad (8)$$

in which $\mathbf{G}_{s,k|k} = \left. \frac{\partial g(\mathbf{Z}_s)}{\partial \mathbf{Z}_s} \right|_{\mathbf{Z}_s = \hat{\mathbf{Z}}_{s,k|k}}$.

Similarly, the measurement equation can be linearized as

$$\mathbf{y}_{s,k+1} = \mathbf{H}_{s,k+1|k} \mathbf{Z}_{s,k+1} + \mathbf{D}_s^u \mathbf{f}_{s,k+1}^u + \mathbf{D}_s^c \mathbf{f}_{s,k+1} + \mathbf{h}_{s,k+1|k} + \mathbf{v}_{s,k+1} \quad (9)$$

where $\mathbf{H}_{s,k+1|k} = \frac{\partial h(\mathbf{Z}_{s,k+1})}{\partial \mathbf{Z}_{s,k+1}} \Big|_{\mathbf{Z}_{s,k+1} = \bar{\mathbf{Z}}_{s,k+1|k}}$; $\mathbf{h}_{s,k+1|k} = h(\bar{\mathbf{Z}}_{s,k+1|k}) - \mathbf{H}_{s,k+1|k} \bar{\mathbf{Z}}_{s,k+1|k}$, and $\bar{\mathbf{Z}}_{s,k+1|k}$ is estimated by

$$\bar{\mathbf{Z}}_{s,k+1|k} = \hat{\mathbf{Z}}_{s,k|k} + \int_{k\Delta t}^{(k+1)\Delta t} \left[g(\hat{\mathbf{Z}}_{s,t|k}) + \mathbf{B}_s^u \hat{\mathbf{f}}_{s,k|k}^u + \mathbf{B}_s^c \mathbf{f}_{s,k} \right] dt \quad (10)$$

If \mathbf{f}_s^u is sampled based on the first-order holder (FOH) [37] within $t \in [t_k, t_{k+1}]$, which means

$$\mathbf{f}_s^u(t) = \mathbf{f}_{s,k}^u + \frac{\mathbf{f}_{s,k+1}^u - \mathbf{f}_{s,k}^u}{\Delta t} (t - t_k) ,$$
 then the discrete form of the state equation can be described in a

recurrence form

$$\mathbf{Z}_{s,k+1} = \mathbf{A}_{s,k} \mathbf{Z}_{s,k} + \mathbf{B}_{s,k}^u \mathbf{f}_{s,k}^u + \mathbf{B}_{s,k+1}^u \mathbf{f}_{s,k+1}^u + \mathbf{B}_{s,k}^c \mathbf{f}_{s,k} + \mathbf{g}_{s,k|k} + \mathbf{w}_{s,k} \quad (11)$$

in which $\mathbf{A}_{s,k} = e^{\mathbf{G}_{s,k|k} \Delta t}$, $\mathbf{g}_{s,k|k} = (\mathbf{A}_{s,k} - \mathbf{I})(\mathbf{G}_{s,k|k} \Delta t)^{-1} \left[g(\hat{\mathbf{Z}}_{s,k|k}) - \mathbf{G}_{s,k|k} \hat{\mathbf{Z}}_{s,k|k} \right] \Delta t$,
 $\mathbf{B}_{s,k}^c = (\mathbf{A}_{s,k} - \mathbf{I})(\mathbf{G}_{s,k|k} \Delta t)^{-1} (\mathbf{B}_s^c \Delta t)$, $\mathbf{B}_{s,k}^u = \left[\mathbf{A}_{s,k} - (\mathbf{A}_{s,k} - \mathbf{I})(\mathbf{G}_{s,k|k} \Delta t)^{-1} \right] (\mathbf{G}_{s,k|k} \Delta t)^{-1} (\mathbf{B}_s^u \Delta t)$,
 $\mathbf{B}_{s,k+1}^u = \left[(\mathbf{A}_{s,k} - \mathbf{I})(\mathbf{G}_{s,k|k} \Delta t)^{-1} - \mathbf{I} \right] (\mathbf{G}_{s,k|k} \Delta t)^{-1} (\mathbf{B}_s^u \Delta t)$.

The detailed derivation of Eqs. (9) and (11) can be referred to [37].

The proposed FGKF-UI has a similar process with GEKF-UI. It is implemented in the following steps:

Time update (prediction):

The time prediction $\tilde{\mathbf{Z}}_{s,k+1|k}^p$ is defined according to Eq.(11):

$$\tilde{\mathbf{Z}}_{s,k+1|k}^p = \mathbf{A}_{s,k} \hat{\mathbf{Z}}_{s,k|k} + \mathbf{B}_{s,k}^u \hat{\mathbf{f}}_{s,k|k}^u + \mathbf{B}_{s,k+1}^u \mathbf{f}_{s,k+1}^u + \mathbf{B}_{s,k}^c \mathbf{f}_{s,k} + \mathbf{g}_{s,k|k} \quad (12)$$

in which $\hat{\mathbf{f}}_{s,k|k}^u$ is the estimated value of $\mathbf{f}_{s,k}^u$.

The predicted error of $\tilde{\mathbf{Z}}_{s,k+1|k}^p$ is defined as $\tilde{\mathbf{e}}_{s,k+1|k}^{Zp} = \mathbf{Z}_{s,k+1} - \tilde{\mathbf{Z}}_{s,k+1|k}^p$, and its corresponding covariance matrix could be presented as:

$$\tilde{\mathbf{P}}_{s,k+1|k}^{Zp} = \Lambda \begin{bmatrix} \mathbf{A}_{s,k} & \mathbf{B}_{s,k}^u \end{bmatrix} \begin{bmatrix} \hat{\mathbf{P}}_{s,k|k}^Z & \hat{\mathbf{P}}_{s,k|k}^{Zf} \\ \hat{\mathbf{P}}_{s,k|k}^{fZ} & \hat{\mathbf{P}}_{s,k|k}^f \end{bmatrix} \begin{bmatrix} \mathbf{A}_{s,k}^T \\ \mathbf{B}_{s,k}^{uT} \end{bmatrix} \Lambda^T + \mathbf{Q}_{s,k} \quad (13)$$

where $\hat{\mathbf{P}}_{s,k|k}^*$ is the corresponding estimation error covariance matrix at $t = k\Delta t$. Noted that Eq. (13) is different from the $\tilde{\mathbf{P}}_{s,k+1|k}^{Zp}$ in GEKF-UI [37], since the fading-factor matrix Λ is introduced as follows to gradually fade the previous information and track the possible changes of the parameter vector

$$\Lambda = \text{diag}[\mathbf{1}_{1 \times 2n}, \lambda \cdot \mathbf{1}_{l \times l}] \quad (14)$$

where $\lambda \geq 1$. In the first step, $\lambda = 2^{2/N_u}$ is adopted based on an existing study [40], which implies that the half-life of the contribution of a data point is N_u time steps.

Measurement update (correction):

The estimation value of $\mathbf{Z}_{s,k+1}$ is defined as $\hat{\mathbf{Z}}_{s,k+1|k+1}^c$:

$$\hat{\mathbf{Z}}_{s,k+1|k+1}^c = \tilde{\mathbf{Z}}_{s,k+1|k}^p + \mathbf{K}_{s,k+1}^g \left(\mathbf{y}_{s,k+1} - \mathbf{H}_{s,k+1|k} \tilde{\mathbf{Z}}_{s,k+1|k}^p - \mathbf{D}_{s^u}^u \mathbf{f}_{s,k+1}^u - \mathbf{D}_{s^c}^c \mathbf{f}_{s,k+1} - \mathbf{h}_{s,k+1|k} \right) \quad (15)$$

in which $\mathbf{K}_{s,k+1}^g$ is the Kalman gain matrix which can be obtained as [37]

$$\mathbf{K}_{s,k+1}^g = \tilde{\mathbf{P}}_{s,k+1|k}^{Zp} \mathbf{H}_{s,k+1|k}^T \left(\mathbf{H}_{s,k+1|k} \tilde{\mathbf{P}}_{s,k+1|k}^{Zp} \mathbf{H}_{s,k+1|k}^T + \mathbf{R}_{s,k+1} \right)^{-1} \quad (16)$$

Given the error of the estimated $\hat{\mathbf{Z}}_{s,k+1|k+1}^c$ as $\hat{\mathbf{e}}_{s,k+1|k+1}^{Zc} = \mathbf{Z}_{s,k+1} - \hat{\mathbf{Z}}_{s,k+1|k+1}^c$, its covariance matrix could be derived as:

$$\hat{\mathbf{P}}_{s,k+1|k+1}^{Zc} = \tilde{\mathbf{P}}_{s,k+1|k}^{Zp} - \mathbf{K}_{s,k+1}^g \mathbf{H}_{s,k+1|k} \tilde{\mathbf{P}}_{s,k+1|k}^{Zp} - \tilde{\mathbf{P}}_{s,k+1|k}^{Zp} \mathbf{H}_{s,k+1|k}^T \mathbf{K}_{s,k+1}^{gT} + \mathbf{K}_{s,k+1}^g \left(\mathbf{H}_{s,k+1|k} \tilde{\mathbf{P}}_{s,k+1|k}^{Zp} \mathbf{H}_{s,k+1|k}^T + \mathbf{R}_{s,k+1} \right) \mathbf{K}_{s,k+1}^{gT} \quad (17)$$

Under the condition that the number of observed measurements (sensors) is larger than that of the unknown excitations, the estimated force vector $\hat{\mathbf{f}}_{s,k+1|k+1}^u$ can be computed by the least-squares estimation as [37]

$$\hat{\mathbf{f}}_{s,k+1|k+1}^u = \mathbf{S}_{s,k+1} \left[\mathbf{y}_{s,k+1} - \mathbf{H}_{s,k+1|k} \left(\mathbf{A}_{s,k} \hat{\mathbf{Z}}_{s,k|k} + \mathbf{B}_{s,k}^u \hat{\mathbf{f}}_{s,k|k}^u + \mathbf{g}_{s,k|k} \right) - \mathbf{D}_{s^c}^c \mathbf{f}_{s,k+1} - \mathbf{h}_{s,k+1|k} \right] \quad (18)$$

where

$$\mathbf{S}_{s,k+1} = \left[\left(\mathbf{H}_{s,k+1|k} \mathbf{B}_{s,k+1}^u + \mathbf{D}_s^u \right)^T \tilde{\mathbf{R}}_{s,k+1}^{-1} \left(\mathbf{H}_{s,k+1|k} \mathbf{B}_{s,k+1}^u + \mathbf{D}_s^u \right) \right]^{-1} \left(\mathbf{H}_{s,k+1|k} \mathbf{B}_{s,k+1}^u + \mathbf{D}_s^u \right)^T \tilde{\mathbf{R}}_{s,k+1}^{-1}$$

$$\tilde{\mathbf{R}}_{s,k+1}^{-1} = \left(\mathbf{H}_{s,k+1|k} \tilde{\mathbf{P}}_{s,k+1|k}^Z \mathbf{H}_{s,k+1|k}^T + \mathbf{R}_{s,k+1} \right)^{-1}$$

And the error covariance matrix of $\hat{\mathbf{e}}_{s,k+1|k+1}^f$ ($\hat{\mathbf{e}}_{s,k+1|k+1}^f = \mathbf{f}_{s,k+1}^u - \hat{\mathbf{f}}_{s,k+1|k+1}^u$) could be given as

$$\hat{\mathbf{P}}_{s,k+1|k+1}^f = \mathbf{S}_{s,k+1} \left(\mathbf{H}_{s,k+1|k} \tilde{\mathbf{P}}_{s,k+1|k}^Z \mathbf{H}_{s,k+1|k}^T + \mathbf{R}_{s,k+1} \right) \mathbf{S}_{s,k+1}^T \quad (19)$$

Thus, by substituting the estimated unknown force vector $\mathbf{f}_{s,k+1}^u$ into Eqs.(12) and (15), the estimation value of augmented state vector could be obtained by accomplishing the process of time prediction and measurement correction.

The time prediction of structural state in FGEKF-UI is given as

$$\tilde{\mathbf{Z}}_{s,k+1|k} = \mathbf{A}_{s,k} \hat{\mathbf{Z}}_{s,k|k} + \mathbf{B}_{s,k}^u \hat{\mathbf{f}}_{s,k|k}^u + \mathbf{B}_{s,k+1}^u \hat{\mathbf{f}}_{s,k+1|k+1}^u + \mathbf{B}_{s,k}^c \mathbf{f}_{s,k} + \mathbf{g}_{s,k|k} \quad (20)$$

And structural state is updated as:

$$\hat{\mathbf{Z}}_{s,k+1|k+1} = \tilde{\mathbf{Z}}_{s,k+1|k} + \mathbf{K}_{s,k+1}^g \left(\mathbf{y}_{s,k+1} - \mathbf{H}_{s,k+1|k} \tilde{\mathbf{Z}}_{s,k+1|k} - \mathbf{D}_{s,k+1}^u \hat{\mathbf{f}}_{s,k+1|k+1}^u - \mathbf{D}_{s,k+1}^c \mathbf{f}_{s,k+1} - \mathbf{h}_{s,k+1|k} \right) \quad (21)$$

In addition, the corresponding error covariance matrices are expressed as [37]

$$\hat{\mathbf{P}}_{s,k+1|k+1}^Z = (\mathbf{I} - \mathbf{K}_{s,k+1}^g \mathbf{H}_{s,k+1|k}) \tilde{\mathbf{P}}_{s,k+1|k}^Z + \left[\mathbf{K}_{s,k+1}^g \left(\mathbf{H}_{s,k+1|k} \mathbf{B}_{s,k+1}^u + \mathbf{D}_s^u \right) - \mathbf{B}_{s,k+1}^u \right] \hat{\mathbf{P}}_{s,k+1|k+1}^f \left[\mathbf{K}_{s,k+1}^g \left(\mathbf{H}_{s,k+1|k} \mathbf{B}_{s,k+1}^u + \mathbf{D}_s^u \right) - \mathbf{B}_{s,k+1}^u \right]^T \quad (22)$$

$$\hat{\mathbf{P}}_{s,k+1|k+1}^{Zf} = \left(\hat{\mathbf{P}}_{s,k+1|k+1}^{fZ} \right)^T = - \left[\mathbf{K}_{s,k+1}^g \left(\mathbf{H}_{s,k+1|k} \mathbf{B}_{s,k+1}^u + \mathbf{D}_s^u \right) - \mathbf{B}_{s,k+1}^u \right] \hat{\mathbf{P}}_{s,k+1|k+1}^f \quad (23)$$

It is concluded from the above formulas that the accuracy of state estimation completely depends on the selection of the fading-factor matrix Λ . Theoretically, the results of estimated physical parameter vector will be more ideal if an optimal Λ is updated with time, but it will undoubtedly increase more workload. Obviously, due to the use of empirical formula in Eq. (14),

the accurate estimated time-varying parameters cannot be obtained herein. It can only roughly determine if a parameter has the time varying property. Then, the parameter vector $\boldsymbol{\theta}_s$ is further divided into a time-varying parameter vector $\boldsymbol{\theta}_{s1}$ and a time-invariant parameter vector $\boldsymbol{\theta}_{s2}$ successfully.

3.2 Step 2: Identify the time-varying physical parameters in the substructure using the integrated WM and GKF-UI method.

In the second step, a novel method based on WM and GKF-UI is proposed to quantitatively identify $\boldsymbol{\theta}_{s2}$ and scale coefficients corresponding to $\boldsymbol{\theta}_{s1}$ in the substructure using partial substructural responses.

3.2.1. Wavelet multiresolution expansion of time-varying parameters

Similar as Eq. (3), the time-varying physical parameter $\theta_{s1,i} (i=1,2,\dots,p)$ is expanded in the wavelet domain as

$$\theta_{s1,i}(t_n) \approx \sum_{l_i} \psi_{J_i, l_i} \phi_{J_i, l_i}(2^{J_i} n - l_i), \quad n=1,2,\dots,Nt \quad (24)$$

where $\theta_{s1,i}$ denotes the i -th time-varying parameter in the target substructure, p is the number of time-varying parameters, ψ_{J_i, l_i} is the scale coefficient at the scale level J_i , l_i is the number of corresponding scale coefficients, and ϕ_{J_i, l_i} is the scale function in WM.

3.2.2 Developing GKF-UI for the identification of time-varying substructure under given scale coefficients and time-invariant parameters

From Eq. (24), the time-varying physical parameter vector $\boldsymbol{\theta}_{s1}$ can be reconstructed based on the given time-invariant scale coefficient vector $\boldsymbol{\Psi}_{J,i}$ accordingly. Thus, together with the given time-invariant parameter vector $\boldsymbol{\theta}_{s2}$, the identification of time-varying parameters is converted into the identification of time-invariant parameters. Recently, the GKF-UI algorithm

has been proposed by the authors to identify the state of time-invariant system and the unknown inputs [36]. This algorithm is implemented under the condition of known physical parameters. It is still workable even when the structural measurement/observation equation does not contain the unknown excitations. Thus, by using limited measurements within the substructure, the GKF-UI algorithm can be adopted herein to estimate the structural state and unknown inputs, including the unknown sub-structural interaction forces when accelerometers are not deployed at interfaces.

The equation of motion of a time-invariant linear system is rewritten as

$$\mathbf{M}_s \ddot{\mathbf{x}}_s(t) + \mathbf{C}_s(\boldsymbol{\psi}_{J,l}, \boldsymbol{\theta}_{s2}) \dot{\mathbf{x}}_s(t) + \mathbf{K}_s(\boldsymbol{\psi}_{J,l}, \boldsymbol{\theta}_{s2}) \mathbf{x}_s(t) = \boldsymbol{\eta}_s \mathbf{f}_s(t) + \boldsymbol{\eta}_s^u \mathbf{f}_s^u(t) \quad (25)$$

Setting the state vector as $\mathbf{X}_s = [\mathbf{x}_s^T \dot{\mathbf{x}}_s^T]^T$, Eq. (25) can be changed into the system state equation as

$$\dot{\mathbf{X}}_s = \mathbf{A}_s^G \mathbf{X}_s + \begin{Bmatrix} \mathbf{0} \\ \boldsymbol{\eta}_s \end{Bmatrix} \mathbf{f}_s + \begin{Bmatrix} \mathbf{0} \\ \boldsymbol{\eta}_s^u \end{Bmatrix} \mathbf{f}_s^u + \mathbf{w}_s = \mathbf{A}_s^G \mathbf{X}_s + \mathbf{B}_s^{Gc} \mathbf{f}_s + \mathbf{B}_s^{Gu} \mathbf{f}_s^u + \mathbf{w}_s \quad (26)$$

in which \mathbf{A}_s^G is the state transformation matrix, and it is the implicit function of physical parameter vectors $\boldsymbol{\theta}_{s1}$ and $\boldsymbol{\theta}_{s2}$. Based on FOH[36], Eq.(26) is discretized into the following equation as

$$\mathbf{X}_{s,k+1} = \mathbf{A}_{s,k}^G \mathbf{X}_{s,k} + \mathbf{B}_{s,k}^G \mathbf{f}_{s,k}^u + \mathbf{B}_{s,k+1}^G \mathbf{f}_{s,k+1}^u + \mathbf{B}_{s,k}^{Gc} \mathbf{f}_{s,k} + \mathbf{w}_{s,k} \quad (27)$$

in which

$$\begin{aligned} \mathbf{A}_{s,k}^G &= e^{\mathbf{A}_s^G \Delta t}; \quad \mathbf{B}_{s,k}^G = \left[\mathbf{A}_{s,k}^G - (\mathbf{A}_{s,k}^G - \mathbf{I})(\mathbf{A}_s^G \Delta t)^{-1} \right] (\mathbf{A}_s^G \Delta t)^{-1} (\mathbf{B}_s^{Gu} \Delta t); \\ \mathbf{B}_{s,k+1}^G &= \left[(\mathbf{A}_{s,k}^G - \mathbf{I})(\mathbf{A}_s^G \Delta t)^{-1} - \mathbf{I} \right] (\mathbf{A}_s^G \Delta t)^{-1} (\mathbf{B}_s^{Gu} \Delta t); \quad \mathbf{B}_{s,k}^{Gc} = (\mathbf{A}_{s,k}^G - \mathbf{I})(\mathbf{A}_s^G \Delta t)^{-1} (\mathbf{B}_s^{Gc} \Delta t) \end{aligned} \quad (28)$$

The observation equation is written in the following form by the data fusion of acceleration and displacement measurements

$$\begin{aligned} \mathbf{y}_{s,k+1} &= \begin{bmatrix} \ddot{\mathbf{x}}_{s,k+1}^m \\ \mathbf{x}_{s,k+1}^m \end{bmatrix} = \mathbf{C}_{s,k+1}^G \mathbf{X}_{s,k+1} + \begin{bmatrix} \mathbf{L}_s^a \mathbf{M}_s^{-1} \boldsymbol{\eta}_s^u \\ \mathbf{0} \end{bmatrix} \mathbf{f}_{s,k+1}^u + \begin{bmatrix} \mathbf{L}_s^a \mathbf{M}_s^{-1} \boldsymbol{\eta}_s \\ \mathbf{0} \end{bmatrix} \mathbf{f}_{s,k+1} + \mathbf{v}_{s,k+1} \\ &= \mathbf{C}_{s,k+1}^G \mathbf{X}_{s,k+1} + \mathbf{D}_s^{Gu} \mathbf{f}_{s,k+1}^u + \mathbf{D}_s^{Gc} \mathbf{f}_{s,k+1} + \mathbf{v}_{s,k+1} \end{aligned} \quad (29)$$

in which $\mathbf{C}_{s,k+1}^G$ is the measurement matrix. Data fusion can prevent the spurious low-frequency drifts in the estimation of displacement and unknown input since acceleration and displacement responses contain high-frequency and low-frequency dynamic characteristics, respectively [36].

It is noted that the previous KF-UI methods request that all the unknown excitations are included in the observation equations, that is, matrix \mathbf{D}_s^{Gu} in Eq. (29) must be a full matrix [41,42]. However, when sub-structural acceleration responses at interfaces are not measured, that is, matrix \mathbf{D}_s^{Gu} becomes non-full rank matrix or even zero matrix, previous KF-UI methods are not applicable. This is the reason to utilize the developed GKF-UI algorithm to estimate the sub-structural state.

The proposed GKF-UI has two procedures [36]. First, the time prediction of structural state $\tilde{\mathbf{X}}_{s,k+1|k}$ is conducted as follows

$$\tilde{\mathbf{X}}_{s,k+1|k} = \mathbf{A}_{s,k}^G \hat{\mathbf{X}}_{s,k|k} + \mathbf{B}_{s,k}^G \hat{\mathbf{f}}_{s,k|k}^u + \mathbf{B}_{s,k+1}^G \hat{\mathbf{f}}_{s,k+1|k+1}^u + \mathbf{B}_{s,k}^{Gc} \mathbf{f}_{s,k} \quad (30)$$

Then the estimated $\hat{\mathbf{X}}_{s,k+1|k+1}$ in the measurement updating procedure is derived as

$$\hat{\mathbf{X}}_{s,k+1|k+1} = \tilde{\mathbf{X}}_{s,k+1|k} + \mathbf{K}_{s,k+1}^G \left(\mathbf{y}_{s,k+1} - \mathbf{C}_{s,k+1}^G \tilde{\mathbf{X}}_{s,k+1|k} - \mathbf{D}_s^{Gu} \hat{\mathbf{f}}_{s,k+1|k+1}^u - \mathbf{D}_s^{Gc} \mathbf{f}_{s,k+1} \right) \quad (31)$$

$$\mathbf{K}_{s,k+1}^G = \tilde{\mathbf{P}}_{s,k+1|k}^Z \left(\mathbf{C}_{s,k+1}^G \right)^T \left(\mathbf{C}_{s,k+1}^G \tilde{\mathbf{P}}_{s,k+1|k}^Z \left(\mathbf{C}_{s,k+1}^G \right)^T + \mathbf{R}_{s,k+1} \right)^{-1} \quad (32)$$

It can be observed from Eq. (30) that the calculation of $\tilde{\mathbf{X}}_{s,k+1|k}$ can proceed unless the value of $\hat{\mathbf{f}}_{s,k+1|k+1}^u$ is already known, which needs to be solved. Herein $\boldsymbol{\Lambda}_{s,k+1}$ is defined as

$$\begin{aligned} \boldsymbol{\Lambda}_{s,k+1} &= \mathbf{y}_{s,k+1} - \hat{\mathbf{y}}_{s,k+1|k+1} \\ &= \left(\mathbf{I} - \mathbf{C}_{s,k+1}^G \mathbf{K}_{s,k+1}^G \right) \left(\mathbf{y}_{s,k+1} - \mathbf{C}_{s,k+1}^G \left(\mathbf{A}_{s,k}^G \hat{\mathbf{X}}_{s,k|k} + \mathbf{B}_{s,k}^G \hat{\mathbf{f}}_{s,k|k}^u \right) - \mathbf{D}_s^{Gc} \mathbf{f}_{s,k+1} - \left(\mathbf{C}_{s,k+1}^G \mathbf{B}_{s,k+1}^G + \mathbf{D}_s^{Gu} \right) \hat{\mathbf{f}}_{s,k+1|k+1}^u \right) \end{aligned} \quad (33)$$

By minimizing $\Delta_{s,k+1}$, $\hat{\mathbf{f}}_{s,k+1|k+1}^u$ can be obtained using the least-squares method when the number of sensors installed on the structure (that is, the number of observed structural responses) is more than the number of unknown external excitations.

$$\hat{\mathbf{f}}_{s,k+1|k+1}^u = \mathbf{S}_{s,k+1}^G \left(\mathbf{y}_{s,k+1} - \mathbf{C}_{s,k+1}^G \left(\mathbf{A}_{s,k}^G \hat{\mathbf{X}}_{s,k|k} + \mathbf{B}_{s,k}^G \hat{\mathbf{f}}_{s,k|k}^u \right) - \mathbf{D}_{s,k+1}^{Gu} \mathbf{f}_{s,k+1} \right) \quad (34)$$

in which

$$\mathbf{S}_{s,k+1}^G = \left[\left(\mathbf{C}_{s,k+1}^G \mathbf{B}_{s,k+1}^G + \mathbf{D}_{s,k+1}^{Gu} \right)^T \tilde{\mathbf{R}}_{s,k+1}^{-1} \left(\mathbf{C}_{s,k+1}^G \mathbf{B}_{s,k+1}^G + \mathbf{D}_{s,k+1}^{Gu} \right) \right]^{-1} \left(\mathbf{C}_{s,k+1}^G \mathbf{B}_{s,k+1}^G + \mathbf{D}_{s,k+1}^{Gu} \right)^T \tilde{\mathbf{R}}_{s,k+1}^{-1} \quad (35)$$

$$\tilde{\mathbf{R}}_{s,k+1}^{-1} = \left(\mathbf{C}_{s,k+1}^G \tilde{\mathbf{P}}_{s,k+1|k}^{\mathbf{x}} \left(\mathbf{C}_{s,k+1}^G \right)^T + \mathbf{R}_{s,k+1} \right)^{-1}$$

The error covariance matrices required in the procedure are expressed as follows. Owing to the page limit, only the main formulas are listed. The detailed derivations can be referred to [36].

$$\tilde{\mathbf{P}}_{s,k+1|k}^{\mathbf{x}} = \begin{bmatrix} \mathbf{A}_{s,k}^G & \mathbf{B}_{s,k}^G \end{bmatrix} \begin{bmatrix} \hat{\mathbf{P}}_{s,k|k}^{\mathbf{x}} & \hat{\mathbf{P}}_{s,k|k}^{\mathbf{x}\mathbf{f}} \\ \hat{\mathbf{P}}_{s,k|k}^{\mathbf{f}\mathbf{x}} & \hat{\mathbf{P}}_{s,k|k}^{\mathbf{f}} \end{bmatrix} \begin{bmatrix} \left(\mathbf{A}_{s,k}^G \right)^T \\ \left(\mathbf{B}_{s,k}^G \right)^T \end{bmatrix} + \mathbf{Q}_{s,k} \quad (36)$$

$$\hat{\mathbf{P}}_{s,k+1|k+1}^{\mathbf{f}} = \mathbf{S}_{s,k+1}^G \left(\mathbf{C}_{s,k+1}^G \tilde{\mathbf{P}}_{s,k+1|k}^{\mathbf{x}} \left(\mathbf{C}_{s,k+1}^G \right)^T + \mathbf{R}_{s,k+1} \right) \mathbf{S}_{s,k+1}^{GT} \quad (37)$$

$$\hat{\mathbf{P}}_{s,k+1|k+1}^{\mathbf{x}} = \left(\mathbf{I} - \mathbf{K}_{s,k+1}^G \mathbf{C}_{s,k+1}^G \right) \tilde{\mathbf{P}}_{s,k+1|k}^{\mathbf{x}} - \tilde{\mathbf{P}}_{s,k+1|k}^{\mathbf{x}} \mathbf{C}_{s,k+1}^{GT} \mathbf{K}_{s,k+1}^{GT} + \mathbf{K}_{s,k+1}^G \left(\mathbf{C}_{s,k+1}^G \tilde{\mathbf{P}}_{s,k+1|k}^{\mathbf{x}} \mathbf{C}_{s,k+1}^{GT} + \mathbf{R}_{s,k+1} \right) \mathbf{K}_{s,k+1}^{GT} \quad (38)$$

$$\hat{\mathbf{P}}_{s,k+1|k+1}^{\mathbf{x}\mathbf{f}} = - \left[\mathbf{K}_{s,k+1}^G \left(\mathbf{C}_{s,k+1}^G \mathbf{B}_{s,k+1}^G + \mathbf{D}_{s,k+1}^{Gu} \right) - \mathbf{B}_{s,k+1}^G \right] \hat{\mathbf{P}}_{s,k+1|k+1}^{\mathbf{f}} \quad (39)$$

$$\hat{\mathbf{P}}_{s,k+1|k+1}^{\mathbf{f}\mathbf{x}} = \left(\hat{\mathbf{P}}_{s,k+1|k+1}^{\mathbf{x}\mathbf{f}} \right)^T \quad (40)$$

3.2.3 Estimation of scale coefficients and time-invariant parameters by nonlinear optimization

As can be seen from the above Section 3.2.2, the estimated state and unknown excitations are implicit functions of scale coefficient vector $\boldsymbol{\Psi}_{Jl}$ and time-invariant parameter vector $\boldsymbol{\theta}_{s2}$

$$\hat{\mathbf{X}}_s = \hat{\mathbf{X}}_s(\boldsymbol{\Psi}_{Jl}, \boldsymbol{\theta}_{s2}); \quad \hat{\mathbf{f}}_s^u = \hat{\mathbf{f}}_s^u(\boldsymbol{\Psi}_{Jl}, \boldsymbol{\theta}_{s2}) \quad (41)$$

in which $\hat{\mathbf{X}}_s$ is the estimated sub-structural state vector, and $\hat{\mathbf{f}}_s^u$ is the estimated unknown excitation vector including unknown interaction forces. Thus, the sub-structural acceleration vector can be obtained as

$$\hat{\ddot{\mathbf{x}}}_s(\boldsymbol{\psi}_{J,l}, \boldsymbol{\theta}_{s2}) = \mathbf{M}_s^{-1} \left(\boldsymbol{\eta}_s \mathbf{f}_s + \boldsymbol{\eta}_s^u \hat{\mathbf{f}}_s^u(\boldsymbol{\psi}_{J,l}, \boldsymbol{\theta}_{s2}) - \mathbf{C}_s(\boldsymbol{\psi}_{J,l}, \boldsymbol{\theta}_{s2}) \hat{\dot{\mathbf{x}}}_s(\boldsymbol{\psi}_{J,l}, \boldsymbol{\theta}_{s2}) - \mathbf{K}_s(\boldsymbol{\psi}_{J,l}, \boldsymbol{\theta}_{s2}) \hat{\mathbf{x}}_s(\boldsymbol{\psi}_{J,l}, \boldsymbol{\theta}_{s2}) \right) \quad (42)$$

where $\hat{\mathbf{x}}_s$ and $\hat{\dot{\mathbf{x}}}_s$ are the estimated sub-structural displacement and velocity response vectors, respectively.

By setting an error function between the measured acceleration $\ddot{\mathbf{x}}_s^m$ and the estimated acceleration $\hat{\ddot{\mathbf{x}}}_s$, the optimal scale coefficient vector $\hat{\boldsymbol{\psi}}_{J,l}$ and optimal time-invariant parameter vector $\hat{\boldsymbol{\theta}}_{s2}$ can be obtained by minimizing the following objective function

$$\left[\hat{\boldsymbol{\psi}}_{J,l}, \hat{\boldsymbol{\theta}}_{s2} \right] = \arg \min_{\boldsymbol{\psi}_{J,l}, \boldsymbol{\theta}_{s2}} \left(\left\| \ddot{\mathbf{x}}_s^m - \mathbf{L}_s^a \hat{\ddot{\mathbf{x}}}_s(\boldsymbol{\psi}_{J,l}, \boldsymbol{\theta}_{s2}) \right\|_2^2 \right) \quad (43)$$

Afterwards, the optimal time-varying parameter vector $\hat{\boldsymbol{\theta}}_{s1}$ in the substructure can be reconstructed successively by using Eq. (24).

3.3 Summary of the identification procedure of the proposed approach

For clear presentation, the flowchart of the proposed approach for identification of time-varying large-scale structures is shown in Fig. 1. A large-scale structure is firstly divided into several substructures, and then parallel identification is conducted for substructures.

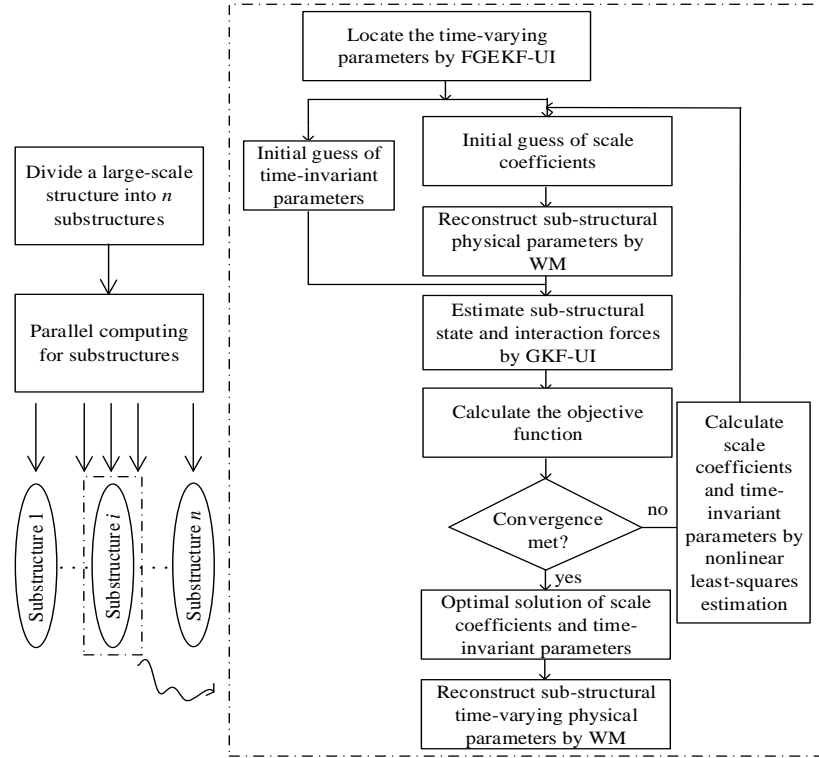


Fig. 1. Flowchart of the proposed identification approach and detail procedure in each substructure

4. Numerical validations

Numerical studies of two time-varying structures, namely, a 30-story shear frame model and a three-span truss bridge model with 55 elements, are conducted to validate the identification accuracy of the proposed approach. Compared with the numerical structures in the previous WM-based studies, for example, a 7-story shear frame by Wang et al. [24], a 10-story shear frame by Shi and Chang [22,23], and a 6-DOF plane frame by Xiang et al. [26], etc., the structures investigated in this paper are of relatively larger-scale.

4.1 Example 1: A 30-story time-varying shear frame under unknown seismic excitations

The stiffness and damping coefficients of the 30-story shear frame are time-varying and to be identified. The mass of each story is assumed to be known with $m_i = 500\text{kg} (i = 1, 2, \dots, 30)$. The shear frame is excited by the 1940 El Centro N-S earthquake excitation, but the excitation is assumed unknown in the identification. The corresponding dynamic responses are computed with

a sampling frequency of 50Hz, and the complete sampling duration is 20s. The equation of motion is given as

$$\mathbf{M}\ddot{\mathbf{x}}(t) + \mathbf{C}(t)\dot{\mathbf{x}}(t) + \mathbf{K}(t)\mathbf{x}(t) = -\mathbf{M}\{\mathbf{I}\}\ddot{x}_g(t) \quad (44)$$

where $\ddot{x}_g(t)$ is the base acceleration. Partial structural responses are used for parameter identification and are polluted by white noises with 2% in root mean square (RMS), namely

$$\ddot{\mathbf{x}}_{noisy} = \ddot{\mathbf{x}}_{clean} + 2\% \times std(\ddot{\mathbf{x}}_{clean}) \times \mathbf{rand} \quad (45)$$

where $\ddot{\mathbf{x}}_{noisy}$ is the simulated noisy acceleration response vector, $\ddot{\mathbf{x}}_{clean}$ is the noisy-free acceleration vector, $std(\ddot{\mathbf{x}}_{clean})$ means the standard deviation of $\ddot{\mathbf{x}}_{clean}$ and \mathbf{rand} is a random standard normal distribution vector.

It should be noticed that Eq. (44) is a relative motion equation. However, only absolute acceleration responses can be measured in the case of unknown base acceleration, and the inter-story displacement responses of the frame structure are easy to be measured by using the displacement sensor in practical engineering applications. The whole shear frame is divided into three substructures, as shown in Fig. 2. According to Yuen *et al.*, [19], the structural physical parameters at the lower part are more likely to change with time. Therefore, the identification of lower and middle substructures is studied in details.

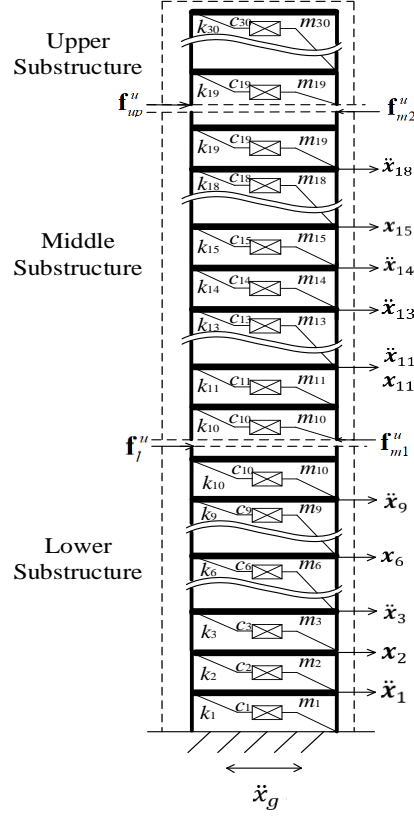


Fig. 2. Substructure for a 30-story shear frame

(1) The lower substructure

It can be observed from Fig. 2 that the lower part is a 10-DOF shear structure subjected to two unknown excitations: one is the earthquake excitation \ddot{x}_g applied to the frame base, and the other one f_l'' is the interaction force imposed on the 10th DOF of the substructure. Thus, the motion equation of the lower substructure is rewritten as

$$\mathbf{M}_s \ddot{\mathbf{x}}_s + \mathbf{C}_s(t) \dot{\mathbf{x}}_s(t) + \mathbf{K}_s(t) \mathbf{x}_s(t) = -\mathbf{M}_s \{\mathbf{I}\} \ddot{x}_g + \boldsymbol{\eta}_l'' f_l'' \quad (46)$$

where $\boldsymbol{\eta}_l''$ is the unknown interaction force location matrix. The physical parameters in the lower substructure are defined as

$$\begin{aligned}
k_2 &= \begin{cases} 1 \times 10^4 \text{ kN/m}, & 0 \text{ s} \leq t < 10.2 \text{ s} \\ 0.8 \times 10^4 \text{ kN/m}, & 10.2 \text{ s} \leq t \leq 20 \text{ s} \end{cases} \\
k_7 &= \begin{cases} 1 \times 10^4 \text{ kN/m}, & 0 \text{ s} \leq t < 15.4 \text{ s} \\ 0.85 \times 10^4 \text{ kN/m}, & 15.4 \text{ s} \leq t \leq 20 \text{ s} \end{cases} \\
k_i &= 1 \times 10^4 \text{ kN/m}, \quad 0 \text{ s} \leq t \leq 20 \text{ s} \quad (i = 1, 3, \dots, 6, 8, 9, 10) \\
c_2 &= \begin{cases} 20 \text{ kN}\cdot\text{s/m}, & 0 \text{ s} \leq t < 10.2 \text{ s} \\ 30 \text{ kN}\cdot\text{s/m}, & 10.2 \text{ s} \leq t \leq 20 \text{ s} \end{cases} \\
c_i &= 20 \text{ kN}\cdot\text{s/m}, \quad 0 \text{ s} \leq t \leq 10 \text{ s} \quad (i = 1, 3, \dots, 10)
\end{aligned}$$

Fig. 2 also shows the location of accelerometers and inter-story displacement gauges for measuring vibration responses. For the lower substructure, the absolute accelerations of the 1st, 3rd, 9th floor and the inter-story displacements of the 2nd-3rd and 6th-7th floors are used as partial measurements. It shall be noted that no sensors have to be placed at the interface DOF in this proposed approach. Thus, the measurement equation of the lower substructure is expressed as

$$\mathbf{y}_{s,k+1} = \begin{bmatrix} \mathbf{L}_s^a (\ddot{\mathbf{x}}_{s,k+1} + \{\mathbf{I}\} \ddot{\mathbf{x}}_g) \\ \mathbf{L}_s^d \cdot \boldsymbol{\zeta}_s^d \cdot \mathbf{x}_{s,k+1} \end{bmatrix} = \begin{bmatrix} \mathbf{L}_s^a \mathbf{M}_s^{-1} (-\mathbf{C}_{s,k+1} \dot{\mathbf{x}}_{s,k+1} - \mathbf{K}_{s,k+1} \mathbf{x}_{s,k+1}) \\ \mathbf{L}_s^d \cdot \boldsymbol{\zeta}_s^d \cdot \mathbf{x}_{s,k+1} \end{bmatrix} + \begin{bmatrix} \mathbf{L}_s^a \mathbf{M}_s^{-1} \boldsymbol{\eta}_l^u \\ \mathbf{0} \end{bmatrix} \mathbf{f}_l^u \quad (47)$$

where $\boldsymbol{\zeta}_s^d$ is the inter-story displacement conversion matrix. It is obvious that the unknown seismic excitation $\ddot{\mathbf{x}}_g$ does not appear in the measurement equation. Furthermore, the unknown interaction force \mathbf{f}_l^u is not included either in the measurement equation without accelerometer placed at the interface story. This explains the motivation why the ‘‘generalized’’ Kalman filter algorithms with unknown input are adopted in the proposed approach to identify the sub-structural time-varying physical parameters.

In the first step, the FGEKF-UI algorithm is implemented to locate the time-varying parameters in the lower substructure. $\lambda = 2^{2/50} = 1.03$ [40] is used in this case, which indicates that the half-life is 50 time steps. Identification results of time-varying stiffness and damping parameters are shown in Figs. 3 and 4.

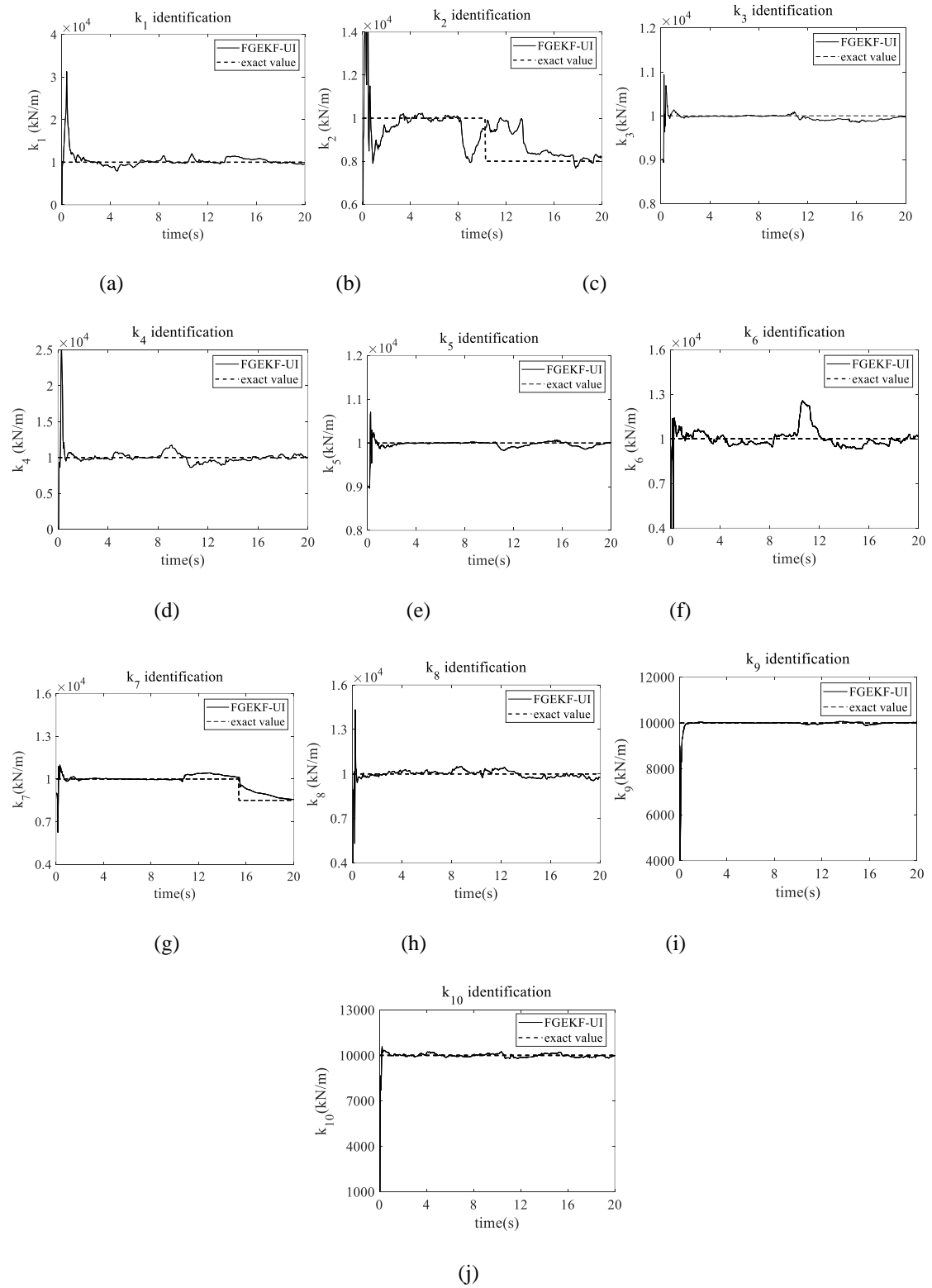


Fig. 3. Location of time-varying stiffness parameters using FGEKF-UI in the lower substructure: (a)

k_1 ; (b) k_2 ; (c) k_3 ; (d) k_4 ; (e) k_5 ; (f) k_6 ; (g) k_7 ; (h) k_8 ; (i) k_9 ; (j) k_{10}

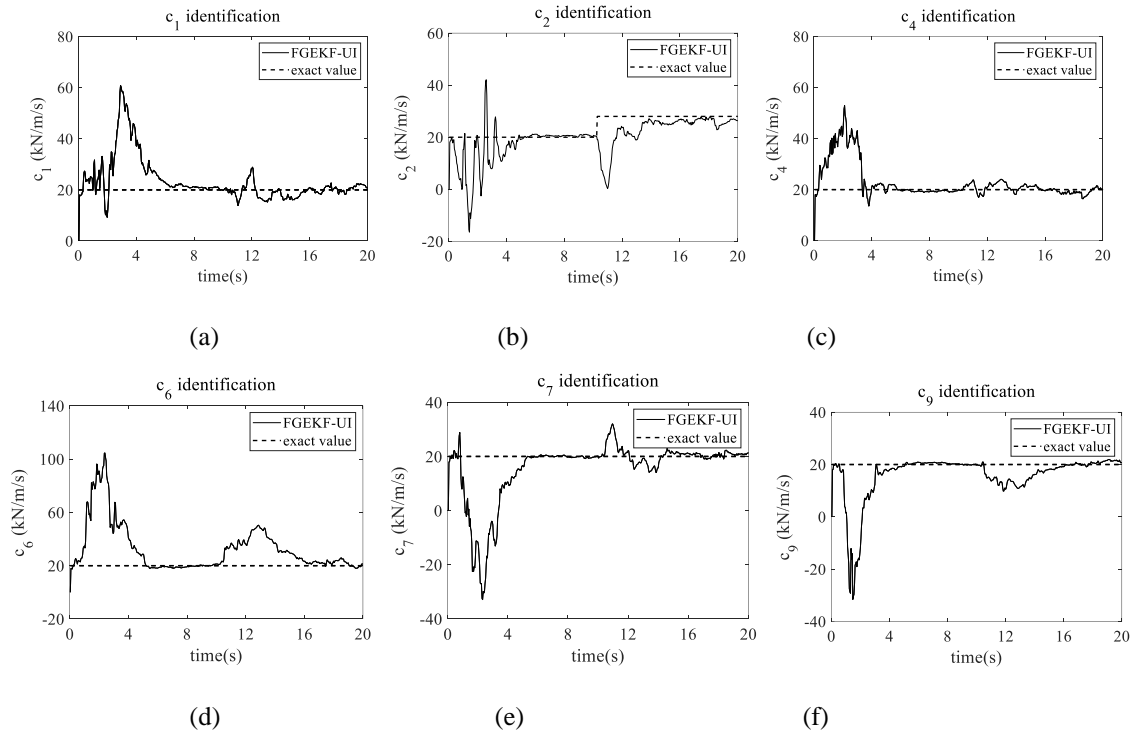


Fig. 4. Location of partial time-varying damping parameters using FGEKF-UI in the lower substructure:

(a) c_1 ; (b) c_2 ; (c) c_4 ; (d) c_6 ; (e) c_7 ; (f) c_9 .

It is observed from Fig. 3 that the stiffness parameters of the second and seventh stories are more likely to have the time-varying properties, while other stiffness values are more likely to remain unchanged. Likewise, the damping of the second story is identified as a time-varying parameter, as shown in Fig. 4. However, since the identified physical parameters are varied gradually, it is difficult to determine the exact beginning and end time instants and the form of stiffness variation.

In the second step, Db1 is adopted as the mother wavelet function for abruptly varying case as suggested by Chang and Shi [43] and the scale level $J = 8$ is used to expand the time-varying stiffness and damping parameters by WM. Thus, the identification of 10,000 unknown stiffness parameter coefficients in the time-domain is converted to the identification of eight scale coefficients of time-varying stiffness parameters k_2 and k_7 , and other eight time-invariant stiffness parameters. Similarly, the dimension of 10,000 damping coefficients in time-domain is reduced to four scale coefficients of time-varying damping parameter c_2 and other nine time-

invariant damping parameters. Based on the integrated WM and GKF-UI method, the time-varying and time-invariant structural stiffness and damping parameters are shown in Figs. 5-6 with comparisons to their exact values.

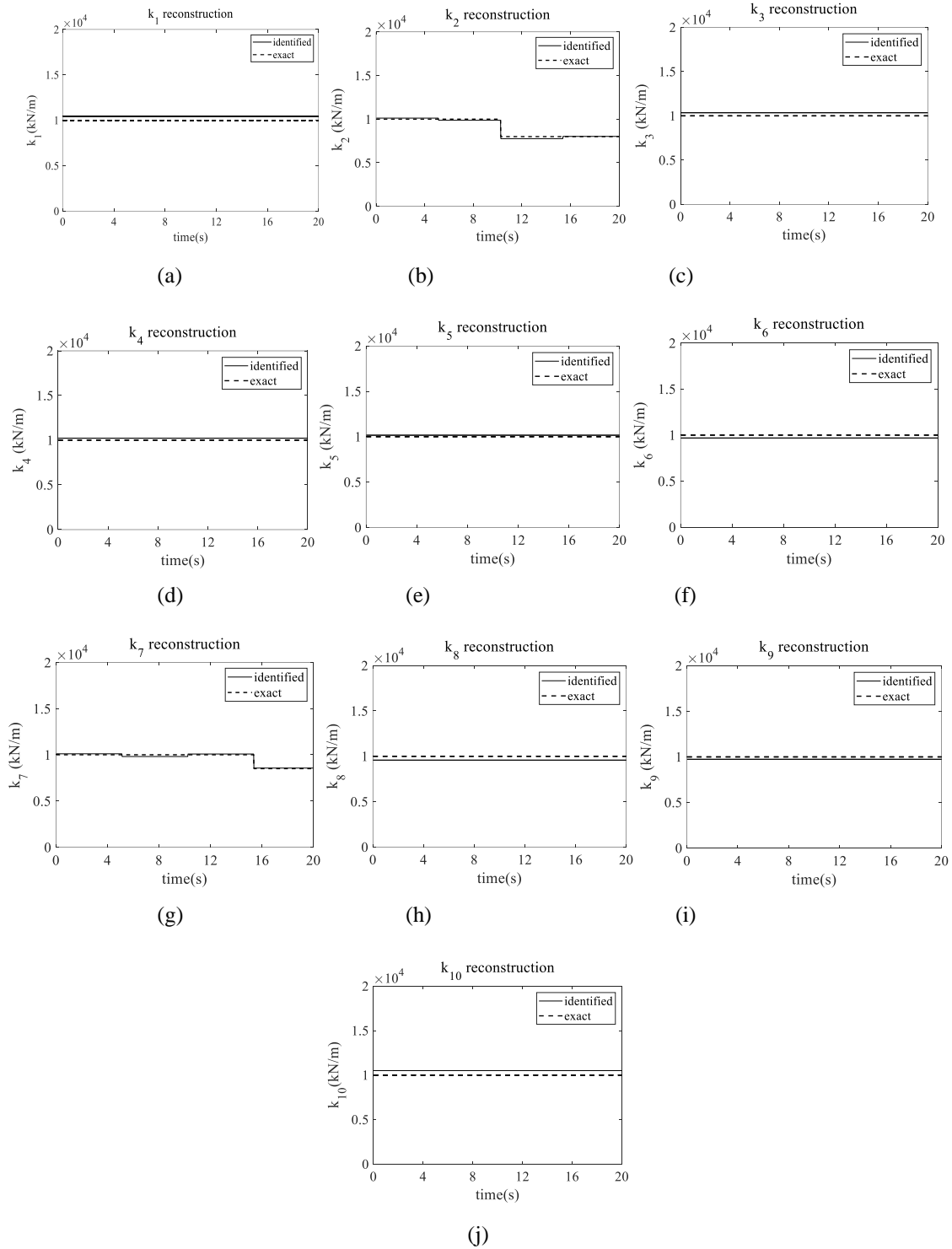


Fig. 5. Comparison of the identified stiffness parameters in the lower substructure: (a) k_1 ; (b) k_2 ; (c) k_3 ; (d) k_4 ; (e) k_5 ; (f) k_6 ; (g) k_7 ; (h) k_8 ; (i) k_9 ; (j) k_{10} .

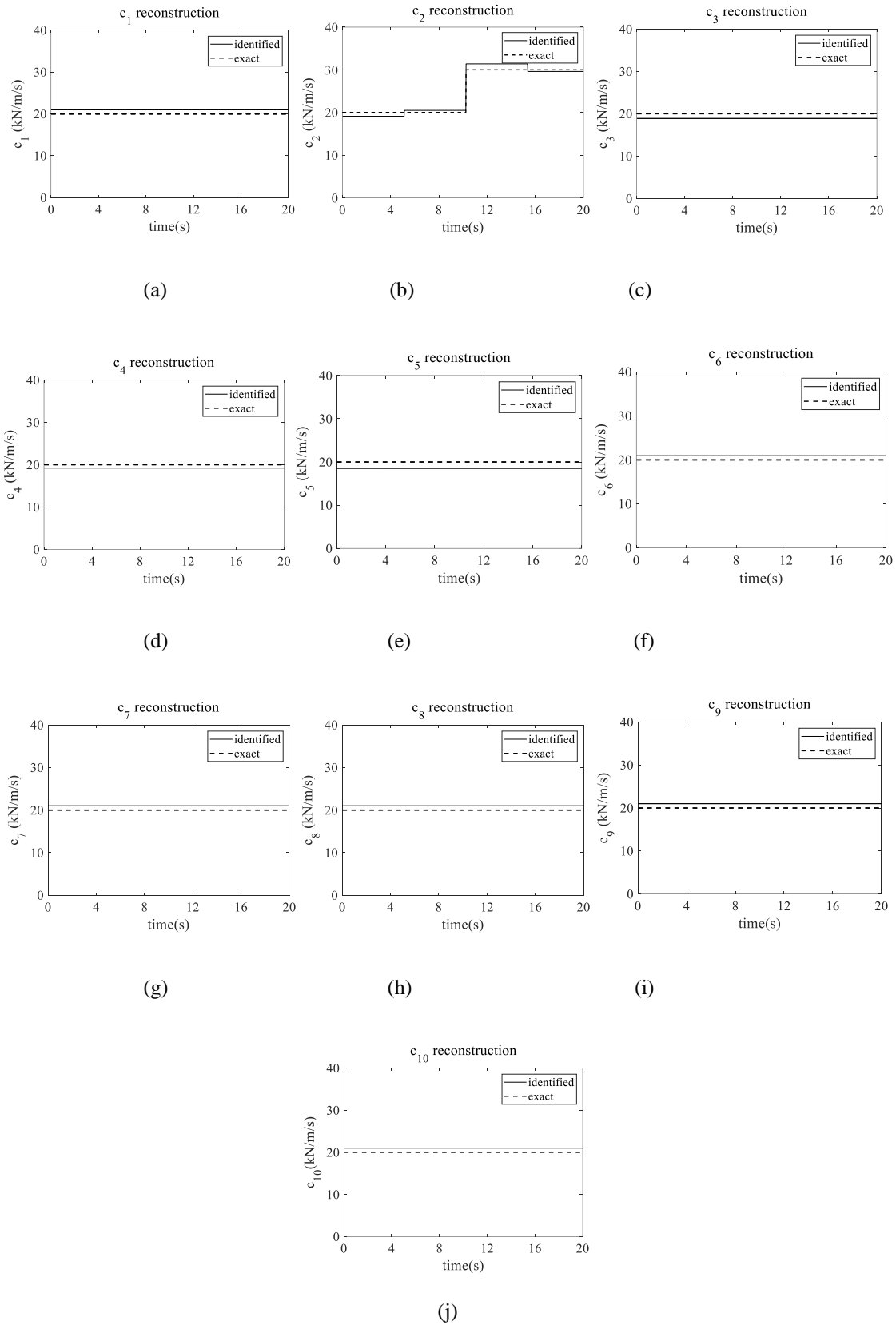


Fig. 6. Comparison of the identified damping parameters in the lower substructure: (a) c_1 ; (b) c_2 ; (c) c_3 ; (d) c_4 ; (e) c_5 ; (f) c_6 ; (g) c_7 ; (h) c_8 ; (i) c_9 ; (j) c_{10}

The precise tracking of the time instant and varying extent illustrate that the proposed approach can effectively track the abrupt change of structural physical parameters in the lower substructure. Furthermore, the identification of other time-invariant parameters also shows a high precision.

(2) The middle substructure

As can be seen from Fig. 2, the middle substructure contains the 10th-19th DOFs, which is subjected to the seismic excitation and two unknown interaction forces. It is assumed that the time-varying stiffness parameter k_{15} is set to be in a linearly changing form, and other stiffness parameters are constant, which are specified as

$$\begin{aligned}
 k_i &= 1 \times 10^4 \text{ kN/m}, \quad 0 \text{ s} \leq t \leq 20 \text{ s} (i = 10, \dots, 14, 16, \dots, 19) \\
 k_{15} &= \begin{cases} 1 \times 10^4 \text{ kN/m}, & 0 \text{ s} \leq t < 5 \text{ s} \\ -250t + 11250 (\text{kN/m}), & 5 \text{ s} \leq t \leq 13 \text{ s} \\ 0.8 \times 10^4 \text{ kN/m}, & 13 \text{ s} < t \leq 20 \text{ s} \end{cases} \\
 c_i &= 20 \text{ kN}\cdot\text{s/m}, \quad 0 \text{ s} \leq t \leq 10 \text{ s} (i = 10, \dots, 19)
 \end{aligned}$$

Four acceleration responses at the 11th, 13th, 14th and 18th DOFs are used in the analysis, with data fusion of inter-story displacement responses at the 11th-12th and 15th-16th DOFs. Because of more interaction forces than that in the lower substructure, more sensors are required for the physical parameter identification of the middle substructure. However, it is noted that it is not necessary to measure the responses at the interface DOFs.

Firstly, the time-varying physical parameters are detected based on the FGEKF-UI algorithm. Only partial identification results are shown in Fig. 7, owing to a large number of parameters in this substructure and page limitation. Most physical parameters converge to fixed values despite occasional fluctuations, except for k_{15} . Then k_{15} is expanded by WM with $J = 6$ using Db3 as the wavelet function as suggested by Chang and Shi [43]. The number of unknown variables in the nonlinear least-squares process is 35 in total, including 16 scale coefficients for k_{15} , 9 parameters for other time-invariant stiffness and 10 parameters for time-invariant damping. Fig. 8 illustrates that both the gradually varying and time-invariant stiffness parameters in the middle

substructure can be accurately identified. The identification results of damping parameters are also acceptable, which are shown in Fig. 9.

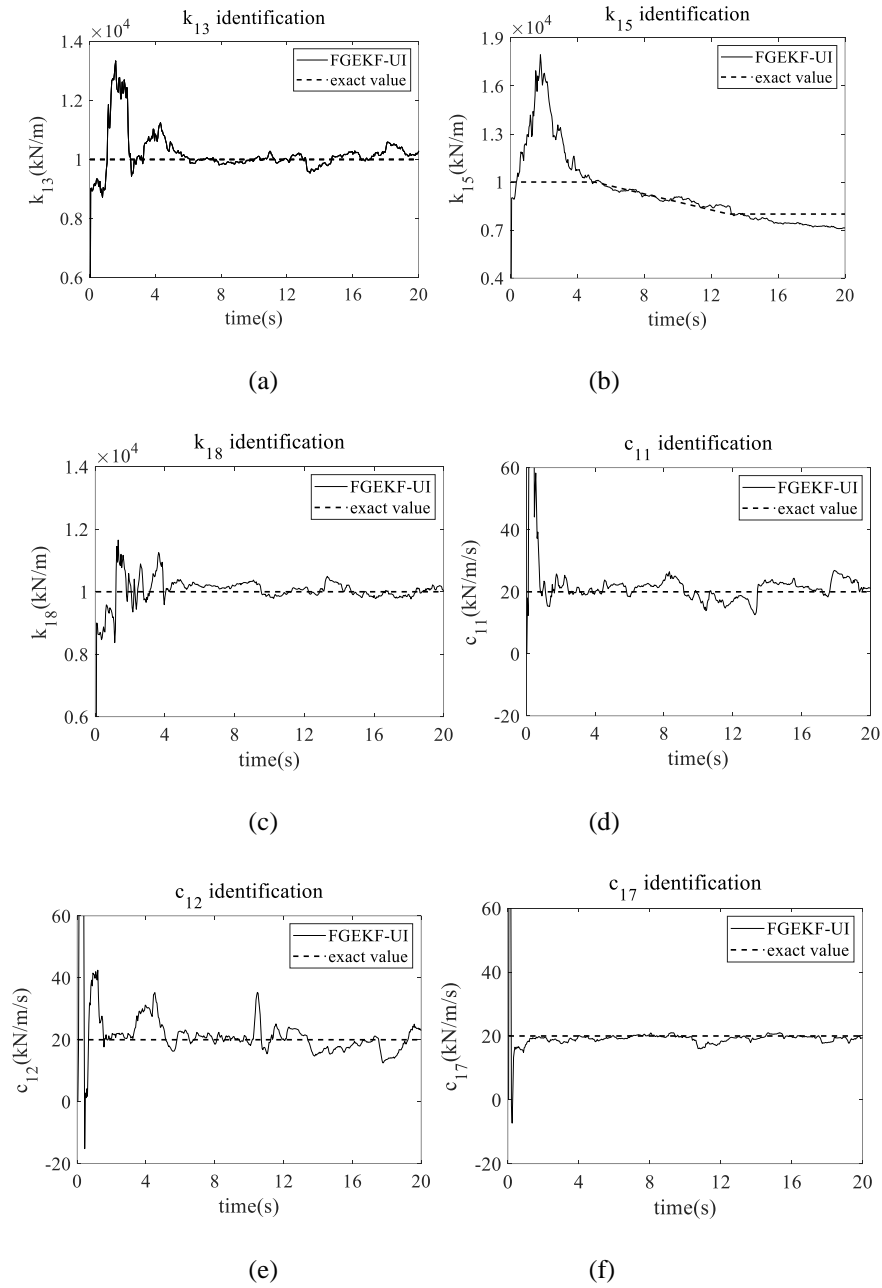


Fig. 7. Location of partial time-varying physical parameters using FGEKF-UI in the middle substructure:

(a) k_{13} ; (b) k_{15} ; (c) k_{18} ; (d) c_{11} ; (e) c_{12} ; (f) c_{17} .

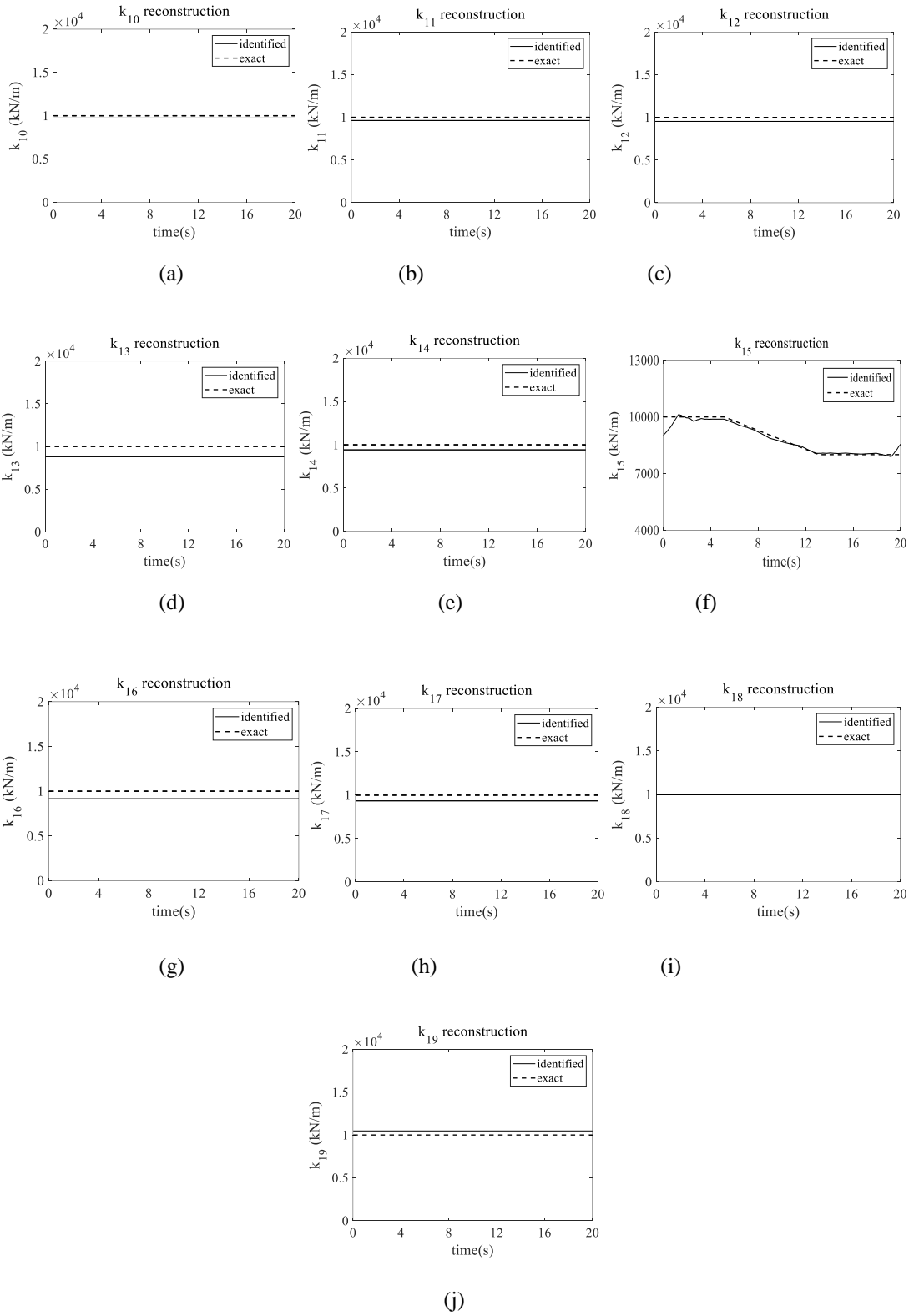


Fig. 8. Comparison of identified stiffness parameters in the middle substructure: (a) k_{10} ; (b) k_{11} ; (c) k_{12} ; (d) k_{13} ; (e) k_{14} ; (f) k_{15} ; (g) k_{16} ; (h) k_{17} ; (i) k_{18} ; (j) k_{19} .

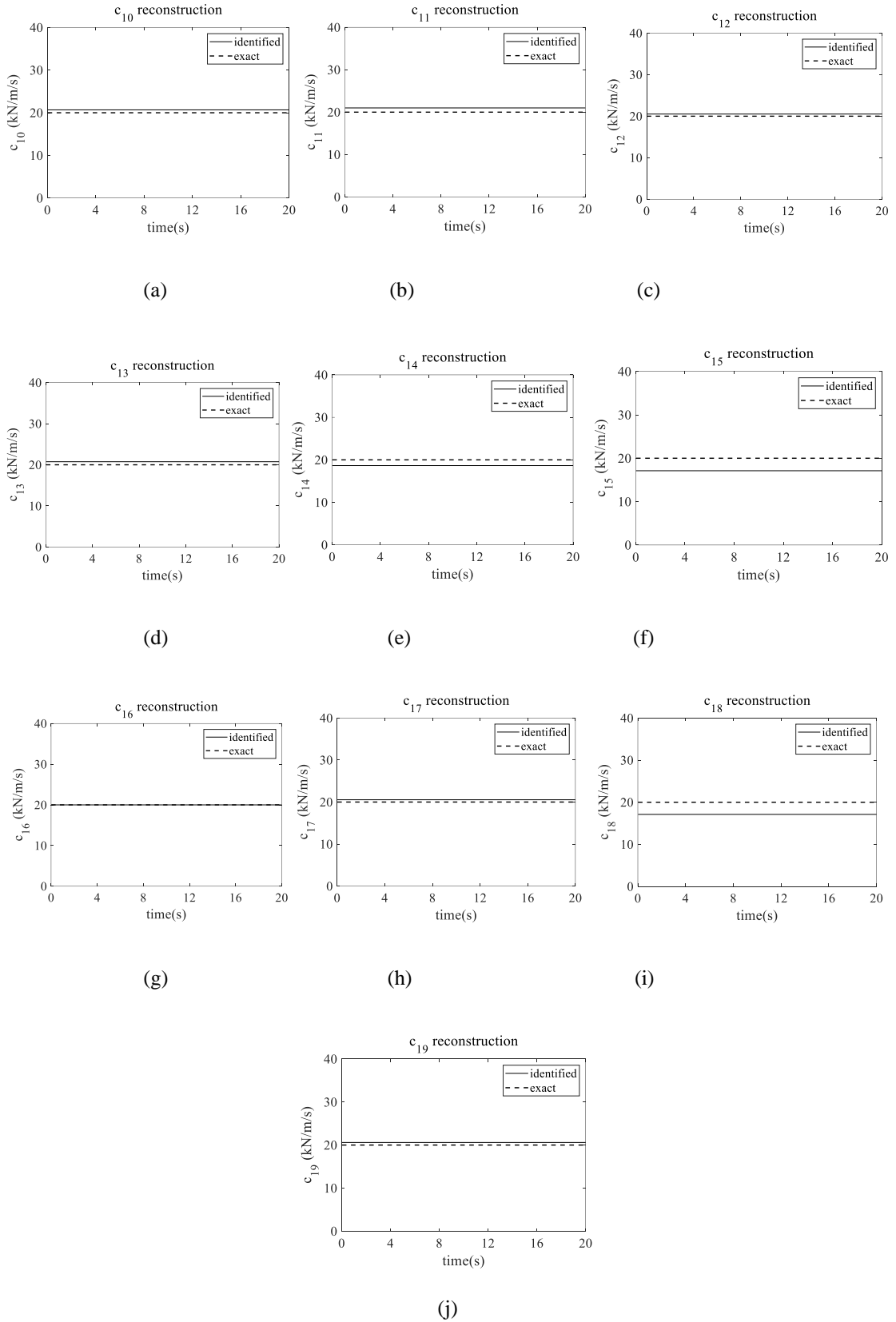


Fig. 9. Comparison of identified damping parameters in the middle substructure: (a) c_{10} ; (b) c_{11} ; (c) c_{12} ; (d) c_{13} ; (e) c_{14} ; (f) c_{15} ; (g) c_{16} ; (h) c_{17} ; (i) c_{18} ; (j) c_{19} .

4.2 Example 2: A three-span truss bridge model under unknown external excitation

To further demonstrate the performance of the proposed approach for the identification of time-varying parameters in other types of structures, a three-span truss bridge model with 55 members as shown in Fig. 10(a) is utilized as another numerical example.

This three-span truss bridge model contains 55 members, 50 DOFs and 29 nodes in total. The length and cross-section of each bar is set to be $l_i=1\text{m}$ and $A_i=0.785\text{cm}^2$ ($i=1,\dots,55$), respectively. The total mass of each bar is constant and known as $m_i=5.495\text{kg}$ ($i=1,\dots,55$). The first four modal frequencies of the time-invariant bridge model are 1.28, 3.13, 5.45 and 5.64Hz. The Rayleigh damping model is adopted with the first two damping ratios assumed as 0.02. An unknown white noise excitation \mathbf{f}_1'' is applied at the 12th DOF. The sampling frequency is set as 50 Hz for dynamic response calculation. The whole truss bridge model is divided into two substructures. Herein only the detailed identification process of the left substructure is presented due to page space.

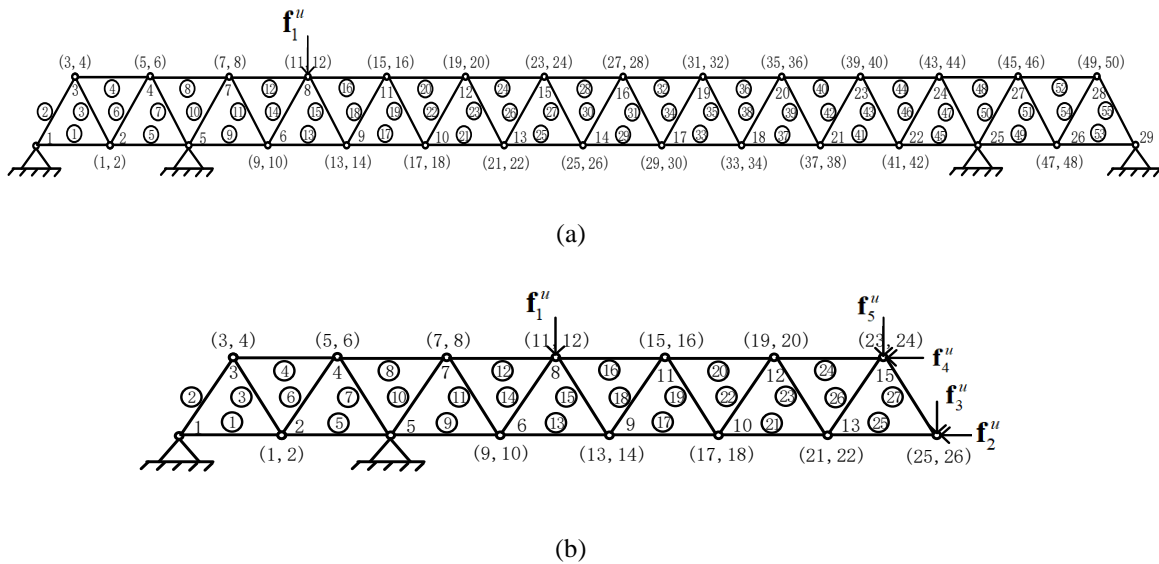


Fig. 10. Substructure formulation in a three-span truss: (a) complete structure; and (b) left substructure.

(Notes: ①,②...are the number of members. (1,2) represents the number of DOFs, in which the former one is the horizontal DOF and the latter one is the vertical DOF, and so on.)

Fig. 10(b) indicates that the left substructure consists of 27 members and 26 DOFs. Apart from unknown white noise excitation \mathbf{f}_1'' , the other four unknown interface forces are also imposed on the substructure which are shown as $\mathbf{f}_i'' (i = 2, \dots, 5)$. These interface forces are generated by the interaction between substructures. The stiffness parameters of the left substructure are to be identified and their changing forms are assumed as

$$k_{14} = \begin{cases} 157 \text{ kN/m}, & 0 \leq t < 10.2 \text{ s} \\ 126 \text{ kN/m}, & 10.2 \leq t \leq 20 \text{ s} \end{cases}$$

$$k_{16} = \begin{cases} 157 \text{ kN/m}, & 0 \leq t < 15.4 \text{ s} \\ 133 \text{ kN/m}, & 15.4 \leq t \leq 20 \text{ s} \end{cases}$$

$$k_i = 157 \text{ kN/m}, \quad 0 \leq t \leq 20 \text{ s} (i = 1, \dots, 13, 15, 17, \dots, 27)$$

Acceleration responses at the 2nd, 8th, 10th, 19th - 22nd and 24th DOFs, and displacement responses at the 4th and 16th DOFs from the left substructure are assumed being recorded and used for identification analysis, and the numerically calculated results are added with a 2% RMS white noise to consider the effect of noise. The proposed approach is used in this case as not all the unknown interaction forces appear in the observation equation.

There are totally 27,000 stiffness coefficients in the time-domain to be identified inside the substructure. Firstly, the proposed FGEKF-UI is applied to find out the time-varying stiffness parameters in the left substructure. Fig. 11 shows the localization results of several elemental stiffness. It is observed that the stiffness parameters of the 14th and 16th elements are more likely to be time varying, since they transit from one stable converged value to another stable value.

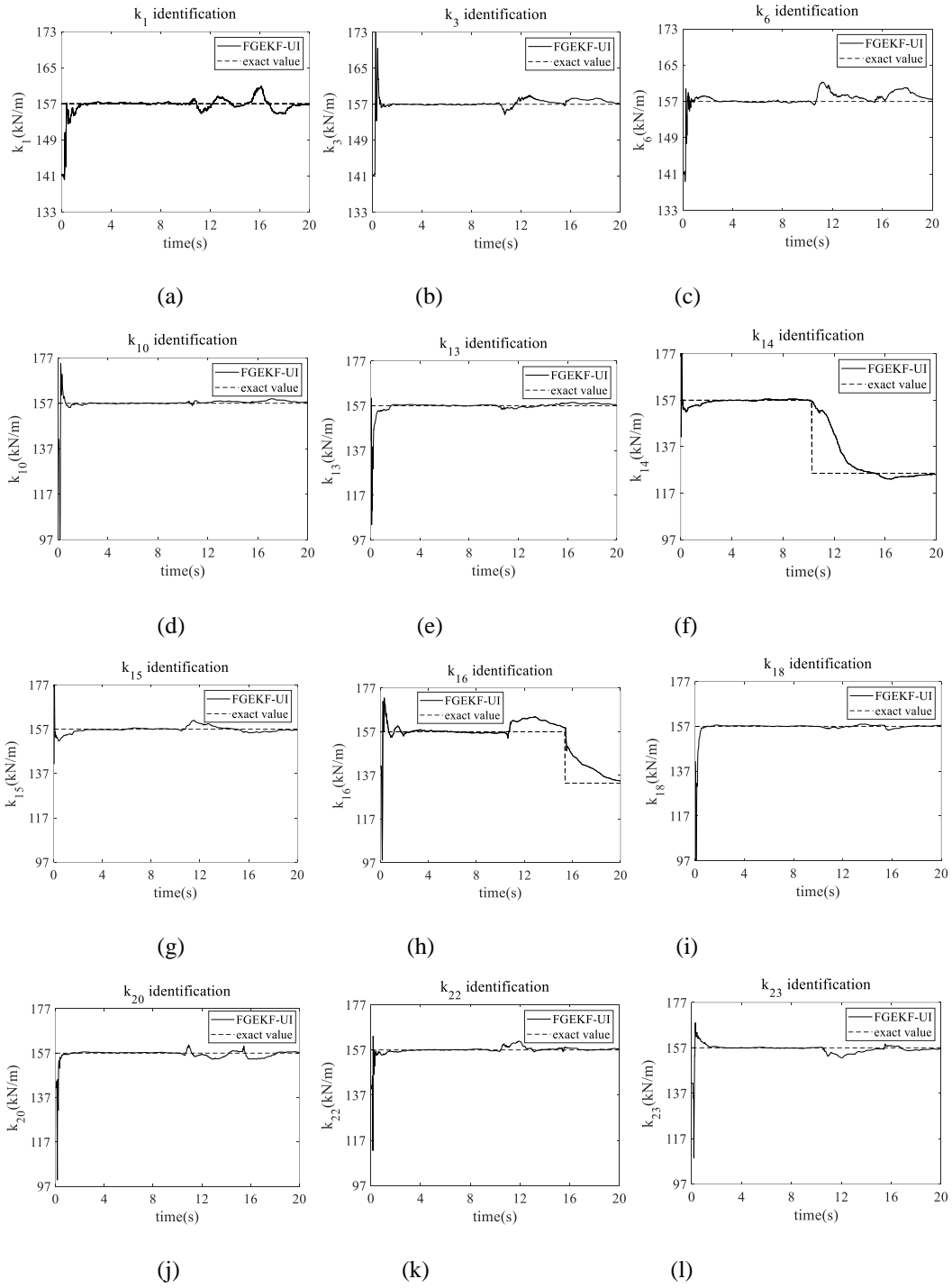


Fig. 11. Location of time-varying stiffness parameters using FGEKF-UI in the left substructure: (a) k_1 ; (b) k_3 ; (c) k_6 ; (d) k_{10} ; (e) k_{13} ; (f) k_{14} ; (g) k_{15} ; (h) k_{16} ; (i) k_{18} ; (j) k_{20} ; (k) k_{22} ; (l) k_{23} .

Secondly, Db1 is applied as the wavelet function according to Chang and Shi [43] and the scale level is defined as $J = 8$ to expand the time-varying stiffness coefficients, transforming the parameters to be identified as 8 scale coefficients and 25 time-invariant stiffness parameters.

According to the identification results as shown in Fig. 12 and Table 1, it is validated that the proposed approach is capable of identifying the time-varying or time-invariant stiffness parameters in the bridge truss model. Only partial results are shown in Fig. 12 due to the page limitation, and more final identified values of time-invariant stiffness can be found in Table 1 in detail. Furthermore, the identification accuracy of the unknown white noise excitation is also good, compared with the exact value used as input in calculating the dynamic responses of the truss model as shown in Fig. 13.

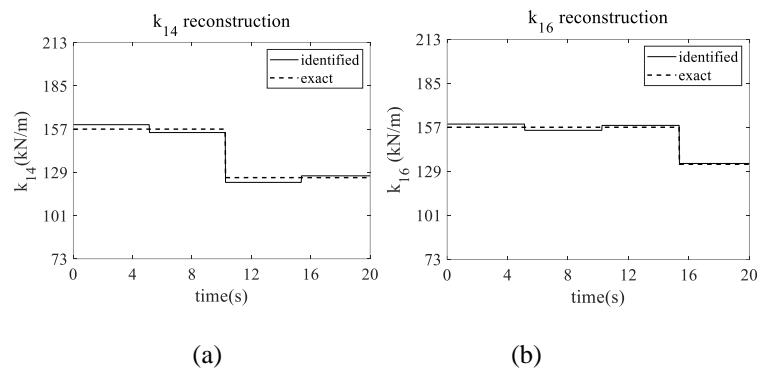


Fig. 12. Comparison of the identified stiffness of members with stiffness change in the left substructure:

(a) k_{14} ; (b) k_{16} .

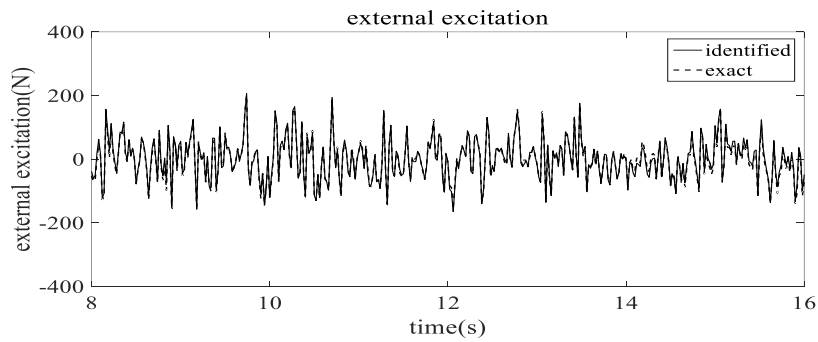


Fig. 13. Comparison of the identified external excitation to the truss structure (8s -16s)

Table 1 Identified stiffness of time-invariant members in the left substructure

Member No.	Actual Stiffness (kN/m)	Identified Stiffness (kN/m)	Relative Error
1	157.00	154.65	-1.50%
2	157.00	160.69	2.35%
3	157.00	149.75	-4.62%
4	157.00	159.34	1.49%
5	157.00	162.57	3.55%
6	157.00	164.68	4.89%
7	157.00	154.31	-1.71%
8	157.00	156.85	-0.10%
9	157.00	157.77	0.49%
10	157.00	155.47	-0.97%
11	157.00	158.99	1.27%
12	157.00	159.17	1.38%
13	157.00	156.28	-0.46%
15	157.00	160.14	2.00%
17	157.00	157.38	0.24%
18	157.00	158.36	0.87%
19	157.00	155.73	-0.81%
20	157.00	156.00	-0.64%
21	157.00	154.59	-1.53%
22	157.00	153.27	-2.38%
23	157.00	157.42	0.27%
24	157.00	156.46	-0.34%
25	157.00	155.98	-0.65%
26	157.00	158.36	0.86%
27	157.00	162.11	3.26%

5. Conclusions

In this paper, a novel two-step approach is proposed to identify the time-varying physical parameters of large-scale structures with incomplete measurements and unknown inputs. The proposed approach is based on the sub-structural technique and conducted in two-step by parallel computing. In the first step, the time-varying physical parameters are localized by the proposed FGEKF-UI algorithm, and then the time-varying physical parameters are identified using the integrated WM and GKF-UI method in the second step. The main contributions of this paper are listed as follows.

- (i) A new two-step approach is proposed for the identification of large-scale linear structure with time-varying physical parameters using only partially measured structural responses;

- (ii) FGEKF-UI is firstly proposed to locate the time-varying parameters and enable dimensionality reduction of scale coefficients to the greatest extent, resulting in only a few variables involved in the optimization process;
- (iii) GKF-UI is used to estimate the sub-structural state, where the known interaction forces and full observations are not required, and observations at the interface are not required either. The effect of measurement noise is minimized, owing to that GKF-UI algorithm itself can include the influence of modelling error and measurement noise;
- (iv) The proposed approach can be applied to each substructure independently by parallel computing, which greatly simplifies the difficulties in identifying large-scale time-varying structural parameters;

Numerical results of identifying time-varying physical parameters of a 30-story shear frame and a three-span truss bridge model demonstrate the proposed approach can effectively identify the abruptly changing, gradually varying and time-invariant stiffness and damping parameters. The structures investigated in this paper are of relatively larger-scale compared with the numerical structures in the previous WM-based studies. Moreover, the external excitations can be unknown in both cases and can also be identified. Experimental studies on a large-scale shear frame structure are being conducted to further verify the effectiveness of the proposed approach, which will be reported subsequently. Further studies on the identification of time-varying physical parameters of large-scale nonlinear structures will be conducted in future.

Acknowledgments

This research is supported by the National Natural Science Foundation of China through the key project No. 51838006.

References

- [1] Bao YQ, Chen ZC, Wei SY, Xu Y, Tang ZY, Li H. The state of the art of data science and engineering in structural health monitoring. *Engineering* 2019; 5(2):234-242.

- [2] Amezcuita-Sanchez JP, Adeli H. Signal processing techniques for vibration-based health monitoring of smart structures. *Archives of Computational Methods in Engineering* 2016; 23(1): 1-15.
- [3] Li JT, Zhu XQ, Law SS, Samali B. Time-varying characteristics of bridges under the passage of vehicles using synchroextracting transform. *Mechanical Systems and Signal Processing* 2020; 140: 106727.1-106727.19.
- [4] Xin Y, Hao H, Li J. Operational modal identification of structures based on improved empirical wavelet transform. *Structural Control and Health Monitoring* 2019; 26: e2323.
- [5] Poulimenos AG, Fassois SD. Parametric time-domain methods for non-stationary random vibration modelling and analysis-A critical survey and comparison. *Mechanical Systems and Signal Processing* 2006; 20(4):763-816.
- [6] Poulimenos AG, Fassois SD. Output-only stochastic identification of a time-varying structure via functional series TARMA models. *Mechanical Systems and Signal Processing* 2009; 23(4): 1180-1204.
- [7] Nagarajaiah S, Basu B. Output only modal identification and structural damage detection using time frequency & wavelet techniques. *Earthquake Engineering and Engineering Vibration* 2009; 8(4): 583-605.
- [8] Wang ZC, Ren WX, Chen GD. Time-frequency analysis and applications in time-varying/nonlinear structural systems: a state-of-the-art review. *Advances in Structural Engineering* 2018; 21: 1562-1584.
- [9] Yang JN, Lei Y, Pan SW, Huang N. System identification of linear structures based on Hilbert-Huang spectral analysis. Part 1: normal modes. *Earthquake Engineering and Structural Dynamics* 2003; 32:1443-1467.
- [10] Ni PH, Li J, Hao H, Xia Y, Wang XY, Lee JM, Jung KH. Time-varying system identification using variational mode decomposition. *Structural Control and Health Monitoring* 2018; 25: e2175.
- [11] Chen GD, Wang ZC. A signal decomposition theorem with Hilbert transform and its application to narrowband time series with closely spaced frequency components. *Mechanical Systems and Signal Processing* 2012; 28: 258-279.
- [12] Qu HY, Li TT, Chen GD. Multiple analytical mode decompositions for nonlinear system identification from forced vibration. *Engineering Structures* 2018; 173: 979-986.
- [13] Xin Y, Hao H, Li J. Time-varying system identification by enhanced Empirical Wavelet Transform based on Synchroextracting Transform. *Engineering Structures* 2019; 196: 109313.

- [14] Yang YC, Nagarajaiah S. Blind identification of damage in time-varying systems using independent component analysis with wavelet transform. *Mechanical Systems and Signal Processing* 2014; 47: 3-20.
- [15] Amezcuita-Sanchez JP, Adeli H. Synchrosqueezed wavelet transform-fractality model for locating, detecting, and quantifying damage in smart highrise building structures. *Smart Materials and Structures* 2015; 24(6):065034.
- [16] Liu JL, Zheng JY, Wei XJ, Ren WX, Laory I. A combined method for instantaneous frequency identification in low frequency structures. *Engineering Structures* 2019; 194: 370-383.
- [17] Lin JW, Betti R, Smyth AW, Longman RW. On-line identification of nonlinear hysteretic structural systems using a variable trace approach. *Earthquake Engineering and Structural Dynamics* 2001; 30(9):1279-1303.
- [18] Mu HQ, Kuok SC, Yuen KV. Stable robust extended Kalman filter. *Journal of Aerospace Engineering* 2016: B4016010.
- [19] Yuen KV, Kuok SC, Dong L. Self-calibrating Bayesian real-time system identification. *Computer-Aided Civil and Infrastructure Engineering* 2019; 34: 806–821.
- [20] Yuen KV, Mu HQ. Real-time system identification: an algorithm for simultaneous model class selection and parametric identification. *Computer-Aided Civil and Infrastructure Engineering* 2015; 30(10):785-801.
- [21] Yang JN, Lin SL. On-line identification of non-linear hysteretic structures using an adaptive tracking technique. *International Journal of Non-Linear Mechanics* 2004; 39(9):1481–1491.
- [22] Shi YF, Chang CC. Substructural time-varying parameter identification using wavelet multiresolution approximation. *Journal of Engineering Mechanics* 2012; 138(1): 50-59.
- [23] Shi YF, Chang CC. Wavelet-based identification of time-varying shear-beam buildings using incomplete and noisy measurement data. *Nonlinear Engineering* 2013; 2 (1-2): 29-37.
- [24] Wang C, Ai DM, Ren WX. A wavelet transform and substructure algorithm for tracking the abrupt stiffness degradation of shear structure. *Advances in Structural Engineering* 2019; 22(5):1136-1148.
- [25] Wang C, Ren WX, Wang ZC, Zhu HP. Time-varying physical parameter identification of shear type structures based on discrete wavelet transform. *Smart Structures and Systems* 2014; 14(5): 831-845.
- [26] Xiang M, Xiong F, Shi YF, Dai KS, Ding ZB. Wavelet multi-resolution approximation of time-varying frame structure. *Advances in Mechanical Engineering* 2018; 10(8):1-19.
- [27] Chen SY, Lu JB, Lei Y. Identification of time-varying systems with partial acceleration measurements by synthesis of wavelet decomposition and Kalman filter. *Advances in Mechanical Engineering* 2020; 12(6):168781402093046.

- [28] Lei Y, Yang N. Simultaneous identification of structural time-varying physical parameters and unknown excitations using partial measurements. *Engineering Structures* 2020; 214:110672.
- [29] Yuen KV, Huang K. Identifiability-enhanced Bayesian frequency-domain substructure identification. *Computer-Aided Civil and Infrastructure Engineering* 2018; 21(4):280-291.
- [30] Lei Y, Liu C, Jiang YQ, Mao YK. Substructure based structural damage detection with limited input and output measurements. *Smart Structures and Systems* 2013; 12(6): 619-640.
- [31] Lei Y, Wu DT, Lin Y. A decentralized control algorithm for large-scale building structures. *Computer-Aided Civil and Infrastructure Engineering* 2012; 27(1): 2-13.
- [32] Li J, Hao H. Substructure damage identification based on wavelet-domain response reconstruction. *Structural Health Monitoring* 2014; 13(4): 389-405.
- [33] Li J, Law SS. Damage identification of a target substructure with moving load excitation. *Mechanical Systems and Signal Processing* 2012; 30: 78-90.
- [34] Weng S, Zhu HP, Li PH, Xia Y, Ye L. Construction of orthogonal projector for the damage identification by measured substructural flexibility. *Measurement* 2016; 88: 441-455.
- [35] Weng S, Zhu HP, Xia Y, Li JJ, Tian W. A review on dynamic substructuring methods for model updating and damage detection of large-scale structures. *Advances in Structural Engineering* 2020; 23(3): 584-600.
- [36] Huang JS, Rao YP, Qiu H, Lei Y. Generalized algorithms for the identification of seismic ground excitations to building structures based on generalized Kalman filtering under unknown input. *Advances in Structural Engineering* 2020; 23(5):136943322090622.
- [37] Lei Y, Lu JB, Huang JS, Chen SY. A general synthesis of identification and vibration control of building structures under unknown excitations. *Mechanical Systems and Signal Processing* 2020; 143:106803.
- [38] Lei Y, Lu JB, Huang JS. Synthesize identification and control for smart structures with time-varying parameters under unknown earthquake excitation. *Structural Control and Health Monitoring* 2020; 27(10).
- [39] Lei Y, Lu JB, Huang JS. Integration of identification and vibration control of time-varying structures subject to unknown seismic ground excitation. *Journal of Vibration and Control* 2020; 26(2):107754631989644.
- [40] Yuen KV, Huang K. Real-time substructural identification by boundary force modeling. *Structural Control and Health Monitoring* 2018; 25(5): e2151.1-e2151.18.
- [41] Liu LJ, Zhu JJ, Su Y, Lei Y. Improved Kalman filter with unknown inputs based on data fusion of partial acceleration and displacement measurement. *Smart Structures and Systems* 2016; 17(6): 903-915.

- [42] Maes K, Smyth AW, Roeck GD, Lombaert G. Joint input-state estimation in structural dynamics. *Mechanical Systems and Signal Processing* 2016; 70: 445-466.
- [43] Chang CC, Shi YF. Identification of time-varying hysteretic structures using wavelet multiresolution analysis. *International Journal of Non-Linear Mechanics* 2010; 45(1): 21-34.

CHAPTER 4 Identification of time-varying nonlinear structural physical parameters by integrated WMA and UKF/UKF-UI

ABSTRACT

The identification of time-varying physical parameters of nonlinear systems is still a challenging task. Limited studies based on the wavelet multiresolution analysis (WMA) have been attempted, which requires full measurements of structural displacement, velocity and acceleration responses of all degrees of freedom and exact information of external excitations. This limits the engineering application of these methods. This paper proposes approaches to identify the time-varying physical parameters of nonlinear structures in three cases using only partially measured structural responses. Firstly, the identification of time-varying nonlinear structures with a small number of elements under known excitations is discussed. The fading-factor unscented Kalman filter (FUKF) method is applied to locate the time-varying parameters, and WMA integrated with UKF method is employed using partially measured acceleration responses. Secondly, it is further extended to the identification of time-varying nonlinear structures with a small number of elements but under unknown excitations. An improved fading-factor unscented Kalman filter under unknown input (FUKF-UI) method is proposed to locate the time-varying parameters, and WMA integrated with UKF-UI method is utilized with partially observed acceleration and displacement responses. Thirdly, for practical engineering applications, the identification of time-varying nonlinear structure with more elements under unknown excitations is conducted. The proposed FUKF-UI method is employed to locate the time-varying parameters of the whole structure. Then the whole structure is divided into several substructures and the unknown interaction forces are regarded as the fictitious unknown inputs to the substructure. Thus, physical parameters of each substructure can be identified in parallel by the combination of WMA and UKF-UI. Three numerical studies corresponding to these three cases are conducted respectively to demonstrate the effectiveness and accuracy of the proposed methods.

Yang N, Li J, Lei Y, Hao H. Identification of time-varying nonlinear structural physical parameters by integrated WMA and UKF/UKF-UI. *Nonlinear Dynamics*, 2021. DOI: 10.1007/s11071-021-06682-y. (In Press)

1 Introduction

Time-varying properties are common for structures in service due to severe natural and manmade hazards, resulting in that the identification of time-varying structural systems is a very important research topic [1-3]. Bao et al. [4] conducted a comprehensive state-of-art review about the latest development of structural health monitoring, pointing out that reliable identification of structural physical parameters has clearer applications, because physical structural parameters correlate with the location and severity of possible damage through the time-varying characteristics of the system. Effective methods have been investigated to identify the time-varying physical parameters, such as the state-space model-based methods [5-7] in the time domain, or the wavelet multiresolution analysis (WMA) based methods [8-12] in the time-frequency domain. In particular, WMA has an excellent function on arbitrarily adjustable time-frequency resolution. Most existing WMA based methods expand the time-varying structural physical parameters into scale coefficients and then identify these coefficients by the linear least-squares estimation [8-10]. However, it is required that the displacement, velocity, acceleration responses at all degrees of freedom (DOFs) and external load information are known in these methods, which is a tough condition in actual applications. To overcome the limitation on full observations, novel methods have been proposed [11, 12] recently by the authors to identify the time-varying linear structures under known or unknown excitations using partial measurements based on the synthesis of WMA and Kalman filter (KF), transforming the solution of scale coefficients into a nonlinear least-squares optimization problem. However, it is required to expand all physical parameters, including time-varying parameters and time-invariant parameters, into

scale coefficients based on WMA. With the growing number of scale coefficients, the difficulty of least-squares optimization is heavily increased.

Moreover, these above-mentioned methods are proposed based on the assumption of the linear model. However, under strong external loads such as earthquake, strong wind, impact and explosion, engineering structural components may present nonlinear behavior intrinsically [13-15]. Xu et al. [14] successfully analyzed the nonlinear failure mechanism of reinforced concrete columns under earthquake based on a region-based deep convolutional neural network. In recent years, many scholars have carried out in-depth researches on the identification of nonlinear structural characteristics and presented a variety of identification methods, including time-domain [16-19], frequency-domain [20] or time-frequency analysis methods [21-27]. However, the parameters of nonlinear models are assumed to be steady in most of these methods, only a few efforts have been attempted on the identification of time-varying nonlinear systems. Adaptive identification techniques based on the Kalman Filter (KF) have the potential to track time-varying parameters of hysterically degrading structures [5-7], which exploited the track factor, adaptive correction factor, or adaptive factor matrix to deal with the evolution of system variation. The challenging issue is that either these adaptive algorithms have strong subjectivity on empirical factors [7], or it is time-consuming in calculating the optimal matrix at each time-step [6]. The WMA based method mentioned above can also be used to identify the time-varying nonlinear systems. For instance, Chang and Shi [27] proposed a method to identify the time-varying physical parameters and model parameters in the Bouc-Wen hysteresis model based on WMA. However, this method needs full information on the structural displacement, velocity, acceleration responses, and excitation. Furthermore, in addition to the stiffness and damping parameters, the

parameters in the nonlinear model are also needed to be expanded by WMA, which increases the complexity than the identification of linear systems.

With partial measurements, the extended Kalman filter (EKF) and unscented Kalman filter (UKF) [28] have been commonly used in the identification of nonlinear time-invariant systems. Compared with EKF, UKF is more superior as it does not need the calculation of the Jacobian matrix and a linearization-based approximation of the nonlinear system, realizing an on-line identification with a better recognition accuracy [29]. Furthermore, UKF method for the case of unknown excitations has been derived and successfully applied to the physical parameter identification of nonlinear systems under unknown loads [30]. However, these methods are only suitable for the time-invariant systems. Adaptive UKF methods have been proposed for the identification of time-varying structures, combining with the adjustment of error covariance [31-33] or the adjustment of noise covariance matrix [34, 35]. This may depend on the fading factors in most of the developed methods. However, if the fading factors are not selected properly, one may only roughly judge which parameter has the most possibility of varying property, but the change degree is difficult to be accurately determined. Moreover, all these adaptive methods are derived on the premise of known excitation. To the best knowledge of the authors, there is a lack in the identification of time-varying nonlinear systems under unknown excitations.

In addition, it should be pointed out that the existing WMA based methods are only applicable to structures with a small number of elements [8-12, 27]. The reason is that the number of scale coefficients in the least-squares process will increase with the number of elements, which makes it difficult to obtain the global optimal solution especially when the quality of observation data is poor. The “divide and conquer” idea of the sub-structural based methods provides a

feasible strategy for the identification of structures with more elements [36-40]. Many scholars have also introduced the concept of substructure into the identification of nonlinear structures [41-44]. However, these methods are mostly used to identify the parameters of time-invariant systems, and they still have some shortcomings such as the difficulties in determining the interface forces, the incapability of parallel identification, and the existence of propagation errors [45]. Shi and Chang [46, 47] presented an offline sub-structural method to identify the time-varying nonlinear shear-type buildings based on WMA. Nevertheless, the method requires all the displacement, velocity and acceleration responses inside and at the interfaces of the substructure. Further development and studies on identification techniques for time-varying nonlinear structures with more elements are still needed.

Based on the above-mentioned detailed literature, most WMA based methods are used to identify the physical parameters of time-varying linear systems, while only a few studies are conducted for the time-varying nonlinear systems. In addition, these methods require full measurements of displacement, velocity, acceleration and external loads. Furthermore, all physical parameters including time-varying and time-invariant parameters are expanded by WMA, which leads to a significant increase in the number of scale coefficients. Therefore, two-step identification processes are proposed in this paper to identify the physical parameters of time-varying nonlinear systems by using partial measurements. Three cases are discussed respectively. The first case is the identification of time-varying nonlinear structures with a small number of elements under known excitations. The time-varying physical parameters are located by the fading-factor unscented Kalman filter (FUKF) in the first step, and the method integrating WMA with UKF is proposed to identify the time-varying physical parameters in the second step, which

uses partially measured acceleration responses. A numerical example of a 6-story time-varying nonlinear shear frame under known seismic acceleration is provided, with abruptly changed or gradually varying parameters, to verify the effectiveness of the first proposed identification process. Considering that the external loads are always hard to measure in practical situations, the study is extended to the second case, that is, the identification of time-varying nonlinear structures with a small number of elements but under unknown excitations. Herein, the improved unscented Kalman filter under unknown input (UKF-UI) method proposed by the authors [30] is adopted. The time-varying physical parameters are located by the proposed fading-factor UKF-UI (FUKF-UI) in the first step, and the method integrating WMA with UKF-UI is proposed to identify the physical parameters using partially measured acceleration and displacement responses in the second step. Numerical study on a truss structure is conducted to identify the time-varying parameters and unknown excitations simultaneously. The last case is the identification of time-varying nonlinear structures with more number of elements under unknown excitations, which is investigated based on the sub-structural method. The time-varying physical parameters of the whole structure are located by the proposed FUKF-UI method in the first step. In the second step, the whole structure is divided into several substructures and the unknown interaction force is considered as the fictitious “unknown input”. Therefore, each substructure can be identified in parallel using the proposed WMA integrated with UKF-UI method. Numerical study on a 10-story shear frame demonstrates that the third proposed identification process is effective for the identification of structures with more number of elements under unknown excitations.

The remaining part of this paper is organized as: Section 2 presents the identification process and numerical validation of time-varying nonlinear structures with a small number of elements

under known excitations. Section 3 is extended to the case of time-varying nonlinear structures with a small number of elements but under unknown excitations. Section 4 further extends the study to the case of time-varying nonlinear structures with more number of elements under unknown excitations by using sub-structural method. Finally, some conclusions with recommendations on the further research are presented in Section 5.

2 Identification of time-varying nonlinear structures with a small number of elements under known excitations

2.1 The proposed two-step identification process

The expansion of all physical parameters, including stiffness parameters, damping parameters and nonlinear model parameters, leads to a large number of scale coefficients. This increases the possibility of not obtaining local optimization solutions, especially for the case with poor-quality measurement data. Thus, it is difficult or even impossible to obtain global optimal scale coefficients when the number of unknown parameters is large. In fact, the time-varying physical parameters are always sparse in the systems [38]. The time-invariant parameter can be identified directly as a time-invariant coefficient. It is not necessary to expand all parameters into scale coefficients by WMA, which increases the number of coefficients to be identified for the time-invariant parameters instead. This paper proposes a two-step identification process for the time-varying nonlinear physical parameters. The time-varying parameters are localized using the FUKF method in the first step. Then an objective function is constructed based on WMA and UKF in the second step, which is the implicit function of the time-invariant physical parameters and scale coefficients of time-varying parameters. Finally, these unknown variables are solved by the nonlinear least-squares optimization. The detailed procedure is introduced as follows.

2.1.1. Locate the time-varying physical parameters by the FUKF method

The equation of motion of a time-varying nonlinear system is described as:

$$\mathbf{M}\ddot{\mathbf{x}}(t) + \mathbf{R}(\boldsymbol{\theta}(t), \mathbf{x}(t), \dot{\mathbf{x}}(t)) = \boldsymbol{\eta}\mathbf{f}(t) \quad (1)$$

in which \mathbf{M} is the time-invariant and known mass matrix, \mathbf{f} is the known excitation with the influence matrix $\boldsymbol{\eta}$, \mathbf{x} , $\dot{\mathbf{x}}$ and $\ddot{\mathbf{x}}$ are displacement, velocity, and acceleration vector, respectively, $\boldsymbol{\theta}$ is the vector of physical parameters including stiffness, damping and nonlinear model parameters, \mathbf{R} is the total restoring force of the structural system.

Supposing an augmented state vector $\mathbf{Z} = \{\mathbf{x}^T, \dot{\mathbf{x}}^T, \boldsymbol{\theta}^T\}^T$, Eq. (1) can be converted into the following state space equation as

$$\dot{\mathbf{Z}} = \begin{Bmatrix} \dot{\mathbf{x}} \\ \ddot{\mathbf{x}} \\ \dot{\boldsymbol{\theta}} \end{Bmatrix} = \begin{Bmatrix} \dot{\mathbf{x}} \\ \mathbf{M}^{-1}[\boldsymbol{\eta}\mathbf{f} - \mathbf{R}(\boldsymbol{\theta}, \mathbf{x}, \dot{\mathbf{x}})] \\ \mathbf{0} \end{Bmatrix} + \mathbf{w} = \mathbf{g}(\mathbf{Z}, \mathbf{f}) + \mathbf{w} \quad (2)$$

in which \mathbf{w} is the process noise that is assumed to be a Gaussian white noise process with zero mean and a covariance matrix $E[\mathbf{w}\mathbf{w}^T] = \mathbf{Q}$.

Given partially measured acceleration responses, the discrete observation equations is expressed as

$$\begin{aligned} \mathbf{y}_{k+1} = \ddot{\mathbf{x}}_{m,k+1} &= \mathbf{L}_a \ddot{\mathbf{x}}_{k+1} + \mathbf{v}_{k+1} = \mathbf{L}_a \mathbf{M}^{-1} [\boldsymbol{\eta}\mathbf{f}_{k+1} - \mathbf{R}(\boldsymbol{\theta}_{k+1}, \mathbf{x}_{k+1}, \dot{\mathbf{x}}_{k+1})] + \mathbf{v}_{k+1} \\ &= \mathbf{h}(\mathbf{Z}_{k+1}, \mathbf{f}_{k+1}) + \mathbf{v}_{k+1} \end{aligned} \quad (3)$$

where \mathbf{y}_{k+1} and $\ddot{\mathbf{x}}_{m,k+1}$ represent the observation and the measured acceleration at the time instant $t = (k+1)\Delta t$, respectively, Δt is the sampling interval, \mathbf{L}_a is the accelerometer position matrix, and \mathbf{v}_{k+1} is the measurement noise assumed as a Gaussian white noise process, with mean value of zero and covariance matrix of $E[\mathbf{v}_{k+1}\mathbf{v}_{k+1}^T] = \mathbf{R}_{k+1}$.

Similar as conventional UKF [28], the FUKF method is implemented based on the following procedure, including sigma point calculation, time predication and measurement updating [31].

Sigma point calculation

A set of $2N + 1$ sigma points $\chi_{i,k|k}$ are generated by using the unscented transform

$$\chi_{i,k|k} = \begin{cases} \hat{\mathbf{z}}_{k|k} & , i = 0 \\ \hat{\mathbf{z}}_{k|k} + \left(\sqrt{(N + \mathcal{G}) \hat{\mathbf{P}}_{\mathbf{z},k|k}} \right)_i & , i = 1, \dots, N \\ \hat{\mathbf{z}}_{k|k} - \left(\sqrt{(N + \mathcal{G}) \hat{\mathbf{P}}_{\mathbf{z},k|k}} \right)_i & , i = N + 1, \dots, 2N \end{cases} \quad (4)$$

where N is the dimension of \mathbf{z} , $\hat{\mathbf{z}}_{k|k}$ is the estimated state at $t = k\Delta t$, $\hat{\mathbf{P}}_{\mathbf{z},k|k}$ is the error covariance matrix that is expressed as $\hat{\mathbf{P}}_{\mathbf{z},k|k} = E \left\{ \left(\mathbf{z}_k - \hat{\mathbf{z}}_{k|k} \right) \left(\mathbf{z}_k - \hat{\mathbf{z}}_{k|k} \right)^T \right\}$, $\mathcal{G} = \kappa_1^2 (N + \kappa_2) - N$, κ_1 and κ_2 are scaling parameters determining the spread of the sigma points.

Time predication

The propagation of the sigma points is predicted based on the state space equation

$$\chi_{i,k+1|k} = \chi_{i,k|k} + \int_{k\Delta t}^{(k+1)\Delta t} \mathbf{g} \left(\mathbf{z}_{t|k}, \mathbf{f} \right) dt \quad (5)$$

The predicted state vector $\tilde{\mathbf{z}}_{k+1|k}$ and error covariance matrix $\tilde{\mathbf{P}}_{\mathbf{z},k+1|k}$ are given as

$$\tilde{\mathbf{z}}_{k+1|k} = \sum_{i=0}^{2N} W_i^m \chi_{i,k+1|k} \quad (6)$$

$$\tilde{\mathbf{P}}_{\mathbf{z},k+1|k} = \lambda \sum_{i=0}^{2N} W_i^c (\chi_{i,k+1|k} - \tilde{\mathbf{z}}_{k+1|k}) (\chi_{i,k+1|k} - \tilde{\mathbf{z}}_{k+1|k})^T + \mathbf{Q}_{k+1} \quad (7)$$

where W_i^m and W_i^c are the weight coefficients of the predicted mean and covariance, respectively. Herein a fading factor $\lambda (\lambda \geq 1)$ is introduced into the conventional UKF. In the first step, $\lambda = 2^{2/N_u}$ is adopted based on an existing study [38], which implies that the half-life of the contribution of a data point is N_u time steps.

Similarly, the estimated measurement vector $\hat{\mathbf{y}}_{k+1|k+1}$ at $t = (k+1)\Delta t$ and its error covariance matrix $\hat{\mathbf{P}}_{\mathbf{y},k+1}$ are computed as

$$\hat{\mathbf{y}}_{i,k+1|k+1} = \mathbf{h}(\boldsymbol{\chi}_{i,k+1|k}, \mathbf{f}_{k+1}); \quad \hat{\mathbf{y}}_{k+1|k+1} = \sum_{i=0}^{2N} W_i^m \hat{\mathbf{y}}_{i,k+1|k+1} \quad (8)$$

$$\hat{\mathbf{P}}_{\mathbf{y},k+1} = \lambda \sum_{i=0}^{2N} W_i^c (\hat{\mathbf{y}}_{i,k+1|k+1} - \hat{\mathbf{y}}_{k+1|k+1})(\hat{\mathbf{y}}_{i,k+1|k+1} - \hat{\mathbf{y}}_{k+1|k+1})^T + \mathbf{R}_{k+1} \quad (9)$$

Besides, the cross-covariance matrix $\hat{\mathbf{P}}_{\mathbf{z}_y,k+1}$ is estimated as

$$\hat{\mathbf{P}}_{\mathbf{z}_y,k+1} = \lambda \sum_{i=0}^{2N} W_i^c \left\{ \boldsymbol{\chi}_{i,k+1|k} - \hat{\mathbf{z}}_{k+1|k} \right\} \left\{ \hat{\mathbf{y}}_{i,k+1|k+1} - \hat{\mathbf{y}}_{k+1|k+1} \right\}^T \quad (10)$$

Measurement Updating

The structural state vector $\hat{\mathbf{z}}_{k+1|k+1}$ and error covariance matrix $\hat{\mathbf{P}}_{\mathbf{z},k+1|k+1}$ are updated as

$$\hat{\mathbf{z}}_{k+1|k+1} = \tilde{\mathbf{z}}_{k+1|k} + \mathbf{K}_{G,k+1} (\mathbf{y}_{k+1} - \hat{\mathbf{y}}_{k+1|k+1}) \quad (11)$$

$$\hat{\mathbf{P}}_{\mathbf{z},k+1|k+1} = \tilde{\mathbf{P}}_{\mathbf{z},k+1|k} - \mathbf{K}_{G,k+1} \hat{\mathbf{P}}_{\mathbf{y},k+1} \mathbf{K}_{G,k+1}^T \quad (12)$$

in which $\mathbf{K}_{G,k+1}$ is the Kalman gain matrix expressed as

$$\mathbf{K}_{G,k+1} = \hat{\mathbf{P}}_{\mathbf{z}_y,k+1} (\hat{\mathbf{P}}_{\mathbf{y},k+1})^{-1} \quad (13)$$

Based on the identification results of FUKF, the physical parameter vector $\boldsymbol{\theta}$ is divided into a time-varying parameter vector $\boldsymbol{\theta}_1$ and a time-invariant parameter vector $\boldsymbol{\theta}_2$ qualitatively. Thus, the time-varying physical parameters can be successfully localized.

2.1.2. Identify the time-varying physical parameters by the proposed WMA integrated with UKF method

In the second step, a novel method based on WMA and UKF is proposed to identify $\boldsymbol{\theta}_2$ and scale coefficients corresponding to $\boldsymbol{\theta}_1$ quantitatively.

Wavelet multiresolution analysis

WMA possesses a strong capability in decomposing any signal into approximate and detailed parts in different scale levels, corresponding to the low-frequency and high-frequency components of the signal respectively [8-12]. Considering that the signal energies in civil engineering are mostly concentrated in the low-frequency component, the time-varying physical parameter $\theta_{1,i}$ ($i=1,2,\dots,m_1$) is expanded in the wavelet domain by only reserving the low-frequency part as

$$\theta_{1,i}(t_n) \approx \sum_{l_i} \psi_{J_i, l_i} \phi_{J_i, l_i}(2^{J_i} n - l_i), \quad n = 1, 2, \dots, Nt \quad (14)$$

where $\theta_{1,i}$ denotes the i -th time-varying parameter, m_1 is the number of time-varying parameters, ψ_{J_i, l_i} is the scale coefficient at the scale level J_i , l_i is the number of corresponding scale coefficients, ϕ_{J_i, l_i} is the scale function in WMA, Nt is the number of sampling points.

Identify structural state by UKF with given scale coefficients and time-invariant physical parameters

By Eq. (14), the time-varying physical parameters can be reconstructed based on the given time-invariant scale coefficient vector $\Psi_{J,l}$ accordingly. Thus, it is transformed into the identification of scale coefficients and time-invariant physical parameters. UKF is utilized to estimate the state under the condition of partial acceleration observations. Owing to page limitation, only main formulas are listed in Eqs. (15)-(22).

The equation of motion, state equation and measurement equation of a nonlinear system are rewritten as

$$\mathbf{M}\ddot{\mathbf{x}}(t) + \mathbf{R}(\boldsymbol{\theta}_1(\Psi_{J,l}), \boldsymbol{\theta}_2, \mathbf{x}(t), \dot{\mathbf{x}}(t)) = \boldsymbol{\eta}\mathbf{f}(t) \quad (15)$$

$$\dot{\mathbf{X}} = \begin{Bmatrix} \dot{\mathbf{x}} \\ \ddot{\mathbf{x}} \end{Bmatrix} = \begin{Bmatrix} \dot{\mathbf{x}} \\ \mathbf{M}^{-1} \left[\boldsymbol{\eta} \mathbf{f} - \mathbf{R}(\boldsymbol{\theta}_1(\boldsymbol{\psi}_{J,l}), \boldsymbol{\theta}_2, \mathbf{x}, \dot{\mathbf{x}}) \right] \end{Bmatrix} + \mathbf{w} = \mathbf{g}(\mathbf{X}, \boldsymbol{\theta}_1(\boldsymbol{\psi}_{J,l}), \boldsymbol{\theta}_2, \mathbf{f}) + \mathbf{w} \quad (16)$$

$$\begin{aligned} \mathbf{y}_{k+1} &= \ddot{\mathbf{x}}_{m,k+1} = \mathbf{L}_a \ddot{\mathbf{x}}_{k+1} + \mathbf{v}_{k+1} = \mathbf{L}_a \mathbf{M}^{-1} \left[\boldsymbol{\eta} \mathbf{f}_{k+1} - \mathbf{R}(\boldsymbol{\theta}_1(\boldsymbol{\psi}_{J,l}), \boldsymbol{\theta}_2, \mathbf{x}_{k+1}, \dot{\mathbf{x}}_{k+1}) \right] + \mathbf{v}_{k+1} \\ &= \mathbf{h}(\mathbf{X}_{k+1}, \boldsymbol{\theta}_1(\boldsymbol{\psi}_{J,l}), \boldsymbol{\theta}_2, \mathbf{f}_{k+1}) + \mathbf{v}_{k+1} \end{aligned} \quad (17)$$

The predicted state vector $\tilde{\mathbf{x}}_{k+1|k}$ and error covariance matrix $\tilde{\mathbf{P}}_{\mathbf{X},k+1|k}$ are given as

$$\boldsymbol{\chi}_{i,k+1|k} = \boldsymbol{\chi}_{i,k|k} + \int_{k\Delta t}^{(k+1)\Delta t} \mathbf{g}(\mathbf{X}_{i|k}, \boldsymbol{\theta}_1(\boldsymbol{\psi}_{J,l}), \boldsymbol{\theta}_2, \mathbf{f}) dt; \quad \tilde{\mathbf{X}}_{k+1|k} = \sum_{i=0}^{2N} W_i^m \boldsymbol{\chi}_{i,k+1|k} \quad (18)$$

$$\tilde{\mathbf{P}}_{\mathbf{X},k+1|k} = \sum_{i=0}^{2N} W_i^c (\boldsymbol{\chi}_{i,k+1|k} - \tilde{\mathbf{X}}_{k+1|k})(\boldsymbol{\chi}_{i,k+1|k} - \tilde{\mathbf{X}}_{k+1|k})^T + \mathbf{Q}_{k+1} \quad (19)$$

The estimated measurement vector $\hat{\mathbf{y}}_{k+1|k+1}$, its error covariance matrix $\hat{\mathbf{P}}_{\mathbf{y},k+1}$, and the cross-covariance matrix $\hat{\mathbf{P}}_{\mathbf{xy},k+1}$ are rewritten as

$$\hat{\mathbf{y}}_{i,k+1|k+1} = \mathbf{h}(\boldsymbol{\chi}_{i,k+1|k}, \boldsymbol{\theta}_1(\boldsymbol{\psi}_{J,l}), \boldsymbol{\theta}_2, \mathbf{f}_{k+1}); \quad \hat{\mathbf{y}}_{k+1|k+1} = \sum_{i=0}^{2N} W_i^m \hat{\mathbf{y}}_{i,k+1|k+1} \quad (20)$$

$$\hat{\mathbf{P}}_{\mathbf{y},k+1} = \sum_{i=0}^{2N} W_i^c (\hat{\mathbf{y}}_{i,k+1|k+1} - \hat{\mathbf{y}}_{k+1|k+1})(\hat{\mathbf{y}}_{i,k+1|k+1} - \hat{\mathbf{y}}_{k+1|k+1})^T + \mathbf{R}_{k+1} \quad (21)$$

$$\hat{\mathbf{P}}_{\mathbf{xy},k+1} = \sum_{i=0}^{2N} W_i^c \left\{ \boldsymbol{\chi}_{i,k+1|k} - \tilde{\mathbf{X}}_{k+1|k} \right\} \left\{ \hat{\mathbf{y}}_{i,k+1|k+1} - \hat{\mathbf{y}}_{k+1|k+1} \right\}^T \quad (22)$$

Finally, the structural state vector and error covariance matrix in Eqs. (11) and (12) are updated, respectively.

Estimate scale coefficients and time-invariant physical parameters by nonlinear optimization

As can be seen from the above sections, the estimated state is an implicit function of the scale coefficient vector $\boldsymbol{\psi}_{J,l}$ and time-invariant physical parameter vector $\boldsymbol{\theta}_2$,

$$\hat{\mathbf{X}} = \hat{\mathbf{X}}(\boldsymbol{\psi}_{J,l}, \boldsymbol{\theta}_2) \quad (23)$$

Then the estimated acceleration is obtained by using the equation of motion in Eq. (15)

$$\hat{\mathbf{x}}(\boldsymbol{\psi}_{J,l}, \boldsymbol{\theta}_2) = \mathbf{M}^{-1} \left(\boldsymbol{\eta} \mathbf{f} - \mathbf{R} \left(\boldsymbol{\theta}_1(\boldsymbol{\psi}_{J,l}), \boldsymbol{\theta}_2, \hat{\mathbf{x}}(\boldsymbol{\psi}_{J,l}, \boldsymbol{\theta}_2), \hat{\mathbf{x}}(\boldsymbol{\psi}_{J,l}, \boldsymbol{\theta}_2) \right) \right) \quad (24)$$

An objective error function is established by integrating the observed acceleration $\ddot{\mathbf{x}}_m$ and the estimated acceleration $\hat{\mathbf{x}}$ as

$$\Delta(\boldsymbol{\psi}_{J,l}, \boldsymbol{\theta}_2) = \left\| \ddot{\mathbf{x}}_m - \mathbf{L}_a \hat{\mathbf{x}}(\boldsymbol{\psi}_{J,l}, \boldsymbol{\theta}_2) \right\|_2^2 \quad (25)$$

The optimal scale coefficient vector $\hat{\boldsymbol{\psi}}_{J,l}$ and optimal time-invariant physical parameter vector $\hat{\boldsymbol{\theta}}_2$ are calculated by minimizing the objective error function

$$\left[\hat{\boldsymbol{\psi}}_{J,l}, \hat{\boldsymbol{\theta}}_2 \right] = \arg \min_{\boldsymbol{\psi}_{J,l}, \boldsymbol{\theta}_2} \left(\left\| \ddot{\mathbf{x}}_m - \mathbf{L}_a \hat{\mathbf{x}}(\boldsymbol{\psi}_{J,l}, \boldsymbol{\theta}_2) \right\|_2^2 \right) \quad (26)$$

Finally, the optimal time-varying physical parameter vector $\hat{\boldsymbol{\theta}}_1$ is reconstructed by using the inverse WMA in Eq. (14).

The procedure of the proposed method is listed in Fig. 1.

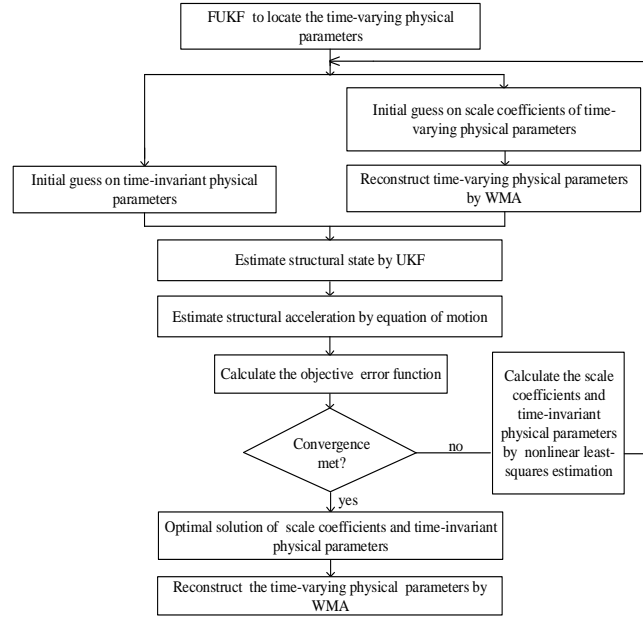


Fig. 1 Procedure of the proposed method to identify the time-varying nonlinear structures with a small number of elements under known excitation

2.2 Numerical verification: Identification of a time-varying nonlinear six-story shear frame subjected to a known seismic acceleration

The first numerical example is a 6-story shear frame with a Bouc-Wen model subjected to the 1940 El Centro N-S earthquake with the peak value scaled to 0.4g. The equation of motion of the structure is given as

$$\mathbf{M}\ddot{\mathbf{x}}(t) + \mathbf{C}(t)\dot{\mathbf{x}}(t) + \mathbf{K}(t)\mathbf{z}(t) = -\mathbf{M}\{\mathbf{I}\}\ddot{x}_g(t) \quad (27)$$

where \mathbf{C} and \mathbf{K} are global damping and stiffness matrices which are composed of the unknown time-varying damping and stiffness parameters, $\{\mathbf{I}\}$ is a unit vector and $\ddot{x}_g(t)$ is the base acceleration. $\mathbf{z}(t)$ is the hysteretic displacement vector with the specific expression as follows

$$\dot{z}_i = \dot{x}_i - \dot{x}_{i-1} - \beta_i |\dot{x}_i - \dot{x}_{i-1}| |\dot{z}_i|^{n_i-1} \dot{z}_i - \gamma_i (\dot{x}_i - \dot{x}_{i-1}) |\dot{z}_i|^{n_i}, \quad (i=1,2,\dots,6) \quad (28)$$

where n_i , β_i , and γ_i ($i=1,2,\dots,6$) are parameters for the Bouc-Wen hysteretic model. It is assumed that the nonlinear damage occurs with the restoring force between the first floor and the ground following the Bouc-Wen model. It should be noted that the Bouc-Wen model is adopted here only as an example to illustrate the proposed method. The proposed approach can be applied to identify structural physical parameters with different nonlinear response characteristics.

Structural parameters are selected as follows: the mass of each story and the Bouc-Wen hysteretic model parameter n_1 are assumed to be known as $m_i=200\text{kg}$ ($i=1,2,\dots,6$) and $n_1 = 1.8$. The corresponding dynamic responses are computed with a sampling frequency of 50Hz, and the complete sampling period is 10s. The acceleration measurements at the 1st, 3rd, and 5th floors are used. Each measured response is polluted by white noise with 2% variance in root mean square (RMS), namely:

$$\ddot{\mathbf{x}}_{i,noisy} = \ddot{\mathbf{x}}_{i,clean} + 2\% \times std(\ddot{\mathbf{x}}_{i,clean}) \times \mathbf{rand}, \quad (i=1,3,5) \quad (29)$$

where $\ddot{\mathbf{x}}_{i,noisy}$ is the measured noisy acceleration vector, $\ddot{\mathbf{x}}_{i,clean}$ is the noisy-free acceleration vector, $std(\ddot{\mathbf{x}}_{i,clean})$ means the standard deviation of $\ddot{\mathbf{x}}_{i,clean}$ and \mathbf{rand} is a random standard normal distribution vector.

The stiffness, viscous damping parameters of each story k_i, c_i ($i = 1, 2, \dots, 6$), and the Bouc-Wen hysteretic model parameters β and γ need to be identified. Two cases are discussed here.

2.2.1. Case I: Identification of abruptly changing physical parameters

The theoretical values of the physical parameters in case I are given below:

$$\begin{aligned} k_1 &= \begin{cases} 1.0 \times 10^5 \text{ N/m}, & 0s \leq t < 5.2s \\ 0.8 \times 10^5 \text{ N/m}, & 5.2s \leq t \leq 10s \end{cases} & k_i = 1.5 \times 10^5 \text{ N/m}, & 0s \leq t \leq 10s \quad (i = 2, \dots, 6) \\ c_1 &= \begin{cases} 800 \text{ N}\cdot\text{s/m}, & 0s \leq t < 5.2s \\ 1120 \text{ N}\cdot\text{s/m}, & 5.2s \leq t \leq 10s \end{cases} & c_i = 1000 \text{ N}\cdot\text{s/m}, & 0s \leq t \leq 10s \quad (i = 2, \dots, 6) \\ \beta_1 &= \begin{cases} 600, & 0s \leq t < 5.2s \\ 780, & 5.2s \leq t \leq 10s \end{cases} & \gamma_1 = 600, & 0s \leq t \leq 10s \end{aligned}$$

Referring to the flowchart in Fig. 1, the identification process is accomplished by the following procedure. Firstly, the time-varying physical parameters are distinguished using the FUKF method, which is shown in Fig. 2. $\lambda = 2^{2/30} = 1.0473$ is used, which indicates the half-life is 30 time steps. It can be seen from Fig. 2 that stiffness parameter k_1 changes gradually from a stable converged value to another stable converged value, implying that k_1 may be a time-varying physical parameter. Similarly, c_1 has the tendency to increase, which can also be selected as another time-varying physical parameter. However, the FUKF method can only roughly determine these physical parameters with the time-varying properties, but it is unable to detect the time-varying instant, time-varying trend and time-varying degree.

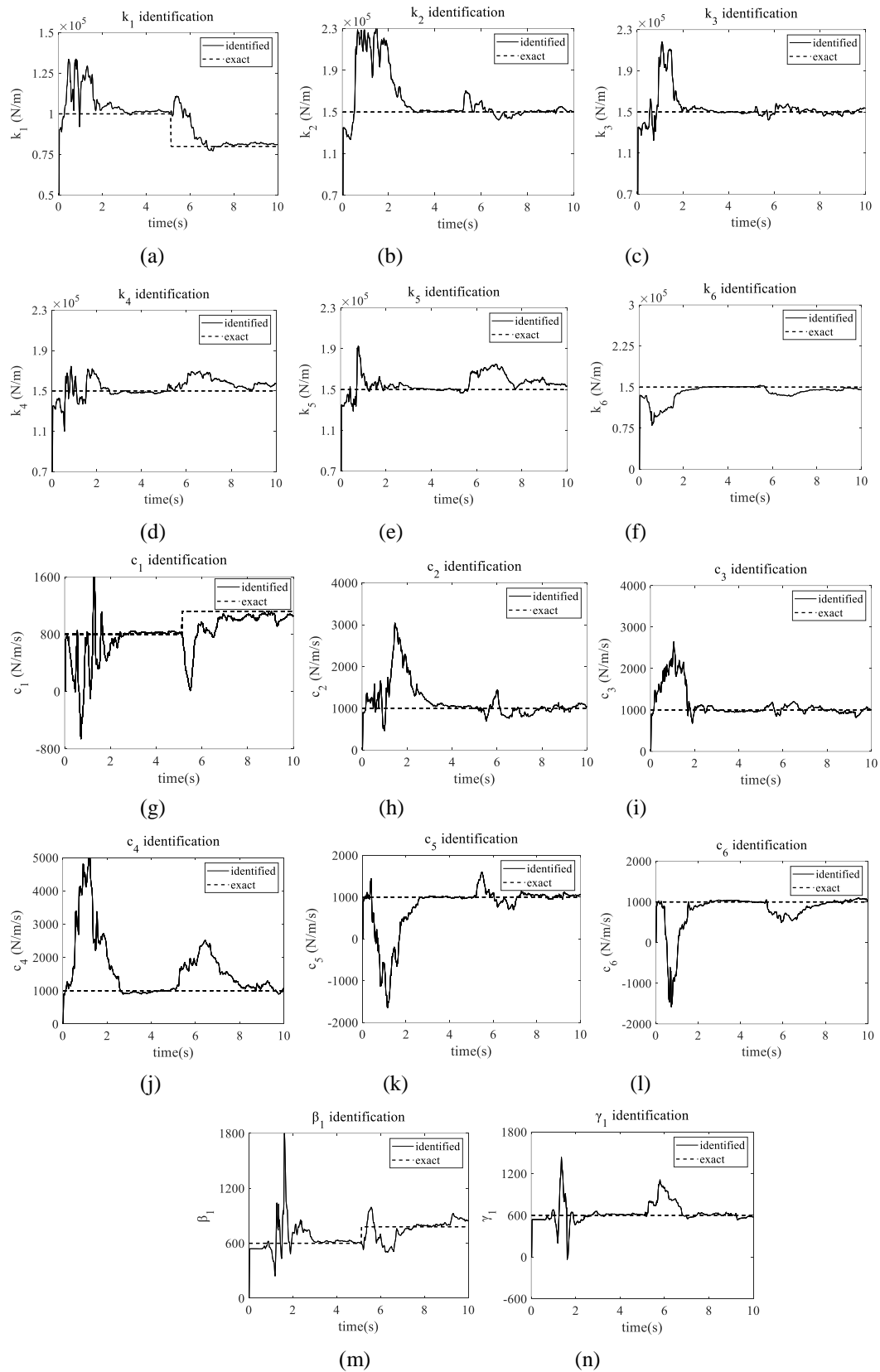


Fig. 2 Identification results using the FUKF method in case I. (a) k_1 ; (b) k_2 ; (c) k_3 ; (d) k_4 ; (e) k_5 ; (f) k_6 ; (g)

c_1 ; (h) c_2 ; (i) c_3 ; (j) c_4 ; (k) c_5 ; (l) c_6 ; (m) β_1 ; (n) γ_1

Secondly, the proposed WMA integrated with UKF method is applied to conduct the identification of time-varying physical parameters. Following the experience in an existing study by Chang and Shi [27], Db1 is adopted herein as the wavelet function to expand the time-varying k_1, c_1 , and nonlinear model parameters β_1 and γ_1 . The scale level is $J = 7$. The number of scale coefficients is 16 in total. The remaining five time-invariant stiffness parameters and five time-invariant damping parameters are not expanded by the WMA, and they are directly included in the nonlinear optimization process.

Figs. 3-5 show the identified physical parameters with comparisons to their exact values, respectively. It can be seen from Figs. 3-4 that the proposed WMA integrated with UKF method can precisely track the sudden change of stiffness and damping parameters, and the identification of time-invariant parameters also shows a high precision. Fig. 5 shows that the proposed method is also effective in identifying the time-varying nonlinear model parameters. It is noted that desirable results are achieved by using only three noisy acceleration responses.

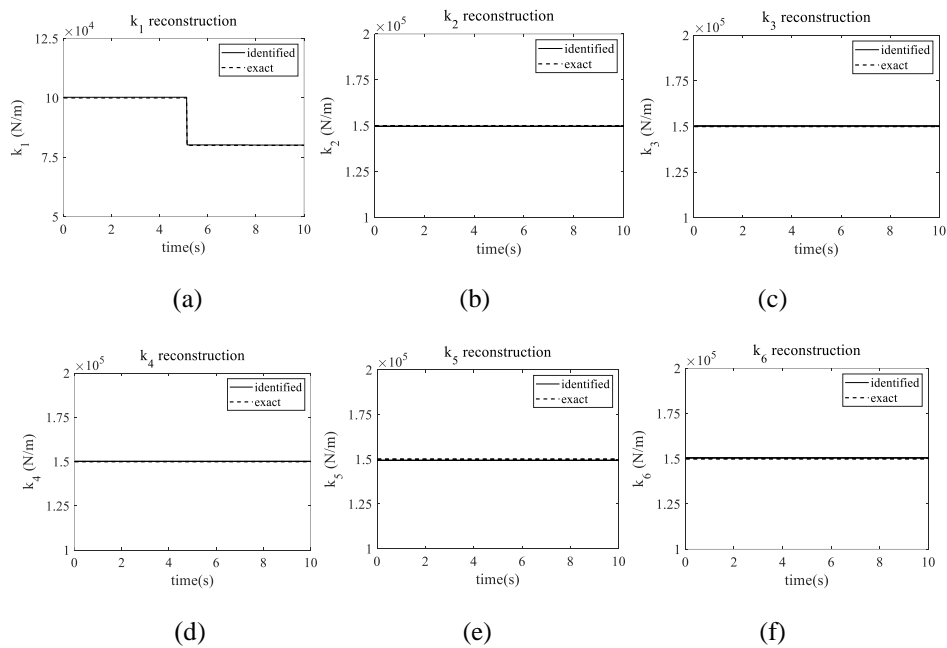


Fig. 3 Comparison of the exact and identified stiffness parameters. (a) k_1 ; (b) k_2 ; (c) k_3 ; (d) k_4 ; (e) k_5 ; (f) k_6

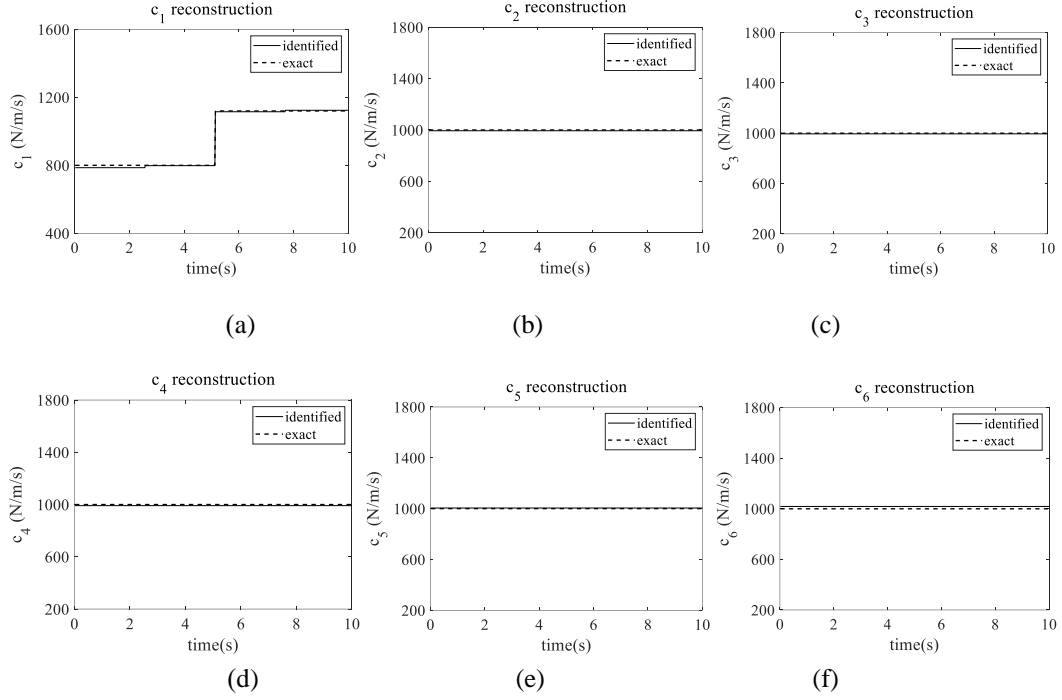


Fig. 4 The exact and identified damping parameters: (a) c_1 ; (b) c_2 ; (c) c_3 ; (d) c_4 ; (e) c_5 ; (f) c_6

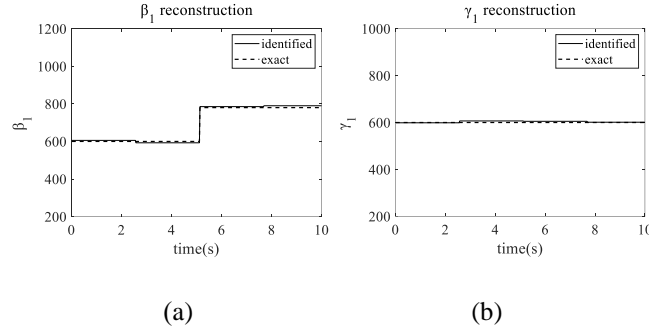


Fig. 5 Comparison of the exact and identified nonlinear model parameters in case I. (a) β_1 ; (b) γ_1

2.2.2. Case II: Identification of gradually varying physical parameters

The theoretical values of the physical parameters in case II are shown below, in which k_1 is gradually varying and expressed as

$$k_1 = \begin{cases} 1.0 \times 10^5 \text{ N/m}, & 0s \leq t < 2s \\ -5360t + 1.1 \times 10^5 \text{ (N/m)}, & 2s \leq t \leq 7.6s \\ 0.7 \times 10^5 \text{ N/m}, & 7.6s < t \leq 10s \end{cases} \quad k_i = 1.5 \times 10^5 \text{ N/m}, \quad 0s \leq t \leq 10s \quad (i = 2, \dots, 6)$$

$$c_1 = 800 \text{ N}\cdot\text{s/m}, \quad 0s \leq t \leq 10s \quad c_i = 1000 \text{ N}\cdot\text{s/m}, \quad 0s \leq t \leq 10s \quad (i = 2, \dots, 6)$$

$$\beta_1 = \begin{cases} 600, & 0s \leq t < 5.2s \\ 780, & 5.2s \leq t \leq 10s \end{cases} \quad \gamma_1 = 600, \quad 0s \leq t \leq 10s$$

The time-varying physical parameters are roughly located using the FUKF method. For brevity and without losing generality, only partial identification results are shown in Fig. 6. It is observed that the identified value of k_1 tends to change gradually, while other stiffness and damping parameters converge to fixed values. However, it should be noted that a relatively large error may be present at the start and end time instants.

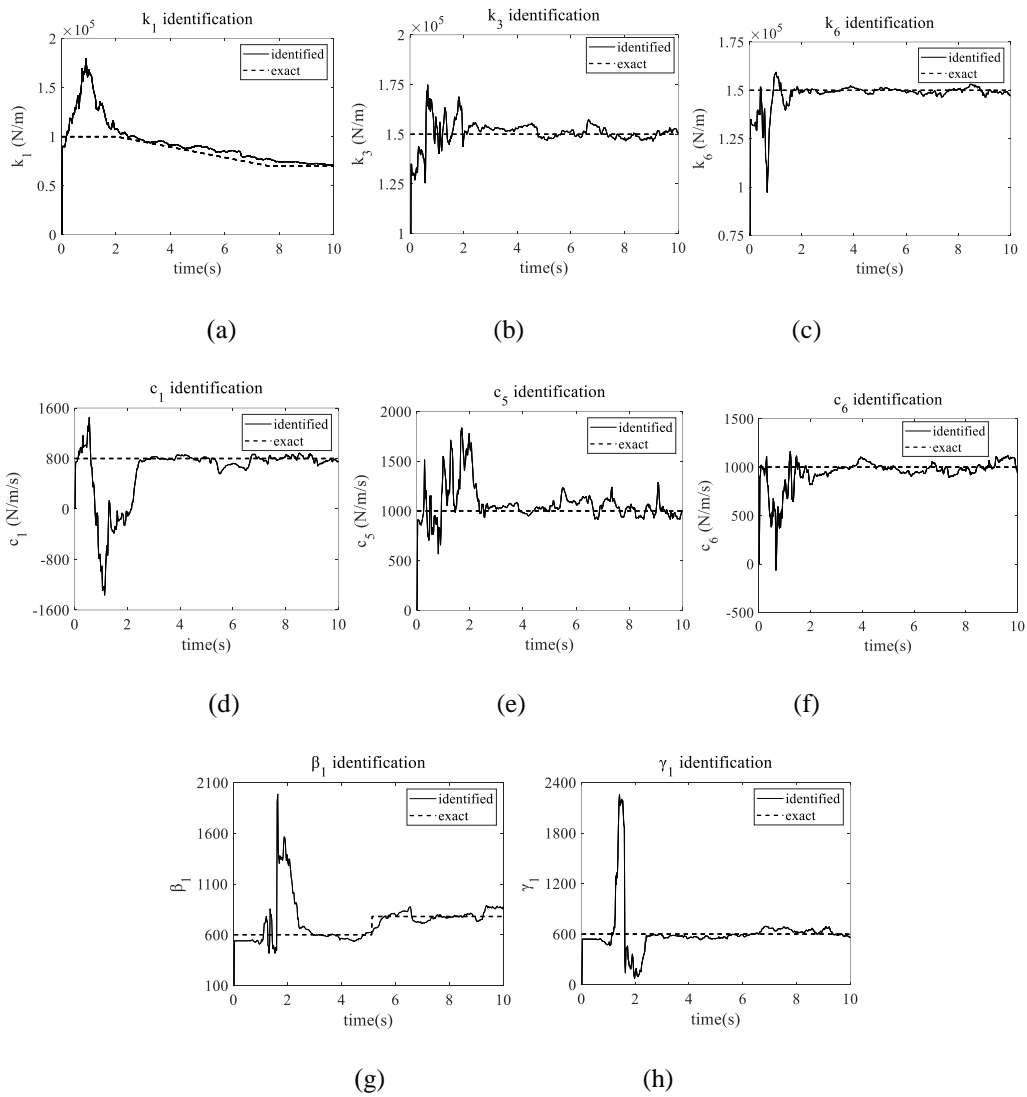


Fig. 6 Partial identification results using the FUKF method in case II. (a) k_1 ; (b) k_3 ; (c) k_6 ; (d) c_1 ; (e) c_5 ;

(f) c_6 ; (g) β_1 ; (h) γ_1

The gradually varying k_1 is expanded using the wavelet function Db3 with the scale level $J = 5$ suggested by Chang and Shi [27]. The time-varying nonlinear model parameters β_1 and γ_1 are also expanded using the wavelet function Db1 with the scale level $J = 7$. Thus, the variables involved in the nonlinear optimization include 24 scale coefficients and 11 time-invariant physical parameters. Identification results are shown in Figs.7-9, demonstrating that the proposed method is also suitable for the identification of gradually changing parameters in the presence of measurement noise. It not only effectively detects the start and end time of the gradual change, but also accurately identifies the degree of the varying parameters. Meanwhile, the identified time-invariant physical parameters are in good agreement with the exact values.

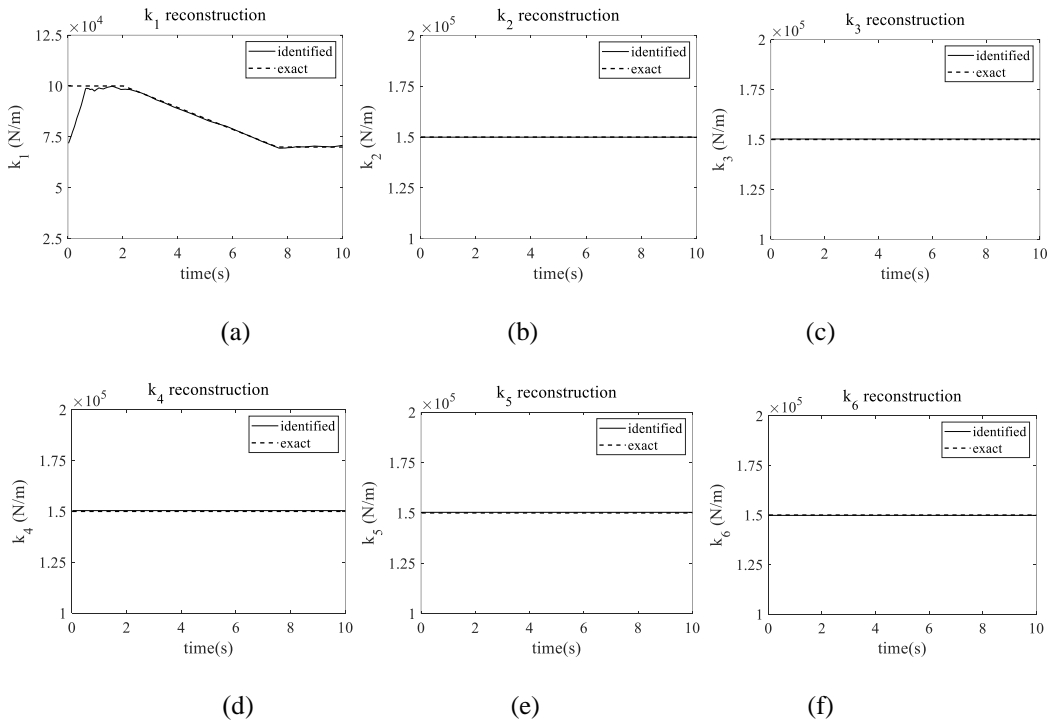


Fig. 7 Comparison of the exact and identified stiffness parameters in case II. (a) k_1 ; (b) k_2 ; (c) k_3 ; (d) k_4 ; (e) k_5 ; (f) k_6

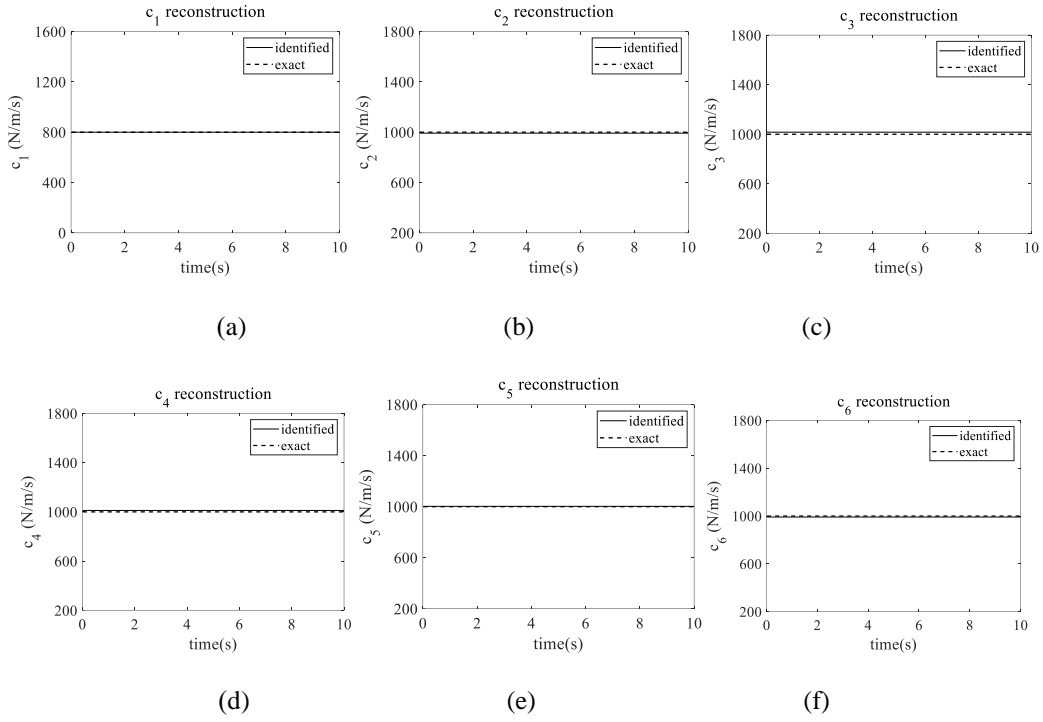


Fig. 8 Comparison of the exact and identified damping parameters in case II. (a) c_1 ; (b) c_2 ; (c) c_3 ; (d) c_4 ;
(e) c_5 ; (f) c_6

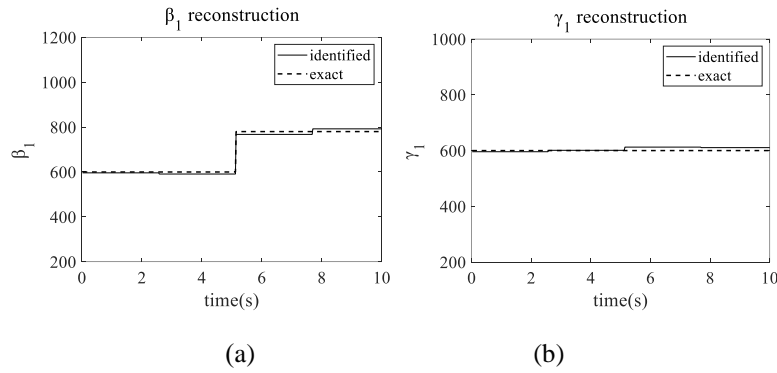


Fig. 9 Comparison of the exact and identified nonlinear model parameters in case II. (a) β_1 ; (b) γ_1

3 Identification of time-varying nonlinear structures with a small number of elements under unknown excitations

It shall be noted that the proposed method in Section 2 is only applicable for the case of known excitations, owing to the limitation of UKF itself. However, external excitations could not be always measured directly and easily in practical engineering applications. To further

generalize the application to a more common case, the identification of time-varying nonlinear structures with a small number of elements but under unknown excitations is discussed in this section.

3.1 The proposed two-step identification process

3.1.1. Locate the time-varying physical parameters by the proposed FUKF-UI method

In this section, the method introduced in Section 2.1.1 is further extended to locate the time-varying physical parameters under unknown excitations. A new method, that is fading-factor unscented Kalman filter under unknown input, is proposed. It is also an improvement for the data fusion based UKF-UI proposed by the authors in 2019 [30], for the reason that the latter is only available for the identification of time-invariant systems under the condition of unknown excitations.

If partial external inputs to the time-varying nonlinear structure are unknown, the equation of motion in Eq. (1) can be rewritten as

$$\mathbf{M}\ddot{\mathbf{x}}(t) + \mathbf{R}(\boldsymbol{\theta}(t), \mathbf{x}(t), \dot{\mathbf{x}}(t)) = \boldsymbol{\eta}\mathbf{f}(t) + \boldsymbol{\eta}^u\mathbf{f}^u(t) \quad (30)$$

where \mathbf{f}^u denotes the unknown input vector with the corresponding influence matrix $\boldsymbol{\eta}^u$. The state space equation can be expressed as

$$\dot{\mathbf{Z}} = \begin{Bmatrix} \dot{\mathbf{x}} \\ \ddot{\mathbf{x}} \\ \dot{\boldsymbol{\theta}} \end{Bmatrix} = \begin{Bmatrix} \dot{\mathbf{x}} \\ \mathbf{M}^{-1}[\boldsymbol{\eta}\mathbf{f} - \mathbf{R}(\boldsymbol{\theta}, \mathbf{x}, \dot{\mathbf{x}})] \\ \mathbf{0} \end{Bmatrix} + \begin{Bmatrix} \mathbf{0} \\ \mathbf{M}^{-1}\boldsymbol{\eta}^u \\ \mathbf{0} \end{Bmatrix} \mathbf{f}^u + \mathbf{w} = \mathbf{g}(\mathbf{Z}, \mathbf{f}) + \boldsymbol{\Phi}^u\mathbf{f}^u + \mathbf{w} \quad (31)$$

where $\boldsymbol{\Phi}^u$ is the influence matrix related to the unknown input \mathbf{f}^u in the above equation.

It should be emphasized that the partially measured acceleration and displacement responses are used in the data fusion based UKF-UI as an on-line technique to restrain the ‘drift’ in identification results [30]. Thus, the observation equation in the discrete form is given as

$$\begin{aligned} \mathbf{y}_{k+1} &= \begin{bmatrix} \ddot{\mathbf{x}}_{m,k+1} \\ \mathbf{x}_{m,k+1} \end{bmatrix} = \begin{bmatrix} \mathbf{L}_a & \mathbf{0} \\ \mathbf{0} & \mathbf{L}_d \end{bmatrix} \begin{bmatrix} \mathbf{M}^{-1} \left[\boldsymbol{\eta} \mathbf{f}_{k+1} - \mathbf{R}(\boldsymbol{\theta}_{k+1}, \mathbf{x}_{k+1}, \dot{\mathbf{x}}_{k+1}) \right] \\ \dot{\mathbf{x}}_{k+1} \end{bmatrix} + \begin{bmatrix} \mathbf{L}_a \mathbf{M}^{-1} \boldsymbol{\eta}^u \mathbf{f}_{k+1}^u \\ \mathbf{0} \end{bmatrix} + \mathbf{v}_{k+1} \quad (32) \\ &= \mathbf{h}(\mathbf{Z}_{k+1}, \mathbf{f}_{k+1}) + \boldsymbol{\lambda}^u \mathbf{f}_{k+1}^u + \mathbf{v}_{k+1} \end{aligned}$$

where $\mathbf{x}_{m,k+1}$ is the measured displacement at $t = (k+1)\Delta t$ with the position matrix \mathbf{L}_d , and $\boldsymbol{\lambda}^u$ is the influence matrix.

The proposed FUKF-UI has a similar process with FUKF. Only the main formulas are briefly presented here.

Sigma point calculation

The same set of sigma points $\boldsymbol{\chi}_{k|k}$ are generated as shown in Eq. (4).

Time predication

Under the premise of zero-order hold (ZOH), the propagation of the sigma points at $t = (k+1)\Delta t$ is expressed as

$$\boldsymbol{\chi}_{i,k+1|k} = \boldsymbol{\chi}_{i,k|k} + \int_{k\Delta t}^{(k+1)\Delta t} \mathbf{g}(\boldsymbol{\chi}_{i,t|k}, \mathbf{f}) dt + \boldsymbol{\Phi}^u \mathbf{f}_{k|k}^u \Delta t \quad (33)$$

The predicted state vector $\tilde{\mathbf{z}}_{k+1|k}$ and its error covariance matrix $\tilde{\mathbf{P}}_{\mathbf{Z},k+1|k}$ are provided by the same formulas in Eqs. (6) and (7), respectively.

The estimated measurement vector $\hat{\mathbf{y}}_{k+1|k+1}$ at $t = (k+1)\Delta t$ is given as

$$\hat{\mathbf{y}}_{k+1|k+1} = \sum_{i=0}^{2N} W_i^m \left[\mathbf{h}(\boldsymbol{\chi}_{i,k+1|k}, \mathbf{f}_{k+1}) \right] + \boldsymbol{\lambda}^u \hat{\mathbf{f}}_{k+1|k+1}^u \quad (34)$$

The error covariance matrix of measurement vector $\hat{\mathbf{P}}_{\mathbf{y},k+1}$ and the cross-covariance matrix $\hat{\mathbf{P}}_{\mathbf{z}_y,k+1}$ are found in Eqs. (9) and (10), respectively.

Unknown input calculation

The state vector is updated by Eq. (11), which is workable only when the unknown input $\hat{\mathbf{f}}_{k+1|k+1}^u$ is given for the reason that $\hat{\mathbf{y}}_{k+1|k+1}$ is a function of $\hat{\mathbf{f}}_{k+1|k+1}^u$, as shown in Eq. (34). To solve the unknown force $\hat{\mathbf{f}}_{k+1|k+1}^u$, the estimated state vector $\hat{\mathbf{z}}_{k+1|k+1}$ in Eq. (11) is substituted into the measurement equation

$$\hat{\mathbf{y}}_{k+1|k+1} = \mathbf{h}\left(\hat{\mathbf{z}}_{k+1|k+1}, \mathbf{f}_{k+1}\right) + \lambda^u \hat{\mathbf{f}}_{k+1|k+1}^u \quad (35)$$

Then an estimation error function is established between the real measurement and the estimated measurement as

$$\Delta_{k+1} = \mathbf{y}_{k+1} - \mathbf{h}\left(\hat{\mathbf{z}}_{k+1|k+1}, \mathbf{f}_{k+1}\right) - \lambda^u \hat{\mathbf{f}}_{k+1|k+1}^u \quad (36)$$

Under the condition that the number of observed measurements is larger than that of the unknown excitations, $\hat{\mathbf{f}}_{k+1|k+1}^u$ can be computed by minimizing the error Δ_{k+1} in Eq. (36) by solving a nonlinear least-squares problem.

Measurement updating

Once $\hat{\mathbf{f}}_{k+1|k+1}^u$ is obtained, the estimated measurement vector $\hat{\mathbf{y}}_{k+1|k+1}$ can be calculated with Eq. (34). Then the estimated state vector $\hat{\mathbf{z}}_{k+1|k+1}$ is solved by Eq. (11). Finally, the error covariance matrix $\hat{\mathbf{P}}_{\mathbf{z},k+1|k+1}$ is updated using Eq. (12).

3.1.2. Identify the time-varying physical parameters by the proposed WMA integrated with UKF-UI method

After the qualitative analysis of time-varying physical parameters under unknown excitations by FUKF-UI, a new method is proposed for quantitative identification of time-varying parameters, which combines the advantage of WMA and UKF-UI under unknown excitations.

The proposed WMA integrated with UKF-UI method has a similar process as WMA integrated with UKF method presented in Section 2.1.2. Firstly, the time-varying physical parameters distinguished in the first step can be reconstructed based on the given time-invariant scale coefficient vector $\boldsymbol{\psi}_{J,l}$ in Eq. (14). Then with the initial time-invariant physical parameter vector $\boldsymbol{\theta}_2$, UKF-UI is applied to obtain the estimated state and input following Eqs. (37)-(41).

The equation of motion, state equation and measurement equation of a nonlinear system under unknown excitations are rewritten as

$$\mathbf{M}\ddot{\mathbf{x}}(t) + \mathbf{R}(\boldsymbol{\theta}_1(\boldsymbol{\psi}_{J,l}), \boldsymbol{\theta}_2, \mathbf{x}(t), \dot{\mathbf{x}}(t)) = \boldsymbol{\eta}\mathbf{f}(t) + \boldsymbol{\eta}^u\mathbf{f}^u(t) \quad (37)$$

$$\dot{\mathbf{x}} = \begin{Bmatrix} \dot{\mathbf{x}} \\ \ddot{\mathbf{x}} \end{Bmatrix} = \begin{Bmatrix} \dot{\mathbf{x}} \\ \mathbf{M}^{-1}[\boldsymbol{\eta}\mathbf{f} - \mathbf{R}(\boldsymbol{\theta}_1(\boldsymbol{\psi}_{J,l}), \boldsymbol{\theta}_2, \mathbf{x}, \dot{\mathbf{x}})] \end{Bmatrix} + \begin{Bmatrix} \mathbf{0} \\ \mathbf{M}^{-1}\boldsymbol{\eta}^u \end{Bmatrix} \mathbf{f}^u + \mathbf{w} = \mathbf{g}(\mathbf{X}, \boldsymbol{\theta}_1(\boldsymbol{\psi}_{J,l}), \boldsymbol{\theta}_2, \mathbf{f}) + \boldsymbol{\phi}^u\mathbf{f}^u + \mathbf{w} \quad (38)$$

$$\begin{aligned} \mathbf{y}_{k+1} &= \begin{bmatrix} \ddot{\mathbf{x}}_{m,k+1} \\ \mathbf{x}_{m,k+1} \end{bmatrix} = \begin{bmatrix} \mathbf{L}_a & \mathbf{0} \\ \mathbf{0} & \mathbf{L}_d \end{bmatrix} \begin{bmatrix} \mathbf{M}^{-1}[\boldsymbol{\eta}\mathbf{f}_{k+1} - \mathbf{R}(\boldsymbol{\theta}_1(\boldsymbol{\psi}_{J,l}), \boldsymbol{\theta}_2, \mathbf{x}_{k+1}, \dot{\mathbf{x}}_{k+1})] \\ \dot{\mathbf{x}}_{k+1} \end{bmatrix} + \begin{bmatrix} \mathbf{L}_a\mathbf{M}^{-1}\boldsymbol{\eta}^u\mathbf{f}_{k+1}^u \\ \mathbf{0} \end{bmatrix} + \mathbf{v}_{k+1} \\ &= \mathbf{h}(\mathbf{X}_{k+1}, \boldsymbol{\theta}_1(\boldsymbol{\psi}_{J,l}), \boldsymbol{\theta}_2, \mathbf{f}_{k+1}) + \boldsymbol{\lambda}^u\mathbf{f}_{k+1}^u + \mathbf{v}_{k+1} \end{aligned} \quad (39)$$

The predicted state vector $\tilde{\mathbf{X}}_{k+1|k}$ is given as

$$\boldsymbol{\chi}_{i,k+1|k} = \boldsymbol{\chi}_{i,k|k} + \int_{k\Delta t}^{(k+1)\Delta t} \mathbf{g}(\boldsymbol{\chi}_{i,t|k}, \boldsymbol{\theta}_1(\boldsymbol{\psi}_{J,l}), \boldsymbol{\theta}_2, \mathbf{f})dt + \boldsymbol{\phi}^u\mathbf{f}_{k|k}^u\Delta t; \quad \tilde{\mathbf{X}}_{k+1|k} = \sum_{i=0}^{2N} W_i^m \boldsymbol{\chi}_{i,k+1|k} \quad (40)$$

The estimated measurement vector $\hat{\mathbf{y}}_{k+1|k+1}$ is rewritten as

$$\hat{\mathbf{y}}_{k+1|k+1} = \sum_{i=0}^{2N} W_i^m \left[\mathbf{h}(\boldsymbol{\chi}_{i,k+1|k}, \boldsymbol{\theta}_1(\boldsymbol{\psi}_{J,l}), \boldsymbol{\theta}_2, \mathbf{f}_{k+1}) \right] + \boldsymbol{\lambda}^u\hat{\mathbf{f}}_{k+1|k+1}^u \quad (41)$$

The related error covariance matrices are shown in Eqs. (19), (21) and (22), respectively.

Under the condition that the number of measurements is larger than that of the unknown excitations, $\hat{\mathbf{f}}_{k+1|k+1}^u$ can be computed by minimizing the error Δ_{k+1}

$$\Delta_{k+1} = \mathbf{y}_{k+1} - \mathbf{h}\left(\hat{\mathbf{X}}_{k+1|k+1}, \boldsymbol{\theta}_1(\boldsymbol{\psi}_{J,l}), \boldsymbol{\theta}_2, \mathbf{f}_{k+1}\right) - \boldsymbol{\lambda}^u \hat{\mathbf{f}}_{k+1|k+1}^u \quad (42)$$

Then the estimated measurement vector $\hat{\mathbf{y}}_{k+1|k+1}$ is obtained by Eq. (34), and the structural state vector $\hat{\mathbf{x}}_{k+1|k+1}$ and error covariance matrix $\hat{\mathbf{P}}_{\mathbf{x},k+1|k+1}$ are updated by Eqs. (11) and (12), respectively.

In conclusion, the estimated state vector $\hat{\mathbf{X}}$ and estimated excitation vector $\hat{\mathbf{f}}^u$ are implicit functions of scale coefficient vector $\boldsymbol{\psi}_{J,l}$ and time-invariant physical parameter vector $\boldsymbol{\theta}_2$, namely:

$$\hat{\mathbf{X}} = \hat{\mathbf{X}}(\boldsymbol{\psi}_{J,l}, \boldsymbol{\theta}_2), \quad \hat{\mathbf{f}}^u = \hat{\mathbf{f}}^u(\boldsymbol{\psi}_{J,l}, \boldsymbol{\theta}_2) \quad (43)$$

Similarly, the estimated acceleration is rewritten as

$$\hat{\mathbf{x}}(\boldsymbol{\psi}_{J,l}, \boldsymbol{\theta}_2) = \mathbf{M}^{-1} \left(\boldsymbol{\eta} \mathbf{f} + \boldsymbol{\eta}^u \hat{\mathbf{f}}^u(\boldsymbol{\psi}_{J,l}, \boldsymbol{\theta}_2) - \mathbf{R} \left(\boldsymbol{\theta}_1(\boldsymbol{\psi}_{J,l}), \boldsymbol{\theta}_2, \hat{\mathbf{x}}(\boldsymbol{\psi}_{J,l}, \boldsymbol{\theta}_2), \hat{\mathbf{x}}(\boldsymbol{\psi}_{J,l}, \boldsymbol{\theta}_2) \right) \right) \quad (44)$$

Finally, the optimal scale coefficient vector $\hat{\boldsymbol{\psi}}_{J,l}$ and optimal time-invariant physical parameter vector $\hat{\boldsymbol{\theta}}_2$ are obtained by minimizing the same objective error function in Eq. (26), and the optimal time-varying physical parameter vector $\hat{\boldsymbol{\theta}}_1$ is reconstructed by the inverse WMA in Eq. (14).

3.2 Numerical verification : Identification of a time-varying nonlinear one-span truss subjected to an unknown force excitation

As shown in Fig. 10, a one-span truss subjected to an unknown white noise excitation is investigated as a more complex numerical example. It is aimed at identifying the stiffness

parameter of each member and the Bouc-Wen model parameters with partial acceleration and displacement measurements.

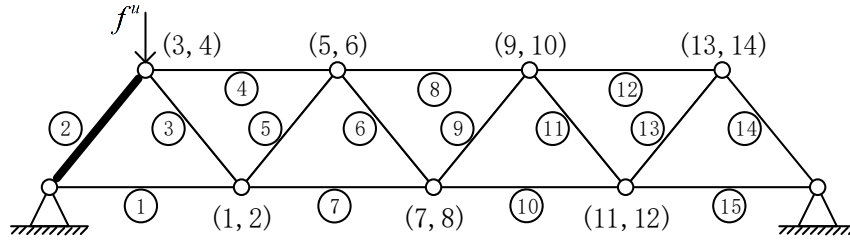


Fig. 10 A one-span truss subjected to an unknown white noise excitation

The truss consists of 15 members and 14 DOFs in total, as shown in Fig. 10. In this numerical example, structural parameters are selected as: The length and cross-section of each bar is $l_i=1\text{m}$ and $A_i=7.85\times 10^{-5}\text{m}^2$ ($i=1,2,\dots,15$), respectively. The total mass of each bar is constant as $m_i=54.95\text{kg}$ ($i=1,2,\dots,15$). The Rayleigh damping is adopted with the first two damping ratios assumed as 0.02. The first five-order natural frequencies of the time-invariant truss are 1.46Hz, 2.99Hz, 3.92Hz, 6.32Hz and 7.31Hz, respectively. An unknown white noise excitation f'' is applied on the 4th DOF of the truss. The sampling frequency is 50Hz during the process of dynamic response calculation and the sampling period is 10s. Six accelerations of the 2nd, 4th, 6th, 8th, 10th, and 12th DOFs and two displacements of the 6th and 14th DOFs are polluted with 2% RMS noise and used as measured responses for identification analysis.

Nonlinear damage is assumed in the 2nd bar element with the Bouc-Wen model governed by Eq. (28). The time-varying physical parameters are defined as

$$k_2 = \begin{cases} 1.57 \times 10^5 \text{ N/m}, & 0s \leq t < 5.2s \\ 1.256 \times 10^5 \text{ N/m}, & 5.2s \leq t \leq 10s \end{cases}$$

$$k_i = 1.57 \times 10^5 \text{ N/m}, \quad 0s \leq t \leq 10s \quad (i = 1, 3, 4, \dots, 15)$$

$$\beta_2 = \begin{cases} 8000, & 0s \leq t < 5.2s \\ 10400, & 5.2s \leq t \leq 10s \end{cases}$$

$$\gamma_2 = \begin{cases} 6000, & 0s \leq t < 5.2s \\ 8400, & 5.2s \leq t \leq 10s \end{cases}$$

The identified stiffness results using the FUKF-UI method are shown in Fig. 11. k_2 and nonlinear model parameters are expanded by the Db1 wavelet function and the scale level is $J = 7$ based on the studies in Ref. [27]. Fig. 12 shows the identified time-varying stiffness parameter and Bouc-Wen model parameters using the proposed WMA integrated with UKF-UI method, which manifests its effectiveness in identifying physical parameters of time-varying nonlinear truss structure with limited number of response measurements and unknown excitations. Meanwhile, the proposed method also gives accurate reconstruction of external force as demonstrated in Fig. 13. Table 1 lists the calculated relative errors of time-invariant stiffness parameters. Most of the relative errors are around 1%, and the maximum value is only 5.29% for the eighth element stiffness parameter.

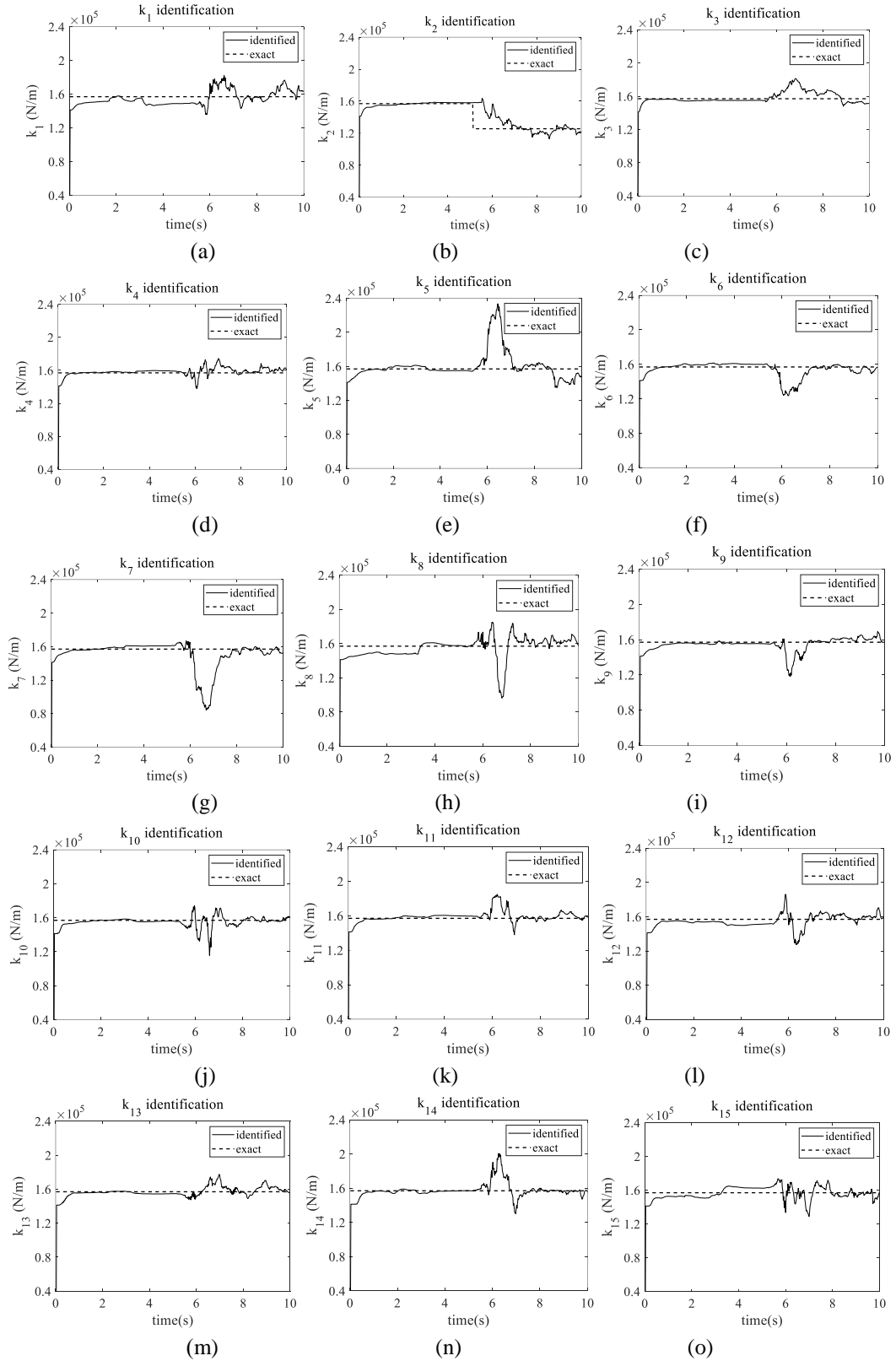


Fig. 11 Identification results of the truss model using the FUKF-UI method. (a) k_1 ; (b) k_2 ; (c) k_3 ; (d) k_4 ;

(e) k_5 ; (f) k_6 ; (g) k_7 ; (h) k_8 ; (i) k_9 ; (j) k_{10} ; (k) k_{11} ; (l) k_{12} ; (m) k_{13} ; (n) k_{14} ; (o) k_{15}

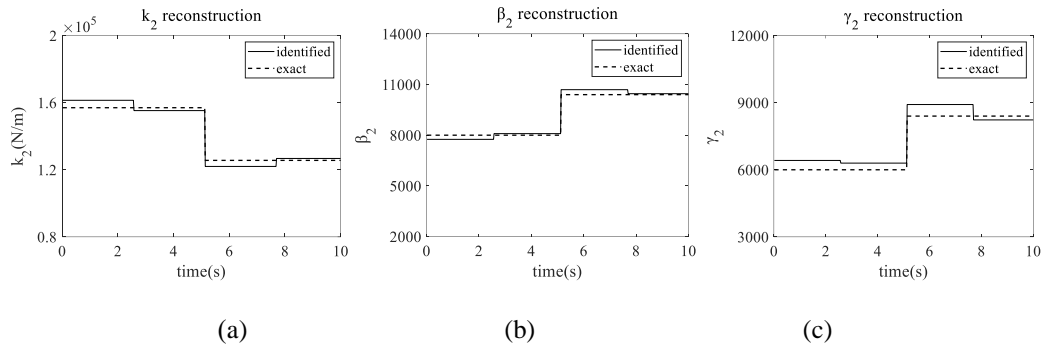


Fig. 12 Comparison of the exact and identified time-varying physical parameters of the truss. (a) k_2 ; (b)

β_2 ; (c) γ_2

Table 1 Identified stiffness of time-invariant members in the truss.

Member No.	Actual stiffness (N/m)	Identified stiffness (N/m)	Relative error
1	157000	159139.70	1.36%
3	157000	158973.71	1.26%
4	157000	155389.34	-1.03%
5	157000	159695.78	1.72%
6	157000	162307.30	3.38%
7	157000	155094.62	-1.21%
8	157000	165298.77	5.29%
9	157000	157728.76	0.46%
10	157000	156832.25	-0.11%
11	157000	156068.42	-0.59%
12	157000	159077.60	1.32%
13	157000	164468.80	4.76%
14	157000	157312.26	0.20%
15	157000	159619.98	1.67%

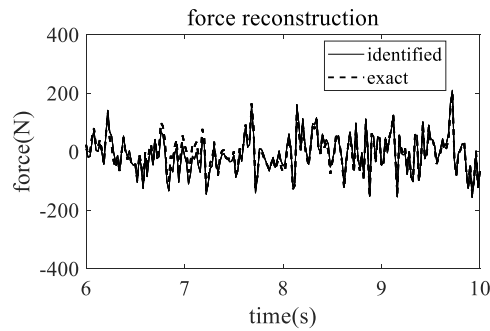


Fig. 13 Comparison of the exact and identified external excitation (6s ~ 10s)

4 Identification of time-varying nonlinear structures with more number of elements under unknown excitations

It should be noted that the cases discussed above are all about the identification of time-varying nonlinear structures with a small number of elements. With the increasing number of elements, the number of expanded scale coefficients is also significantly increased. Since the basis of the proposed methods in Section 2.1.2 and Section 3.1.2 is a nonlinear least-squares optimization, a large number of scale coefficients may result in convergence to local optimization results, especially when the quality of the collected data is poor. Herein, combining the sub-structural method, a two-step identification process is proposed for the identification of time-varying nonlinear structures with more number of elements under unknown excitations.

4.1 The proposed two-step identification process

4.1.1. Locate the time-varying physical parameters of the whole structure by the proposed FUKF-UI method

The FUKF-UI method proposed in Section 3.1.1 is used here to locate the time-varying physical parameters of the whole structure.

4.1.2. Divide into substructures and identify the sub-structural time-varying physical parameters by the proposed WMA integrated with UKF-UI method

As demonstrated above the proposed WMA integrated with UKF-UI method can accurately identify the actual unknown external loads. Therefore, it can be used to determine the unknown interaction forces acting on the divided substructures in the following sub-structural based method.

When aiming at the identification of time-varying nonlinear structures with more elements, the whole structure is divided into several substructures to limit the number of parameters in each

optimization analysis. For each substructure, the initial time-varying physical parameter vector $\boldsymbol{\theta}_{s1}$ can be reconstructed by the given time-invariant scale coefficient vector $\boldsymbol{\psi}_{J_s, l_s}$ by Eq. (14). Thus, it is converted into the identification of a time-invariant nonlinear system. The equation of motion of the substructure is written as

$$\begin{aligned} \mathbf{M}_s \ddot{\mathbf{x}}_s + \mathbf{R}_s \left(\boldsymbol{\theta}_{s1} \left(\boldsymbol{\psi}_{J_s, l_s} \right), \boldsymbol{\theta}_{s2}, \mathbf{x}_s, \dot{\mathbf{x}}_s \right) &= \boldsymbol{\eta}_s \mathbf{f}_s + \boldsymbol{\eta}_s^u \mathbf{f}_s^u \\ \left\{ \begin{array}{l} \boldsymbol{\eta}_s^u = \left[\boldsymbol{\eta}_{se}^u \quad \boldsymbol{\eta}_{sb}^* \right] \\ \mathbf{f}_s^u = \left[\mathbf{f}_{se}^u \quad \mathbf{f}_{sb}^* \right]^T \end{array} \right. & \end{aligned} \quad (45)$$

in which the subscript “ s ” indicates that these properties are possessed by the substructure. \mathbf{M}_s is the mass matrix of the substructure. \mathbf{x}_s , $\dot{\mathbf{x}}_s$, and $\ddot{\mathbf{x}}_s$ are displacement, velocity, and acceleration response vector of substructure, respectively. $\boldsymbol{\theta}_{s2}$ is the time-invariant physical parameter vector of the substructure, \mathbf{f}_s is the known excitation (if have) of the substructure with the influence matrix $\boldsymbol{\eta}_s$, and \mathbf{f}_s^u is the unknown input of the substructure with the influence matrix $\boldsymbol{\eta}_s^u$. \mathbf{f}_s^u is composed of the actual unknown external excitation \mathbf{f}_{se}^u and the unknown sub-structural interaction force \mathbf{f}_{sb}^* , $\boldsymbol{\eta}_{se}^u$ and $\boldsymbol{\eta}_{sb}^*$ are their influence matrix, respectively.

The state space equation and measurement equation are given as

$$\begin{aligned} \dot{\mathbf{X}}_s &= \begin{Bmatrix} \dot{\mathbf{x}}_s \\ \ddot{\mathbf{x}}_s \end{Bmatrix} = \begin{Bmatrix} \dot{\mathbf{x}}_s \\ \mathbf{M}_s^{-1} \left[\boldsymbol{\eta}_s \mathbf{f}_s - \mathbf{R}_s \left(\boldsymbol{\theta}_{s1} \left(\boldsymbol{\psi}_{J_s, l_s} \right), \boldsymbol{\theta}_{s2}, \mathbf{x}_s, \dot{\mathbf{x}}_s \right) \right] \end{Bmatrix} + \begin{Bmatrix} \mathbf{0} \\ \mathbf{M}_s^{-1} \boldsymbol{\eta}_s^u \end{Bmatrix} \mathbf{f}_s^u + \mathbf{w}_s \\ &= \mathbf{g}_s \left(\mathbf{X}_s, \boldsymbol{\theta}_{s1} \left(\boldsymbol{\psi}_{J_s, l_s} \right), \boldsymbol{\theta}_{s2}, \mathbf{f}_s \right) + \boldsymbol{\eta}_s^u \mathbf{f}_s^u + \mathbf{w}_s \end{aligned} \quad (46)$$

$$\begin{aligned} \mathbf{y}_{s,k+1} &= \begin{bmatrix} \ddot{\mathbf{x}}_{sm,k+1} \\ \mathbf{x}_{sm,k+1} \end{bmatrix} \\ &= \begin{bmatrix} \mathbf{L}_{sa} & \mathbf{0} \\ \mathbf{0} & \mathbf{L}_{sd} \end{bmatrix} \begin{bmatrix} \mathbf{M}_s^{-1} \left[\boldsymbol{\eta}_s \mathbf{f}_{s,k+1} - \mathbf{R}_s \left(\boldsymbol{\theta}_{s1} \left(\boldsymbol{\psi}_{J_s, l_s} \right), \boldsymbol{\theta}_{s2}, \mathbf{x}_{s,k+1}, \dot{\mathbf{x}}_{s,k+1} \right) \right] \\ \dot{\mathbf{x}}_{s,k+1} \end{bmatrix} + \begin{bmatrix} \mathbf{L}_{sa} \mathbf{M}_s^{-1} \boldsymbol{\eta}_s^u \mathbf{f}_{s,k+1}^u \\ \mathbf{0} \end{bmatrix} + \mathbf{v}_{s,k+1} \\ &= \mathbf{h}_s \left(\mathbf{X}_{s,k+1}, \boldsymbol{\theta}_{s1} \left(\boldsymbol{\psi}_{J_s, l_s} \right), \boldsymbol{\theta}_{s2}, \mathbf{f}_{s,k+1} \right) + \boldsymbol{\lambda}_s^u \mathbf{f}_{s,k+1}^u + \mathbf{v}_{s,k+1} \end{aligned} \quad (47)$$

where \mathbf{W}_s is the process noise, $\mathbf{y}_{s,k+1}$ is the sub-structural measurements at the time instant $t=(k+1)\Delta t$ including the partially measured acceleration response $\ddot{\mathbf{x}}_{sm,k+1}$ and displacement response $\mathbf{x}_{sm,k+1}$. \mathbf{L}_{sa} and \mathbf{L}_{sd} are position matrices of accelerometer and displacement responses in the substructure, respectively. \mathbf{v}_s is the measurement noise.

Following the procedure of UKF-UI, the estimated state vector of substructure $\hat{\mathbf{X}}_s$ and unknown excitation vector $\hat{\mathbf{f}}_s^u$ can be obtained, which are implicit functions of scale coefficient vector $\boldsymbol{\Psi}_{J_s, J_s}$ and time-invariant physical parameter vector $\boldsymbol{\theta}_{s2}$, that is

$$\hat{\mathbf{X}}_s = \hat{\mathbf{X}}_s(\boldsymbol{\Psi}_{J_s, J_s}, \boldsymbol{\theta}_{s2}), \quad \hat{\mathbf{f}}_s^u = \hat{\mathbf{f}}_s^u(\boldsymbol{\Psi}_{J_s, J_s}, \boldsymbol{\theta}_{s2}) \quad (48)$$

Similarly, the estimated acceleration is rewritten as

$$\hat{\ddot{\mathbf{x}}}_s(\boldsymbol{\Psi}_{J_s, J_s}, \boldsymbol{\theta}_{s2}) = \mathbf{M}_s^{-1} \left(\boldsymbol{\eta}_s \mathbf{f}_s + \boldsymbol{\eta}_s^u \hat{\mathbf{f}}_s^u(\boldsymbol{\Psi}_{J_s, J_s}, \boldsymbol{\theta}_{s2}) - \mathbf{R}_s \left(\boldsymbol{\theta}_{s1}(\boldsymbol{\Psi}_{J_s, J_s}), \boldsymbol{\theta}_{s2}, \hat{\mathbf{x}}_s(\boldsymbol{\Psi}_{J_s, J_s}, \boldsymbol{\theta}_{s2}), \hat{\ddot{\mathbf{x}}}_s(\boldsymbol{\Psi}_{J_s, J_s}, \boldsymbol{\theta}_{s2}) \right) \right) \quad (49)$$

Finally, the optimal scale coefficient vector $\hat{\boldsymbol{\Psi}}_{J_s, J_s}$ and optimal time-invariant physical parameter vector $\hat{\boldsymbol{\theta}}_{s2}$ for the substructure are obtained by minimizing the objective error function in Eq. (50). Then the optimal time-varying physical parameter vector $\hat{\boldsymbol{\theta}}_{s1}$ is reconstructed by the inverse WMA.

$$[\hat{\boldsymbol{\Psi}}_{J_s, J_s}, \hat{\boldsymbol{\theta}}_{s2}] = \arg \min_{\boldsymbol{\Psi}_{J_s, J_s}, \boldsymbol{\theta}_{s2}} \left(\left\| \ddot{\mathbf{x}}_{sm} - \mathbf{L}_{sa} \hat{\ddot{\mathbf{x}}}_s(\boldsymbol{\Psi}_{J_s, J_s}, \boldsymbol{\theta}_{s2}) \right\|_2^2 \right) \quad (50)$$

Considering that every substructure is independent of each other, the time-varying physical parameters can be identified by using the proposed WMA integrated with UKF-UI method in parallel, which greatly improves the computational efficiency.

4.2 Numerical verification: Identification of a time-varying nonlinear 10-story shear frame with an unknown excitation using the sub-structural method

In this section, a 10-story shear frame under unknown excitation is used to demonstrate the feasibility of the sub-structural method for the identification of a time-varying nonlinear structure with more number of elements. The mass of each story is $m_i=2000\text{kg}$ ($i=1,2,\dots,10$). The first five-order natural frequencies of the time-invariant system are 0.31Hz, 0.92Hz, 1.52Hz, 2.08Hz and 2.60Hz, respectively. It is assumed that the nonlinear damage occurs in the first floor and the Bouc-Wen model governed by Eq. (28) is assumed. $n_1=1.8$. A white noise excitation is imposed on the top floor to excite the structure, which is assumed unknown in the identification analysis. The corresponding dynamic responses are computed with a sampling frequency of 50Hz, and the complete sampling period is 10s. The specific expressions of other physical parameters are given as

$$\begin{aligned}
k_1 &= \begin{cases} 3.0 \times 10^5 \text{ N/m}, & 0 \leq t < 5.2 \text{ s} \\ 2.4 \times 10^5 \text{ N/m}, & 5.2 \text{ s} \leq t \leq 10 \text{ s} \end{cases} & k_7 &= \begin{cases} 3.5 \times 10^5 \text{ N/m}, & 0 \leq t < 5.2 \text{ s} \\ 2.73 \times 10^5 \text{ N/m}, & 5.2 \text{ s} \leq t \leq 10 \text{ s} \end{cases} \\
k_{10} &= \begin{cases} 3.5 \times 10^5 \text{ N/m}, & 0 \leq t < 5.2 \text{ s} \\ 2.975 \times 10^5 \text{ N/m}, & 5.2 \text{ s} \leq t \leq 10 \text{ s} \end{cases} & k_i &= 3.5 \times 10^5 \text{ N/m}, \quad 0 \leq t \leq 10 \text{ s} \quad (i=2, \dots, 6, 8, 9) \\
c_i &= 1000 \text{ N}\cdot\text{s/m}, \quad 0 \leq t \leq 10 \text{ s} \quad (i=1, \dots, 10) \\
\beta_1 &= \begin{cases} 600, & 0 \leq t < 5.2 \text{ s} \\ 780, & 5.2 \text{ s} \leq t \leq 10 \text{ s} \end{cases} & \gamma_1 &= 600, \quad 0 \leq t \leq 10 \text{ s}
\end{aligned}$$

The FUKF-UI method is implemented to roughly locate the changing physical parameters. Six acceleration measurements at the 1st, 3rd, 5th, 7th, 8th, and 10th floors and two interlayer displacements of the 1st-2nd and 9th-10th floors are used. Each response is contaminated with a 2% RMS white noise. Stiffness identification results are shown in Fig. 14. The stiffness of the 1st, 7th, and 10th stories are more likely to change, as they transit from one stable convergence value to the other stable value, while other stiffness values are more likely to remain unchanged, since only one convergence value appears despite occasional fluctuations.

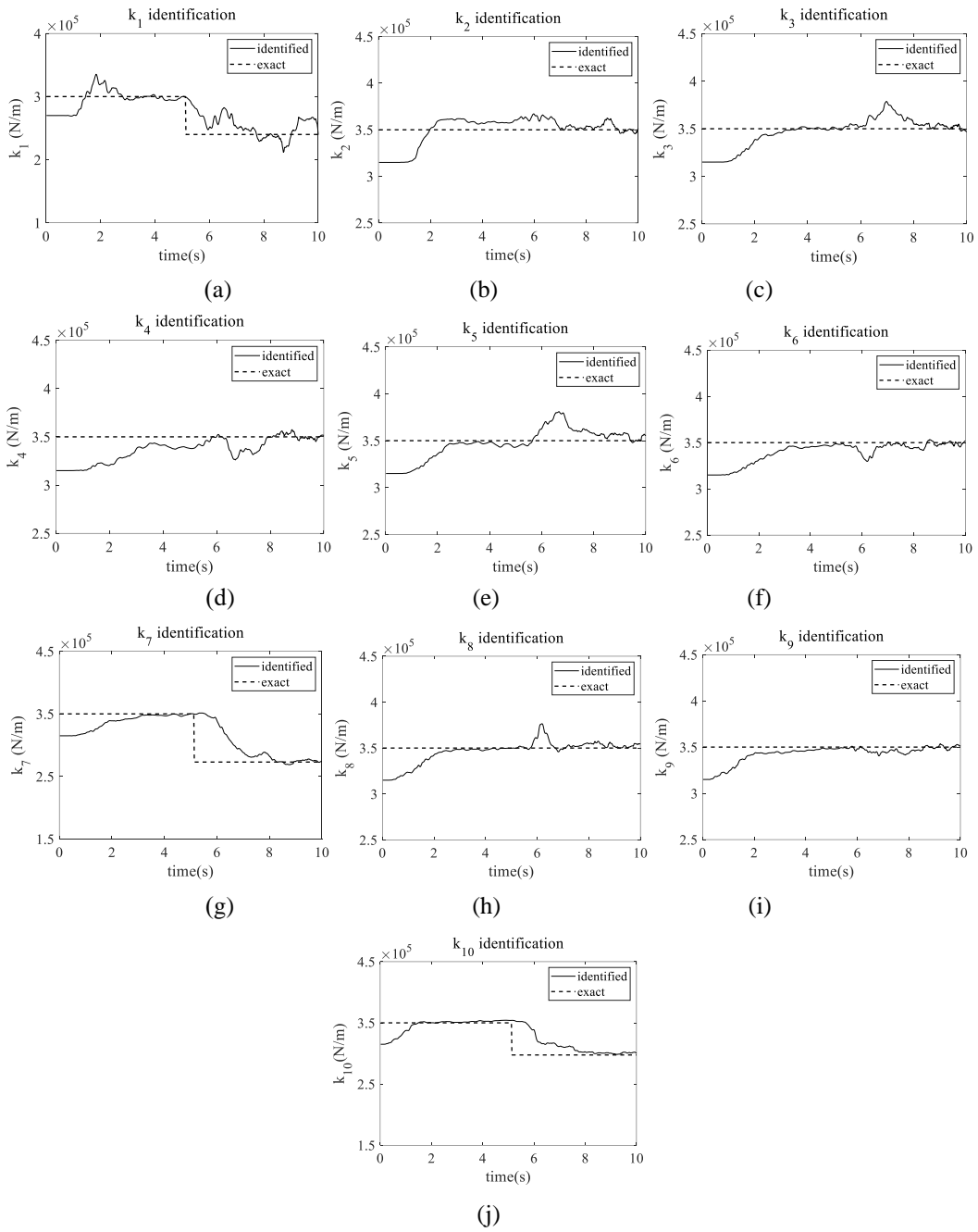


Fig. 14 Identification results using the FUKF-UI method in the shear frame. (a) k_1 ; (b) k_2 ; (c) k_3 ; (d) k_4 ;

(e) k_5 ; (f) k_6 ; (g) k_7 ; (h) k_8 ; (i) k_9 ; (j) k_{10}

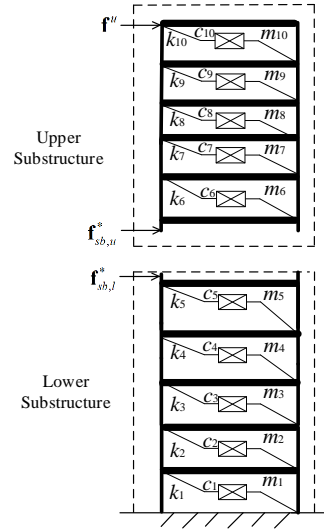


Fig. 15 Substructures of a 10-story shear frame

The whole structure is divided into two substructures as illustrated in Fig. 15, and the physical parameters in each substructure are identified using the proposed WMA integrated with UKF-UI method in parallel.

Lower substructure

In this numerical example, the 1st~5th DOFs are in the scope of the lower substructure. The accelerations of the 1st, 3rd, and 5th floors and interlayer displacement of the 1st-2nd floors are measured with a 2% RMS noise and used as recorded responses for the identification analysis. k_1 , β_1 and γ_1 are expanded by the Db1 wavelet function and the scale level is $J = 7$ [27]. Fig. 16 exhibits the identified stiffness and nonlinear model parameters inside the lower substructure employing the WMA integrated with UKF-UI method. The results demonstrate that the identification accuracy is good, even the step changes in time-varying physical parameters can be identified accurately.

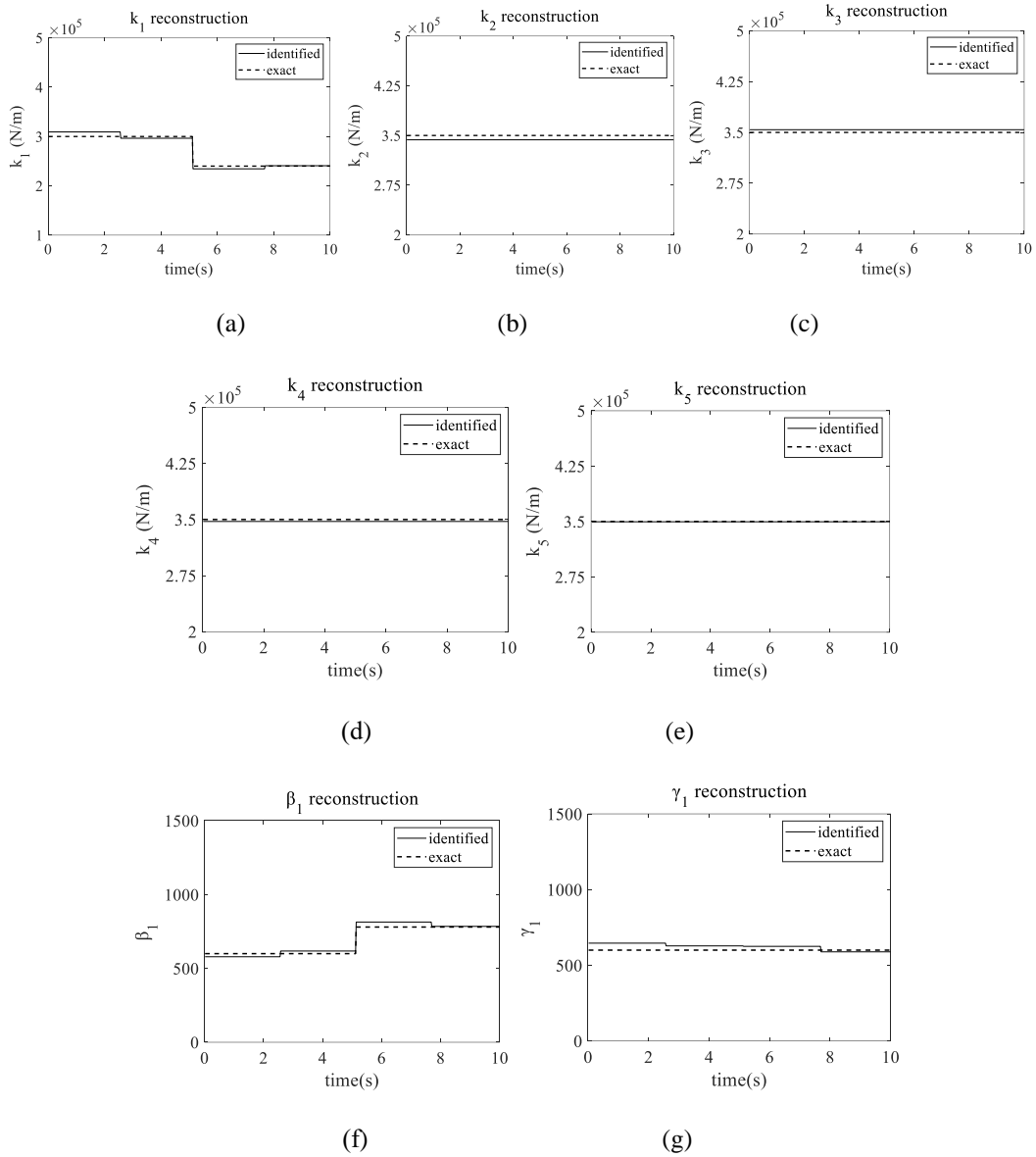


Fig. 16 Comparison of the exact and identified physical parameters of the lower substructure. (a) k_1 ; (b)

k_2 ; (c) k_3 ; (d) k_4 ; (e) k_5 ; (f) β_1 ; (g) γ_1

Upper substructure

The upper substructure is composed of 6~10 DOFs. The accelerations of the 6th, 8th and 10th floors and interlayer displacement of the 9th-10th floors are used as measurements with a 2% RMS noise for the identification analysis. k_7 and k_{10} are expanded by the Db1 wavelet function and the scale level is $J = 7$. Fig. 17 displays the identified stiffness parameters inside

the upper substructure, which demonstrates that the proposed WMA integrated with UKF-UI method is capable of the parametric identification of structures with more number of elements when combining with the sub-structural method. The external load applied on the top floor can also be identified as shown in Fig. 18, which shows that the identified force matches well with the exact one.

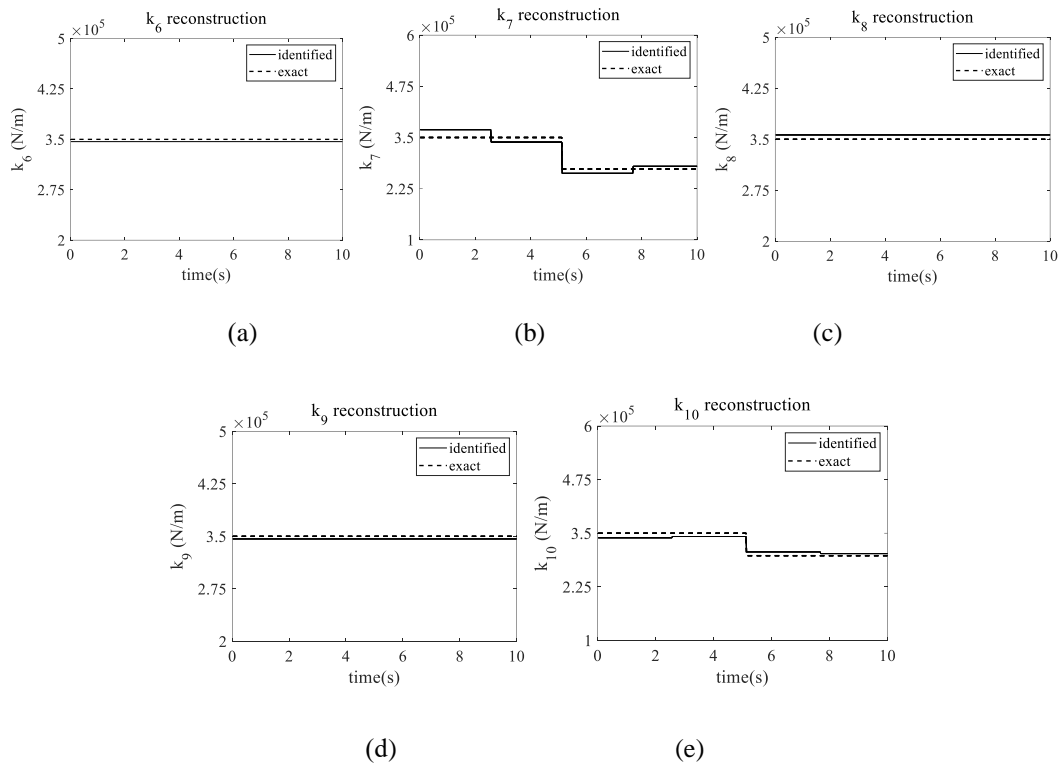


Fig. 17 Comparison of the exact and identified physical parameters of the upper substructure. (a) k_6 ; (b)

k_7 ; (c) k_8 ; (d) k_9 ; (e) k_{10}

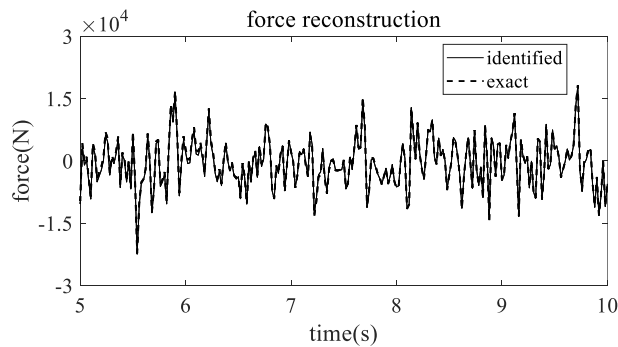


Fig. 18 Comparison of the exact and identified external excitations (5s ~ 10s)

5 Conclusions

The identification of time-varying nonlinear structural physical parameters is an important research topic with practical applications. Methods based on WMA can not only identify the time-varying physical parameters such as stiffness and damping coefficients but also the time-varying parameters in the nonlinear model. However, they require displacement, velocity, and acceleration responses of all DOFs, and known excitations to be used in the analysis. Moreover, all physical parameters are expanded into scale coefficients by WMA, which leads to a large number of scale coefficients and increases the difficulties in nonlinear system identification. This paper presents two-step identification processes using partial measurements to identify the time-varying physical parameters of nonlinear systems.

Firstly, the identification of time-varying nonlinear structures with a small number of elements under known excitations is conducted. The time-varying physical parameters are distinguished using the FUKF method. Then a method integrating WMA and UKF is proposed to identify the physical parameters in the case of known excitations. The proposed identification process contributes to reduce the number of scale coefficients, since not all physical parameters are required to be expanded after the locations of time-varying physical parameters are detected. Most importantly, only partial response measurements are needed in the identification process, a clear improvement of the previous WMA based methods which require response measurements at all DOFs.

Secondly, it is extended to the identification of time-varying nonlinear structures with a small number of elements but under unknown excitations. The time-varying physical parameters are localized using the proposed FUKF-UI method, and then all the physical parameters, as well as

the excitations are identified by the proposed WMA integrated with UKF-UI method. The proposed identification process meets the needs of practical engineering applications, since the physical parameters of time-varying nonlinear system can be identified by using partial response measurements under unknown excitations.

Thirdly, combining with the sub-structural method, it is further extended to identify the time-varying nonlinear structures with more number of elements under unknown excitations. The time-varying physical parameters of the whole structure are located by the proposed FUKF-UI method. Then the whole structure is divided into several substructures. Based on the proposed WMA integrated with UKF-UI method, each substructure is identified by considering the unknown interaction forces as the fictitious unknown inputs. With partial response measurements, each substructure can be identified in parallel without measuring the interaction forces.

Three numerical examples with noisy measurement data are conducted to verify the effectiveness and accuracy of the proposed identification methods. Experimental verification is still required in future to further demonstrate the efficiency of the proposed methods.

Acknowledgments

This research is supported by the National Natural Science Foundation of China through the key project No. 51838006.

Compliance with ethical standards

Conflict of interest: The authors declare that they have no conflict of interest concerning the publication of this manuscript.

References

1. Xin, Y., Hao, H., Li, J.: Time-varying system identification by enhanced Empirical Wavelet Transform

- based on Synchroextracting Transform. *Engineering Structures* **196**, 109313 (2019)
2. Li, J.T., Zhu, X.Q., Law, S.S., Samali, B.: Time-varying characteristics of bridges under the passage of vehicles using synchroextracting transform. *Mechanical systems and signal processing* **140**, 106727.1-106727.19 (2020)
 3. Ni, P.H., Li, J., Hao, H., Xia, Y., Wang, X.Y., Lee, J.M., Jung, K.H.: Time-varying system identification using variational mode decomposition. *Structural Control and Health Monitoring* **25**, e2175(2018)
 4. Bao, Y.Q., Chen, Z.C., Wei, S.Y., Xu, Y., Tang, Z.Y., Li, H.: The state of the art of data science and engineering in structural health monitoring. *Engineering* **5**(2), 234-242 (2019)
 5. Huang, Q., Xu, Y.L., Liu, H.J.: An efficient algorithm for simultaneous identification of time-varying structural parameters and unknown excitations of a building structure. *Eng Struct* **98**, 29–37(2015)
 6. Yang, J.N., Lin, S.L.: On-line identification of non-linear hysteretic structures using an adaptive tracking technique. *Int J Non Linear Mech* **39**(9), 1481–1491(2004)
 7. Mu, H.Q., Kuok, S.C., Yuen, K.V.: Stable robust extended Kalman filter. *J Aerosp Eng*, B4016010 (2016)
 8. Wang, C., Ren, W.X., Wang, Z.C., Zhu, H.P.: Time-varying physical parameter identification of shear type structures based on discrete wavelet transform. *Smart Structures and Systems* **14**(5), 831-845(2014)
 9. Xiang, M., Xiong, F., Shi, Y.F., Dai, K.S., Ding, Z.B.: Wavelet multi-resolution approximation of time-varying frame structure. *Advances in Mechanical Engineering* **10**(8),1–19(2018)
 10. Wang, C., Ai, D.M., Ren, W.X.: A wavelet transform and substructure algorithm for tracking the abrupt stiffness degradation of shear structure. *Advances in Structural Engineering* **22**(5), 1136-1148(2019)
 11. Chen, S.Y., Lu, J.B., Lei, Y.: Identification of time-varying systems with partial acceleration measurements by synthesis of wavelet decomposition and Kalman filter. *Advances in Mechanical Engineering* **12**(6), 168781402093046 (2020)
 12. Lei, Y., Yang, N.: Simultaneous identification of structural time-varying physical parameters and unknown excitations using partial measurements. *Engineering Structures*, **214**,110672 (2020)

13. Quaranta, G., Lacarbonara, W., Masri, S.F.: A review on computational intelligence for identification of nonlinear dynamical systems. *Nonlinear Dynamics* **99**,1709-1761(2020)
14. Xu, Y., Wei, S.Y., Bao, Y.Q., Li, H.: Automatic seismic damage identification of reinforced concrete columns from images by a region-based deep convolutional neural network. *Structural Control and Health Monitoring* **26**(3), e2313 (2019)
15. Xu, B., He, J., Dyke, S.J.: Model-free nonlinear restoring force identification for SMA dampers with double Chebyshev polynomials: approach and validation. *Nonlinear Dynamics* **82**(3), 1-16 (2015)
16. Wei, S., Peng, Z.K., Dong, X.J., Zhang, W.M.: A nonlinear subspace-prediction error method for identification of nonlinear vibrating structures. *Nonlinear Dynamics* **91**,1605-1617(2018)
17. He, J., Xu, B., Masri, S. F.: Restoring force and dynamic loadings identification for a nonlinear chain-like structure with partially unknown excitations. *Nonlinear Dynamics* **69**(1-2), 231-245 (2012)
18. Lei, Y., Luo, S.J., He, M.Y.: Identification of model-free structural nonlinear restoring forces using partial measurements of structural responses. *Advances in Structural Engineering* **20**(1), 69-80(2016)
19. Xu, B., Li, J., Dyke, S.J., Deng, B.C., He, J.: Nonparametric identification for hysteretic behavior modelled with a power series polynomial using EKF-WGI approach under limited acceleration and unknown mass. *International Journal of Non-linear Mechanics*, 103324(2019)
20. Cheng, C.M., Peng, Z.K., Zhang, W.M., Meng, G.: Volterra-series-based nonlinear system modeling and its engineering applications: a state-of-the-art review. *Mechanical Systems and Signal Processing* **87**, 340-364(2017)
21. Wang, Z.C., Ren, W.X., Chen, G.D.: Time-frequency analysis and applications in time-varying/nonlinear structural systems: A state-of-the-art review. *Advances in Structural Engineering* **21**, 1562-1584 (2018)
22. Qu, H.Y., Li, T.T., Chen, G. D.: Multiple analytical mode decompositions for nonlinear system identification from forced vibration. *Engineering Structures* **173**, 979-986(2018)
23. Li, H., Mao, C.X., Ou, J.P.: Identification of hysteretic dynamic systems by using hybrid extended Kalman filter and wavelet multiresolution analysis with limited observation. *Journal of Engineering Mechanics* **139**(5),547-558(2013)
24. Ghanem, R., Romeo, F.: A wavelet-based approach for model and parameter identification of non-linear systems. *International Journal of Non-Linear Mechanics* **36**(5), 835-859(2001)

25. Kougioumtzoglou, I.A., Spanos, P.D.: An identification approach for linear and nonlinear time-variant structural systems via harmonic wavelets. *Mechanical Systems & Signal Processing* **37**(1-2), 338-352(2013)
26. Yang, Y., Peng, Z.K., Dong, X. J., Zhang, W. M., Meng, G.: Nonlinear time-varying vibration system identification using parametric time–frequency transform with spline kernel. *Nonlinear Dynamics* **85**(3), 1679-1694 (2016)
27. Chang, C.C., Shi, Y.F.: Identification of time-varying hysteretic structures using wavelet multiresolution analysis. *International Journal of Non-Linear Mechanics* **45**(1), 21-34(2010)
28. Julier, S. J., Uhlmann, J. K., Durrant-Whyte, H.F.: A new approach for filtering nonlinear systems. *Proc. Am. Control Conf.* **3**, 1628–1632(1995)
29. Astroza, R., Alessandri, A., Conte, J. P.: Finite element model updating accounting for modeling uncertainty. *Mechanical Systems & Signal Processing*, **115**(15), 782-800 (2019)
30. Lei, Y., Xia, D.D., Erazo, K., Nagarajaiah, S.: A novel unscented Kalman filter for recursive state-input-system identification of nonlinear systems. *Mechanical Systems and Signal Processing* **127**(15),120-135(2019)
31. Jwo, D.J., Yang, C. F., Chuang, C.H., Lee, T.Y.: Performance enhancement for ultra-tight GPS/INS integration using a fuzzy adaptive strong tracking unscented Kalman filter. *Nonlinear Dynamics* **73**(1-2), 377-395(2013)
32. Hu, G.G., Wang, W., Zhong, Y.M., Gao, B.B., Gu, C.F.: A new direct filtering approach to INS/GNSS integration. *Aerospace Science and Technology* **77**,755-764(2018)
33. Bisht, S.S., Singh, M.P.: An adaptive unscented Kalman filter for tracking sudden stiffness changes. *Mechanical Systems & Signal Processing* **49**(1-2),181-195(2014)
34. Wang, N., Li, L., Wang, Q.: Adaptive UKF-based parameter estimation for Bouc-Wen model of magnetorheological elastomer materials. *Journal of Aerospace Engineering* **32**(1), 04018130 (2019)
35. Gaviria, C.A., Montejo, L.A.: Monitoring physical and dynamic properties of reinforced concrete structures during seismic excitations. *Construction and Building Materials* **196**, 43-53 (2019)
36. Koh, C.G., See, L.M., Balendra, T.: Estimation of structural parameters in time domain: A substructure approach. *Earthquake Engineering and Structural Dynamics* **20**(8), 787-801(1991)

37. Weng, S., Zhu, H.P., Xia, Y., Gao, F.: Substructuring Method in Structural Health Monitoring. *Structural Health Monitoring - Measurement Methods and Practical Applications* (2017)
38. Yuen, K.V., Huang, K.: Real-time substructural identification by boundary force modeling. *Structural Control and Health Monitoring* **25**(5), e2151.1-e2151.18 (2018)
39. Li, J., Hao, H.: Substructure damage identification based on wavelet-domain response reconstruction. *Structural Health Monitoring* **13**(4), 389-405(2014)
40. Liu, K., Law, S.S., Zhu, X.Q.: Substructural condition assessment based on force identification and interface force sensitivity. *International Journal of Structural Stability & Dynamics* **15**(2), 1450046 (2015)
41. Ni, P.H., Xia, Y., Li, J., Hao, H.: Improved decentralized structural identification with output only measurements. *Measurement* **122**, 597–610 (2018)
42. Su, T.L., Tang, Z.Y., Peng, L.Y., Bai, Y.T., Kong, J.L.: Model updating for real time dynamic substructures based on UKF algorithm. *Earthquake Engineering and Engineering Vibration* **19**(2), 413-421 (2020)
43. Kumar, R.K., Shankar, K.: Parametric identification of structures with nonlinearities using global and substructure approaches in the time domain. *Advances in Structural Engineering* **12**(2),195-210(2009)
44. Tao, D.W., Zhang, D.Y., Li, H.: Structural seismic damage detection using fractal dimension of time-frequency feature. *Key Engineering Materials* 558,554-560(2013)
45. Lei, Y., He, M.Y., Liu, C., Lin, S.Z.: Identification of tall shear buildings under unknown seismic excitation with limited output measurements. *Advances in Structural Engineering* **16**(11),1839-1850(2013)
46. Shi, Y.F., Chang, C.C.: Substructural time-varying parameter identification using wavelet multiresolution approximation. *Journal of Engineering Mechanics* **138**(1), 50-59 (2012)
47. Shi, Y.F., Chang, C.C.: Wavelet-based identification of time-varying shear-beam buildings using incomplete and noisy measurement data. *Nonlinear Engineering* **2**, 29-37 (2013)

CHAPTER 5 Identification of gradually varying physical parameters based on discrete cosine transform using partial measurements

ABSTRACT

Structural physical parameters often vary gradually due to the degradation of material properties or effects of environment. In this paper, two novel approaches are proposed to identify the gradually varying physical parameters based on the discrete cosine transform (DCT) using partial measurements of structural responses. Approach I is proposed for the circumstance of known excitations. The gradually varying physical parameters are firstly located by the fading-factor extended Kalman filter (FEKF), and then identified by the proposed DCT integrated with Kalman filter (KF) method. Approach II is proposed for the identification of gradually varying physical parameters under unknown excitations. The gradually varying physical parameters are firstly localized by the proposed fading-factor extended Kalman filter under unknown input (FEKF-UI), and then identified by the proposed DCT integrated with Kalman filter under unknown input (KF-UI). Numerical examples demonstrate that the proposed approaches can identify the gradually varying physical parameters accurately with incomplete measurement data. Moreover, the identification of time-varying cable force in cable-stayed bridge is also discussed as a case study of the proposed approach I. Both numerical example and experimental verification show that it provides a new path to identify the time-varying cable force by only using one acceleration response measurement of the cable.

Ning Yang, Ying Lei, Jun Li, Hong Hao. Identification of gradually varying physical parameters based on discrete cosine transform using partial measurements, *Structural Control & Health Monitoring*, 2021. (Under review)

1. Introduction

Direct identification of physical parameters, such as physical stiffness and damping parameters of linear structures, plays an indispensable role in structural health assessment.

Vibration-based techniques have been developed to identify the physical parameters of time-invariant structures in the field of structural health monitoring (SHM)¹. However, structural physical parameters often vary owing to severe hazards, such as strong seismic and wind loads, as well as other environmental effects, e.g., temperature or corrosion effect. Bao and Li² conducted a comprehensive review about the recent methodologies for SHM, especially machine learning paradigm for SHM. However, effective methods are still needed to describe the dynamic characteristics of time-varying structures, adaptively assess and evaluate the performance of time-varying structural systems^{3,4}.

Relevant studies have been conducted in the time-domain and time-frequency domain. The state space model based methods have shown a high efficiency in the time-domain to track the change of physical parameters⁵⁻¹⁴. Among these methods, the Kalman filter (KF) series methods have been commonly used with an outstanding feature that only incomplete measurements are required in the identification process⁷⁻¹⁴. Based on KF series methods, the time-varying physical parameters are able to be identified by introducing the fading-factor to adjust the state prediction covariance matrix in real time. However, it is difficult to determine the optimal fading-factor. Therefore, some of these methods were proposed based on an empirical factor⁷ or the empirical formula⁸⁻⁹. Furthermore, the method was modified by updating the factor matrix at each time instant, but it is computationally expensive.¹⁰⁻¹¹ In addition, the time-varying physical parameters can be identified by updating the process noise covariance in KF series methods,¹²⁻¹³ which also depends on the selection of empirical factors. Most recently, a novel method combining the sparse Bayesian learning and KF was proposed by Huang *et al.*¹⁴ to identify the abruptly changed physical parameters, but further exploration is still needed in the identification of gradually changing physical parameters.

The time-frequency domain methods that are developed to identify the structural time-varying physical parameters mainly refer to the wavelet multiresolution (WM) based methods.¹⁵⁻
²³ Most of these methods expand the time-varying structural physical parameters into scale

coefficients, and then identify these coefficients by the linear least-squares estimation.¹⁵⁻²¹ However, complete measurements of structural responses at all degrees of freedom (DOFs) are required in these methods, which is impractical for real applications. To conquer the limitation on full observations, novel methods have been proposed recently by the authors to identify the time-varying physical parameters of linear structures under known or unknown excitations based on partial measurements.²²⁻²³ Nevertheless, the methods require to expand all physical parameters (including time-varying parameters and time-invariant parameters) into scale coefficients based on WM. The number of expanded coefficients increases greatly as the structural size increases, making it difficult to obtain a global optimal solution especially when the quality of the collected data is poor. Additionally, more low-frequency scale coefficients need be retained to ensure the accuracy of reconstructing the gradually changing parameters, which also leads to the growth in the number of scale coefficients. Furthermore, the determination of appropriate mother function and decomposition level in WM is a pending issue that is not yet well resolved.²⁴ Besides, the boundary effect of WM is also inevitable.

In fact, the change in physical parameters of civil engineering structures is a gradual process in most circumstances. For instance, the cumulative structural damage evolves from minor to severe, leading to gradually changing vibration characteristics.²⁵ For the vehicle-bridge coupling system, the mass distribution of the system varies with time due to the vehicle movement, which also results in the gradually varying features of the system.²⁶⁻²⁸ Tracking the gradual evolution process and identifying the gradually changing physical parameters accurately is still a challenging issue that is worth of investigation. The core of the WM-based method is to reparametrize the time-varying model by wavelet basis for the purpose of reducing the dimensionality of unknown parameters in the inverse problem. Then, the unknown physical parameters are equal to the product of the scale coefficients and the base functions. However, the wavelet basis function is not particularly suitable for the decomposition of gradually changing parameters. The reason is that relatively more scale coefficients should be retained to guarantee the accuracy of reconstructed gradually changing parameters, while a large number of scale

coefficients may result in the convergence to local optimization results, especially when the structural responses for analysis are polluted by high-level noise. Therefore, other decomposition basis which is more suitable for gradually changing parameters should be investigated to reduce the number of coefficients as much as possible. Discrete cosine transform (DCT) is a kind of transformation defined for analyzing real signals.²⁹ A series of DCT coefficients are obtained in frequency domain after transformation. Most importantly, energy concentration is a very valuable property of DCT, that is, a majority of energy in natural signals (e.g., sound and image) is concentrated in the low frequency range, promoting the wide application of DCT in data compression.^{30, 31} In addition, some researchers have adopted DCT for the identification of unknown parameters benefitting from the dimensional reduction of DCT. For example, Eom³² expanded the time-varying autoregressive parameters by using a low-order DCT to analyze the acoustic signatures from moving vehicles. Aleardi³³ proposed a novel method using DCT to reparametrize and reduce dimensionality of parameters. The unknown parameters became the coefficient sequence related to DCT basis functions. Zhang³⁴ used the DCT basis and wavelet basis to expand the same gradually changing signal, and then compared the sparsity of DCT coefficients and scale coefficients, respectively. Results showed that DCT coefficients contained more coefficients close to zero, demonstrating a better sparsity. It means that DCT instead of WM can use less coefficients to express the original gradually changing signal. By considering the energy of vibration of civil structures is mainly distributed in the low-frequency component²¹, it is worth decomposing the gradually varying physical parameters into low-order DCT coefficients, especially when the measured responses are polluted by high-level noise.

Cable force in a cable-stayed bridge is time-varying. With the advantages of low cost, high bearing capacity and wind stability, cables have been widely used as the main components in long-span bridges.³⁵⁻³⁷ The healthy state of cables is of great significance to the safety of the whole cable-stayed bridge, Li *et al.*³⁶ proposed diagnostic approach through the variation of pattern parameters, and the results are so promising and validated through an actual long-span cable-stayed bridge. Under complex load effects and formidable natural conditions, the cable is

inevitably damaged by a number of issues, such as fatigue, corrosion and prestress loss. Damage can introduce negative effects on the cable, such as weakening the stiffness and reducing the bearing capacity, and eventually leading to cable fracture, which endangers the safety of the cable-supported bridges.³⁸ Therefore, the identification of cable force plays an indispensable role in the SHM of cable-supported bridges. Li and Ou³⁹, and Zhang *et al.*⁴⁰ have conducted comprehensive literature reviews on the methods of monitoring and identifying cable tension force, which can be roughly divided into five categories: lift-off method, load cell method, magnetic flux leakage method, fiber Bragg grating method and vibration-based method.^{39,40} Among these methods, the vibration-based method is adopted as an indirect way to obtain the cable force by inverse analysis, with the advantages of simple installation, convenient operation, reusability, high precision and low cost.⁴⁰ Although many in-depth studies have been carried out, most of the proposed methods can only acquire the average value of cable force in a specific duration. However, the cable force is time-varying subjected to the live load in the long-span cable-supported bridge. The average cable force value may not be used to evaluate the fatigue damage of the cable accurately. Therefore, it is of great theoretical significance and engineering application importance to develop the identification method of time-varying cable force for the safety assessment of bridges.

Some attempts have been conducted to identify the time-varying cable tension from the dynamic responses of cable. Li *et al.*⁴¹ proposed a real-time method to estimate the time-varying cable forces based on the extended Kalman filter (EKF). However, the influence of process noise and measurement noise in EKF on identification results cannot be ignored. Bao *et al.*⁴² presented an adaptive sparse time-frequency (ASTF) analysis method to identify the instantaneous frequency of cables, and then obtain the time-varying cable force according to the tension string theory. Furthermore, to solve the non-convex least-squares optimization in the algorithm, a machine learning-based method was developed by Bao *et al.*⁴³ to enhance the ASTF method. However, the selection of initial phase in these methods has influence on the identification result. Yang *et al.*⁴⁴ proposed a data-driven method for real-time identification of time-varying cable tension force based on the complexity pursuit algorithm using more than two monitored

acceleration responses of the cable. In addition, depending on the time-frequency analysis method, some studies have been conducted to obtain the time-varying cable force by identifying the instantaneous frequency. For example, Xue and Shen⁴⁵ performed cable force identification by combining the short time sparse time domain algorithm and the simplified half wave method. Zhang *et al.*³⁸ presented the synchrosqueezing short-time Fourier transform to identify the instantaneous frequency and time-varying cable force. Wang *et al.*⁴⁶ developed a method which combines the variational mode decomposition and generalized Morse wavelet to identify the instantaneous frequency and time-varying cable force. Obviously, the accuracy of using these methods to identify the time-varying cable force depends on the resolution of time-frequency analysis method both in time and frequency domains. Additionally, it shall be noted that the varying cable force is in the form of gradual change in all of the studies mentioned above.

Inspired by the merits of DCT and KF series methods, this paper proposes novel two-step approaches for the identification of structural gradually varying physical parameters under known or unknown excitations, respectively. In this study, the structural mass is a known and time-invariant parameter, and only partially measured structural responses are used for the identification of other gradually varying physical parameters. Approach I is proposed for the case of time-varying system identification under known excitations. The gradually varying physical parameters are localized by the fading-factor extended Kalman filter (FEKF) algorithm in the first step, and then identified by the proposed DCT integrated with KF method. Approach II is proposed to conduct the time-varying system identification under unknown excitations. In this approach, the gradually varying physical parameters are localized by the proposed fading-factor extended Kalman filter under unknown input (FEKF-UI) algorithm, and identified by the proposed DCT integrated with Kalman filter under unknown input (KF-UI) method. Moreover, by considering that the stay cable is a time-varying system as its cable force changes with time under the joint action of vehicle and wind loads, it is investigated as a case study in this paper. The discrete equation of motion of stay cables in modal domain is given and the steps of identifying the time-varying cable force by the proposed approach I are presented. Numerical

studies on Nanjing Yangtze River No. 3 Bridge and experimental tests on the scaled cable are conducted by using only one acceleration response on the cable, with or without the anemometer installed on the bridge.

The rest of the paper is organized as follows. The theoretical background and development of the proposed approach I (identification under known excitations) and approach II (identification under unknown excitations) are presented in Section 2 and Section 3, respectively. Then in Section 4.1, numerical models including a gradually varying truss and a gradually varying bridge under known excitations are used to demonstrate the performance of the proposed approach I, and in Section 4.2, the same models under unknown excitations are employed to validate the effectiveness of the proposed approach II. In Section 5, the procedures to identify the time-varying cable force are presented based on the proposed approach I. Numerical example and experimental verification results are given to verify the effectiveness of the proposed cable force identification method. Finally, conclusions and discussions are presented in the conclusion section.

2. The proposed approach I: two-step approach to identify the gradually varying physical parameters under known excitations

Considering that the gradually varying physical parameters are expected to be sparse in the systems⁴⁷, it is unnecessary to consider that all physical parameters are time-varying and then expanded into corresponding numerical coefficients. It is more feasible and effective to distinguish the time-varying parameters qualitatively and then concentrate on identifying those time-varying parameters. Therefore, the proposed approaches in this paper are conducted in two steps. The detailed procedures are introduced as follows.

2.1 Step 1: Locating the gradually varying physical parameters by the FEKF algorithm

In the first step, the gradually varying physical parameters, including stiffness and damping parameters, are localized by using the FEKF algorithm.

The governing equation of a multi-DOF time-varying linear structure is expressed as

$$\mathbf{M}\ddot{\mathbf{x}}(t) + \mathbf{C}(t)\dot{\mathbf{x}}(t) + \mathbf{K}(t)\mathbf{x}(t) = \boldsymbol{\eta}\mathbf{f}(t) \quad (1)$$

where $\ddot{\mathbf{x}}(t)$, $\dot{\mathbf{x}}(t)$ and $\mathbf{x}(t)$ are the structural acceleration, velocity, and displacement response vectors, respectively; \mathbf{M} is the matrix of structural mass, and it is time-invariant and known; $\mathbf{K}(t)$ and $\mathbf{C}(t)$ denote the stiffness and damping matrices, respectively, and are assembled by the time-varying physical parameters; $\mathbf{f}(t)$ is a known external excitation vector with the influence matrix $\boldsymbol{\eta}$.

An augmented state vector with a dimension of $(2n+l) \times 1$ is defined as $\mathbf{Z} = \{\mathbf{x}^T, \dot{\mathbf{x}}^T, \boldsymbol{\theta}^T\}^T$, in which n is the number of DOF, l is the number of unknown structural parameters, and $\boldsymbol{\theta}$ is the vector of unknown structural physical parameters including stiffness and damping parameters. Rewritten Eq. (1) into the following state space equation as

$$\dot{\mathbf{Z}} = \begin{Bmatrix} \dot{\mathbf{x}} \\ \ddot{\mathbf{x}} \\ \dot{\boldsymbol{\theta}} \end{Bmatrix} = \begin{Bmatrix} \dot{\mathbf{x}} \\ \mathbf{M}^{-1}[\boldsymbol{\eta}\mathbf{f} - \mathbf{C}(t)\dot{\mathbf{x}}(t) - \mathbf{K}(t)\mathbf{x}(t)] \\ \mathbf{0} \end{Bmatrix} = \mathbf{g}(\mathbf{Z}, \mathbf{f}) + \mathbf{w} \quad (2)$$

in which $\mathbf{g}(\cdot)$ is a nonlinear function, \mathbf{W} is the process noise (or model noise) with zero mean and a covariance matrix $E[\mathbf{w}\mathbf{w}^T] = \mathbf{Q}$.

When only partial acceleration responses are provided as available measurements, the discrete observation equation is expressed as

$$\mathbf{y}_{k+1} = \ddot{\mathbf{x}}_{m,k+1} = \mathbf{L}_a \ddot{\mathbf{x}}_{k+1} + \mathbf{v}_{k+1} = \mathbf{L}_a \mathbf{M}^{-1}[\boldsymbol{\eta}\mathbf{f}_{k+1} - \mathbf{C}_{k+1}\dot{\mathbf{x}}_{k+1} - \mathbf{K}_{k+1}\mathbf{x}_{k+1}] + \mathbf{v}_{k+1} = \mathbf{h}(\mathbf{Z}_{k+1}, \mathbf{f}_{k+1}) + \mathbf{v}_{k+1} \quad (3)$$

where \mathbf{y}_{k+1} represents the observation vector at the time instant $t = (k+1)\Delta t$, $\ddot{\mathbf{x}}_{m,k+1}$ is the measured acceleration response vector, Δt is the sampling interval, \mathbf{L}_a denotes the mapping matrix of measurement locations, and \mathbf{v}_{k+1} is the measurement noise which is assumed as a Gaussian white noise process, with mean value of zero and covariance matrix of $E[\mathbf{v}_{k+1}\mathbf{v}_{k+1}^T] = \mathbf{R}_{k+1}$.

Let $\hat{\mathbf{Z}}_{k|k}$ be the estimated state vector at the time instant $t = k\Delta t$ and $\tilde{\mathbf{Z}}_{k+1|k}$ be the predicted state vector at the time instant $t = (k+1)\Delta t$, Eqs. (2) and (3) are linearized at $\hat{\mathbf{Z}}_{k|k}$ and $\tilde{\mathbf{Z}}_{k+1|k}$ by using the first order Taylor series expansion and expressed as

$$\mathbf{g}(\mathbf{Z}, \mathbf{f}) \approx \mathbf{g}(\hat{\mathbf{Z}}_{k|k}, \mathbf{f}) + \mathbf{G}_{k|k} (\mathbf{Z} - \hat{\mathbf{Z}}_{k|k}); \quad \mathbf{G}_{k|k} = \left. \frac{\partial \mathbf{g}(\mathbf{Z}, \mathbf{f})}{\partial \mathbf{Z}} \right|_{\mathbf{Z}=\hat{\mathbf{Z}}_{k|k}} \quad (4)$$

$$\mathbf{h}(\mathbf{Z}_{k+1}, \mathbf{f}_{k+1}) \approx \mathbf{h}(\tilde{\mathbf{Z}}_{k+1|k}, \mathbf{f}_{k+1}) + \mathbf{H}_{k+1|k} (\mathbf{Z}_{k+1} - \tilde{\mathbf{Z}}_{k+1|k}); \quad \mathbf{H}_{k+1|k} = \left. \frac{\partial \mathbf{h}(\mathbf{Z}, \mathbf{f})}{\partial \mathbf{Z}} \right|_{\mathbf{Z}=\tilde{\mathbf{Z}}_{k+1|k}} \quad (5)$$

Similar to the conventional EKF which is used in the estimation of time-invariant systems, the FEKF algorithm is implemented in the following two steps:

1) Time update (prediction) procedure

$$\tilde{\mathbf{Z}}_{k+1|k} = \hat{\mathbf{Z}}_{k|k} + \int_{k\Delta t}^{(k+1)\Delta t} \mathbf{g}(\hat{\mathbf{Z}}_{t|k}, \mathbf{f}) dt; \quad \tilde{\mathbf{P}}_{k+1|k} = \Lambda \Theta_{k|k} \hat{\mathbf{P}}_{k|k} \Theta_{k|k}^T \Lambda^T + \mathbf{Q}_k \quad (6)$$

where $\tilde{\mathbf{P}}_{k+1|k}$ is the prediction error covariance matrix, $\hat{\mathbf{P}}_{k|k}$ is the estimation error covariance matrix, and $\Theta_{k|k} \approx \mathbf{I}_{2n+l} + \mathbf{G}_{k|k} \Delta t$ where \mathbf{I}_{2n+l} is an unit matrix. It is noted that Eq. (6) is different from the conventional EKF, since the fading factor matrix Λ is introduced as follows to gradually fade the previous information and track the possible changes of the parameter vector

$$\Lambda = \text{diag}[\mathbf{1}_{1 \times 2n}, \lambda \cdot \mathbf{1}_{1 \times l}] \quad (7)$$

where $\lambda \geq 1$. In the first step, $\lambda = 2^{2/N_u}$ is adopted based on an existing study, which implies that the half-life of the contribution of a data point is N_u time steps.⁸

2) Measurement update (correction) procedure

$$\hat{\mathbf{Z}}_{k+1|k+1} = \tilde{\mathbf{Z}}_{k+1|k} + \mathbf{K}_{G,k+1} (\mathbf{y}_{k+1} - \mathbf{h}(\tilde{\mathbf{Z}}_{k+1|k}, \mathbf{f}_{k+1})) \quad (8)$$

where $\hat{\mathbf{Z}}_{k+1|k+1}$ is the estimated state vector at the time instant $t = (k+1)\Delta t$, and $\mathbf{K}_{G,k+1}$ is the Kalman gain matrix which can be derived as

$$\mathbf{K}_{G,k+1} = \tilde{\mathbf{P}}_{k+1|k} \mathbf{H}_{k+1|k}^T \left(\mathbf{H}_{k+1|k} \tilde{\mathbf{P}}_{k+1|k} \mathbf{H}_{k+1|k}^T + \mathbf{R}_{k+1} \right)^{-1} \quad (9)$$

In addition, the updated error covariance matrix $\hat{\mathbf{P}}_{k+1|k+1}$ is obtained as

$$\hat{\mathbf{P}}_{k+1|k+1} = \left(\mathbf{I}_{2n+l} - \mathbf{K}_{G,k+1} \mathbf{H}_{k+1|k} \right) \tilde{\mathbf{P}}_{k+1|k} \left(\mathbf{I}_{2n+l} - \mathbf{K}_{G,k+1} \mathbf{H}_{k+1|k} \right)^T + \mathbf{K}_{G,k+1} \mathbf{R}_{k+1} \mathbf{K}_{G,k+1}^T \quad (10)$$

Thus, the time-varying physical parameter vector $\hat{\boldsymbol{\theta}}_{k+1|k+1}$ can be updated in real time since they are included in the augmented vector $\hat{\mathbf{z}}_{k+1|k+1}$. It is concluded from the above formulas that the accuracy of state estimation completely depends on the selection of fading factor matrix Λ . Theoretically, the results of estimated physical parameter vector will be more ideal when Λ is updated with time, however, it will undoubtedly increase more workload. Obviously, owing to the use of empirical formula in Eq. (7), the accurate estimation of gradually varying parameters cannot be obtained herein. It can be used to roughly determine which physical parameter has the greatest possibility of time-varying changes. Thus, the physical parameter vector $\boldsymbol{\theta}$ is divided into two parts including a gradually varying parameter vector $\boldsymbol{\theta}_1$ and a time-invariant parameter vector $\boldsymbol{\theta}_2$.

2.2 Step 2: Identifying the gradually varying physical parameters by the proposed DCT integrated with KF method

In the second step, based on DCT and KF, the time-invariant parameter vector $\boldsymbol{\theta}_2$ and the DCT coefficients corresponding to $\boldsymbol{\theta}_1$ can be identified more exactly.

2.2.1 Expansion of gradually varying physical parameters by using discrete cosine transform

Supposing that the number of gradually varying elements is M and the number of sampled points is N , the DCT of the i -th gradually varying physical parameter $\theta_{1,i}(t_n)$ ($i=1,2,\dots,M;n=1,2,\dots,N$) can be written as follows

$$r_i(m) = \sqrt{\frac{2}{N}} \sum_{p=1}^N \theta_{1,i}(t_p) \frac{1}{\sqrt{1+\delta_{m1}}} \cos\left(\frac{\pi}{2N}(2p-1)(m-1)\right) \quad (11)$$

where r_i denotes the DCT coefficients that fully describe the i -th gradually varying physical parameter $\theta_{1,i}$ in the transformed DCT space, δ_{m1} represents the Kronecker delta, and m represents the order of each DCT coefficient. Rewritten Eq. (11) into the matrix form as

$$\mathbf{r} = \mathbf{B}\boldsymbol{\theta}_1 \quad (12)$$

in which \mathbf{r} represents the transformed DCT coefficient vector, and \mathbf{B} is an orthonormal matrix composed of the cosine functions which is N -by- N . $\mathbf{B}\mathbf{B}^T = \mathbf{I}$, where \mathbf{I} is the identity matrix. Eq. (12) shows that DCT is a linear and reversible transformation.

Energy concentration is an important property of DCT, that is, most of the energy in natural signals is concentrated in the low frequency components (the low order DCT coefficients). The energy of vibration of civil structures is mainly distributed in the low-frequency component.²¹ This means that an approximation of the time-varying physical parameter can be obtained by considering only the first q DCT coefficients

$$\boldsymbol{\theta}_1 \approx \tilde{\boldsymbol{\theta}}_1 = \mathbf{B}_q^T \mathbf{r}_q \quad (13)$$

in which $\tilde{\boldsymbol{\theta}}_1$ is the approximated gradually varying physical parameter vector, \mathbf{B}_q^T is a partition of the matrix \mathbf{B} , which is N -by- q representing that the first q DCT base functions are used, and \mathbf{r}_q only contains the first q coefficients in \mathbf{r} . Thus, the identification of N -dimensional gradually varying physical parameter is transformed into the determination of q -dimensional DCT coefficients. The dimension of unknown parameters is greatly reduced.

Then an example is provided to prove the superiority of DCT in decomposing gradually changing parameters. A pre-set gradient physical parameter k_1 is decomposed and reconstructed by WM and DCT, respectively. In this example, the sampling interval is 0.01s and the entire

sampling duration is 20s, thus the total number of the discrete points in the time-domain is 2000. Fig. 1(a) shows the reconstructed results by WM. a represents the number of scale coefficients at the scale level J . With a lower scale level, more scale coefficients are retained to provide a more accurate reconstruction result. However, the boundary effect is still obvious even when the scale level is low, owing to the characteristics of wavelet basis function. Fig. 1(b) presents the reconstruction results of using DCT. The reconstructed signals are always consistent with the exact stiffness parameter even when the number of DCT coefficients is $q=8$. However, when the number of wavelet scale coefficients is $a=8$, the reconstructed signal differs greatly from the original one. It is demonstrated that DCT is better than WM in reducing the dimensionality of gradually changing physical parameters. In addition, the boundary effect is mitigated when using DCT to decompose and reconstruct signals.

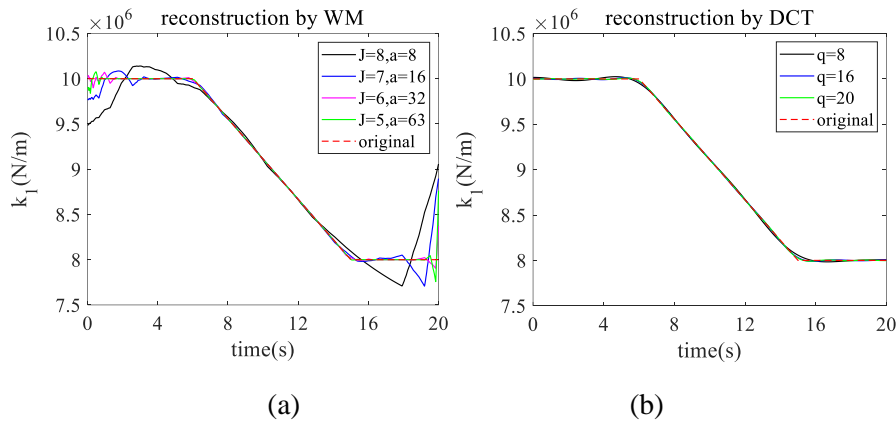


FIGURE 1 Decomposition and reconstruction of gradually varying k_1 by: (a) WM; and (b) DCT

2.2.2 Identification of structural state by KF under given DCT coefficients

By Eq. (13), the gradually varying physical parameter vector θ_1 is reconstructed based on the given time-invariant DCT coefficient vector \mathbf{r}_q accordingly. Thus, the identification of original physical parameters is converted into the identification of time-invariant DCT coefficient vector \mathbf{r}_q and time-invariant physical parameter vector θ_2 . The equation of motion of a time-invariant linear system is rewritten as

$$\mathbf{M}\ddot{\mathbf{x}}(t) + \mathbf{C}(\mathbf{r}_q, \boldsymbol{\theta}_2)\dot{\mathbf{x}}(t) + \mathbf{K}(\mathbf{r}_q, \boldsymbol{\theta}_2)\mathbf{x}(t) = \boldsymbol{\eta}\mathbf{f}(t) \quad (14)$$

KF is adopted to estimate the state (including displacement and velocity) of all DOFs with partial measurements when the external excitations are known. Owing to page limitation, only main formulas are listed in Eqs. (15)- (19).

Defining the state vector $\mathbf{X} = \{\mathbf{x}^T, \dot{\mathbf{x}}^T\}^T$, the state equation can be described in the discrete form as:

$$\mathbf{X}_{k+1} = \mathbf{A}_k \mathbf{X}_k + \mathbf{B}_k \mathbf{f}_k + \mathbf{w}_k \quad (15)$$

in which \mathbf{X}_k is the system state vector at the time instant $t = k\Delta t$, \mathbf{A}_k is the state transformation matrix which is the implicit function of vectors \mathbf{r}_q and $\boldsymbol{\theta}_2$, and \mathbf{B}_k is the influence matrix of \mathbf{f}_k . The discrete measurement equation is expressed as

$$\mathbf{y}_{k+1} = \ddot{\mathbf{x}}_{m,k+1} = \mathbf{C}_{k+1} \mathbf{X}_{k+1} + \mathbf{D}_{k+1} \mathbf{f}_{k+1} + \mathbf{v}_{k+1} \quad (16)$$

in which \mathbf{C}_{k+1} is the measurement matrix related to vectors \mathbf{r}_q and $\boldsymbol{\theta}_2$, and \mathbf{D}_{k+1} is the measurement matrix associated with the external force vector \mathbf{f}_{k+1} .

The KF algorithm includes two main procedures. The time update (prediction) is the first procedure, which is expressed as

$$\tilde{\mathbf{X}}_{k+1|k} = \mathbf{A}_k \hat{\mathbf{X}}_{k|k} + \mathbf{B}_k \mathbf{f}_k; \quad \tilde{\mathbf{P}}_{k+1|k} = \mathbf{A}_k \hat{\mathbf{P}}_{k|k} \mathbf{A}_k^T + \mathbf{Q}_k \quad (17)$$

The second procedure is the measurement update (correction). It can be expressed as

$$\hat{\mathbf{X}}_{k+1|k+1} = \tilde{\mathbf{X}}_{k+1|k} + \mathbf{K}_{G,k+1} (\mathbf{y}_{k+1} - \mathbf{C}_{k+1} \tilde{\mathbf{X}}_{k+1|k} - \mathbf{D}_{k+1} \mathbf{f}_{k+1}); \quad \mathbf{K}_{G,k+1} = \tilde{\mathbf{P}}_{k+1|k} \mathbf{C}_{k+1}^T (\mathbf{C}_{k+1} \tilde{\mathbf{P}}_{k+1|k} \mathbf{C}_{k+1}^T + \mathbf{R}_{k+1})^{-1} \quad (18)$$

$$\hat{\mathbf{P}}_{k+1|k+1} = (\mathbf{I} - \mathbf{K}_{G,k+1} \mathbf{C}_{k+1}) \tilde{\mathbf{P}}_{k+1|k} \quad (19)$$

Following the procedures of KF, the structural state vector is updated finally.

2.2.3 Estimation of DCT coefficients and time-invariant parameters by nonlinear optimization

As can be seen from the above sections, the estimated state is an implicit function of DCT coefficient vector \mathbf{r}_q and time-invariant parameter vector $\boldsymbol{\theta}_2$, that is

$$\hat{\mathbf{X}} = \hat{\mathbf{X}}(\mathbf{r}_q, \boldsymbol{\theta}_2) \quad (20)$$

Then the estimated acceleration vector can be obtained by Eq. (14) as

$$\hat{\mathbf{x}}(\mathbf{r}_q, \boldsymbol{\theta}_2) = \mathbf{M}^{-1} \left(\boldsymbol{\eta} \mathbf{f} - \mathbf{C}(\mathbf{r}_q, \boldsymbol{\theta}_2) \hat{\mathbf{x}}(\mathbf{r}_q, \boldsymbol{\theta}_2) - \mathbf{K}(\mathbf{r}_q, \boldsymbol{\theta}_2) \hat{\mathbf{x}}(\mathbf{r}_q, \boldsymbol{\theta}_2) \right) \quad (21)$$

Finally, the optimal DCT coefficient vector $\hat{\mathbf{r}}_q$ and the optimal time-invariant parameter vector $\hat{\boldsymbol{\theta}}_2$ are estimated by minimizing the following objective error function

$$\left[\hat{\mathbf{r}}_q, \hat{\boldsymbol{\theta}}_2 \right] = \arg \min_{\mathbf{r}_q, \boldsymbol{\theta}_2} \left(\left\| \ddot{\mathbf{x}}_m - \mathbf{L}_a \hat{\mathbf{x}}(\mathbf{r}_q, \boldsymbol{\theta}_2) \right\|_2^2 \right) \quad (22)$$

Thus, the optimal gradually varying parameter vector $\hat{\boldsymbol{\theta}}_1$ can be reconstructed by using Eq. (13).

In conclusion, the procedures of the proposed approach I to identify the gradually varying physical parameters under known excitations are shown in Fig. 2.

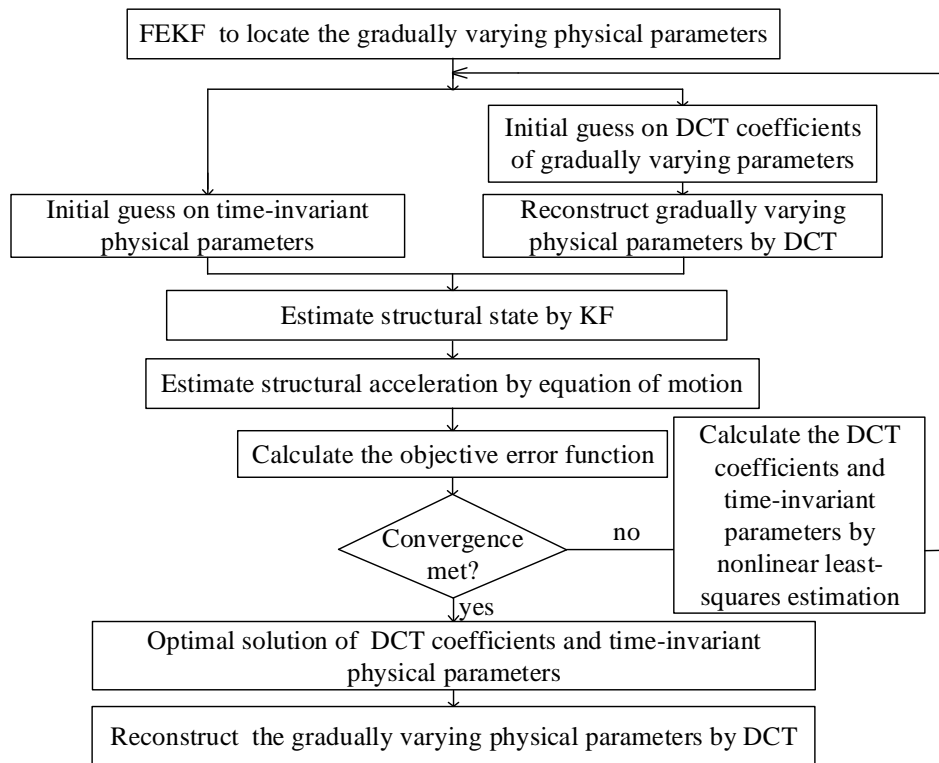


FIGURE 2 Procedures of the proposed approach I under known excitations

3. The proposed approach II: two-step approach to identify the gradually varying physical parameters under unknown excitations

The proposed approach I is developed to identify the gradually varying physical parameters under known excitations by using partially measured acceleration responses. However, external excitations could not be always measured directly and easily in practical engineering applications^{48,49}. To further generalize the application to a more common case, the identification of gradually varying physical parameters under unknown excitations is discussed in this section.

3.1 Step 1: Locating the gradually varying physical parameters by the proposed FEKF-UI algorithm

In this section, a new algorithm, that is fading-factor extended Kalman filter under unknown input, is proposed. It is improved from the data fusion based EKF-UI proposed in 2016 by the authors,⁵⁰ as the latter one is only efficient to identify the time-invariant systems under unknown excitations. This study extends the algorithm for the identification of time-varying systems.

When the time-varying linear system is also subjected to partial unknown external inputs, the equation of motion in Eq. (1) can be rewritten as

$$\mathbf{M}\ddot{\mathbf{x}}(t) + \mathbf{C}(t)\dot{\mathbf{x}}(t) + \mathbf{K}(t)\mathbf{x}(t) = \boldsymbol{\eta}\mathbf{f}(t) + \boldsymbol{\eta}^u\mathbf{f}^u(t) \quad (23)$$

in which $\boldsymbol{\eta}^u$ is the influence matrix of unknown input vector \mathbf{f}^u .

The state space equation is expressed as

$$\dot{\mathbf{Z}} = \begin{Bmatrix} \dot{\mathbf{x}} \\ \ddot{\mathbf{x}} \\ \dot{\boldsymbol{\theta}} \end{Bmatrix} = \begin{Bmatrix} \dot{\mathbf{x}} \\ \mathbf{M}^{-1}[\boldsymbol{\eta}\mathbf{f} - \mathbf{C}(t)\dot{\mathbf{x}}(t) - \mathbf{K}(t)\mathbf{x}(t)] \\ \mathbf{0} \end{Bmatrix} + \begin{Bmatrix} \mathbf{0} \\ \mathbf{M}^{-1}\boldsymbol{\eta}^u \\ \mathbf{0} \end{Bmatrix} \mathbf{f}^u + \mathbf{w} = \mathbf{g}(\mathbf{Z}, \mathbf{f}, \mathbf{f}^u) + \mathbf{w} \quad (24)$$

Let $\hat{\mathbf{f}}_{k|k}^u$ be the estimation at $t = k\Delta t$, Eq. (24) is linearized at $\hat{\mathbf{Z}}_{k|k}$ and $\hat{\mathbf{f}}_{k|k}^u$ by the first order Taylor series expansion

$$\mathbf{g}(\mathbf{Z}, \mathbf{f}, \mathbf{f}^u) \approx \mathbf{g}(\hat{\mathbf{Z}}_{k|k}, \mathbf{f}, \hat{\mathbf{f}}_{k|k}^u) + \mathbf{G}_{k|k}(\mathbf{Z} - \hat{\mathbf{Z}}_{k|k}) + \mathbf{B}_{k|k}^u(\mathbf{f}^u - \hat{\mathbf{f}}_{k|k}^u) \quad (25)$$

where

$$\mathbf{G}_{k|k} = \left. \frac{\partial \mathbf{g}(\mathbf{Z}, \mathbf{f}, \mathbf{f}^u)}{\partial \mathbf{Z}} \right|_{\mathbf{Z}=\hat{\mathbf{Z}}_{k|k}; \mathbf{f}^u=\hat{\mathbf{f}}_{k|k}^u}; \quad \mathbf{B}_{k|k}^u = \left. \frac{\partial \mathbf{g}(\mathbf{Z}, \mathbf{f}, \mathbf{f}^u)}{\partial \mathbf{f}^u} \right|_{\mathbf{Z}=\hat{\mathbf{Z}}_{k|k}; \mathbf{f}^u=\hat{\mathbf{f}}_{k|k}^u} \quad (26)$$

When using the EKF-UI algorithm to identify time-invariant systems under unknown excitations, partial acceleration and displacement (or strain) responses are fused as observations, which can be used to restrain the ‘drift’ in recognition results⁵⁰. The observation equation herein can be expressed as:

$$\mathbf{y}_{k+1} = \begin{bmatrix} \ddot{\mathbf{x}}_{m,k+1} \\ \mathbf{x}_{m,k+1} \end{bmatrix} = \begin{bmatrix} \mathbf{L}_a & \mathbf{0} \\ \mathbf{0} & \mathbf{L}_d \end{bmatrix} \begin{bmatrix} \mathbf{M}^{-1}[\boldsymbol{\eta}\mathbf{f}_{k+1} - \mathbf{C}_{k+1}\dot{\mathbf{x}}_{k+1} - \mathbf{K}_{k+1}\mathbf{x}_{k+1}] \\ \dot{\mathbf{x}}_{k+1} \end{bmatrix} + \begin{bmatrix} \mathbf{L}_a\mathbf{M}^{-1}\boldsymbol{\eta}^u\mathbf{f}_{k+1}^u \\ \mathbf{0} \end{bmatrix} + \mathbf{v}_{k+1} = \mathbf{h}(\mathbf{Z}_{k+1}, \mathbf{f}_{k+1}, \mathbf{f}_{k+1}^u) + \mathbf{v}_{k+1} \quad (27)$$

where $\mathbf{x}_{m,k+1}$ is the measured displacement (or strain) responses at $t = (k+1)\Delta t$ with the position matrix \mathbf{L}_d .

Eq. (27) can be linearized at $\tilde{\mathbf{Z}}_{k+1|k}$ and $\hat{\mathbf{f}}_{k|k}^u$ by using the first order Taylor series

expansion

$$\mathbf{h}(\mathbf{Z}_{k+1}, \mathbf{f}_{k+1}, \mathbf{f}_{k+1}^u) \approx \mathbf{h}(\tilde{\mathbf{Z}}_{k+1|k}, \mathbf{f}_{k+1}, \hat{\mathbf{f}}_{k|k}^u) + \mathbf{H}_{k+1|k} (\mathbf{Z}_{k+1} - \tilde{\mathbf{Z}}_{k+1|k}) + \mathbf{D}_{k+1|k}^u (\mathbf{f}_{k+1}^u - \hat{\mathbf{f}}_{k|k}^u) \quad (28)$$

where

$$\mathbf{H}_{k+1|k} = \left. \frac{\partial \mathbf{h}(\mathbf{Z}, \mathbf{f}, \mathbf{f}^u)}{\partial \mathbf{Z}} \right|_{\mathbf{Z}=\tilde{\mathbf{Z}}_{k+1|k}; \mathbf{f}^u=\hat{\mathbf{f}}_{k|k}^u}; \quad \mathbf{D}_{k+1|k}^u = \left. \frac{\partial \mathbf{h}(\mathbf{Z}, \mathbf{f}, \mathbf{f}^u)}{\partial \mathbf{f}^u} \right|_{\mathbf{Z}=\tilde{\mathbf{Z}}_{k+1|k}; \mathbf{f}^u=\hat{\mathbf{f}}_{k|k}^u} \quad (29)$$

The proposed FEKF-UI has a similar process with FEKF. Only some main formulas are briefly presented here.

1) Time update (prediction)

$$\tilde{\mathbf{Z}}_{k+1|k} = \hat{\mathbf{Z}}_{k|k} + \int_{k\Delta t}^{(k+1)\Delta t} \mathbf{g}(\hat{\mathbf{Z}}_{t|k}, \mathbf{f}, \hat{\mathbf{f}}_{k|k}^u) dt; \quad \tilde{\mathbf{P}}_{k+1|k}^{\mathbf{Z}} = \Lambda \begin{bmatrix} \mathbf{\Theta}_{k|k} & \Delta t \mathbf{B}_{k|k}^u \\ \hat{\mathbf{P}}_{k|k}^{\mathbf{z}} & \hat{\mathbf{P}}_{k|k}^{\mathbf{f}} \end{bmatrix} \begin{bmatrix} \hat{\mathbf{P}}_{k|k}^{\mathbf{Z}} & \hat{\mathbf{P}}_{k|k}^{\mathbf{z}\mathbf{f}} \\ \hat{\mathbf{P}}_{k|k}^{\mathbf{f}\mathbf{z}} & \hat{\mathbf{P}}_{k|k}^{\mathbf{f}} \end{bmatrix} \begin{bmatrix} \mathbf{\Theta}_{k|k}^T \\ \Delta t \mathbf{B}_{k|k}^{uT} \end{bmatrix} \Lambda^T + \mathbf{Q}_k \quad (30)$$

where $\tilde{\mathbf{P}}_{k+1|k}^{\mathbf{Z}}$ is the prediction error covariance matrix of state at $t=(k+1)\Delta t$, $\hat{\mathbf{P}}_{k|k}^*$ is the corresponding estimation error covariance matrix at $t=k\Delta t$, and $\mathbf{\Theta}_{k|k} \approx \mathbf{I}_{2n+t} + \mathbf{G}_{k|k} \Delta t$. It is noted that the same fading factor matrix Λ is used for the identification of time-varying systems, which can be found in Eq. (7).

2) Unknown excitation calculation

Under the condition that the number of observed measurements (sensors) is larger than that of the unknown excitations, $\hat{\mathbf{f}}_{k+1|k+1}^u$ can be computed as⁵⁰

$$\hat{\mathbf{f}}_{k+1|k+1}^u = \mathbf{S}_{k+1} \mathbf{D}_{k+1|k}^{uT} \mathbf{R}_{k+1}^{-1} \left(\mathbf{I} - \mathbf{H}_{k+1|k} \mathbf{K}_{G,k+1} \right) \left(\mathbf{y}_{k+1} - \mathbf{h}(\tilde{\mathbf{Z}}_{k+1|k}, \mathbf{f}_{k+1}, \hat{\mathbf{f}}_{k|k}^u) + \mathbf{D}_{k+1|k}^u \hat{\mathbf{f}}_{k|k}^u \right) \quad (31)$$

$$\mathbf{S}_{k+1} = \left[\mathbf{D}_{k+1|k}^{uT} \mathbf{R}_{k+1}^{-1} \left(\mathbf{I} - \mathbf{H}_{k+1|k} \mathbf{K}_{G,k+1} \right) \mathbf{D}_{k+1|k}^u \right]^{-1} \quad (32)$$

where $\hat{\mathbf{f}}_{k+1|k+1}^u$ is the estimation of \mathbf{f}^u at $t=(k+1)\Delta t$, and $\mathbf{K}_{G,k+1}$ is the Kalman gain matrix which can be found in Eq. (9).

3) Measurement update (correction)

$$\hat{\mathbf{Z}}_{k+1|k+1} = \tilde{\mathbf{Z}}_{k+1|k} + \mathbf{K}_{G,k+1} \left(\mathbf{y}_{k+1} - \mathbf{h}(\tilde{\mathbf{Z}}_{k+1|k}, \mathbf{f}_{k+1}, \hat{\mathbf{f}}_{k|k}^u) - \mathbf{D}_{k+1|k}^u (\hat{\mathbf{f}}_{k+1|k+1}^u - \hat{\mathbf{f}}_{k|k}^u) \right) \quad (33)$$

In addition, the error covariance matrices are expressed as⁵⁰

$$\hat{\mathbf{P}}_{k+1|k+1}^Z = (\mathbf{I} + \mathbf{K}_{G,k+1} \mathbf{D}_{k+1|k}^u \mathbf{S}_{k+1} \mathbf{D}_{k+1|k}^{uT} \mathbf{R}_{k+1}^{-1} \mathbf{H}_{k+1|k}^T) (\mathbf{I} - \mathbf{K}_{G,k+1} \mathbf{H}_{k+1|k}) \tilde{\mathbf{P}}_{k+1|k}^Z \quad (34)$$

$$\hat{\mathbf{P}}_{k+1|k+1}^f = \mathbf{S}_{k+1}; \quad \hat{\mathbf{P}}_{k+1|k+1}^{Zf} = (\hat{\mathbf{P}}_{k+1|k+1}^Z)^T = -\mathbf{K}_{G,k+1} \mathbf{D}_{k+1|k}^u \mathbf{S}_{k+1} \quad (35)$$

Similarly, based on the identification results of FEKF-UI, the parameter vector $\boldsymbol{\theta}$ is divided into a gradually varying parameter vector $\boldsymbol{\theta}_1$ and a time-invariant parameter vector $\boldsymbol{\theta}_2$ qualitatively.

3.2 Step 2: Identification of the gradually varying physical parameters by the proposed DCT integrated with KF-UI method

After the localization of gradually varying physical parameters by using FEKF-UI, a new method is proposed for the identification of the time-invariant parameter vector $\boldsymbol{\theta}_2$ and the DCT coefficient vector \mathbf{r}_q corresponding to $\boldsymbol{\theta}_1$ under unknown excitations, which combines the advantages of DCT and KF-UI. KF-UI was proposed by the authors in previous studies to estimate the structural state of a time-invariant system by using partial measurements when the external excitations are unknown.⁵¹ Physical parameters of the time-invariant system should be known in advance when performing KF-UI. Thus, given the assumed \mathbf{r}_q and $\boldsymbol{\theta}_2$, KF-UI can be applied herein to estimate the structural state and unknown excitations simultaneously.

The proposed method by using DCT integrated with KF-UI has a similar process as method in Section 2.2. Firstly, the gradually varying physical parameters distinguished in the first step can be reconstructed based on the given time-invariant DCT coefficient vector \mathbf{r}_q in Eq. (13).

Then with the initial time-invariant parameter vector $\boldsymbol{\theta}_2$, KF-UI is applied to obtain the estimated state and input.

The equation of motion of a time-invariant linear system under unknown excitations is rewritten as:

$$\mathbf{M}\ddot{\mathbf{x}}(t) + \mathbf{C}(\mathbf{r}_q, \boldsymbol{\theta}_2)\dot{\mathbf{x}}(t) + \mathbf{K}(\mathbf{r}_q, \boldsymbol{\theta}_2)\mathbf{x}(t) = \boldsymbol{\eta}\mathbf{f}(t) + \boldsymbol{\eta}^u\mathbf{f}^u(t) \quad (36)$$

The state equation can be described in the discrete form as

$$\mathbf{X}_{k+1} = \mathbf{A}_k\mathbf{X}_k + \mathbf{B}_k\mathbf{f}_k + \mathbf{B}_k^u\mathbf{f}_k^u + \mathbf{w}_k \quad (37)$$

where \mathbf{B}_k^u is the influence matrix of \mathbf{f}_k^u .

The discrete measurement equation is expressed as

$$\mathbf{y}_{k+1} = \begin{bmatrix} \ddot{\mathbf{x}}_{m,k+1} \\ \mathbf{x}_{m,k+1} \end{bmatrix} = \mathbf{C}_{k+1}\mathbf{X}_{k+1} + \mathbf{D}_{k+1}\mathbf{f}_{k+1} + \mathbf{D}_{k+1}^u\mathbf{f}_{k+1}^u + \mathbf{v}_{k+1} \quad (38)$$

The main formulas of KF-UI are briefly presented as follows:

1) Time update (prediction)

$$\tilde{\mathbf{X}}_{k+1|k} = \mathbf{A}_k\hat{\mathbf{X}}_{k|k} + \mathbf{B}_k\mathbf{f}_k + \mathbf{B}_k^u\hat{\mathbf{f}}_{k|k}^u; \quad \tilde{\mathbf{P}}_{k+1|k}^{\mathbf{X}} = \begin{bmatrix} \mathbf{A}_k & \mathbf{B}_k^u \end{bmatrix} \begin{bmatrix} \hat{\mathbf{P}}_{k|k}^{\mathbf{X}} & \hat{\mathbf{P}}_{k|k}^{\mathbf{Xf}} \\ \hat{\mathbf{P}}_{k|k}^{\mathbf{fX}} & \hat{\mathbf{P}}_{k|k}^{\mathbf{f}} \end{bmatrix} \begin{bmatrix} \mathbf{A}_k^T \\ \mathbf{B}_k^T \end{bmatrix} + \mathbf{Q}_k \quad (39)$$

2) Unknown excitation calculation

Under the condition that the number of observed measurements (sensors) is larger than that of the unknown excitations, $\hat{\mathbf{f}}_{k+1|k+1}^u$ can be computed as⁵¹

$$\hat{\mathbf{f}}_{k+1|k+1}^u = \mathbf{S}_{k+1}\mathbf{D}_{k+1}^{uT}\mathbf{R}_{k+1}^{-1}(\mathbf{I} - \mathbf{C}_{k+1}\mathbf{K}_{G,k+1})(\mathbf{y}_{k+1} - \mathbf{C}_{k+1}\tilde{\mathbf{X}}_{k+1|k} - \mathbf{D}_{k+1}\mathbf{f}_{k+1}) \quad (40)$$

in which $\mathbf{S}_{k+1} = [\mathbf{D}_{k+1}^{uT}\mathbf{R}_{k+1}^{-1}(\mathbf{I} - \mathbf{C}_{k+1}\mathbf{K}_{G,k+1})\mathbf{D}_{k+1}^u]^{-1}$, and $\mathbf{K}_{G,k+1}$ can be found in Eq. (18).

3) Measurement update (correction)

$$\hat{\mathbf{X}}_{k+1|k+1} = \tilde{\mathbf{X}}_{k+1|k} + \mathbf{K}_{G,k+1}(\mathbf{y}_{k+1} - \mathbf{C}_{k+1}\tilde{\mathbf{X}}_{k+1|k} - \mathbf{D}_{k+1}\mathbf{f}_{k+1} - \mathbf{D}_{k+1}^u\hat{\mathbf{f}}_{k+1|k+1}^u) \quad (41)$$

In addition, the error covariance matrices are expressed as⁵¹

$$\hat{\mathbf{P}}_{k+1|k+1}^{\mathbf{x}} = (\mathbf{I} + \mathbf{K}_{G,k+1} \mathbf{D}_{k+1}^u \mathbf{S}_{k+1} \mathbf{D}_{k+1}^{uT} \mathbf{R}_{k+1}^{-1} \mathbf{C}_{k+1}^T) (\mathbf{I} - \mathbf{K}_{G,k+1} \mathbf{C}_{k+1}) \tilde{\mathbf{P}}_{k+1|k}^{\mathbf{x}} \quad (42)$$

$$\hat{\mathbf{P}}_{k+1|k+1}^{\mathbf{f}} = \mathbf{S}_{k+1}; \quad \hat{\mathbf{P}}_{k+1|k+1}^{\mathbf{x}\mathbf{f}} = (\hat{\mathbf{P}}_{k+1|k+1}^{\mathbf{x}})^T = -\mathbf{K}_{G,k+1} \mathbf{D}_{k+1}^u \mathbf{S}_{k+1} \quad (43)$$

Thus, following the procedures of KF-UI, the structural state vector and unknown input are updated as

$$\hat{\mathbf{X}} = \hat{\mathbf{X}}(\mathbf{r}_q, \boldsymbol{\theta}_2); \quad \hat{\mathbf{f}}^u = \hat{\mathbf{f}}^u(\mathbf{r}_q, \boldsymbol{\theta}_2) \quad (44)$$

Similarly, the estimated acceleration is rewritten as

$$\hat{\mathbf{x}}(\mathbf{r}_q, \boldsymbol{\theta}_2) = \mathbf{M}^{-1} \left(\boldsymbol{\eta} \mathbf{f} + \boldsymbol{\eta}^u \hat{\mathbf{f}}^u(\mathbf{r}_q, \boldsymbol{\theta}_2) - \mathbf{C}(\mathbf{r}_q, \boldsymbol{\theta}_2) \hat{\mathbf{x}}(\mathbf{r}_q, \boldsymbol{\theta}_2) - \mathbf{K}(\mathbf{r}_q, \boldsymbol{\theta}_2) \hat{\mathbf{x}}(\mathbf{r}_q, \boldsymbol{\theta}_2) \right) \quad (45)$$

Finally, the optimal DCT coefficient vector $\hat{\mathbf{r}}_q$ and the optimal time-invariant physical parameter vector $\hat{\boldsymbol{\theta}}_2$ are obtained by minimizing the same objective error function in Eq. (22), and the optimal gradually varying physical parameter vector $\hat{\boldsymbol{\theta}}_1$ can be reconstructed by DCT in Eq. (13). The detailed procedures of the proposed approach II are shown in Fig. 3.

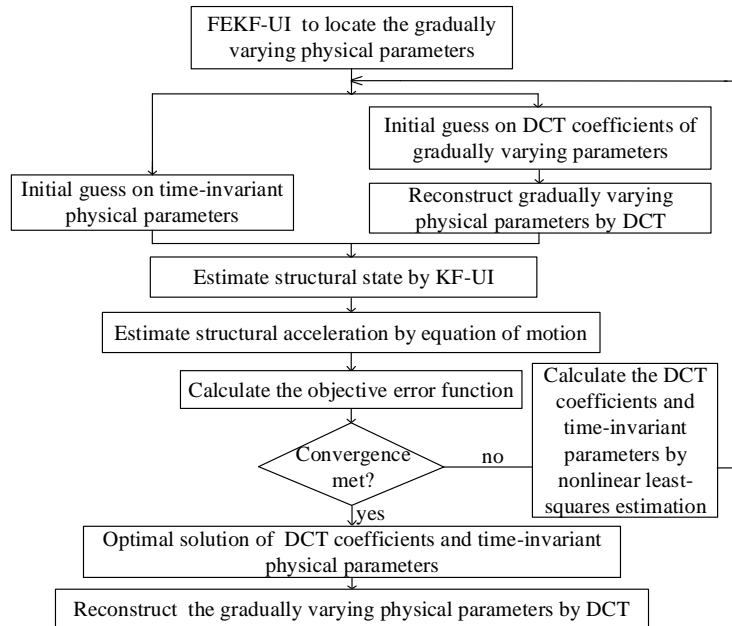


FIGURE 3 Procedures of the proposed approach II under unknown excitations

4. Numerical verifications

4.1 Identification of gradually varying physical parameters subjected to known excitations

Example 1: A gradually varying truss model subjected to a known external excitation

As shown in Fig. 4, a one-span truss structure subjected to a known white noise excitation is investigated. The proposed approach I is used to identify the stiffness parameter of each member using only partially measured acceleration responses.

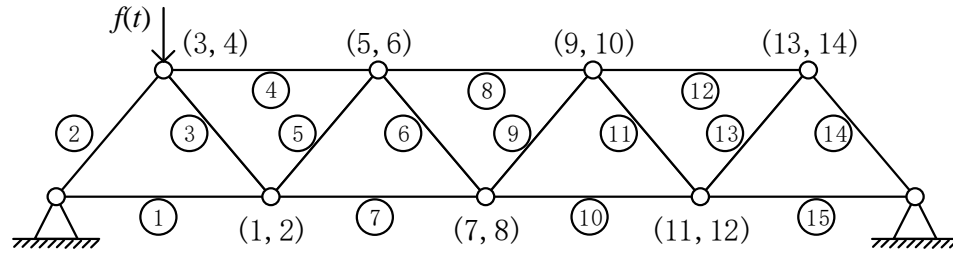


FIGURE 4 A one-span truss subjected to a white noise excitation

(Note: the symbols ①,②.. represent the number of member. (1, 2) means the horizontal and vertical DOFs of a specific node.)

The truss structure contains 15 members and 14 DOFs in total. The length and cross-section of each bar is $l_i=1\text{m}$ and $A_i=7.85 \times 10^{-5}\text{m}^2$ ($i=1,2,\dots,15$), respectively. The total mass of each bar is $m_i=54.95\text{kg}$ ($i=1,2,\dots,15$). The Rayleigh damping is adopted with the first two damping ratios assumed as 0.02. The first five natural frequencies of the time-invariant truss are 1.48Hz, 2.99Hz, 4.03Hz, 6.38Hz and 7.42Hz, respectively. The truss model is subjected to a white noise excitation $f(t)$, which acts on the 4th DOF. The sampling frequency is 100Hz during the process of dynamic response calculation, and the sampling duration is 10s. Seven acceleration responses of the 2nd, 4th, 6th, 8th, 10th, 12th and 14th DOFs are used as measured responses for the identification. They are the vertical acceleration responses of nodes. Each measured response is polluted by white noise with 3% variance in root mean square (RMS), namely

$$\ddot{\mathbf{x}}_{i,\text{noisy}} = \ddot{\mathbf{x}}_{i,\text{clean}} + 3\% \times \text{std}(\ddot{\mathbf{x}}_{i,\text{clean}}) \times \mathbf{rand} \quad (i = 2, 4, 6, 8, 10, 12, 14) \quad (46)$$

where $\ddot{\mathbf{x}}_{i,noisy}$ is the simulated ‘measured’ noisy acceleration vector, $\ddot{\mathbf{x}}_{i,clean}$ is the noisy-free acceleration vector, $std(\ddot{\mathbf{x}}_{i,clean})$ means the standard deviation of $\ddot{\mathbf{x}}_{i,clean}$ and **rand** is a random standard normal distribution vector.

In the truss model, single gradual change of the member stiffness is assumed. The stiffness parameter change in the truss is defined as

$$k_i = 1.57 \times 10^5 \text{ N/m} \quad (i = 1, 3, 4, \dots, 15)$$

$$k_2 = \begin{cases} 1.57 \times 10^5 \text{ N/m}, & 0 \text{ s} \leq t < 2 \text{ s} \\ -3.62 \times 10^3 t + 1.64 \times 10^5 \text{ (N/m)}, & 2 \text{ s} \leq t \leq 8.5 \text{ s} \\ 1.33 \times 10^7 \text{ N/m}, & 8.5 \text{ s} < t \leq 10 \text{ s} \end{cases}$$

In the first step, the FEKF algorithm is implemented to locate the gradually varying parameters in the truss. $\lambda = 2^{2/70} = 1.02$ is used in this case.⁸ Results of locating time-varying stiffness parameters are shown in Fig. 5. It is observed from Fig. 5 that the stiffness parameter of the second element is more likely to have the time-varying property, since it transits from one stable converged value to the other stable value, while other stiffness values are more likely to remain unchanged with occasional fluctuations. However, it is difficult to determine the exact beginning and end time instants and the specific form of stiffness variation.

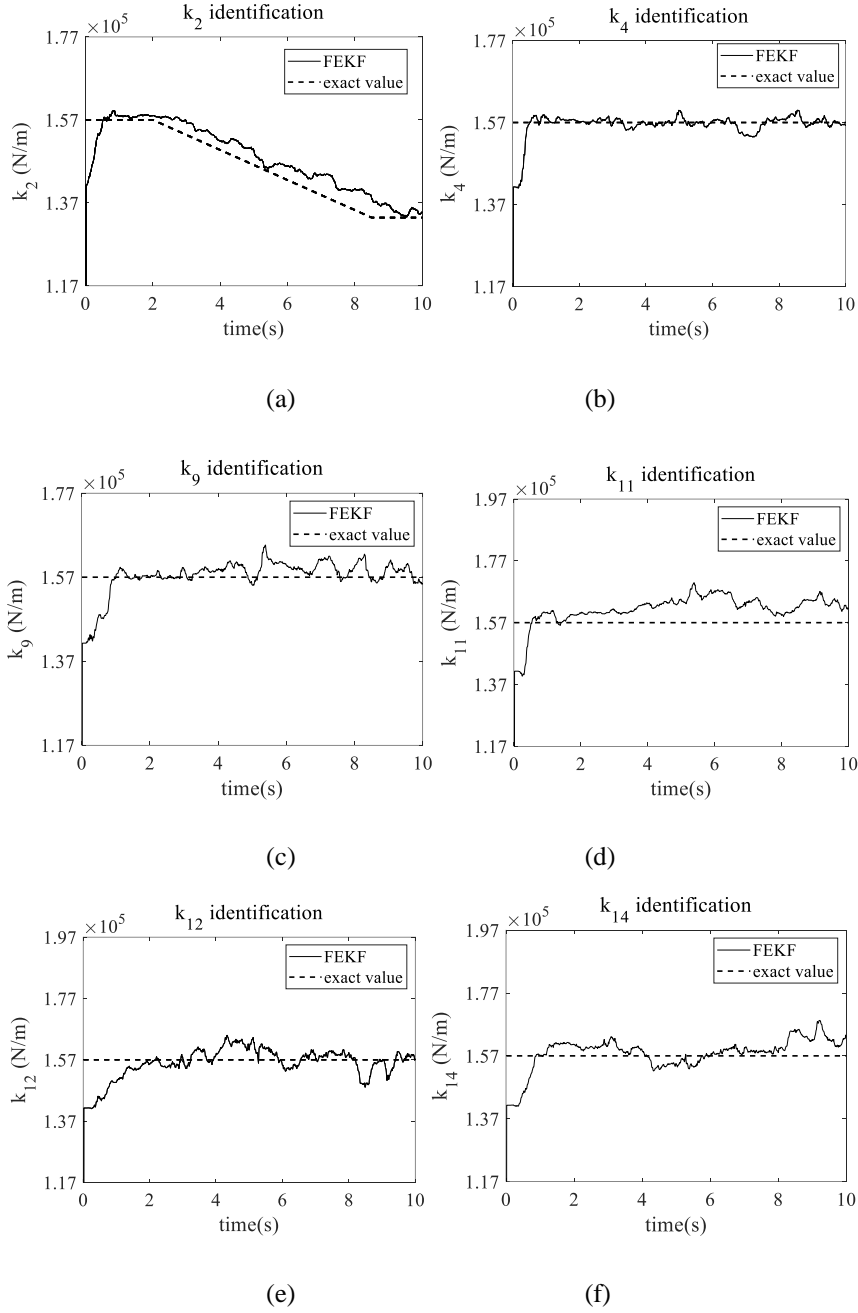


FIGURE 5 Location of time-varying stiffness parameters using FEKF (3% noise): (a) k_2 ; (b) k_4 ; (c) k_9 ; (d) k_{11} ; (e) k_{12} ; (f) k_{14}

In the second step, k_2 is expanded by DCT with $q=8$. Thus, the identification of 15,000 unknown stiffness parameter coefficients in the time-domain is converted to the identification of eight DCT coefficients of k_2 and other 14 time-invariant stiffness parameters. Based on the proposed approach I which integrating DCT and KF, the gradually changing and time-invariant

structural stiffness parameters are identified and shown in Fig. 6 with comparisons to the exact values. It is illustrated that the proposed approach I can effectively track the gradually change of structural physical parameters in the truss. Furthermore, the identification of other time-invariant parameters also shows a high precision. Most of the identified time-invariant parameters are identical to the exact values, and the maximum relative error is around 0.5% for the twelfth element stiffness parameter.

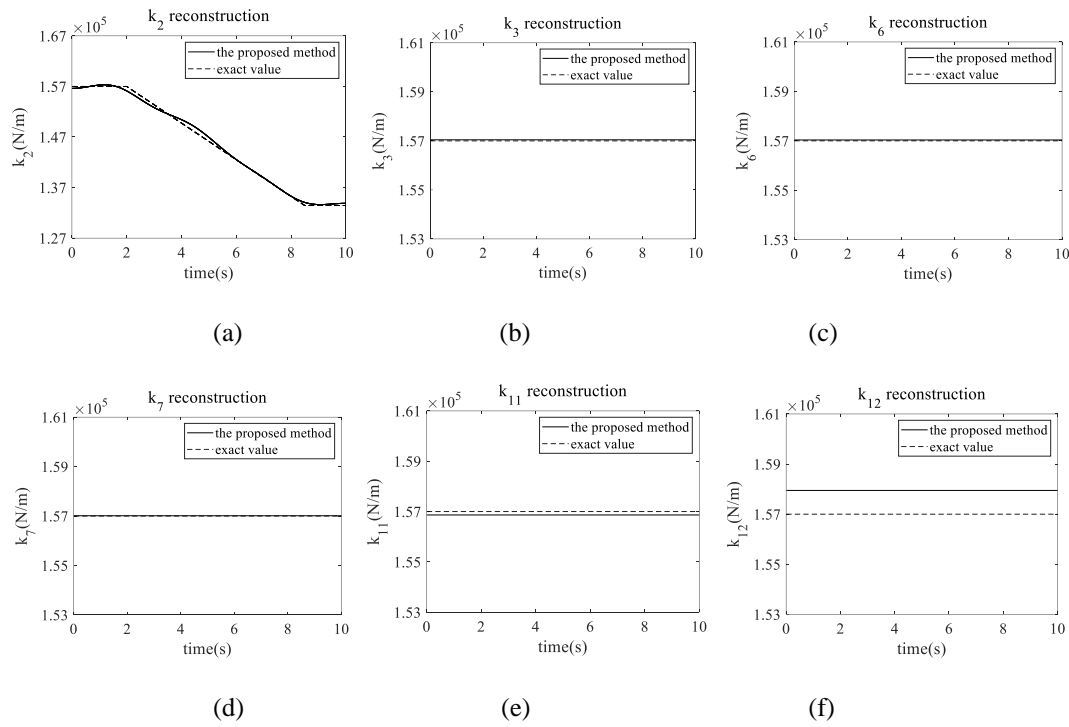


FIGURE 6 Identification of partial stiffness parameters: (a) k_2 ; (b) k_3 ; (c) k_6 ; (d) k_7 ; (e) k_{11} ; (f) k_{12}

Example 2: A gradually varying bridge model subjected to a known ground excitation

As shown in Fig. 7, the finite element model of a bridge is composed of three-span main beam models and two pier models. The whole model is divided into 16 elements. Each element contains two nodes and three DOFs in the horizontal, vertical, and rotational directions. The beam has a uniform cross section with area $A_b = 1.56\text{m}^2$ and moment of inertia $I_b = 4.02\text{m}^4$. The length of beam element between two adjacent nodes is $l_b = 12\text{m}$. The cross section area of the two piers is $A_p = 1.57\text{m}^2$ and the element length is $l_p = 5\text{m}$. The mass density is $\rho = 300\text{kg/m}^3$ and the modulus of elasticity is assumed as $E = 10^8\text{Pa}$. Rayleigh damping model is used and the damping

ratios of the first two modes of the bridge are 2%. The first four modal frequencies for the time-invariant bridge are 0.516 Hz, 1.296 Hz, 1.513 Hz and 1.758 Hz.

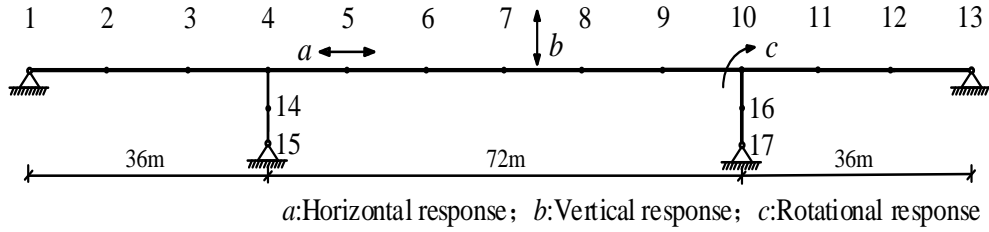


FIGURE 7 A bridge model

The dynamic responses are computed with a sampling frequency of 100 Hz and a sampling duration of 10 s. The bridge model is subjected to the 1940 El Centro N-S earthquake with the peak value scaled to 0.2g. The vertical acceleration responses at the nodes No. 2, 3, 5, 6, 7, 8, 9, 11 and 12, and the horizontal acceleration responses at the nodes No. 14 and 16 are used as measurements. Each measured response is polluted by white noise with 3% RMS as

$$\ddot{\mathbf{x}}_{i,\text{noisy}} = \ddot{\mathbf{x}}_{i,\text{clean}} + 3\% \times \text{std}(\ddot{\mathbf{x}}_{i,\text{clean}}) \times \mathbf{rand} \quad (i = 3, 6, 10, 13, 16, 19, 22, 26, 29, 32, 33, 36, 37) \quad (47)$$

Two pier elements are assumed to be gradually varying. The theoretical values of the stiffness parameters are given as below

$$k_i = 3.35 \times 10^7 \text{ N/m} \quad (i = 1, 2, \dots, 12); \quad k_i = 3.14 \times 10^7 \text{ N/m} \quad (i = 14, 15)$$

$$k_{13} = \begin{cases} 3.35 \times 10^7 \text{ N/m}, & 0 \text{ s} \leq t < 3 \text{ s} \\ -8.38 \times 10^5 t + 3.60 \times 10^7 \text{ (N/m)}, & 3 \text{ s} \leq t \leq 7 \text{ s} \\ 3.02 \times 10^7 \text{ N/m}, & 7 \text{ s} < t \leq 10 \text{ s} \end{cases}$$

$$k_{16} = \begin{cases} 3.14 \times 10^7 \text{ N/m}, & 0 \text{ s} \leq t < 2 \text{ s} \\ -1.22 \times 10^6 t + 3.38 \times 10^7 \text{ (N/m)}, & 2 \text{ s} \leq t \leq 8.5 \text{ s} \\ 2.35 \times 10^7 \text{ N/m}, & 8.5 \text{ s} < t \leq 10 \text{ s} \end{cases}$$

The time-varying stiffness parameters are localized using the FEKF algorithm. For brevity and without losing generality, only partial identification results are shown in Fig. 8. Herein, the fading factor is adopted as $\lambda = 2^{2/70} = 1.02$.⁸ According to the identification results in Fig. 8, the stiffness of pier element between nodes 4 and 14 (k_{13}), and the stiffness of pier element between

nodes 16 and 17 (k_{16}), have the highest possibility of having changes. However, it is difficult to determine the pattern and degree of change accurately owing to the coarse identification results.

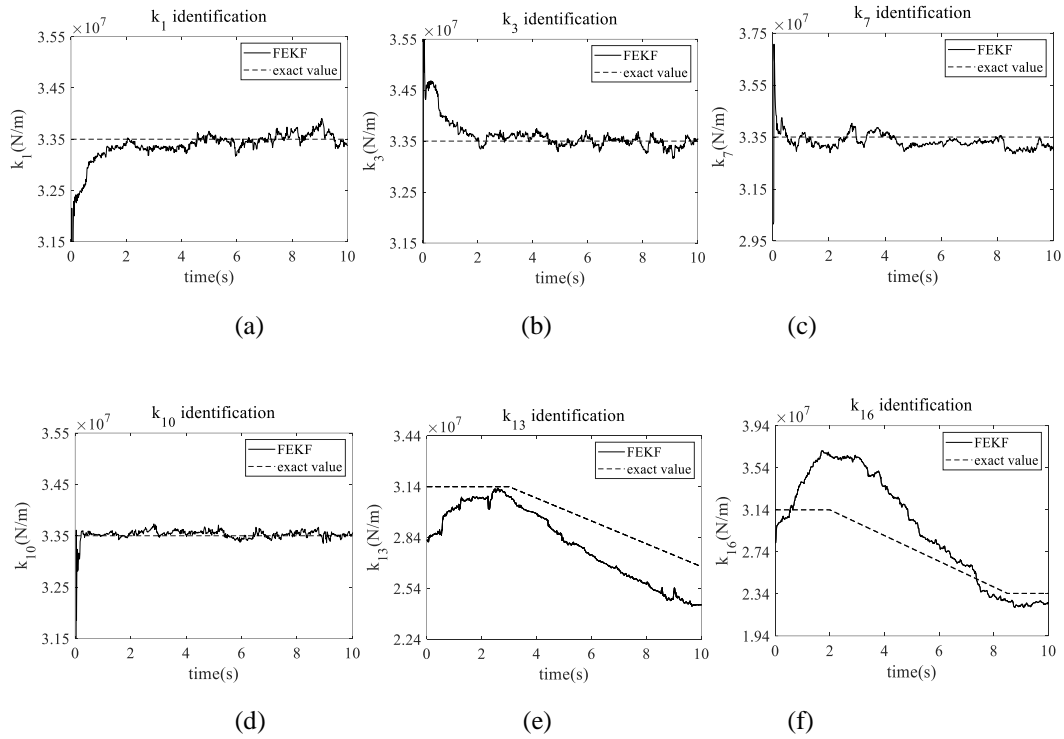


FIGURE 8 Location of time-varying stiffness parameters: (a) k_1 ; (b) k_3 ; (c) k_7 ; (d) k_{10} ; (e) k_{13} ; (f) k_{16}

According to the localization results of time-varying parameters in Fig.8, k_{13} and k_{16} are expanded by using DCT with $q=6$. Therefore, the unknown variables in the nonlinear least-squares optimization process include 6 DCT coefficients for k_{13} , 6 DCT coefficients for k_{16} and 14 parameters for other time-invariant stiffness. Fig. 9 shows the optimization results of gradually varying stiffness parameters using the proposed DCT integrated with KF method when the RMS level of noise is 3%. The identification results are consistent with the exact values. The proposed approach I can accurately track the start and end time instants of the gradual change, the form of varying, and the time-varying stiffness values with changes.

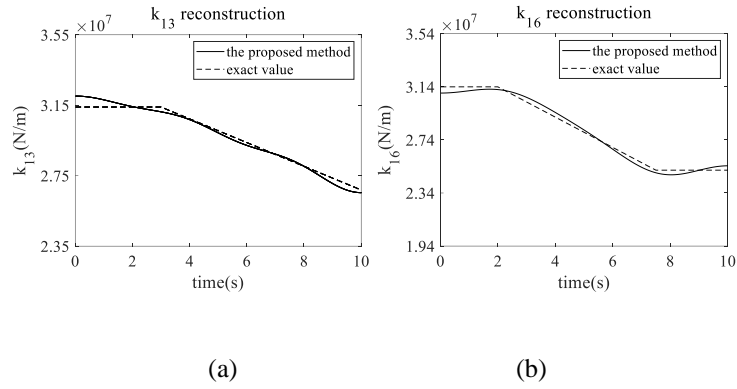


FIGURE 9 Identification of gradually varying stiffness parameters (3% noise): (a) k_{13} ; (b) k_{16}

Fig. 10 shows the identification results of partial time-invariant stiffness parameters. It can be observed that most stiffness parameters are identified accurately. It should be noted that k_{15} has the maximum identification error, however, the relative error is only 1.2%. The desirable identification results are obtained using only partial acceleration responses which are polluted by a high level of measurement noise.

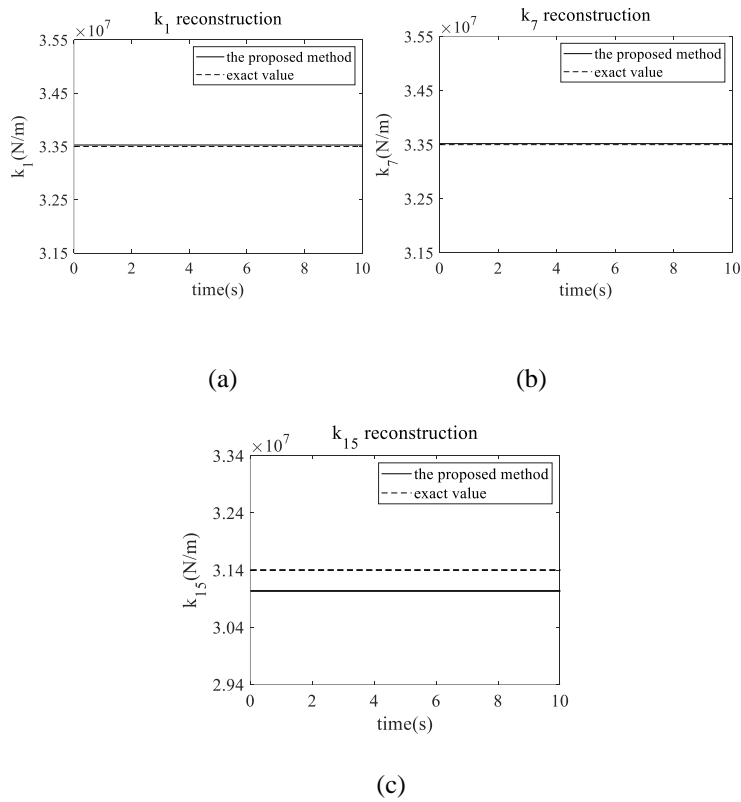


FIGURE 10 Identification of partial time-invariant stiffness parameters of the bridge: (a) k_1 ; (b) k_7 ; (c) k_{15}

4.2 Identification of gradually varying physical parameters subjected to unknown excitations

Example 1: A gradually varying truss model subjected to an unknown external excitation

The same truss model in Fig. 4 is utilized to validate the effectiveness of the proposed approach II with unknown excitations. The external white noise excitation is assumed unknown in the identification analysis. The acceleration responses of the 2nd, 4th, 6th, 8th, 10th, 12th and 14th DOFs are collected as measurements for identification. Additionally, the displacement responses of the 4th and 10th DOFs are measured as a supplement for data fusion. White noise with 3% variance in RMS is added to all the measured responses.

There are totally 15,000 stiffness coefficients in the time-domain to be identified in the truss. First, the proposed FEKF-UI is applied to locate the gradually varying stiffness parameters. Fig. 11 shows the localization results of some elemental stiffness. It is noted that k_2 is likely to be time varying as it transits from one converged value to another value.

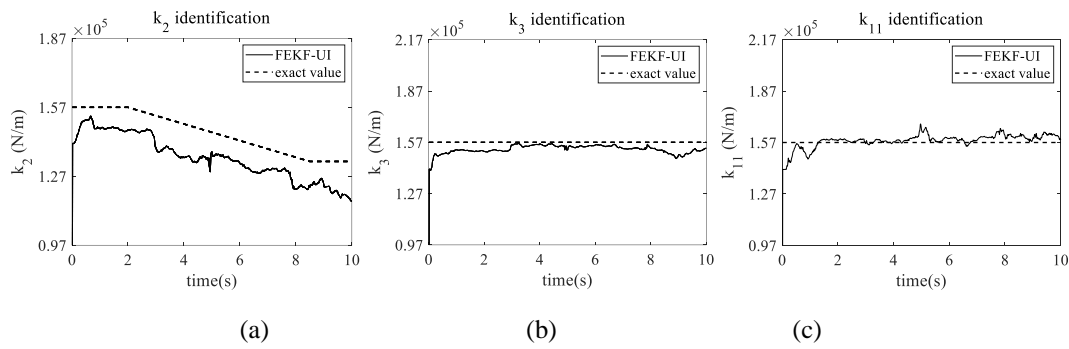


FIGURE 11 Location of time-varying stiffness parameters using FEKF-UI (3% noise): (a) k_2 ; (b) k_3 ; (c) k_{11}

Then, k_2 is expanded by DCT with $q=6$, transforming the parameters to be identified into 6 DCT coefficients and 14 time-invariant stiffness parameters. The identification results shown in Fig.12 validate that the proposed approach II could identify the gradually varying or time-

invariant stiffness parameters in the truss model. Furthermore, the identification accuracy of the unknown white noise excitation is good by comparing with its exact value as shown in Fig. 13.

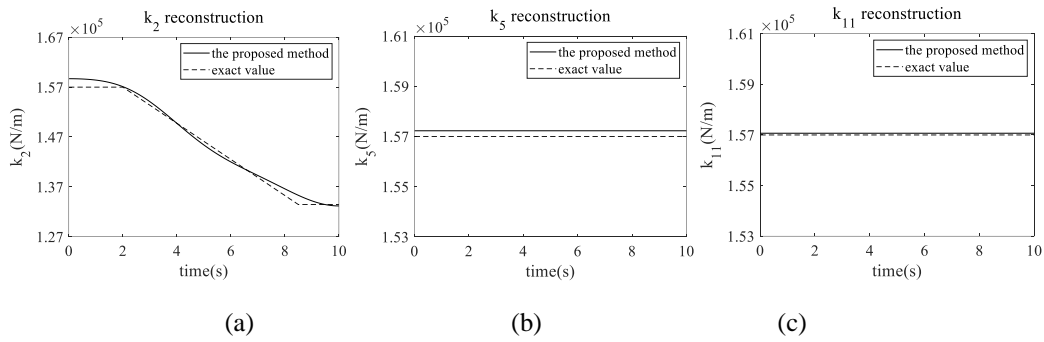


FIGURE 12 Identification of partial stiffness parameters in the truss: (a) k_2 ; (b) k_5 ; (c) k_{11}

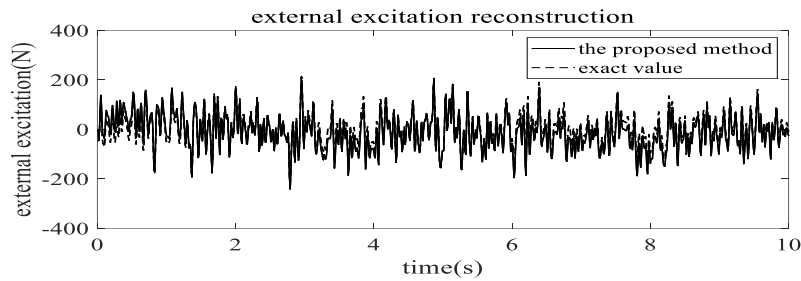


FIGURE 13 Identification of external excitation (3% noise)

Example 2: A gradually varying bridge model subjected to an unknown ground excitation

In this section, the same bridge model in Fig. 7 is used to verify the effectiveness of the proposed approach II, and the ground excitation is assumed unknown in the identification. Partial measurements include the vertical acceleration responses at the nodes No. 2, 3, 5, 6, 7, 8, 9, 11 and 12, the horizontal acceleration responses at the nodes No. 14 and 16, and the strain responses on the top surface of the 2nd, 3rd and 14th nodes. Each measured response is polluted by white noise with 3% variance in RMS.

The proposed FEKF-UI is applied to locate the gradually varying stiffness parameters when the external excitations are unknown. Fig. 14 shows the localization results of some elemental stiffness values.

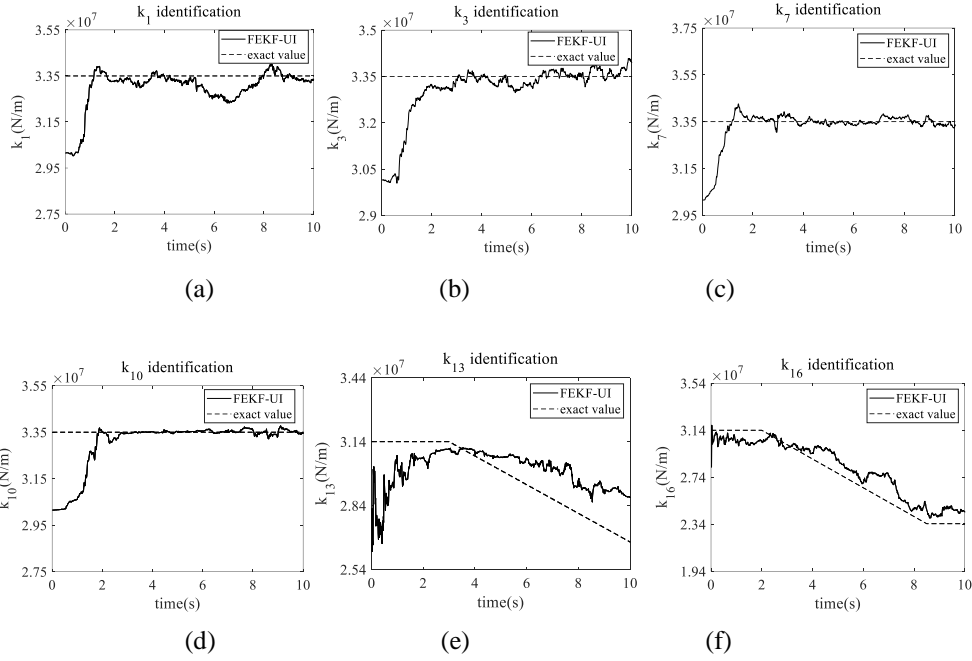


FIGURE 14 Location of time-varying stiffness parameters using FEKF-UI (3% noise):(a) k_1 ; (b) k_3 ; (c) k_7 ; (d) k_{10} ; (e) k_{13} ; (f) k_{16}

The stiffness of the 13th and 16th elements are more likely to be time varying since their stiffness values transit from one stable convergence value to the other stable one. Then DCT is utilized to transform the time-varying stiffness parameters k_{13} and k_{16} with $q=6$ into the corresponding coefficients. The number of unknown DCT coefficients and the time-invariant stiffness parameters in the nonlinear least-squares optimization process is 26 in total, and these DCT coefficients and time-invariant stiffness parameters are identified by the proposed method. Fig. 15 shows the reconstructed gradually varying stiffness parameters based on the optimized DCT coefficients. In addition, for brevity and without losing generality, part of the optimized time-invariant physical parameters are shown in Fig. 16. The results demonstrate that the identification accuracy is good when the noise RMS degree is 3%. The proposed approach II can be used to identify the external excitations simultaneously, as shown in Fig. 17. It is demonstrated that the proposed approach II is effective in identifying the gradually varying physical parameters under unknown excitations with a relatively high level of noise.

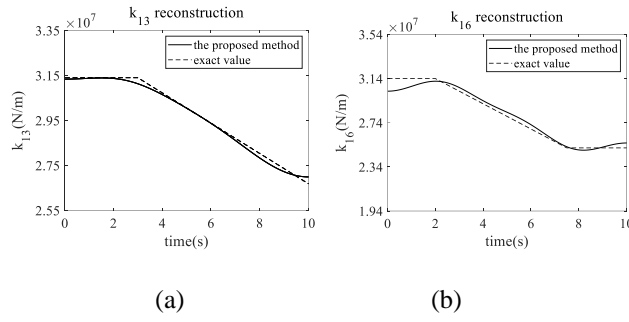


FIGURE 15 Identification of gradually varying stiffness parameters of the bridge: (a) k_{13} ; (b) k_{16}

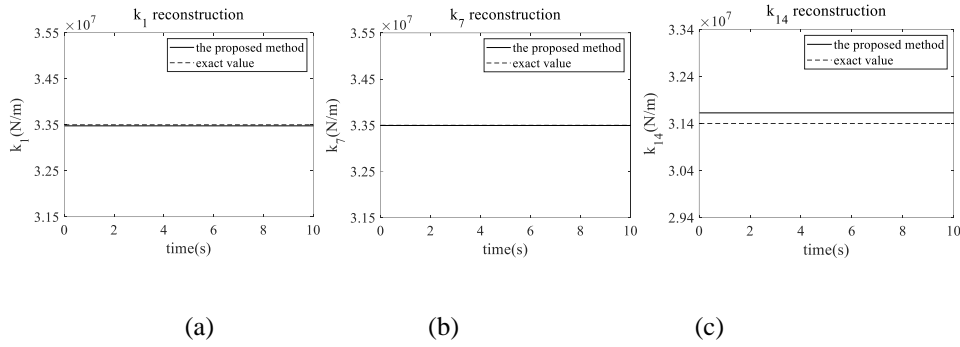


FIGURE 16 Identification of partial time-invariant stiffness parameters of the bridge: (a) k_1 ; (b) k_7 ; (c) k_{14}

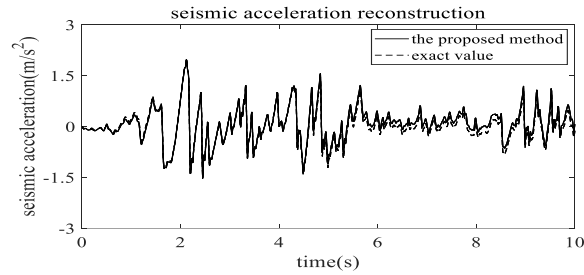


FIGURE 17 Identification of seismic acceleration (3% noise)

5. Case study: Identification of time-varying cable forces in cable-stayed bridges

5.1 Using the proposed approach I to identify the time-varying cable force

Under the influence of external excitations such as wind and vehicle loads, the cable tension force of a cable-stayed bridge can vary gradually with time. The proposed approach I provides an idea to identify the cable force using only one monitored acceleration response of the cable.

The motion of equation of a cable subjected to distributed force along the cable length (such as wind) has been investigated by many researchers.⁴¹ Assuming that the vibration of the cable

contains only r modes, the governing equation of the first r -order can be written in the matrix form as

$$\mathbf{M}_r \ddot{\mathbf{q}}_r + \mathbf{C}_r \dot{\mathbf{q}}_r + a(t) \mathbf{K}_r \mathbf{q}_r + \mathbf{\Lambda}_r \mathbf{q}_r = \mathbf{f}_r \quad (t=1, 2, \dots, Nt) \quad (48)$$

in which $\ddot{\mathbf{q}}_r$, $\dot{\mathbf{q}}_r$, and \mathbf{q}_r are the first r -order modal acceleration, modal velocity and modal displacement vectors, respectively; $a(t)$ denotes the variation coefficient of the cable tension force, namely $a(t)=T(t)/T_0$, where T_0 is the static tension, $T(t)$ is the varied cable force, Nt is the number of time steps. The term $\mathbf{\Lambda}_r$ is related to the nonlinear vibrations, which reflects the axial elongation effect due to the transverse vibration of the cable. \mathbf{f}_r is the modal input vector; \mathbf{M}_r , \mathbf{C}_r and \mathbf{K}_r are mass, damping and stiffness matrices, which can be expressed as

$$\mathbf{M}_r = \frac{\mu L}{2} \begin{bmatrix} 1 & 0 & \dots & \dots & 0 \\ 0 & 1 & \ddots & & \vdots \\ \vdots & \ddots & \ddots & \ddots & \vdots \\ \vdots & & \ddots & 1 & 0 \\ 0 & \dots & \dots & 0 & 1 \end{bmatrix}_{r \times r}, \quad \mathbf{K}_r = \frac{\pi^2 T_0}{2L} \begin{bmatrix} 1 & 0 & \dots & \dots & 0 \\ 0 & 2^2 & \ddots & & \vdots \\ \vdots & \ddots & \ddots & \ddots & \vdots \\ \vdots & & \ddots & (r-1)^2 & 0 \\ 0 & \dots & \dots & 0 & r^2 \end{bmatrix}_{r \times r}, \quad \mathbf{C}_r = \mu L \omega_1 \begin{bmatrix} \xi_1 & 0 & \dots & \dots & 0 \\ 0 & 2\xi_2 & \ddots & & \vdots \\ \vdots & \ddots & \ddots & \ddots & \vdots \\ \vdots & & \ddots & (r-1)\xi_{r-1} & 0 \\ 0 & \dots & \dots & 0 & r\xi_r \end{bmatrix}_{r \times r} \quad (49)$$

where μ is the mass density per unit length of cable, L is the cable length under the static tension, ω_1 is the first order natural circular frequency, ξ_n ($1, 2, \dots, r$) is the damping ratio of the mode n .

It shall be noted that the varied cable tension force can be determined when $a(t)$ is identified. \mathbf{f}_r is the modal input of the applied wind load. Considering two common cases in engineering applications with and without anemometers installed on the bridge, the identification of $a(t)$ based on the integrated DCT with KF method is discussed.

5.1.1 Case I: Identification of time-varying cable force when anemometer installed on the bridge

For most long-span cable-stayed bridges, wind anemoscopes are required for SHM and used to provide the data of wind speed and wind load. Thus, the identification of $a(t)$ can be

conducted by the proposed approach I under the case of known excitations. In addition, considering $a(t)$ is an unknown scalar, the first step of time-varying parameter localisation in the proposed approach I can be omitted. The following section presents the identification procedures of variation coefficient $a(t)$ using the method in the second step of the proposed approach I.

(1) Decompose the Nt -dimensional $a(t)$ into q coefficients by DCT.

(2) Given initial guess of DCT coefficients $d(i)(i=1,2,\dots,q)$, the initial value of $a(t)$ can be reconstructed. Then the process in Step 2 of the proposed approach I is followed to identify the structural state by KF.

The state vector is defined as $\mathbf{X}_r = [\mathbf{q}_r^T, \dot{\mathbf{q}}_r^T]^T$. Considering that the transverse vibration amplitude of the cable is small, the nonlinear item $\Lambda_r \mathbf{q}_r$ can be ignored. Thus, the state equation can be rewritten as:

$$\dot{\mathbf{X}}_r = \mathbf{g}(\mathbf{X}_r) = \left(\begin{array}{c} \dot{\mathbf{q}}_r \\ \mathbf{M}_r^{-1}(\mathbf{f}_r - \mathbf{C}_r \dot{\mathbf{q}}_r - a(\mathbf{d})\mathbf{K}_r \mathbf{q}_r) \end{array} \right) + \mathbf{w} \quad (50)$$

In practice, accelerometers are commonly used to measure the vibration of stay cables. Therefore, the measurement equation is rewritten as

$$\mathbf{Y}_{k+1} = \begin{bmatrix} \mathbf{0}_{1 \times r} & \varphi_1(l_a^{(1)}) & \cdots & \varphi_r(l_a^{(1)}) \\ \vdots & \vdots & \ddots & \vdots \\ \mathbf{0}_{1 \times r} & \varphi_1(l_a^{(p)}) & \cdots & \varphi_r(l_a^{(p)}) \end{bmatrix} \mathbf{g}(\mathbf{X}_{r,k+1}) + \mathbf{v}_{k+1} \quad (51)$$

in which p is the number of accelerometers, $l_a^{(j)}$ represents the position of the j -th accelerometer. $\varphi_r(\cdot)$ is the mode shape function of mode r and $\varphi_r(x) = \sin(ix/L)$.

Formulas of KF used to estimate the structural state can be referred to Eqs. (17)-(19). The estimated acceleration response can be obtained as

$$\hat{\mathbf{q}}_r(\mathbf{d}) = \mathbf{M}_r^{-1}(\mathbf{f}_r - \mathbf{C}_r \hat{\mathbf{q}}_r(\mathbf{d}) - a(\mathbf{d}) \mathbf{K}_r \hat{\mathbf{q}}_r(\mathbf{d})) \quad (52)$$

(3) Estimate DCT coefficients by nonlinear optimization and reconstruct $a(t)$.

The optimal DCT coefficient $\hat{d}(i)(i=1,2,\dots,q)$ can be estimated by minimising the following objective error function

$$[\hat{\mathbf{d}}] = \arg \min_{\mathbf{d}} \left(\left\| \mathbf{Y}_{k+1} - \mathbf{L}_{qa} \hat{\mathbf{q}}_r(\mathbf{d}) \right\|_2^2 \right) \quad (53)$$

where $\mathbf{L}_{qa} = \begin{bmatrix} \varphi_1(l_a^{(1)}) & \cdots & \varphi_r(l_a^{(1)}) \\ \vdots & \ddots & \vdots \\ \varphi_1(l_a^{(p)}) & \cdots & \varphi_r(l_a^{(p)}) \end{bmatrix}$. Thus, the optimal variation coefficient of the cable tension

force $\hat{a}(t)$ can be reconstructed by Eq. (13).

5.1.2 Case II: Identification of time-varying cable force when no anemometer on the bridge

When no anemometer is installed on the bridge, the wind load can be included in the process noise according to previous studies⁴¹ to simplify the complexity of the problem. Thus, the above proposed approach in case I is modified to identify the time-varying cable force when the anemometer is not installed on the bridge.

The state equation is rewritten as

$$\dot{\mathbf{X}}_r = \mathbf{g}(\mathbf{X}_r) = \left(\mathbf{M}_r^{-1}(-\mathbf{C}_r \dot{\mathbf{q}}_r - a(\mathbf{d}) \mathbf{K}_r \mathbf{q}_r) \right) + \mathbf{w} \quad (54)$$

The state equation is discretized into

$$\mathbf{X}_{r,k+1} = \mathbf{A}_k \mathbf{X}_{r,k} + \mathbf{w}_k \quad (55)$$

The observation equation is rewritten as

$$\mathbf{Y}_{k+1} = \begin{bmatrix} \mathbf{0}_{1 \times r} & \varphi_1(l_a^{(1)}) & \cdots & \varphi_r(l_a^{(1)}) \\ \vdots & \vdots & \ddots & \vdots \\ \mathbf{0}_{1 \times r} & \varphi_1(l_a^{(p)}) & \cdots & \varphi_r(l_a^{(p)}) \end{bmatrix} \mathbf{g}(\mathbf{X}_{r,k+1}) + \mathbf{v}_{k+1} = \mathbf{C}_{k+1} \mathbf{X}_{r,k+1} + \mathbf{v}_{k+1} \quad (56)$$

The main formulas of KF algorithm are modified as

$$\tilde{\mathbf{X}}_{r,k+1|k} = \mathbf{A}_k \hat{\mathbf{X}}_{r,k|k}; \quad \tilde{\mathbf{P}}_{k+1|k} = \mathbf{A}_k \hat{\mathbf{P}}_{k|k} \mathbf{A}_k^T + \mathbf{Q}_k \quad (57)$$

$$\hat{\mathbf{X}}_{r,k+1|k+1} = \tilde{\mathbf{X}}_{r,k+1|k} + \mathbf{K}_{G,k+1} (\mathbf{Y}_{k+1} - \mathbf{C}_{k+1} \tilde{\mathbf{X}}_{r,k+1|k}); \quad \mathbf{K}_{G,k+1} = \tilde{\mathbf{P}}_{k+1|k} \mathbf{C}_{k+1}^T (\mathbf{C}_{k+1} \tilde{\mathbf{P}}_{k+1|k} \mathbf{C}_{k+1}^T + \mathbf{R}_{k+1})^{-1} \quad (58)$$

$$\hat{\mathbf{P}}_{k+1|k+1} = (\mathbf{I} - \mathbf{K}_{G,k+1} \mathbf{C}_{k+1}) \tilde{\mathbf{P}}_{k+1|k} \quad (59)$$

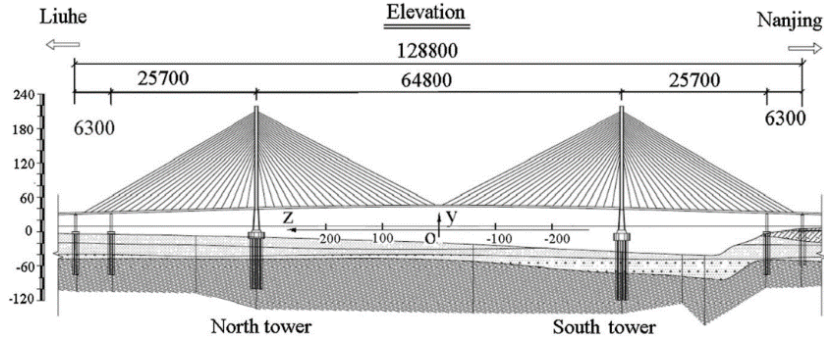
The estimation of acceleration response is derived as

$$\hat{\mathbf{q}}_r(\mathbf{d}) = \mathbf{M}_r^{-1} (-\mathbf{C}_r \hat{\mathbf{q}}_r(\mathbf{d}) - \mathbf{a}(\mathbf{d}) \mathbf{K}_r \hat{\mathbf{q}}_r(\mathbf{d})) \quad (60)$$

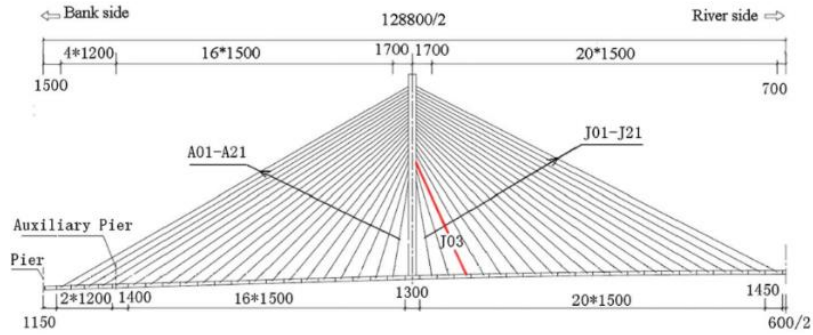
Finally, the optimal DCT coefficient $\hat{d}(i) (i=1,2,\dots,q)$ can be estimated by Eq. (53).

5.2 Numerical verification

The Nanjing Yangtze River No. 3 Bridge is adopted in the numerical study to validate the effectiveness of the proposed approach in case I (with anemometer installed on the bridge). Fig. 18 shows the structural geometric information. The details of the whole bridge model can be referred to Li *et al.*⁴¹, which are not introduced herein owing to the page limitation. There are totally 168 stay cables installed on the bridge. Among these, the No. J03 cable, which is marked red in Fig. 18 (b), is investigated as the target cable. The parameters of No. J03 cable is: the length is 112.029m; the section area is 41.948cm²; the unit length mass is 32.929kg/m; the static tension is $T_0=1470\text{kN}$; the fundamental frequency at the initial tension is 0.9031Hz; and the damping ratio is assumed to be 0.01.



(a)



(b)

FIGURE 18 Geometric dimensions of the cable-stayed bridge: (a) elevation of the bridge (unit: cm. The unit of height is meter.) and (b) sequential numbers of cables (unit: cm). (Referred to Li *et al.*⁴¹)

It is assumed that the time-varying cable force of No. J03 cable is induced by a truck weighted 100t passing over the bridge with a speed of 20 m/s. Then the real variation coefficient of the cable tension force can be obtained by $a(t)=T(t)/T_0$. Additionally, the fluctuating wind load causes the vibration of the cable, and the wind load can be generated by Davenport spectrum⁵². Since an anemometer is installed on the bridge, the wind force is assumed known in the identification process. Thus, the modal input vector \mathbf{f}_r can be calculated accordingly. \mathbf{f}_r is applied in Eq. (48) together with the real variation coefficient $a(t)$. When given $r=11$ as in reference⁴¹ the modal acceleration responses of the target cable can be calculated by solving Eq. (48). In addition, the calculated acceleration responses are polluted by white noise with 5%

variance in RMS. Only one acceleration at one sixth of the length from the bottom of the cable is used as the measurement for identification.

The variation coefficient of the cable force $a(t)$ is expanded by DCT with $q=30$. Then the optimal DCT coefficient $\hat{\mathbf{a}}$ is identified following the procedures of the integrated DCT with KF method. The identified cable tension force is shown in Fig. 19 compared with the exact value. Results indicate that even in the case of high level noise, the gradually varying cable force can be identified accurately by using the proposed approach I when only one acceleration sensor is fixed on the cable and the wind load are available.

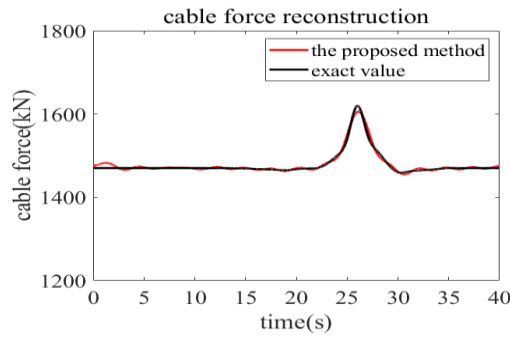


FIGURE 19 Identified cable force by the proposed approach I with anemometer on the bridge

5.3 Experimental verification

A scaled steel stay cable experiment carried out at Harbin Institute of Technology⁴² is further employed to validate the effectiveness of the proposed approach in case II (without anemometer installed on the bridge). The length, mass per unit length, damping ratio and natural frequency of the cable model are 14.03 m, 1.33 kg/m, 0.012 and 2.493 Hz, respectively. The experimental setup is shown in Fig. 20. Two 550kw blower fans (marked as Blower No.1 and Blower No.2 in Fig.20) are utilized to simulate the influence of wind and excite the vibrations of the cable both in-plane and out-of-plane. The cable tension can be adjusted by a threaded rod, since the rod is installed in a series connection with the cable and can be operated manually to produce a changing cable

force. Then the real cable force is measured simultaneously by the load cell installed between the left anchorage and the sliding bearing. Herein, the in-plane acceleration response measured by an accelerometer installed 3.6m from the sliding bearing is employed to identify the varied cable force using the proposed approach. The acceleration and cable tension data are recorded by the DSpace data acquisition system and its sampling frequency is 200 Hz. More details of this experiment can be referred to Bao *et al.*⁴².

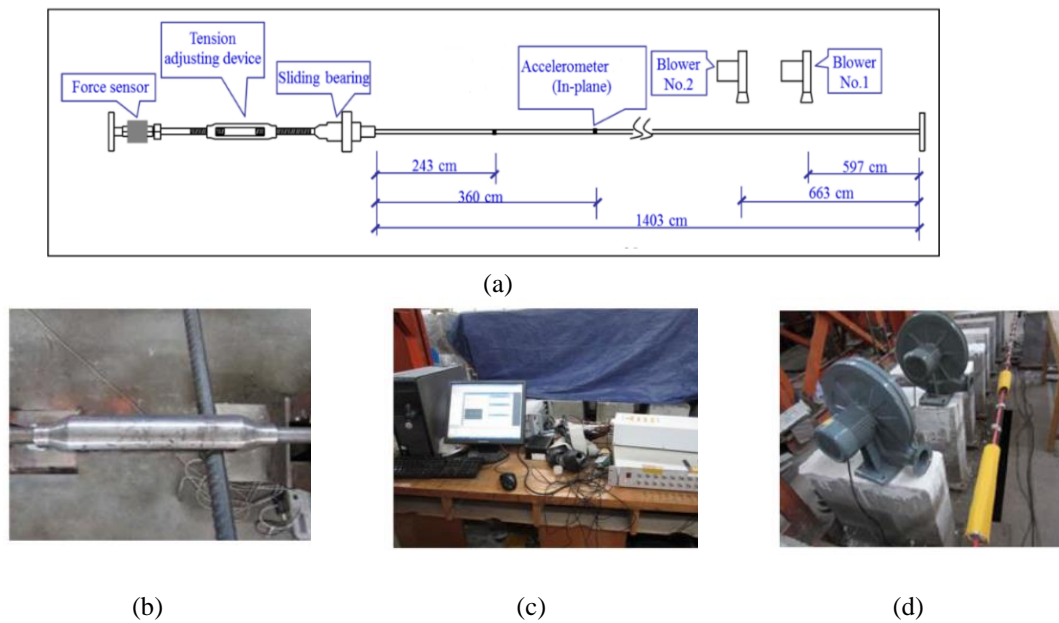


FIGURE 20 Experiment setup: (a) experimental model; (b) tension adjusting device; (c) data acquisition system; and (d) blowers and cable. (Referred to Bao *et al.*⁴²)

Since the fluctuating wind cannot be measured in the test, the wind load is unknown in the identification. Therefore, the proposed approach in case II (without anemometer installed on the bridge) is applied to identify the time-varying force of the cable in test. The variation coefficient of the cable force $a(t)$ is expanded by DCT with $q=30$. Then the initial value of $a(t)$ is reconstructed by the given initial guess of DCT coefficients, and the structural state is estimated by KF using the measured in-plane acceleration response. The optimal DCT coefficient $\hat{\mathbf{a}}$ estimated by the nonlinear optimization in Eq. (53), and the optimal variation coefficient of the

cable force $\hat{a}(t)$ is reconstructed by DCT. Afterwards, the cable force can be obtained by $\hat{T}(t)=\hat{a}(t)T_0$, which is shown in Fig. 21.

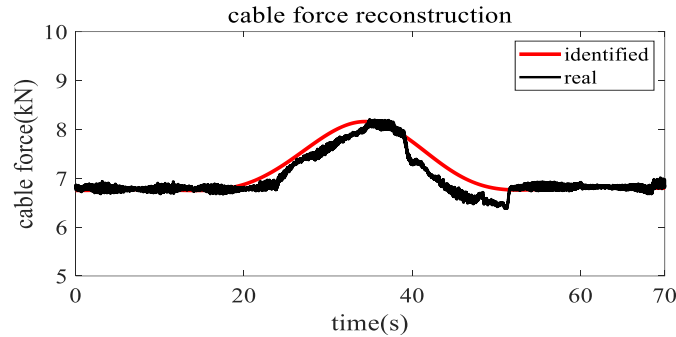


FIGURE 21 Identified cable force by the proposed approach I without anemometer on the bridge

The identification results show that the proposed approach I can track the change of cable force accurately when no anemometer is installed on the bridge. This result validates that the proposed approach I can be applied to conduct the identification of time-varying cable forces in practical engineering applications. When no load cell and anemometer are installed on the cable, it is very economical and practical to identify the change of cable force by using the measured acceleration response of an accelerometer mounted on the cable.

6. Conclusions

In this paper, two approaches are proposed to identify the gradually varying physical parameters under known/unknown excitations by using the limited number of measurements. The proposed approaches are based on the FEKF/ FEKF-UI for locating time-varying physical parameters, DCT analysis for expanding time-varying parameters, KF/KF-UI for identifying structural state by using partial measurements and nonlinear optimization for estimating coefficients. The main contributions of this paper are listed as follows.

- (i) Two-step approaches are proposed for the identification of gradually varying physical parameters of linear structures using only partially measured structural responses. FEKF-UI is firstly proposed to locate the time-varying parameters under unknown excitations, which aids to reduce the number of coefficients involved in the optimization process;

- (ii) DCT is used to expand the gradually varying physical parameters instead of previous WM analysis. It is demonstrated that DCT is more suitable for the decomposition of gradually varying parameters, which retains less coefficients to reconstruct the original varying parameters. As the number of unknown coefficients involved in the optimization is reduced, the proposed approaches are more efficient and robust to measurement noise than previous WM based methods. In addition, the boundary effect of WM can be avoided;
- (iii) It is further extended to the identification of gradually changing physical parameters under unknown excitations. Both the time-varying parameters and unknown excitations are identified simultaneously.

Numerical identification results of a truss and a bridge model validate that the proposed approaches can effectively identify the gradually varying and time-invariant physical parameters under known/unknown excitations. Moreover, the identification of time-varying cable force of cable-stayed bridges is investigated as a case study of the proposed approach I. Both the numerical and experimental results show that the proposed approach can be used to identify the time-varying cable force by only using the measurement of one accelerometer installed on the cable.

Acknowledgments

This research is supported by the National Natural Science Foundation of China through the key project No. 51838006. The authors also appreciate the support from Professor Hui Li and Professor Yuequan Bao at Harbin Institute of Technology for providing experimental data of the time-varying cable force. Finally, contributions by the anonymous reviewers are also highly appreciated.

References

- [1] Hou RR, Xia Y. Review on the new development of vibration-based damage identification for civil engineering structures: 2010-2019. *Journal of Sound and Vibration*. 2020; 491(9): 115741.
- [2] Bao YQ, Li H. Machine learning paradigm for structural health monitoring. *Structural health monitoring*. 2020; 4:147592172097241.

- [3] Wang ZC, Ren WX, Chen GD. Time-frequency analysis and applications in time-varying/nonlinear structural systems: A state-of-the-art review. *Advances in Structural Engineering*. 2018; 21: 1562-1584.
- [4] Ni PH, Li J, Hao H, Xia Y, Wang X, Lee JM, Jung KH. Time-varying system identification using variational mode decomposition. *Structural Control & Health Monitoring*. 2018; 25(6): e2175.
- [5] Lin JW, Betti R, Smyth AW, Longman RW. On-line identification of nonlinear hysteretic structural systems using a variable trace approach. *Earthquake Engineering and Structural Dynamics*. 2001; 30(9):1279-1303.
- [6] Askari M, Yu Y, Zhang CW, Samali B, Gu XY. Real-time tracking of structural stiffness reduction with unknown inputs, using self-adaptive recursive least-square and curvature-change techniques. *International Journal of Structural Stability and Dynamics*. 2019; 19(10):1950123.
- [7] Bisht SS, Singh MP. An adaptive unscented Kalman filter for tracking sudden stiffness changes. *Mechanical Systems and Signal Processing*. 2014; 49(1-2):181-195.
- [8] Yuen KV, Kuok SC. Online updating and uncertainty quantification using nonstationary output-only measurement. *Mechanical Systems and Signal Processing*. 2016; 66-67:62-77.
- [9] Yuen KV, Kuok SC, Dong L. Self-calibrating Bayesian real-time system identification. *Computer-Aided Civil and Infrastructure Engineering*. 2019; 34: 806-821.
- [10] Yang JN, Lin SL, Huang HW, Zhou L. An adaptive extended Kalman filter for structural damage identification. *Structural Control & Health Monitoring*. 2006; 13: 849-867.
- [11] Huang Q, Xu YL, Liu HJ. An efficient algorithm for simultaneous identification of time-varying structural parameters and unknown excitations of a building structure. *Engineering Structures*. 2015; 98:29-37.
- [12] Yang YH, Nagayama T, Xue K. Structure system estimation under seismic excitation with an adaptive extended Kalman filter. *Journal of Sound and Vibration*. 2020; 489:115690.
- [13] Wang N, Li L, Wang Q. Adaptive UKF-based parameter estimation for Bouc-Wen model of magnetorheological elastomer materials. *Journal of Aerospace Engineering*. 2019; 32(1): 04018130.
- [14] Huang Y, Yu JQ, Beck JL, Zhu HP, Li H. Novel sparseness-inducing dual Kalman filter and its application to tracking time-varying spatially-sparse structural stiffness changes and inputs. *Computer Methods in Applied Mechanics and Engineering*. 2020; 372:113411.
- [15] Ghanem R, Romeo F. A wavelet-based approach for the identification of linear time-varying dynamical systems. *Journal of Sound and Vibration*. 2000; 234(4):555-576.

- [16] Chang CC, Shi YF. Identification of time-varying hysteretic structures using wavelet multiresolution analysis. *International Journal of Non-Linear Mechanics*. 2010; 45(1): 21-34.
- [17] Shi YF, Chang CC. Substructural time-varying parameter identification using wavelet multiresolution approximation. *Journal of Engineering Mechanics*. 2012; 138(1):50-59.
- [18] Shi YF, Chang CC. Wavelet-based identification of time-varying shear-beam buildings using incomplete and noisy measurement data. *Nonlinear Engineering*. 2013; 2(1-2): 29-37.
- [19] Xiang M, Xiong F, Shi YF, Dai KS, Ding ZB. Wavelet multi-resolution approximation of time-varying frame structure. *Advances in Mechanical Engineering*. 2018; 10(8):1-19.
- [20] Wang C, Ren WX, Wang ZC, Zhu HP. Time-varying physical parameter identification of shear type structures based on discrete wavelet transform. *Smart Structures and Systems*. 2014; 14(5): 831-845.
- [21] Wang C, Ai DM, Ren WX. A wavelet transform and substructure algorithm for tracking the abrupt stiffness degradation of shear structure. *Advances in Structural Engineering*. 2019; 22(5): 1136-1148.
- [22] Chen SY, Lu JB, Lei Y. Identification of time-varying systems with partial acceleration measurements by synthesis of wavelet decomposition and Kalman filter. *Advances in Mechanical Engineering*. 2020; 12(6):168781402093046.
- [23] Lei Y, Yang N. Simultaneous identification of structural time-varying physical parameters and unknown excitations using partial measurements. *Engineering Structures*. 2020; 214: 110672.
- [24] Silik A, Noori M, Altabey WA, Ghiasi R. Selecting optimum levels of wavelet multi-resolution analysis for time-varying signals in structural health monitoring. *Structural Control & Health Monitoring*. 2021; e2762.
- [25] Xin Y, Li J, Hao H. Enhanced vibration decomposition method based on multisynchrosqueezing transform and analytical mode decomposition. *Structural Control & Health Monitoring*. 2021; 28: e2730.
- [26] Li JT, Zhu XQ, Law SS, Samali B. Time-varying characteristics of bridges under the passage of vehicles using synchroextracting transform. *Mechanical Systems and Signal Processing*. 2020; 140:106727.1-106727.19.
- [27] Zhu XQ, Law SS. Recent developments in inverse problems of vehicle-bridge interaction dynamics. *Journal of Civil Structural Health Monitoring*. 2016; 6(1): 107-128.
- [28] Tian YD, Wang L, Zhang J. Time-varying frequency-based scaled flexibility identification of a posttensioned concrete bridge through vehicle-bridge interaction analysis. *Structural Control & Health Monitoring*. 2021; 28: e2631.

- [29] Ahmed N, Natarajan T, Rao KR. Discrete cosine transform. *IEEE Transactions on Computers*. 1974; C-23:90-93.
- [30] Garcia-Hernandez JJ, Gomez-Flores W. Detection of AAC compression using MDCT-based features and supervised learning. *Journal of Experimental & Theoretical Artificial Intelligence*. 2021; 10:1-18.
- [31] Holub V, Fridrich J. Low-complexity features for JPEG steganalysis using undecimated DCT. *IEEE Transactions on Information Forensics & Security*. 2015; 10(2):219-228.
- [32] Eom KB. Analysis of acoustic signatures from moving vehicles using time-varying autoregressive models. *Multidimensional Systems and Signal Processing*. 1999; 10(4):357-378.
- [33] Aleardi M. Discrete cosine transform for parameter space reduction in linear and non-linear AVA inversions. *Journal of Applied Geophysics*. 2020; 179:104106.
- [34] Zhang S. Study the method of under sampling flight data reconstruction based on compressive sensing. Master Thesis, Civil Aviation University of China, China, May 2015. (In Chinese)
- [35] Alamdari MM, Khoa NLD, Wang Y, Samali B, Zhu XQ. A multi-way data analysis approach for structural health monitoring of a cable-stayed bridge. *Structural Health Monitoring*. 2019; 18(1):35-48.
- [36] Li SL, Wei SY, Bao YQ, Li H. Condition assessment of cables by pattern recognition of vehicle-induced cable tension ratio. *Engineering Structures*. 2018; 155(15): 1-15.
- [37] Kim SW, Jeon BG, Kim NS, Park JC. Vision-based monitoring system for evaluating cable tensile forces on a cable-stayed bridge. *Structural Health Monitoring*. 2013; 12(5-6): 440-456.
- [38] Zhang X, Peng JY, Cao MS, Damjanovic D, Ostachowicz W. Identification of instantaneous tension of bridge cables from dynamic responses: STRICT algorithm and applications. *Mechanical Systems and Signal Processing*. 2020; 142: 106729.
- [39] Li H, Ou JP. The state of the art in structural health monitoring of cable-stayed bridges. *Journal of Civil Structural Health Monitoring*. 2016; 6:43-67.
- [40] Zhang LX, Qiu GY, Chen ZS. Structural health monitoring methods of cables in cable-stayed bridge: a review. *Measurement*. 2020; 168:108343.
- [41] Li H, Zhang FJ, Jin YZ. Real-time identification of time-varying tension in stay cables by monitoring cable transversal acceleration. *Structural Control & Health Monitoring*. 2014; 21:1100–1117.
- [42] Bao YQ, Shi ZQ, Beck JL, Li H, Hou TY. Identification of time-varying cable tension forces based on adaptive sparse time-frequency analysis of cable vibrations. *Structural Control & Health Monitoring*. 2016; 24(3).

- [43] Bao YQ, Guo YB, Li H. A machine learning-based approach for adaptive sparse time-frequency analysis used in structural health monitoring. *Structural Health Monitoring*. 2020; 19(6): 1963–1975
- [44] Yang YC, Li SL, Nagarajaiah S, Li H, Zhou P. Real-time output-only identification of time-varying cable tension from accelerations via complexity pursuit. *Journal of Structural Engineering*. 2016; 142(1):1-10.
- [45] Xue SL, Shen RL. Real time cable force identification by short time sparse time domain algorithm with half wave. *Measurement*. 2020; 152:107355.
- [46] Wang C, Zhang J, Zhu HP. A combined method for time-varying parameter identification based on variational mode decomposition and generalized Morse wavelet. *International Journal of Structural Stability and Dynamics*. 2020; 10:2050077.
- [47] Hou RR, Wang XY, Xia Y. Sparse damage detection via the elastic net method using modal data. *Structural Health Monitoring*. 2021; 0(0):1-17.
- [48] Zhang CD, Xu YL. Structural damage identification via response reconstruction under unknown excitation. *Structural Control & Health Monitoring*. 2016; 24(8):e1953.1-e1953.11.
- [49] He J, Xu YL, Zhan S, Huang Q. Structural control and health monitoring of building structures with unknown ground excitations: Experimental investigation. *Journal of Sound and Vibration*. 2017; 390:23-38.
- [50] Liu LJ, Su Y, Zhu JJ, Lei Y. Data fusion based EKF-UI for real-time simultaneous identification of structural systems and unknown external inputs. *Measurement*. 2016; 88: 456–467.
- [51] Liu LJ, Zhu JJ, Su Y, Lei Y. Improved Kalman filter with unknown inputs based on data fusion of partial acceleration and displacement measurements. *Smart Structures and Systems*. 2016; 17(6): 903-915.
- [52] Achkire Y. Active tendon control of cable-stayed bridges. Ph.D. Thesis, ULB, Belgium, May 1997.

CHAPTER 6 Structural damage diagnosis based on the temporal moment of partially measured structural responses

ABSTRACT

Structural damage diagnosis is still a challenging task, as current methods are either insensitive to local structural damage or sensitive to measurement noise. Statistical moment-based structural damage detection (SMBDD) algorithm has been proposed to locate and detect damages, revealing superiority in noise immunity. However, it requests the number of measured responses should be no less than that of unknown structural parameters. In this paper, to reduce the number of measurements required in the SMBDD algorithm, an improved method for damage diagnosis is proposed based on the temporal moment of partially measured structural responses. First, structural partial acceleration responses are measured and split into several time segments. Then, the temporal moment in each segment of measured acceleration response time history is estimated. Finally, an objective error function is established by the temporal moments of measured accelerations and calculated accelerations, and structural stiffness can be identified by minimizing the objective error function. The proposed method is simple and feasible with a robust anti-noise property and can identify structural damage when the number of measured responses is less than that of the structural stiffness. Numerical simulations and experimental study are conducted respectively to verify the feasibility and effectiveness of the proposed method.

This chapter was published in *Journal of Aerospace Engineering* with the full bibliographic citation as follows: Yang N, Luo SJ, Lei Y. Structural damage detection based on the temporal moments of partially measured structural responses. *Journal of Aerospace Engineering*, 2021, 34(1): 04020106.

Introduction

In recent years, based on advanced sensing technology and data-driven techniques, structural health monitoring (SHM) has made great progress in many fields such as civil engineering,

mechanical engineering, aerospace, etc. (Ou and Li 2010; Chen and Ni 2018). Structural damage occurs unavoidably due to hazard environment (e.g., earthquake, typhoon and fire, etc.) and deterioration of structural performance. How to locate and quantify the potential damage, assess the structural integrity and security, and predict the remaining service life has always been an important research topic in SHM. The vibration-based structural damage detection approaches have attracted extensive attention in recent years and the development is becoming more and more mature. Most vibration-based structural damage diagnosis methods are established on the idea that the measured modal parameters or the parameters derived from these modal parameters are closely related to the physical characteristics of the structure, therefore, the change of physical characteristics can be reflected by detecting the change of modal parameters (Doebbling *et al.* 1998). Researches on different modal damage indices have been performed to recognize structural damage, including the change in natural frequency (Mekjavić and Damjanović 2017), mode shape (Chen and Büyüköztürk 2017), mode shape curvature (Shokrani *et al.* 2018), flexibility matrix (Katebi *et al.* 2018), and modal strain energy (Yang *et al.* 2019), etc. Among those, damage detection method based on natural frequency change is proved to be relatively easy with higher precision, but it has low sensitivity to local damages (Salawu 1997) and is failure to locate damage effectively. On the contrary, the change in mode shape can provide the spatial damaged location information in theory, but they can not quantify the damage along with other limitations including requirements on numerous sensors and poor noise resistance (Farrar and Jauregui 1998). Alvandi and Cremona found that the modal strain energy performed best in noise resistance, but even so, 3% noise had seriously affected the accuracy of damage identification in practice (Alvandi and Cremona 2006).

In conclusion, damage detection of civil structures is still a challenging task, as current damage detection methods are either insensitive to local structural damage or sensitive to measurement noise. It's noted that methods based on structural response statistical moment are proposed and shown to be an efficient tool because of its good noise immunity. Farrar *et al.* set up a statistical pattern recognition paradigm for damage detection in SHM (Farrar *et al.* 2000).

Sohn *et al.* combined autoregressive (AR) model and Auto-Regressive with exogenous inputs (ARX) prediction model in the context of a statistical pattern recognition paradigm to diagnose damage (Sohn *et al.* 2003). Zhang and Xu in the Hong Kong Polytechnic University proposed a novel damage detection method called statistical moment-based structural damage detection (SMBDD) method and have published a series of papers (Zhang *et al.* 2008,2011a,2011b,2013; Xu *et al.* 2009,2011). The sensitivity of statistical moment to structural damage was discussed and the formula was derived under a random excitation for the first time, and numerical examples including single and multi-story shear buildings were both employed to illustrate the accuracy of the method (Zhang *et al.* 2008). Then a shaking table test of a three shear building model subjected to ground motions was completed to further prove the validity of the proposed method (Xu *et al.* 2009). The displacement and acceleration responses were analyzed to locate damages and quantify severities. After that, the SMBDD method was extended in theory with more a general application (Zhang *et al.* 2011b). Particularly, the applicability of the SMBDD method under the conditions of non-Gaussian and non-stationary excitations was discussed with emphasis (Zhang *et al.* 2013). Considering the uncertainties in the first modal damping ratio, a method to identify damage for buildings with parametric uncertainties was presented by the combination of the SMBDD and the probability density evolution method (Xu *et al.* 2011). Besides, component and system reliability were evaluated taking advantage of the SMBDD account for the uncertainties in both the structure model and the external excitation (Zhang *et al.* 2011a). Also, Zhu and Wang in Huazhong University of Science and Technology in China came up with an idea of a two-step damage identification method based on the fourth strain statistical moment (FSSM) (Wang *et al.* 2014a, 2014b, 2016). This method has been verified by numerical simulation of beams (Wang *et al.* 2014a), numerical simulation of plates (Wang *et al.* 2014b), and experiments of beams (Wang *et al.* 2016), successively. Furthermore, Zhou *et al.* utilized a novel structural damage detection indicator called fourth-order voltage statistical moment (FVSM) which was established on the electromechanical impedance (EMI) principle to locate the damage element (Zhou *et al.* 2018). Xia and Hao took the uncertainties in random noise into consideration and assumed it had normal

distribution (Xia and Hao 2003). They put forward a statistical damage detection algorithm according to the change in frequency. Yu and Zhu applied higher statistical moments of structural responses to assess the nonlinear damaged behaviors (Yu and Zhu 2015). Impollonia *et al.* used the second-order moments of displacement and velocity to diagnose the change in stiffness and modal damping parameters (Impollonia *et al.* 2016). Lei *et al.* proposed two probabilistic structural damage detection approaches based on the SMBDD method when considering various uncertainties in structural parameters and external excitation (Lei *et al.* 2017). The probability density model of the parameter was discussed both in Gaussian distribution and logarithmic Gaussian distribution, respectively. Yang *et al.* fused two different statistical moments of structural dynamic responses including the fourth-order statistical moment of displacement and the eighth-order statistical moment of acceleration to identify damage in structures (Yang *et al.* 2018).

Generally speaking, a significant advantage of the method based on structural response statistical moment is that it is not only sensitive to local structural damage but also insensitive to measurement noise. However, the limitation is that it can only be applied when the number of measured responses is less than that of the structural stiffness, greatly restricting the application in engineering practice. Given the above, an improved temporal moment-based damage detection (TMBDD) method is proposed in this paper. Firstly, structural incomplete acceleration responses are measured and divided into a series of time segments. Then, the temporal moments of the measured accelerations and those of the calculated accelerations are obtained respectively, and the objective error function between them is constructed. Finally, the structural stiffness can be estimated by minimizing the objective error function. The innovation of the method is that it takes the advantage of statistical moment method on good anti-noise performance but only needs partial observations, i.e., it is effective when the number of observations is less than that of the structural stiffness to be identified. The validity of the method is confirmed by numerical examples and experimental model respectively.

The rest of the paper is organized as follows: Section 2 gives a detailed introduction to the process of the TMBDD method. In Section 3, four numerical examples are completed and analyzed for different structural types under various load styles, which prove the universality of the method. Section 4 presents a five-story shear frame test model to verify the effectiveness of the method from the experimental point of view, and its merits are demonstrated by comparing it with the traditional method. Section 5 gives information on the main contents and innovations to summarize.

The Proposed Algorithm

The motion equation of a linear structure under external excitation can be written as:

$$\mathbf{M}\ddot{\mathbf{x}}(t) + \mathbf{C}\dot{\mathbf{x}}(t) + \mathbf{K}\mathbf{x}(t) = \mathbf{B}\mathbf{f}(t) \quad (1)$$

where \mathbf{x} , $\dot{\mathbf{x}}$, and $\ddot{\mathbf{x}}$ are the vectors of displacement, velocity, and acceleration responses, respectively. Only part of acceleration responses is measured herein. $\mathbf{f}(t)$ is a known external excitation vector with the position matrix \mathbf{B} . \mathbf{M} and \mathbf{C} are the mass matrix and the damp matrix of the structure which are assumed to be known. \mathbf{K} is the global stiffness matrix of the structure, and it can be expressed as:

$$\mathbf{K} = \sum_{i=1}^n a_i \mathbf{k}_i = \alpha_1 \mathbf{k}_1 + \alpha_2 \mathbf{k}_2 + \cdots + \alpha_n \mathbf{k}_n \quad (2)$$

where a_i is unknown and denotes the i -th elemental relative stiffness coefficient of the reference FE model. n is the number of elements in the structure; \mathbf{k}_i is the i -th elemental stiffness matrix.

The proposed TMBDD method can be implemented in the following steps:

First, acquire calculated acceleration response $\ddot{\mathbf{x}}^c$ and measured acceleration responses $\ddot{\mathbf{x}}^m$ respectively: $\ddot{\mathbf{x}}^c$ can be computed by Eq. (1) when the initial values of the stiffness are known and $\ddot{\mathbf{x}}^m$ can be obtained by accelerometers installed on practical structures.

Equations can be solved only if the number of equations is greater than or equal to the number of unknowns. Therefore, a partial observation method is proposed in this paper to satisfy

the above conditions, which splits the acceleration responses into time segments to ensure that temporal moments in each segment are different, namely:

$$\mathbf{t} = \{t_1, t_2, t_3, \dots, t_N; t_{N+1}, t_{N+2}, \dots, t_{2N}, \dots, t_{dN}\} \quad (3)$$

in which N is the number of sample points in each response time segments; d represents the number of time segments.

Then, calculate temporal moments of measured acceleration \mathbf{M}^m and temporal moments of calculated acceleration \mathbf{M}^c in each segment.

$$\mathbf{M}_j^m = \frac{1}{N} \sum_{k=(j-1)N+1}^{jN} (\ddot{\mathbf{x}}_k^m)^2 - \left(\frac{1}{N} \sum_{k=(j-1)N+1}^{jN} \ddot{\mathbf{x}}_k^m \right)^2 \quad (j=1, 2, \dots, d) \quad (4)$$

$$\mathbf{M}_j^c = \frac{1}{N} \sum_{k=(j-1)N+1}^{jN} (\ddot{\mathbf{x}}_k^c)^2 - \left(\frac{1}{N} \sum_{k=(j-1)N+1}^{jN} \ddot{\mathbf{x}}_k^c \right)^2 \quad (j=1, 2, \dots, d) \quad (5)$$

where the subscript j denotes the temporal moment of acceleration response of the j -th time segment.

If the number of measured accelerations is l , the number of responses time segment is d , then the temporal moments can be written as:

$$\begin{bmatrix} \mathbf{M}^c(\mathbf{a}) \end{bmatrix} = \begin{bmatrix} \mathbf{M}_1^c \\ \mathbf{M}_2^c \\ \vdots \\ \mathbf{M}_{ld}^c \end{bmatrix} \quad \begin{bmatrix} \mathbf{M}^m(\mathbf{a}) \end{bmatrix} = \begin{bmatrix} \mathbf{M}_1^m \\ \mathbf{M}_2^m \\ \vdots \\ \mathbf{M}_{ld}^m \end{bmatrix} \quad (6)$$

For a structure with n degrees of freedom and m elements, the number of acceleration observations must satisfy the following constraints:

$$l \cdot d \geq n \quad (7)$$

Finally, the stiffness is estimated by solving the optimization problem.

The main idea of this method is to identify structural stiffness by using the relationship between the temporal moments of measured acceleration and those of calculated acceleration.

Therefore, compute the residual between these two temporal moments as:

$$\mathbf{F}_j(\boldsymbol{\alpha}) = \mathbf{M}_j^c(\boldsymbol{\alpha}) - \mathbf{M}_j^m(\boldsymbol{\alpha}) \quad (j = 1, 2, \dots, d) \quad (8)$$

$$\mathbf{g}(\boldsymbol{\alpha}) = \sum_{j=1}^d \|\mathbf{F}_j(\boldsymbol{\alpha})\|^2 \quad (9)$$

Ideally, if the given stiffness vector parameter is equal to the actual value, the 2-norm of the residual vector $\|\mathbf{F}_j(\boldsymbol{\alpha})\|^2$ will be zero. Herein, the FMINCON function in MATLAB is used to minimize the objective error function $\mathbf{g}(\boldsymbol{\alpha})$. It can be expressed as:

$$\min_{\boldsymbol{\alpha}} \mathbf{g}(\boldsymbol{\alpha}) \quad \text{subject to} \quad \mathbf{lb} \leq \boldsymbol{\alpha} \leq \mathbf{ub} \quad (10)$$

where \mathbf{lb} and \mathbf{ub} denote the lower bound and upper bound in the optimization process, respectively.

Numerical Examples

Damage Detection on Truss with Incomplete Measurement

A numerical example in this section is given to recognize truss stiffness under two separate white noise excitations. The structural parameters of truss are as follows:

As shown in Fig.1, the truss consists of 11 bars with the same cross section area $A = 7.854 \times 10^{-5} \text{ m}^2$, Young's modulus $E = 2 \times 10^8 \text{ N} \cdot \text{m}^{-2}$, and the mass density $\rho = 7850 \text{ kg} \cdot \text{m}^{-3}$.

The length of each horizontal bar is $l = 2 \text{ m}$ while the length of each inclined bar is $l = \sqrt{2} \text{ m}$. The finite element model of the truss has 11 members with 10 degrees of freedom (DOFs), i.e. each free node has the lateral and vertical DOFs. Structural global stiffness matrix \mathbf{K} can be formulated as the summation of each element stiffness matrix, in which the stiffness of i -th truss element is defined as $k_i = EA/l_i$ ($i = 1, \dots, 11$). The mass is concentrated on each node. The damping of the truss is assumed as viscous damping.

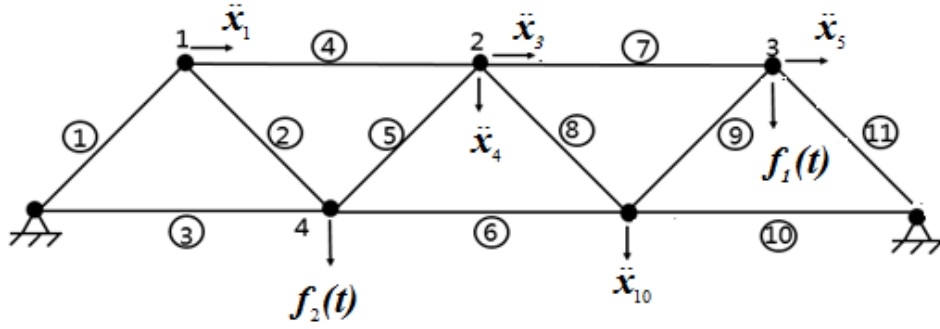


Fig. 1. A truss model subjected to two external excitations

In this numerical example, the duration of the excitation time history is 100s with the sampling frequency of 1000 Hz. The number of response time segments is 20; the initial value of relative stiffness coefficient is 0.8 and the domain of lower and upper bound is [0.8,1.2]. The truss is subjected to two external excitations of a band-limited white noise sequence in the vertical direction at node 3 and node 4. Only five accelerometers are deployed on the 1st, 3rd, 4th, 5th, and 10th DOFs. All the measured acceleration responses of structure are polluted by white noises with 10% root mean square (RMS).

Stiffness reduction of the element is given to simulate the damage. Single-damage and multi-damage are considered, respectively. Table 1 and Table 2 list the recognized stiffness coefficients of the undamaged and damaged elements. Table 1 is the case of single-damage with a 10% stiffness reduction on the 6th element. Table 2 shows the multi-damage with an 8% stiffness reduction on the 3rd element, a 10% stiffness reduction on the 6th element, and a 12% stiffness reduction on the 9th element. In these tables, α^u and α^d are relative stiffness parameters of undamaged structure and damaged structure, respectively. μ is the theoretical damage scenario. $\hat{\mu}$ is the identified damage scenario, namely:

$$\hat{\mu} = \frac{\alpha^d - \alpha^u}{\alpha^u} \times 100\% \quad (11)$$

Table 1. The results of the truss single damage identification

Element Number	α^u	α^d	μ	$\hat{\mu}$
1	1.0044	1.0044	0	0.00%
2	1.0121	1.0126	0	0.05%
3	0.9836	0.9919	0	0.84%
4	0.9660	0.9693	0	0.34%
5	1.0171	1.0139	0	-0.31%
6	1.0007	0.9114	-10%	-8.92%
7	1.0316	1.0250	0	-0.64%
8	1.0073	0.9962	0	-1.10%
9	1.0143	1.0137	0	-0.06%
10	1.0058	1.0042	0	-0.16%
11	0.9896	0.9927	0	0.31%

Note: α^u and α^d are relative stiffness parameters of undamaged structure and damaged structure, respectively. μ is the theoretical damage scenario. $\hat{\mu}$ is the identified damage scenario

$$\hat{\mu} = \frac{\alpha^d - \alpha^u}{\alpha^u} \times 100\% .$$

Table 2. The results of the truss multi-damage identification

Element Number	α^u	α^d	μ	$\hat{\mu}$
1	1.0044	1.0041	0	-0.03%
2	1.0121	1.0070	0	-0.50%
3	0.9836	0.9090	-8%	-7.58%
4	0.9660	0.9552	0	-1.12%
5	1.0171	1.0141	0	-0.29%
6	1.0007	0.9114	-10%	-8.92%
7	1.0316	1.0142	0	-1.69%
8	1.0073	0.9945	0	-1.27%
9	1.0143	0.8967	12%	-11.59%
10	1.0058	1.0064	0	0.06%
11	0.9896	1.0041	0	1.47%

Note: α^u and α^d are relative stiffness parameters of undamaged structure and damaged structure, respectively. μ is the theoretical damage scenario. $\hat{\mu}$ is the identified damage scenario

$$\hat{\mu} = \frac{\alpha^d - \alpha^u}{\alpha^u} \times 100\% .$$

Table 1 and Table 2 show that noise has little effect on recognition results even when the measurement noise intensity is as high as 10%, and the damage severities and locations can be properly discovered. Although only part of the accelerations are measured, the relative error is less than 1.69% for both single damage and multi-damage. Therefore, this method is not only insensitive to measurement noise, but also sensitive to damage with strong robustness and reliability. More importantly, it has a significant advantage that the number of observations is less than that of the structural stiffness.

Damage Detection on Continuous Beam with Incomplete Measurement

A continuous beam is selected as another numerical example to demonstrate the accuracy of the proposed method for identifying more complicated damage. The continuous beam is divided into ten finite elements and it has 19 DOFs (Fig. 2). The structural parameters of continuous beam are as follows: The length of each element is $l = 1\text{m}$; uniformly distributed mass is $785\text{ kg}\cdot\text{m}^{-1}$; and the exact stiffness of each element is $k_1 = k_2 = \dots = k_{10} = 1.111 \times 10^5\text{ N}\cdot\text{m}^{-1}$. A white noise excitation acts on the 6th DOF. Only seven accelerometers are installed at the 2nd, 4th, 6th, 8th, 11th, 15th, and 17th DOFs, which means only partial vertical accelerations are observed, and the rotation accelerations are non-essential. In this numerical example, the duration of the excitation time history is 200s with 1000 Hz sampling frequency. And the number of response time segments is 100; the initial value of relative stiffness coefficient is 0.8. 10% RMS noise intensity is considered in this case.

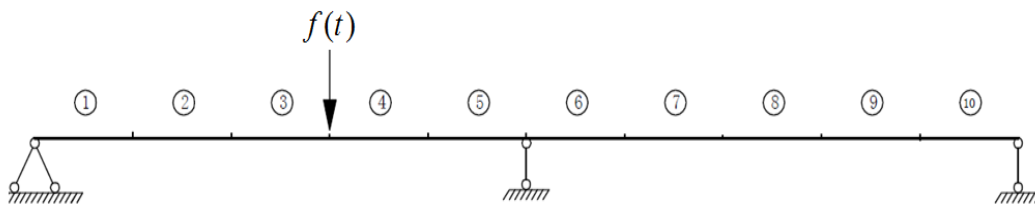


Fig. 2. A continuous beam model

The identification results are shown in Table 3 and Table 4. Table 3 proves that the identified results are accurate for single damage detection, in which case the theoretical stiffness value of the 4th element is reduced by 10%. The relative errors of the recognized values are less than 0.5% for all elements compared with the exact values when 10% noise intensity is considered. Table 4 shows that this method can locate and determine the multi-damage severity precisely. To simulate the multi-damage, an 8% stiffness reduction and a 12% stiffness reduction occurs on the 2nd and 7th element, respectively. It is obvious that the proposed algorithm can distinguish the structural stiffness accurately based on partial measured responses for continuous beam, demonstrating its reliability and feasibility again.

Table 3. The results of single damage identification of the continuous beam

Element Number	α^u	α^d	μ	$\hat{\mu}$
1	1.0265	1.0260	0	-0.05%
2	1.0024	1.0005	0	-0.19%
3	0.9758	0.9735	0	-0.24%
4	0.9791	0.8819	-10%	-9.93%
5	1.0255	1.0303	0	0.47%
6	1.0026	1.0023	0	-0.03%
7	1.0273	1.0257	0	-0.16%
8	1.0312	1.0293	0	-0.18%
9	0.9693	0.9692	0	-0.01%
10	0.9826	0.9835	0	0.09%

Note: α^u and α^d are relative stiffness parameters of undamaged structure and damaged structure, respectively. μ is the theoretical damage scenario. $\hat{\mu}$ is the identified damage scenario

$$\hat{\mu} = \frac{\alpha^d - \alpha^u}{\alpha^u} \times 100\% .$$

Table 4. The results of multi-damage identification of the continuous beam

Element Number	α^u	α^d	μ	$\hat{\mu}$
1	1.0265	1.0260	0	-0.05%
2	1.0024	0.9222	-8%	-8.00%
3	0.9758	0.9735	0	-0.24%
4	0.8820	0.8819	0	-0.01%
5	1.0255	1.0303	0	0.47%
6	1.0026	1.0023	0	-0.03%
7	1.0273	0.9065	-12%	-11.76%
8	1.0312	1.0293	0	-0.18%
9	0.9693	0.9692	0	-0.01%
10	0.9826	0.9835	0	0.09%

Note: α^u and α^d are relative stiffness parameters of undamaged structure and damaged structure, respectively. μ is the theoretical damage scenario. $\hat{\mu}$ is the identified damage scenario

$$\hat{\mu} = \frac{\alpha^d - \alpha^u}{\alpha^u} \times 100\% .$$

Damage Detection on Shear Frame with Incomplete Measurement

An eight-story shear frame under colored noise ground excitation is investigated in this section. The ground acceleration is modeled as a colored noise with the Kanai-Tajimi spectrum having parameters $\omega_g = 15.6 \text{ rad} \cdot \text{s}^{-1}$ and $\xi_g = 15.6$. Structural parameters of the building are $m_i = 2500 \text{ kg}$, $k_i = 7.0 \times 10^6 \text{ N} \cdot \text{m}^{-1}$, $c_i = 5.0 \times 10^4 \text{ N} \cdot \text{s} \cdot \text{m}^{-1}$, ($i = 1, \dots, 8$). In this case, only five accelerometers are deployed at the 1st, 2nd, 4th, 6th, and 8th stories. The duration of the excitation time history is 100s with 1000 Hz sampling frequency. And the number of response time segments is 20; the initial value of stiffness is 80% of exact value.

Table 5 and Table 6 show the identified stiffness coefficients for all stories of the undamaged and damaged building with 10% RMS noise level. Table 5 is the identification results of the single-damage case, where the 2nd element has an 8% stiffness reduction. Table 6 is the identification results of the multi-damage case. Herein the 2nd element has an 8% stiffness reduction and the 6th element has a 10% stiffness reduction. It is noted that there is no much

difference between the estimated damage scenarios and the theoretical damage scenarios when the structure is subjected to colored noise ground excitation. It proves that the proposed method is not only suitable under Gaussian white noise excitation but also appropriate under non-Gaussian colored noise ground excitation.

Table 5. The results of single damage identification of the shear frame with colored noise ground excitation

Element Number	α^u	α^d	μ	$\hat{\mu}$
1	0.9899	0.9767	0	-1.33%
2	1.0070	0.9221	-8%	-8.43%
3	1.0024	0.9983	0	-0.41%
4	0.9905	0.9903	0	-0.02%
5	1.0089	1.0042	0	-0.47%
6	0.9835	0.9895	0	0.61%
7	1.0562	1.0479	0	-0.79%
8	1.0181	1.0212	0	0.30%

Note: α^u and α^d are relative stiffness parameters of undamaged structure and damaged structure, respectively. μ is the theoretical damage scenario. $\hat{\mu}$ is the identified damage scenario

$$\hat{\mu} = \frac{\alpha^d - \alpha^u}{\alpha^u} \times 100\%$$

Table 6. The results of multi-damage identification of the shear frame with colored noise ground excitation

Element Number	α^u	α^d	μ	$\hat{\mu}$
1	0.9899	0.9685	0	-2.16%
2	1.0066	0.9324	-8%	-7.37%
3	1.0098	0.9981	0	-1.16%
4	0.9978	0.9934	0	-0.44%
5	0.9778	0.9848	0	0.72%
6	0.9983	0.9043	-10%	-9.42%
7	1.0552	1.0441	0	-1.05%
8	1.0184	1.0245	0	0.60%

Note: α^u and α^d are relative stiffness parameters of undamaged structure and damaged structure, respectively. μ is the theoretical damage scenario. $\hat{\mu}$ is the identified damage scenario

$$\hat{\mu} = \frac{\alpha^d - \alpha^u}{\alpha^u} \times 100\%$$

Damage Detection on Shear Frame with Non-stationary Excitation

In this section another shear frame numerical investigation is analyzed to further extend the proposed method from non-Gaussian colored noise ground excitation to non-stationary and non-Gaussian colored noise ground excitation. The utilized non-stationary external excitation takes the form of

$$\ddot{x}_g(t) = \ddot{x}_{gG}(t) \cdot g(t) \quad (12)$$

in which $\ddot{x}_{gG}(t)$ is the aforementioned Gaussian colored noise, $g(t)$ is a specified envelope or modulation function as:

$$g(t) = \begin{cases} 0 & t < 0 \\ 2.5974[\exp(-0.2t) - \exp(-0.6t)] & t \geq 0 \end{cases} \quad (13)$$

Parameters of shear frame are the same with the third numerical example. Only seven accelerometers are mounted at the 1st, 2nd, 4th, 6th, 9th, 10th, and 12th stories. The duration of the excitation time history is 100s with the sampling frequency of 1000Hz. And the number of response time segments is 20; the initial value of stiffness is 80% of exact value.

The calculating results are listed in Table 7 and Table 8. In Table 7, the theoretical stiffness value of the 2nd element is reduced by 10%. In Table 8, the stiffness of the 2nd and 10th element is damaged by 10% and 8% respectively. It can be seen from Table 7 and Table 8 that the damage locations of all the concerned damage scenarios can be accurately discovered when the measurement noise RMS is 10%, with the maximal relative error being less than 1%. Therefore, the sensitivity to structural local damage, insensitivity to measurement noise and applicability to non-stationary external excitations are demonstrated.

Table 7. Results of single damage identification of the shear frame with non-stationary colored noise ground excitation

Element Number	α^u	α^d	μ	$\hat{\mu}$
1	1.0033	1.0042	0	0.09%
2	1.0038	0.9005	10%	-10.29%
3	1.0289	1.0242	0	-0.46%
4	0.9634	0.9694	0	0.62%
5	0.9839	0.9869	0	0.30%
6	1.0295	1.0256	0	-0.38%
7	0.9937	0.9961	0	0.24%
8	0.9839	0.9860	0	0.21%
9	1.0276	1.0211	0	-0.63%
10	0.9984	0.9986	0	0.02%
11	0.9881	0.9910	0	0.29%
12	1.0299	1.0225	0	-0.72%

Note: α^u and α^d are relative stiffness parameters of undamaged structure and damaged structure, respectively. μ is the theoretical damage scenario. $\hat{\mu}$ is the identified damage scenario

$$\hat{\mu} = \frac{\alpha^d - \alpha^u}{\alpha^u} \times 100\% .$$

Table 8. Results of multi-damage identification of the shear frame with non-stationary colored noise ground excitation

Element Number	α^u	α^d	μ	$\hat{\mu}$
1	1.0033	1.0039	0	0.06%
2	1.0038	0.9003	10%	-10.31%
3	1.0289	1.0237	0	-0.51%
4	0.9634	0.9702	0	0.71%
5	0.9839	0.9869	0	0.30%
6	1.0295	1.0260	0	-0.34%
7	0.9937	0.9968	0	0.31%
8	0.9839	0.9859	0	0.20%
9	1.0276	1.0209	0	-0.65%
10	0.9984	0.9186	8%	-7.99%
11	0.9881	0.9904	0	0.23%
12	1.0162	1.0230	0	0.67%

Note: α^u and α^d are relative stiffness parameters of undamaged structure and damaged structure, respectively. μ is the theoretical damage scenario. $\hat{\mu}$ is the identified damage scenario

$$\hat{\mu} = \frac{\alpha^d - \alpha^u}{\alpha^u} \times 100\% .$$

Experimental Validation

In this section, a five-story shear frame (as shown in Fig. 3) subjected to white noise excitation has been used as experimental model to validate the proposed method. The length, width, and height of each story is 0.35m, 0.25m, and 0.2m, respectively. The junction nodes are connected to double bolts, it can be approximated that the connection between the support columns and the floors is consolidation. The structural materials are all steel with the Young's modulus $E = 2 \times 10^{11} \text{ N} \cdot \text{m}^{-2}$ and the mass density $\rho = 7850 \text{ kg} \cdot \text{m}^{-3}$. The mass of each story (including the floor and steel column's weights concentrating to the floor) and theoretical stiffness are shown in Table 9. The white noise excitation acts on the third floor in this experiment. The duration of the excitation time history is 40s with the sampling frequency of 1024Hz. Five accelerometers are deployed at the 1st, 2nd, 3rd, 4th, and 5th stories.

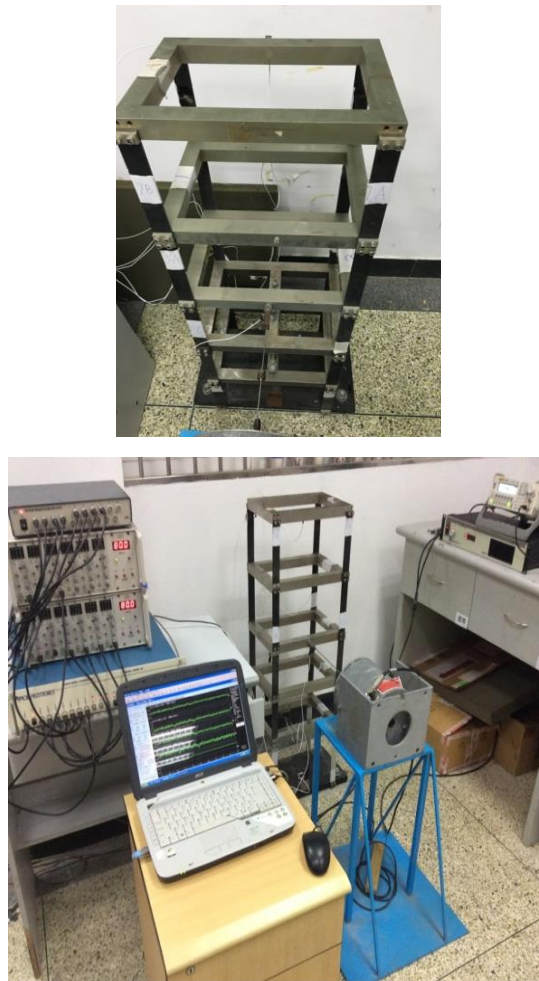


Fig. 3. An experimental study on a five-story building

Table 9. The mass and theoretical stiffness of frame

Story	Mass (kg)	Theoretical Stiffness ($\text{kN}\cdot\text{m}^{-1}$)
1	9.945	125.20
2	10.171	74.80
3	8.355	129.57
4	8.732	112.87
5	7.983	141.95

The effectiveness of the proposed method is proved by comparing with the existing SMBDD method. Firstly, apply SMBDD method to identify the structural parameters by measuring all the accelerations. Secondly, utilize the proposed method (TMBDD) to recognize the structural parameters with partial accelerations. The number of response time segments is 100. Only the 30000 sample points of accelerations on the 1st, 2nd and 5th story have been used to estimate the parameters. Recognition results of the two methods are presented in Table 10.

Table 10. The recognition results of the two methods

Story	Results of SMBDD	Results of TMBDD	Relative Error (%)
1	1.002	1.017	1.49
2	0.974	0.994	2.05
3	1.000	0.993	-0.70
4	1.020	0.994	-2.55
5	1.003	0.993	-0.99

It can be found from Table 10 that the results of TMBDD method is close to SMBDD with the maximal relative error being less than 3%. It testifies that the TMBDD method can check the structural parameters exactly only using partial response measurements, and retains the advantages of good anti-noise performance of the SMBDD method.

Conclusions

In this paper, a structural damage detection algorithm based on incomplete measured structural response is proposed. It divides the responses into time segments to ensure that the

sampling time is different in each segment. In order to improve the noise immunity, the response time should be as long as possible but ensure that temporal moments in each segment are different. Then, the structural stiffness is identified by the relationship between the temporal moments of the measured and the calculated accelerations. Four numerical examples are given to demonstrate the effectiveness of the proposed method. In addition, the reliability and feasibility are proved by a five-story shear frame experimental test.

Compared with the previous work, the proposed algorithm has the following innovations: 1) The proposed algorithm only needs partial observed structural acceleration responses. Moreover, the number of measured acceleration responses is less than that of the structural stiffness. 2) This method shows good accuracy in structural damage diagnosis with noise resistance.

Data Availability Statement

All data, models, and code generated or used during the study are available from the corresponding author upon reasonable request.

Acknowledgements

This work was supported by the Natural Science Foundation of China (NSFC) through the Grant No. 51678509.

References

- Alvandi, A., and C. Cremona. 2006. "Assessment of vibration-based damage identification techniques." *Journal of Sound and Vibration*. 292 (1-2):179-202. <https://doi.org/10.1016/j.jsv.2005.07.036>.
- Chen H.P., and Y.Q. Ni. 2018. "Introduction to structural health monitoring." *Structural Health Monitoring of Large Civil Engineering Structures*. <https://doi.org/10.1002/9781119166641.ch1>.
- Chen, J.G., and O. Büyüköztürk. 2017. "A symmetry measure for damage detection with mode shapes." *Journal of Sound and Vibration*. 408:123-137. <https://doi.org/10.1016/j.jsv.2017.07.022>.
- Doebling, S.W., C.R. Farrar, and M.B. Prime. 1998. "A summary review of vibration-based damage identification methods." *The Shock and Vibration Digest*. 30(2): 91-105. <https://doi.org/10.1.1.57.9721>.
- Farrar, C.R., T.A. Duffey, S.W. Doebling, and D.A. Nix. 2000. "A statistical pattern recognition paradigm for vibration-based structural health monitoring." *Structural & Multidisciplinary Optimization*. 41 (1):57-64. <https://doi.org/10.1007/s00158-009-0407-z>.

- Farrar, C.R., and D.A. Jauregui. 1998. "Comparative study of damage identification algorithms applied to a bridge: I. experiment." *Smart Materials and Structures*. 7(5): 704-719. <https://doi.org/10.1088/0964-1726/7/5/013>.
- Impollonia, N., I. Failla, and G. Ricciardi. 2016. "Parametric statistical moment method for damage detection and health monitoring." *ASCE-ASME Journal of Risk and Uncertainty in Engineering Systems, Part A: Civil Engineering*. C4016001. <https://doi.org/10.1061/AJRUA6.0000863>.
- Katebi, L., M. Tehranizadeh, and N. Mohammadgholibeyki. 2018. "A generalized flexibility matrix-based model updating method for damage detection of plane truss and frame structures." *Journal of Civil Structural Health Monitoring*. 8(2): 301-314. <https://doi.org/10.1007/s13349-018-0276-5>.
- Lei, Y., N. Yang, and D.D. Xia. 2017. "Probabilistic structural damage detection approaches based on structural dynamic response moments." *Smart Structures and Systems*. 20(2):207-217. <https://doi.org/10.12989/sss.2017.20.2.207>.
- Mekjavić, I., and D. Damjanović. 2017. "Damage assessment in bridges based on measured natural frequencies." *International Journal of Structural Stability and Dynamics*. 17(2):1750022. <https://doi.org/10.1142/S0219455417500225>.
- Ou, J.P., and H. Li. 2010. "Structural health monitoring in mainland China: review and future trends." *Structural Health Monitoring*. 9(3):219-231. <https://doi.org/10.1177/1475921710365269>.
- Salawu, O.S. 1997. "Detection of structural damage through changes in frequency: a review." *Engineering Structures*, 19 (9):718-723. [https://doi.org/10.1016/S0141-0296\(96\)00149-6](https://doi.org/10.1016/S0141-0296(96)00149-6).
- Shokrani, Y., V. K. Dertimanis, E. N. Chatzi, and M.N. Savoia. 2018. "On the use of mode shape curvatures for damage localization under varying environmental conditions." *Structural Control & Health Monitoring*. 25(4):e2132.1-e2132.20. <https://doi.org/10.1002/stc.2132>.
- Sohn, H., C.R. Farrar, N.F. Hunter, and K. Worden. 2003. "Structural health monitoring using statistical pattern recognition techniques." *Journal of Dynamic Systems Measurement and Control*. 123(4):706-711. <https://doi.org/10.1115/1.1410933>.
- Wang, D.S., Z. Chen, X. Wei, and H.P. Zhu. 2016. "Experimental investigation of damage identification in beam structures based on the strain statistical moment." *Advances in Structural Engineering*. 20(5):747-758. <https://doi.org/10.1177/1369433216664349>.
- Wang, D.S., W. Xiang, and H.P. Zhu. 2014a. "Damage identification in beam type structures based on statistical moment using a two-step method." *Journal of Sound and Vibration*. 333(3):745-760. <https://doi.org/10.1016/j.jsv.2013.10.007>.
- Wang, D.S., W. Xiang, and H.P. Zhu. 2014b. "Damage identification in a plate structure based on strain statistical moment." *Advances in Structural Engineering*. 17(11):1639-1655. <https://doi.org/10.1260/1369-4332.17.11.1639>.
- Xia, Y., and H. Hao. 2003. "Statistical damage identification of structures with frequency changes." *Journal of Sound and Vibration*. 263(4):853-870. [https://doi.org/10.1016/S0022-460X\(02\)01077-5](https://doi.org/10.1016/S0022-460X(02)01077-5).
- Xu, Y.L., J. Zhang, J. Li, and X.M. Wang. 2011. "Stochastic damage detection method for building structures with parametric uncertainties." *Journal of Sound and Vibration*. 330(20):4725-4737. <https://doi.org/10.1016/j.jsv.2011.03.026>.

- Xu, Y.L., J. Zhang, J.C. Li, and Y. Xia. 2009. "Experimental investigation on statistical moment-based structural damage detection method." *Structural Health Monitoring*. 8(6):555-571. <https://doi.org/10.1177/1475921709341011>.
- Yang, D.L., C.Y. Kang, Z.M. Hua, B.L. Ye, and P. Xiang. 2019. "On the study of element modal strain energy sensitivity for damage detection of functionally graded beams." *Composite Structures*. 224: 110989. <https://doi.org/10.1016/j.compstruct.2019.110989>.
- Yang, Y., J.L. Li, C.H. Zhou, S.S. Law, and L. Lv. 2018. "Damage detection of structures with parametric uncertainties based on fusion of statistical moments." *Journal of Sound and Vibration*. 442:200-219. <https://doi.org/10.1016/j.jsv.2018.10.005>.
- Yu, L., and J.H. Zhu. 2015. "Nonlinear damage detection using higher statistical moments of structural responses." *Structural Engineering and Mechanics*. 54(2):221-237. <https://doi.org/10.12989/sem.2015.54.2.221>.
- Zhang, J., Y.L. Xu, and J. Li. 2011a. "Integrated system identification and reliability evaluation of stochastic building structures." *Probabilistic Engineering Mechanics*. 26(4):528-538. <https://doi.org/10.1016/j.probengmech.2011.04.002>.
- Zhang, J., Y.L. Xu, J. Li, Y. Xia, and J.C. Li. 2008. "A new statistical moment-based structural damage detection method." *Earthquake Engineering & Engineering Vibration*. 12(1). <https://doi.org/10.1007/s11803-012-0147-8>.
- Zhang, J., Y. L. Xu, J. Li, Y. Xia, and J.C. Li. 2013. "Statistical moment-based structural damage detection method in time domain." *Earthquake Engineering and Engineering Vibration*. 1291(1):1671-3664. <https://doi.org/10.1007/s11803-012-0147-8>.
- Zhang, J., Y.L. Xu, Y. Xia, and J. Li. 2011b. "Generalization of the statistical moment-based damage detection method." *Structural Engineering and Mechanics*. 38(6):715-732. <https://doi.org/10.12989/sem.2011.38.6.715>.
- Zhou, P., D.S. Wang, and H.P. Zhu. 2018. "A novel damage indicator based on the electromechanical impedance principle for structural damage identification." *Sensors*. 18(7):2199. <https://doi.org/10.3390/s18072199>.

APPENDIX I
ATTRIBUTION OF AUTHORSHIP

To whom it may concern

I, Ning Yang, conducted numerical, experimental investigations, data processing, analysis and wrote manuscript of the paper titled as follows, which was revised and edited by the first co-author. He also provided insights on data processing and data analysis.

Simultaneous identification of structural time-varying physical parameters and unknown excitations using partial measurements

()

I, as a co-author, endorse that this level of contribution by the candidate indicated above is appropriate.

(Prof. Ying Lei)

()

To whom it may concern

I, Ning Yang, conducted numerical, data processing, analysis and wrote manuscript of the paper titled as follows, which was revised and edited by the first, third and the fourth co-authors. They also provided insights on data processing and data analysis. The last co-author helped conduct the numerical studies.

Identification of time-varying large-scale structures by integrated sub-structural and wavelet multiresolution approach with partial measurements

()

I, as a co-author, endorse that this level of contribution by the candidate indicated above is appropriate.

(Prof. Ying Lei) ()

(Associate Prof. Jun Li) ()

(Prof. Hong Hao) ()

(Dr. Jinshan Huang) (.)

To whom it may concern

I, Ning Yang, conducted numerical, data processing, analysis and wrote manuscript of the paper titled as follows, which was revised and edited by other co-authors. They also provided insights on data processing and data analysis.

Identification of time-varying nonlinear structural physical parameters by integrated WMA and UKF/UKF-UI

()

I, as a co-author, endorse that this level of contribution by the candidate indicated above is appropriate.

(Associate Prof. Jun Li) ()

(Prof. Ying Lei) ()

(Prof. Hong Hao) ()

To whom it may concern

I, Ning Yang, conducted numerical, experimental investigations, data processing, analysis and wrote manuscript of the paper titled as follows, which was revised and edited by other co-authors. They also provided insights on data processing and data analysis. The third co-author also helped to provide test data of the cable force experiment.

Identification of gradually varying physical parameters based on discrete cosine transform using partial measurements

()

I, as a co-author, endorse that this level of contribution by the candidate indicated above is appropriate.

(Prof. Ying Lei) ()

(Associate Prof. Jun Li) ()

(Prof. Hong Hao) ()

To whom it may concern

I, Ning Yang, conducted numerical, experimental investigations, data processing, analysis and wrote manuscript of the paper titled as follows, which was revised and edited by the last co-author. The second author helped conduct the numerical studies and experimental test.

Structural damage diagnosis based on the temporal moment of partially measured structural responses

()

I, as a co-author, endorse that this level of contribution by the candidate indicated above is appropriate.

(Mrs. Sujuan Luo) ()


(Prof. Ying Lei) ()

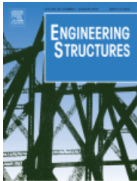
APPENDIX II

COPYRIGHT CLEARANCE

The proof of the rights, granted by publishers for the publication that forms the chapters of this thesis, to reproduce the contribution in the thesis are attached below.

Lei Y, Yang N. Simultaneous identification of structural time-varying physical parameters and unknown excitations using partial measurements. *Engineering Structures*, 2020, 214:110672.

Home ? Help ▾ 🗨️ Live Chat 👤 Sign in 👤+ Create Account



Simultaneous identification of structural time-varying physical parameters and unknown excitations using partial measurements

Author: Ying Lei, Ning Yang

Publication: Engineering Structures

Publisher: Elsevier

Date: 1 July 2020

© 2020 Elsevier Ltd. All rights reserved.

Journal Author Rights

Please note that, as the author of this Elsevier article, you retain the right to include it in a thesis or dissertation, provided it is not published commercially. Permission is not required, but please ensure that you reference the journal as the original source. For more information on this and on your other retained rights, please visit: <https://www.elsevier.com/about/our-business/policies/copyright#Author-rights>

BACK

CLOSE WINDOW

Yang N, Li J, Lei Y, Hao H. Identification of time-varying nonlinear structural physical parameters by integrated WMA and UKF/UKF-UI. *Nonlinear Dynamics*, 2021. DOI: 10.1007/s11071-021-06682-y. (In Press)

发件人: "Nonlinear Dynamics (NODY)"
<em@editorialmanager.com>
发送时间: 2021-06-24 05:38:44 (星期四)
收件人: "ying lei" <ylei@xmu.edu.cn>
抄送:
主题: Your Submission NODY-D-20-02665 -
[EMID:719377d7453690f0]

Dear Prof lei,

We are very pleased to inform you that your manuscript, "Identification of time-varying nonlinear structural physical parameters by integrated WMA and UKF/UKF-UI", has been accepted for publication in *Nonlinear Dynamics*. We apologize for the long processing time.

Please remember to quote the manuscript number, NODY-D-20-02665, whenever inquiring about your manuscript.

Thank you very much.

With best regards,
Walter Lacarbonara, Ph.D.
Editor in Chief
Nonlinear Dynamics

Please note that this journal is a Transformative Journal (TJ). Authors may publish their research with us through the traditional subscription access route or make their paper immediately open access through payment of an article-processing charge (APC). Authors will not be

发件人: Spr_corrections1@springer.com
发送时间: 2021-07-13 01:10:15 (星期二)
收件人: ylei@xmu.edu.cn
抄送:
主题: Proofs for your article in NONLINEAR DYNAMICS (6682) [First Reminder]

Dear Author,

The message below was sent to you more than 48 hours ago but we have not yet received your corrections. Please return your proof as soon as possible so as not to delay the publication of your article.

Yours sincerely,
Springer Corrections Team

PS: This is an auto reminder generated 48 hours after you have received proofs for corrections. Keeping in mind the global time difference, you may receive reminders even after you have sent in your corrections. If you already have sent us the necessary corrections, kindly ignore this email.

Identification of time-varying nonlinear structural physical parameters by integrated WMA and UKF/UKF-UI

Article DOI: 10.1007/s11071-021-06682-y

Editorial manuscript number:NODY-D-20-02665R0

Dear Author,

We are pleased to inform you that your paper is nearing publication. You can help us facilitate quick and accurate publication by using our e-Proofing system. The system will show you PDF-version of the article that you can

Rights and Permissions

- » [Permissions](#)
- » [Obtaining translation and reprint rights](#)
- » [Rights and Permissions at book fairs](#)
- » [Contacts](#)
- » [Anti-piracy strategies for Springer eBooks](#)
- » [Springer's text- and data-mining policy](#)

Permissions

Get permission to reuse Springer Nature content

Springer Nature is partnered with the Copyright Clearance Center to meet our customers' licensing and permissions needs.

Copyright Clearance Center's RightsLink® service makes it faster and easier to secure permission for the reuse of Springer Nature content to be published, for example, in a journal/magazine, book/textbook, coursepack, thesis/dissertation, annual report, newspaper, training materials, presentation/slide kit, promotional material, etc.

Simply visit [SpringerLink](#) and locate the desired content;

- Go to the article or chapter page you wish to reuse content from. (Note: permissions are granted on the article or chapter level, not on the book or journal level). Scroll to the bottom of the page, or locate via the side bar, the "Reprints and Permissions" link at the end of the chapter or article.
- Select the way you would like to reuse the content;
- Complete the form with details on your intended reuse. Please be as complete and specific as possible so as not to delay your permission request;
- Create an account if you haven't already. A RightsLink account is different than a SpringerLink account, and is necessary to receive a licence regardless of the permission fee. You will receive your licence via the email attached to your RightsLink receipt;
- Accept the terms and conditions and you're done!

For questions about using the RightsLink service, please contact Customer Support at Copyright Clearance Center via phone +1-855-239-3415 or +1-978-646-2777 or email springematuresupport@copyright.com.

Yang N, Luo SJ, Lei Y. Structural damage diagnosis based on the temporal moment of partially measured structural responses. *Journal of Aerospace Engineering*, 2021, 34(1): 04020106.

CCC | Marketplace™ Sign In Cart Help Live Chat

Publications To Search Permissions Enter Title, Keywords, PMID, ISSN, ISBN, Authors, etc... Advanced Search Search Tips

[Return to Search](#)

Journal of Aerospace Engineering
Publication type: Journal

ISSN: 0893-1321
Publication Year: 1988 - Present
Publisher: American Society of Civil Engineers

Language: English
Country: United States of America
Authors: American Society of Civil Engineers

Order License ID	1137700-1
Order detail status	Completed
ISSN	0893-1321
Type of use	Republish in a thesis/dissertation
Publisher	American Society of Civil Engineers

ASCE LIBRARY Access provided by Xiamen University SEARCH CART LOG IN / REGISTER FIND MY INSTITUTION

JOURNALS BOOKS MAGAZINES AUTHOR SERVICES USER SERVICES

- Guidelines for Permission Request
- ASCE Terms and Conditions for

REUSE AUTHOR'S OWN MATERIAL

As the original author of an ASCE journal article or proceedings paper, you are permitted to reuse your own content for another ASCE or non-ASCE publication.

BIBLIOGRAPHY DISCLAIMER

Every reasonable effort has been made to acknowledge the owners of copyright material. I would be pleased to hear from any copyright owner who has been omitted or incorrectly acknowledged.